

STOICHIOMETRIC AND CATALYTIC  
C–H BORYLATIONS OF ARENES

By

Sean Michael Preshlock

A DISSERTATION

Submitted to  
Michigan State University  
in partial fulfillment of the requirements  
for the degree of

Chemistry – Doctor of Philosophy

2013

## ABSTRACT

### STOICHIOMETRIC AND CATALYTIC C–H BORYLATIONS OF ARENES

By

Sean Michael Preshlock

Regioselective catalytic transformation of carbon-hydrogen bonds to other functional groups represents a long-standing challenge in homogeneous and heterogeneous catalysis. The Ir-catalyzed C–H activation/borylation has emerged as a useful method for synthesizing various aryl and heteroaryl boronic esters with regiochemistry complimentary to traditional methods and tolerant of various functional groups. The steric dominance of C–H activation/borylation has allowed for the synthesis of new aromatic building blocks which were previously inaccessible or hard to synthesize.

With the aid of high throughput experimentation (HTE), we designed reaction screens that would not only optimize Ir-catalyzed C-H borylation reactions for more challenging substrates, but also broaden the scope of this chemistry by assessing the efficiency and compatibility of the reactions as functions of precatalyst, boron reagent, ligand, order of addition, temperature, solvent and substrate.

We then sought to apply these results to unprotected anilines which were inert under conventional Ir-catalyzed C-H borylation conditions. Building off a recent report from our research group that utilized a unique outer sphere directing effect to obtain *ortho* functionalized C-H borylation products from NBoc protected anilines, we investigated whether we could use HBPin as a traceless protecting/directing group for the borylation of primary anilines under more forcing conditions. Our attempts were successful and provided for a one-pot protection/deprotection procedure that used a lower

catalyst loading and gave products in better to comparable yields than the NBoc protected borylation reaction.

Using an  $(\eta^6\text{-C}_6\text{Me}_3\text{H}_3)\text{Ir}(\text{BPin})_3$  as starting material, five-coordinate bisphosphine complexes can be synthesized by displacement of the  $\eta^6\text{-C}_6\text{Me}_3\text{H}_3$  with the incoming phosphine ligands. Using this method we have isolated the *trans*- $\text{Ir}(\text{PAr}_3^{\text{F}})_2\text{BPin}_3$  complex which is thought to be the active catalyst for the *ortho*-C-H directed borylation of benzoate esters first discovered by Miyaura. The *trans*- $\text{Ir}(\text{PAr}_3^{\text{F}})_2\text{BPin}_3$  complex is not catalytically competent with HBPin as borylating reagent. We have since been able to develop silylphosphine chelates (Figure 8) that are compatible with HBPin while retaining the unique selectivity shown with the  $\text{Ir}(\text{PAr}_3^{\text{F}})_2\text{BPin}_3$  complex. Studies to further improve on the silylphosphine ligand design and extend the substrate scope are ongoing.

Copyright by  
SEAN MICHAEL PRESHLOCK  
2013

*Tacos and candy bars*

## ACKNOWLEDGMENTS

I would like to thank, first and foremost, my lab mates in the Mitch Smith Research group. It is true that you are influenced by your surroundings and they undoubtedly had the largest impact on my development as a chemist. I would like to thank my seniors, Abbas, Britt and Appi, for welcoming me into the group and relating all of the borylation lab lore that had come before my time. I would like to thank the chemist who came and went while I was in the lab, Bala, Jon and Phil, I learned a lot from them and we shared many adventures. I would also like to thank the next generation of Junior Borylation Rangers, Behnaz, Don, Buddha, Dmitry, Kristen, and Tim, it is up to you to carry on the borylation torch and I wish you the best in publishing my unfinished projects. Yu Ling and Olive Oyl, you guys are great too and I wish you the best of luck with your research.

I would like to offer a very special thanks to Mitch. The C-H borylation chemistry he discovered was an absolute joy to work on and it was a fulfilling and enlightening experience to take part in its further development. I would also like to thank Mitch for the great opportunity I had while doing research at Rahway.

I owe a great many thanks to Rob Maleczka for the excellent discussions and suggestions along the way. The members of his group who worked on the borylation project along with me, Luis, Monica, Li, Suzi, Damith, Fung Yi and Ruwi, all did exceptional work and I learned a great deal from their research as well.

During my time as a graduate student, I also had the tremendous opportunity to do research in an industrial environment at Merck. Shane and Peter offered exceptional guidance while I was there and it was a remarkable learning experience.

I would like to thank dynamic duo Dan and Kermit for all the help with NMR at MSU and Richard for his help with X-Ray structures; I know it was not easy with some of my less than stellar crystals. Also, Pete Dormer and Thomas Williamson gave me great help with the NMR instruments at Merck. The members of Merck's Automation and Catalysis group were a joy to work with and gave great guidance.

I would like to offer a special thanks to the brave men and women I served with during my time as a CEM 415 TA (Thanks, Phil, Colin and Behnaz, those were certainly the days of high adventure).

My parents Mike and Debra and my brother Phil offered great moral support among so many other things that I will forever be grateful for. I could always tell you were proud of me.

I would like to thank the Spencer family for being my home away from home. I could never ask for better friends. I would also like to thank the Comptons for making my long stay in East Lansing such an enjoyable one.

I would also like to thank my old roommate Alex for always assuring me that no matter what, I was still good enough for government work; Strength and Honor, bud.

## TABLE OF CONTENTS

LIST OF TABLES .....	xi
LIST OF FIGURES .....	xiii
KEY TO SYMBOLS AND ABBREVIATIONS .....	xviii
<b>CHAPTER 1</b>	
INTRODUCTION .....	1
C-H Bond Activation and Functionalization in Aromatic Compounds.....	1
Arylboronic Acids.....	4
Ir C-H Borylation Chemistry .....	6
Chemoselectivity of C-H Activation/Borylation Catalysts.....	8
Regioselectivity of Ir C-H Activation/Borylation Catalysis.....	8
Mechanism.....	9
Deviations From Sterically Directed Regioselectivity via Electronic Bias .....	11
REFERENCES .....	19
<b>CHAPTER 2</b>	
OPTIMIZATION OF Iridium CATALYZED C-H BORYLATIONS.....	22
Introduction.....	22
Identification of Reaction Variables .....	23
Orders of Addition Effects for Room Temperature Reactions .....	28
Effects of Borylating Reagent on Relative Reactivity .....	29
General Ligand and Precatalyst Trends for Room Temperature Reaction Screen .....	29
Temperature effects on optimization screens .....	31
Solvent Effects on Catalyst Formation at Room Temperature .....	33
Solvent Effects on Catalyst Formation at Elevated Temperature .....	37
Elevated Temperature Reaction Screen Performed on <b>5a</b> in Multiple Solvents .....	38
Phosphine Ligated Iridium Borylation Catalysts .....	41
Ligand Effects; Electron Donating Ability and Constrained Geometry .....	43
Kinetic Experiments with (tmphen)Ir(BPin) <sub>3</sub> (COE) and (dtbpy)Ir(BPin) <sub>3</sub> (COE).....	46
C-H Borylation in Open vs. Closed Systems.....	50
Ligand to Metal Ratio and Catalyst Loading Study.....	52
Precatalyst Stability and Aging Studies .....	55
REFERENCES .....	58
<b>CHAPTER 3</b>	
CHELATE DIRECTED C-H BORYLATIONS .....	61
Ester directed C-H borylation .....	61



Synthesis of Discrete 5 Coordinate $(Ar^F_3P)_2Ir(BPin)_3$ Trisboryl Complex.....	62
Mechanistic Insights into $(Ar^F_3P)_2Ir(BPin)_3$ Catalytic Cycle.....	66
REFERENCES .....	81

#### CHAPTER 4

BPIN AS A TRACELESS DIRECTING GROUP FOR C-H BORYLATIONS .....	83
Traceless BPin protected borylation of heterocycles.....	83
Application of BPin as traceless protecting group with primary anilines .....	87
Optimization .....	89
Solvent Effects on Regioselectivity .....	92
Ligand Effects on Regioselectivity.....	93
Applications .....	96
Borylation of Aminopyridines .....	98
REFERENCES .....	100

#### CHAPTER 5

EXPERIMENTAL.....	102
REFERENCES .....	249

## LIST OF TABLES

Table 1.1	Regioselectivity for C-H borylations with veratrole ( <b>1</b> ) and benzodioxole ( <b>2</b> ).....	14
Table 2.1	Temperature Effects on Relative Conversions for 1,2,3-trimethoxybenzene ( <b>4a</b> )..	30
Table 2.2	Temperature Effect on Catalyst Stability.....	40
Table 2.3	Borylation of 2,6-dimethylanisole ( <b>7a</b> ) .....	44
Table 2.4	Ligand to Metal Ratios and Catalyst Loading Study .....	52
Table 2.5	Ligand to Metal Ratio with preformed (tmphen)Ir(COE)BPin <sub>3</sub> .....	53
Table 2.6	Metal Additive Screen for In-Situ Precatalyst Generation .....	57
Table 3.1	Borane effects on <i>ortho</i> -directed borylation of <b>10a</b> .....	72
Table 3.2	Ligand effects on <i>ortho</i> -directed borylation of methyl benzoate ( <b>10a</b> ) .....	78
Table 3.3	Borane effects on <i>ortho</i> -directed borylation of methyl benzoate ( <b>10a</b> ).....	79
Table 4.1	Borane and Solvent Effects on Borylation of 3-chloroaniline ( <b>22a</b> ) with tmphen ...	90
Table 4.2	Borane and Solvent Effects on Borylation of 3-chloroaniline ( <b>22a</b> ) with dtbpy .....	91
Table 4.3	Solvent Screen for 3-(trifluoromethyl)anilines ( <b>20a</b> ) .....	92
Table 4.4	Ligand effects on borylation of 3-(trifluoromethyl)anilines ( <b>20a</b> ) .....	94
Table 4.5	Traceless BPin protected borylation of anilines .....	95
Table 5.1	Ligand to Metal Ratio with preformed (tmphen)Ir(COE)BPin <sub>3</sub> .....	131

Table 5.2	Solvent Screen for 3-(trifluoromethyl)anilines ( <b>20</b> ) .....	153
Table 5.3	Crystal data and structure refinement for <b>37</b> .....	182
Table 5.4	Crystal data and structure refinement for <i>Trans</i> -(Ar <sup>F</sup> <sub>3</sub> P) <sub>2</sub> Ir(BPin) <sub>3</sub> ( <b>12</b> ) .....	183
Table 5.5	Crystal data and structure refinement for <i>Trans</i> -(Ar <sup>F</sup> <sub>3</sub> P) <sub>2</sub> Ir(H)(BPin) <sub>2</sub> ( <b>13</b> ) .....	184

## LIST OF FIGURES

Figure 1.1	Synthesis of organo ruthenium aryl complexes by Chatt and Davidson .....	1
Figure 1.2	Synthesis of $\text{Fe}(\text{dmpe})_2(\text{H})(\text{C}_6\text{H}_4\text{Me})$ .....	2
Figure 1.3	Catalytic intramolecular cyclization of 2,6-xylyl isocyanide .....	2
Figure 1.4	Intermolecular C-H activation/ functionalization reactions with trialkylsilanes .....	3
Figure 1.5	Thermodynamics of methane borylation .....	5
Figure 1.6	Stoichiometric C-H borylation of aromatic and aliphatic substrates .....	6
Figure 1.7	First catalytic aromatic C-H activation /borylation reaction .....	7
Figure 1.8	Chemo- and regioselective comparisons for iridium and rhodium catalysts .....	8
Figure 1.9	Borylation of benzene with $(\eta^6\text{-C}_6\text{H}_3\text{Me}_3)\text{Ir}(\text{BPin})_3$ .....	10
Figure 1.10	Proposed catalytic cycle.....	11
Figure 1.11	Electronic effects in product distribution.....	12
Figure 1.12	Steric hinderance of veratrole ( <b>1</b> ) and benzodioxole ( <b>2</b> ) .....	13
Figure 1.13	5-coordinate Iridium Catalyst .....	13
Figure 1.14	Limiting descriptions of the C-H activation transition states .....	15
Figure 1.15	. Correlation of $\Delta E$ with the charge developed on the aryl group (TS 1 in Figure 1.14). For interpretation of references color in this and all other figures, the reader is referred to the electronic version of this dissertation.....	16

Figure 1.16	Ligand design for enhanced regioselectivity .....	17
Figure 1.17	Regioselective borylations with 1,3-difluorobenzene .....	18
Figure 2.1	Precatalysts Selected for Reaction Screens .....	23
Figure 2.2	Room Temperature Reaction Screen With 3-bromotoluene.....	25
Figure 2.3	Precatalyst and ligand complexation .....	28
Figure 2.4	Rate equation .....	29
Figure 2.5	Elevated temperature reaction screen performed on N,N-dimethyltoluidine ( <b>5a</b> ) ...	32
Figure 2.6	(dtbpy)Ir(BPin) <sub>3</sub> (COE) and (tmphen)Ir(BPin) <sub>3</sub> (COE).....	34
Figure 2.7	Solvent Effects on Catalyst Generation at Room Temperature.....	35
Figure 2.8	[(tmphen)Ir(CH(BPin) <sub>2</sub> Cl) <sub>2</sub> ]......	36
Figure 2.9	Solvent effects on catalyst generation with 1,3-dimethoxybenene ( <b>6a</b> ) .....	37
Figure 2.10	Multivariable Solvent Screen.....	39
Figure 2.11	Phosphine Ligand Screen.....	41
Figure 2.12	Elevated Temperature Phosphine Ligand Screen .....	42
Figure 2.13	(dmpbz-κ <sup>2</sup> P)Ir((BPin) <sub>3</sub> (dmpbz-κ <sup>1</sup> P) .....	43
Figure 2.14	Decay of <b>6a</b> during the reaction with HBPIn or B <sub>2</sub> pin <sub>2</sub> .....	45

Figure 2.15	$\ln[\text{arene}]$ vs. time over two half-lives .....	47
Figure 2.16	Catalytic resting states for kinetic experiments with $(\text{tmphen})\text{Ir}(\text{BPin})_3(\text{COE})$ with $\text{B}_2\text{Pin}_2$ ( <b>A</b> ) and $\text{HBPin}$ ( <b>B</b> ) .....	48
Figure 2.17	Proposed catalytic cycle for $(\text{dtbpy})\text{Ir}(\text{BPin})_3(\text{COE})$ from ref. 5 .....	48
Figure 2.18	Kinetic Experiments with $(\text{tmphen})\text{Ir}(\text{BPin})_3(\text{COE})$ at variable catalyst loadings ..	49
Figure 2.18	C-H Borylation in Open vs. Closed Systems with <b>8a</b> .....	51
Figure 2.20	Precatalyst Stability and Aging Study .....	54
Figure 3.1	Ester directed C-H borylation .....	61
Figure 3.2	<i>Cis</i> and <i>Trans</i> - $(\text{Ar}^{\text{F}}_3\text{P})_2\text{Ir}(\text{BPin})_3$ .....	62
Figure 3.3	<i>Trans</i> - $(\text{Ar}^{\text{F}}_3\text{P})_2\text{Ir}(\text{BPin})_3$ ( <b>9b</b> ) .....	63
Figure 3.4	Variable temperature $^{31}\text{P}$ NMR of <i>Cis</i> and <i>Trans</i> - $(\text{Ar}^{\text{F}}_3\text{P})_2\text{Ir}(\text{BPin})_3$ .....	65
Figure 3.5	Ester coordination to $(\text{Ar}^{\text{F}}_3\text{P})_2\text{Ir}(\text{BPin})_3$ complex.....	66
Figure 3.6	Stoichiometric borylation of methyl 3-(trifluoromethyl)benzoate ( <b>11a</b> ) .....	67
Figure 3.7	<i>Trans</i> - $(\text{Ar}^{\text{F}}_3\text{P})_2\text{Ir}(\text{H})(\text{BPin})_2$ ( <b>12</b> ) .....	68
Figure 3.8	Borylation of methyl benzoate ( <b>10a</b> ) with excess $(\text{Ar}^{\text{F}}_3\text{P})_2\text{Ir}(\text{BPin})_3$ .....	69
Figure 3.9	<i>Trans</i> - $(\text{Ar}^{\text{F}}_3\text{P})_2\text{Ir}(\text{H}_2\text{BPin})(\text{BPin})_2$ ( <b>13</b> ) .....	70

Figure 3.10 Proposed catalytic cycle for the chelate directed borylation of aryl esters with $(\text{Ar}^{\text{F}}_3\text{P})_2\text{Ir}(\text{BPin})_3$ .....	71
Figure 3.11 Designing more reactive Iridium catalysts .....	73
Figure 3.12 Synthesis of silylboranes .....	74
Figure 3.13 Silyl-directed <i>ortho</i> borylation of alkylamines .....	75
Figure 3.14 N-(dimethylsilyl)-N,N-bis(2-pyridyl)amine ( <b>14b</b> ) .....	76
Figure 3.15 Synthesis of $\text{Ir}(\kappa^2\text{-SiNpy}_2)_3$ .....	76
Figure 3.16 Synthesis of SiPbz ligands.....	77
Figure 4.1 Borylation of indole .....	83
Figure 4.2 Base assisted protection of heterocycles with HBPin.....	84
Figure 4.3 In-situ protection of heterocycles with HBPin .....	85
Figure 4.4 Comparison of Boc and traceless directed borylation of heterocycles .....	86
Figure 4.5 Outer-sphere <i>ortho</i> directed iridium catalyzed C-H borylation of aniline.....	87
Figure 4.6 Synthesis of N-BPin-3-(trifluoromethyl)aniline ( <b>20b</b> ) .....	88
Figure 4.7 <i>Ortho</i> borylation of N-BPin-3-(trifluoromethyl)aniline ( <b>20b</b> ) .....	88
Figure 4.8 Proposed Reaction Mechanism.....	89
Figure 4.9 Borylation of 3-chloro-N-methylaniline ( <b>21a</b> ) .....	89
Figure 4.10 Borylation of <i>o</i> -anisidine .....	97

Figure 4.11	Putative transition state for <i>ortho</i> -borylation of 2-substituted anilines .....	98
Figure 4.12	Traceless BPin protected borylation of amino pyridines.....	99
Figure 5.1	2-methoxy-4-(4,4,5,5-tetramethyl-1,3,2-dioxaborolan-2yl)-benzenamine ( <b>37</b> ) ....	173



## KEY TO SYMBOLS AND ABBREVIATIONS

acac	acetylacetonate
Å	Ångstrom
bbnbox	2,2'-bis[(4S)-4-benzyl-2-oxazoline]
$\beta$	bite angle
BCat	catecholatorboryl
BCat*	4- <i>tert</i> -butyl-catecholatorboryl
Beg	1,3,2-dioxborolane
Boc	<i>tert</i> -butoxycarbonyl
box	2,2'-bisoxazoline
BPin	pinacolatoboryl
COE	<i>cis</i> -cyclooctene
COD	1,5-cyclooctadiene
Cpme	cyclopentyl methylether
Cp	cyclopentadienyl
Cp*	pentamethylcyclopentadienyl

dcpe	1,2-bis(dicyclohexylphosphino)ethane
diim	(2,3,5,6,8,9-hexahydrodiimidazo[1,2-a:2',1'-c]pyrazine)
dippe	1,2-bis(di- <i>iso</i> -propylphosphino)ethane
dmabpy	(4,4'-bis(dimethylamino)-2,2'-bipyridine)
dmpbz	1,2-bis(dimethylphosphino)benzene
dmpe	1,2-bis(dimethylphosphino)ethane
dppbz	1,2-bis(diphenylphosphino)benzene
dppe	1,2-bis(diphenylphosphino)ethane
dtbpe	1,2-bis(di- <i>tert</i> -butylphosphino)ethane
dtbpy	4,4'-di- <i>tert</i> -butyl bipyridine
EAS	electrophilic aromatic substitution
equiv	equivalent
GC-FID	gas chromatography flame ionization detection
gCOSY	gradient-selected correlated spectroscopy
$\eta$	eta, hapticity
Ind	indenyl
<sup><i>i</i></sup> Pr	<i>iso</i> -propyl

$\kappa$	kappa, denotes how many and which atoms of a ligand are binding
K	equilibrium constant
M	metal
<i>m</i>	<i>meta</i>
MesH	mesitylene
$\mu$	mu, denotes bridging ligand
<i>n</i>	<i>normal</i> (straight chain hydrocarbon)
NMR	Nuclear Magnetic Resonance
<i>o</i>	<i>ortho</i>
ORTEP	Oak Ridge Thermal Ellipsoid Plot Program
<i>p</i>	para
phen	(1,10-phenanthroline)
$\pi$	pi, degree of pyramidalicity
ppm	parts per million
R	general substituent
<i>t</i> <sub>1/2</sub>	half-life
tmphen	3,4,7,8-tetramethyl-1,10-phenanthroline

# CHAPTER 1

## INTRODUCTION

### C-H Bond Activation and Functionalization in Aromatic Compounds

The catalytic transformation of carbon-hydrogen bonds to other functional groups represents a long-standing challenge in homogeneous and heterogeneous catalysis as C-H bonds are the most ubiquitous chemical linkages in Nature. Unfortunately, hydrocarbons are also among the least reactive organic compounds. The C-H bonds in aromatics are of very low acidity/ basicity, low polarity, and bond energies typically in the range of 115 Kcal/mol, accounting for their relative lack of reactivity. Over the past several decades, significant advances have been made in the use of transition metal complexes to facilitate the cleavage of these bonds and for the inclusion of these organometallic complexes in organic transformations.<sup>1</sup>

Perhaps, the earliest example of C-H activation by a transition metal complex was reported in 1963 for the reaction of nickelocene and azobenzene, although the reaction was not well defined.<sup>2</sup> By 1965, Chatt found that  $\text{Ru}(\text{dmpe})_2$ , (dmpe is (1,2-bis(dimethylphosphino)ethane), generated from the reduction of  $\text{Ru}(\text{dmpe})_2\text{Cl}_2$ , was capable of giving intermolecular C-H oxidative addition of the aromatic solvent (Figure 1.1).<sup>3</sup>

**Figure 1.1.** Synthesis of organo ruthenium aryl complexes by Chatt and Davidson.

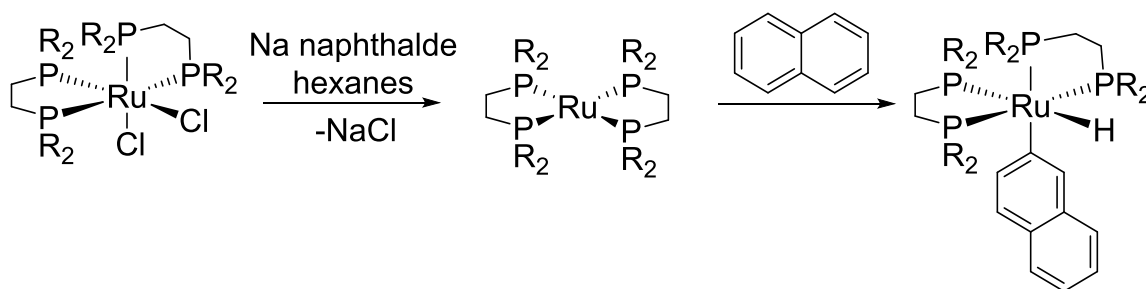
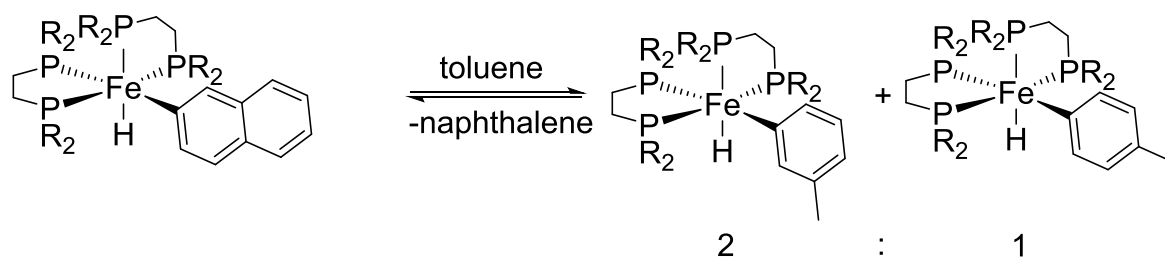
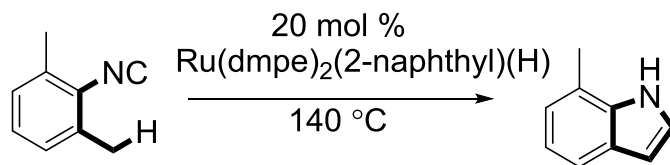


**Figure 1.2.** Synthesis of  $\text{Fe}(\text{dmpe})_2(\text{H})(\text{C}_6\text{H}_4\text{Me})$ .



Years later, Ittel and coworkers found that the related iron analogue of the Chatt compound could undergo reversible C-H reductive elimination/oxidative addition with a variety of monosubstituted arenes.<sup>4</sup> The most intriguing aspect of this reaction was that the product distribution of isomers of  $\text{Fe}(\text{dmpe})_2(\text{H})(\text{C}_6\text{H}_4\text{Me})$  showed a near statistical distribution of *meta* and *para*-tolyl regioisomers with no evidence of the *ortho* regioisomer, showing that the C-H activation event was governed by sterics rather than electronics (Figure 1.2). This was in stark contrast to the more well known main group metalation reactions which give products dependant on directing groups or the electrophilic aromatic substitution reactions that are governed by electronics.

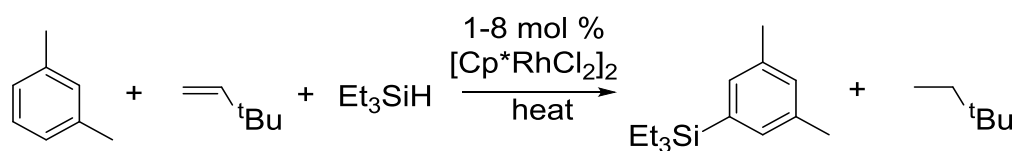
**Figure 1.3.** Catalytic intramolecular cyclization of 2,6-xylyl isocyanide.



The further functionalization of the metal-carbon bonds that result from C-H activation has proven to be far more difficult than C-H bond activation itself. In order for a transition metal to enact the functionalization of C-H bonds, the initial C-H activation step needs to be followed by a successive functionalization step. This involves the replacement of a carbon-hydrogen bond

with a carbon functional group bond. Jones and co-workers were able to demonstrate this by using the original  $\text{Ru}(\text{dmpe})_2(\text{H})(\text{naphtyl})$  to achieve catalytic intramolecular cyclizations of 2,6-xylyl isocyanide (Figure 1.3).<sup>5</sup>

**Figure 1.4.** Intermolecular C-H activation/ functionalization reactions with trialkylsilanes.



Despite the huge achievement that the intramolecular C-H activation/ functionalization demonstrated, a more desirable system would involve C-H activation of one molecule followed by coupling of an external functional group of a separate molecule. Berry and co-workers were able to provide an excellent example of an intermolecular C-H activation/ functionalization reaction coupling various aromatic substituents with trialkylsilanes using a rhodium catalyst (Figure 1.4).<sup>6</sup> Still, selective C-H bond activation and subsequent functionalization of unreactive hydrocarbons remains among the most significant challenges in homogeneous catalyst design.<sup>7</sup> The requirement that these transformations provide good chemo-, regio-, stereo-, and enantioselective products further increases the difficulty of these reactions.

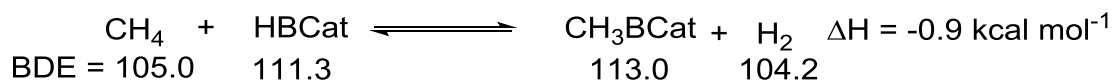
## Arylboronic Acids

The use of organoboron reagents in reactions with carbon electrophiles, such as organic halides, has seen tremendous attention with the development of transition metal catalyzed coupling reactions over the last few decades. Transition metal catalysts, especially those containing Pd<sup>8</sup> and Ni<sup>9</sup>, have been found to convert the otherwise relatively unreactive organoboron derivatives into highly versatile reagents for the formation of carbon-carbon bonds. It is reasonable to state that Zn, B, and Sn are currently the three most commonly used metals in Pd catalyzed cross-coupling.<sup>10</sup> Some of the advantages organoboron derivatives have over organozinc compounds in these cross coupling reactions are represented by their greater stability towards air and moisture and lower reactivity towards common organic electrophiles. A significant advantage of organoboron reagents relative to organostannanes is their reduced toxicity. However, there have been some reports of boronic acid genotoxicity.

The traditional method for the synthesis of organoboronic acids and esters is the reaction of alkoxyboranes with alkyllithiums or Grignard reagents. Although this method is common for the large-scale production of organoboranes, catalyzed reactions are of interest for obtaining organoboranes with different chemo and regioselectivities than that provided by the uncatalyzed synthesis. Palladium-catalyzed cross-coupling reactions with tetraalkoxydiboron<sup>11</sup> and dialkoxyboranes<sup>12</sup> provided a one-step procedure for deriving aromatic boronates from various organic electrophiles, such as aromatic halides and triflates. The discovery of these novel cross-coupling reactions provided access to a variety of boronic esters directly from arylhalides with increased functional group tolerance. Yet, the regioselectivity of the arylboronic esters produced

from the Pd-catalyzed cross-coupling reaction as well as the alkyllithium and Grignard reagents is dependent on the availability of the corresponding arylhalides. Since the mechanism for halogenation of aromatics is a form of electrophilic substitution, which is governed by electronics, many simple *meta* substituted reagents require overly elaborate and inefficient syntheses. A number of transition metal-mediated C-H activation reactions are known to produce products determined by the sterics of a substrate more so than its electronics<sup>22</sup>, raising the possibility that metal mediated C-H functionalization reactions could be able to give products with selectivities complementary to those of electrophilic aromatic substitution and directed ortho metallation reactions.

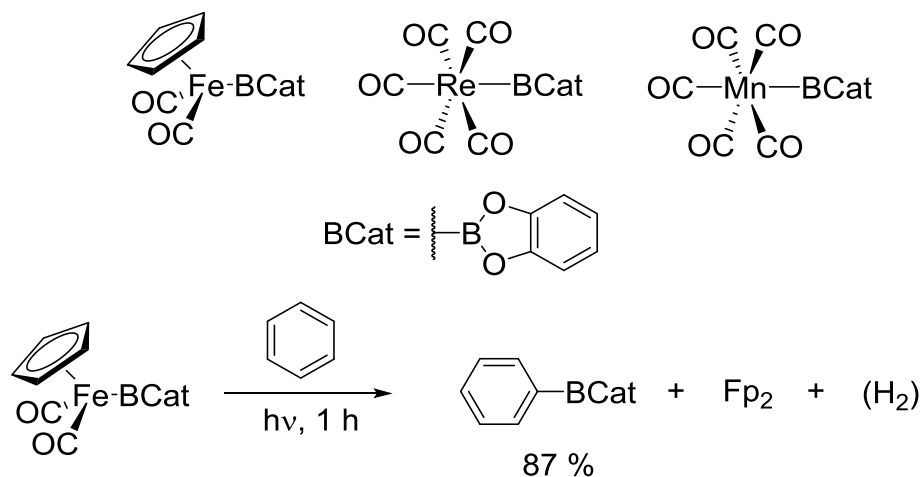
**Figure 1.5.** Thermodynamics of methane borylation.



Studies concerning the fundamental properties and reaction chemistry of transition metal boryl complexes were initiated in the early 1990s. Transition metal-ligand covalent bond energies are important in understanding the catalysis. However, there have been few data available for boranes and no thermochemical data for transition metal boryl complexes until 1994. In that year, the theoretical estimation of B-H and B-C bond enthalpies reported by Rablen and Hartwig<sup>13</sup> gave credence in organoborane synthesis *via* direct borylation of unsubstituted hydrocarbons. From the established thermochemical and computational data of borane reagents, the reaction in figure 1.5 is essentially thermoneutral. Moreover, from the calculated BDE's for B-H, C-H, and B-C bonds synthesis of aryl boronic esters directly from boranes and arenes should be thermodynamically feasible.



**Figure 1.6.** Stoichiometric C-H borylation of aromatic and aliphatic substrates.

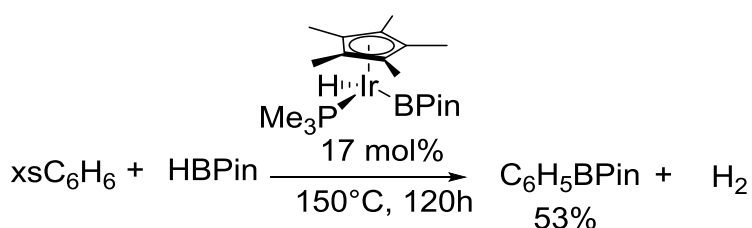


### Ir C-H Borylation Chemistry

Aromatic C-H activation/ borylation was first observed in 1993 by Marder and co-workers during the synthesis of  $\text{Ir}(\eta^6\text{-C}_6\text{H}_5\text{Me})(\text{BCat})_3$ , ( $\text{BCat}$  = catecholboryl), from  $(\eta^5\text{-C}_9\text{H}_7)\text{Ir}(\text{COD})$ , ( $\text{COD}$  = 1,5 cyclooctadiene).<sup>14</sup> Trace amounts of borylated products were detected in the filtrate by GCMS provided in the supplementary information section, resulting from the reaction of  $\text{Ir}(\eta^6\text{-C}_6\text{H}_5\text{Me})(\text{BCat})_3$  and toluene solvent. No mention of this appeared in the accompanying manuscript, no attempts were made to increase the efficiency of this reaction, and there was no evidence of catalysis. The first report of C-H activation/ borylation reactions with moderate to high yields appeared in the literature in 1995.<sup>15</sup> These reactions, shown in Figure 1.6, involved stoichiometric amounts of monocatecholboryltransition metal complexes which were capable of borylating both aromatic and aliphatic substrates when subjected to photolytic dissociation of carbonyl ligands. Regeneration of the boryl complex from the resulting

metal hydride products required several steps and external reagents, precluding these complexes from being catalytically viable.<sup>16</sup>

**Figure 1.7.** First catalytic aromatic C-H activation /borylation reaction.



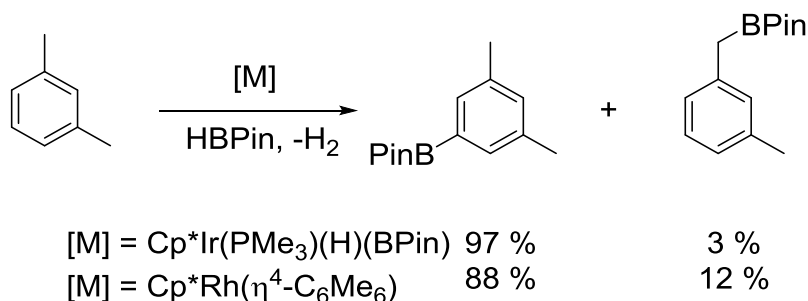
In 1999 the Smith research group demonstrated the first catalytic aromatic C-H activation /borylation reaction with a Cp\*Ir(PMe<sub>3</sub>)BPin(H) complex in the presence of HBPIn, (BPin = pinacolborane), under thermal conditions (Figure 1.7).<sup>17</sup> Ensuing studies lead to vastly more efficient catalysts.<sup>18,19</sup> Catalyst generated from readily made ( $\eta^5$ -C<sub>9</sub>H<sub>7</sub>)Ir(COD) and 1,2-bis(dimethylphosphino)ethane, dmpe, at 150 °C yielded 4500 TON.

Later in 1999, a photochemical Re-catalyzed C-H activation/ borylation reaction using Cp\*Re(CO)<sub>3</sub> and B<sub>2</sub>Pin<sub>2</sub> under CO (2 atm) was shown to be able to effectively borylate alkanes with great regioselectivity for primary carbons.<sup>20</sup> Later, Hartwig demonstrated that Cp\*Rh(I) complexes, generated by loss of hexamethylbenzene from Cp\*Rh( $\eta^4$ -C<sub>6</sub>Me<sub>6</sub>), are highly effective catalysts for both aliphatic and aromatic C-H borylation under thermal conditions.<sup>19</sup> Similar to the previous systems, alkanes reacted regiospecifically at the terminal carbon.

## Chemoselectivity of C-H Activation/Borylation Catalysts

Following reports of  $\text{Cp}^*\text{Rh}(\eta^4\text{-C}_6\text{Me}_6)$  showing viability as a catalyst for C-H activation/borylation, our group did a comparative study focusing on the functional group tolerance of the Ir- and Rh- precatalysts used.<sup>21</sup> Resulting from this study, was the realization that although the Rh derived catalysts display good reactivity, their chemo- and regioselectivity is inferior to that of the Ir based systems. Reactions between  $\text{Cp}^*\text{Rh}(\eta^4\text{-C}_6\text{Me}_6)$  and fluorinated aromatics lead to substantial defluorinated/borylated by products demonstrating the Rh catalysts inability to tolerate aromatic-halogen bonds, an exceptionally important class of compounds. The Rh catalyst also showed to be far less selective for discerning between aromatic and benzylic C-H activation and sizeable amounts of benzylic borylated products were present in the reaction mixtures with *m*-xylene as substrate (Figure 1.8).

**Figure 1.8.** Chemo- and regioselective comparisons for iridium and rhodium catalysts.



## Regioselectivity of Ir C-H Activation/Borylation Catalysis

The regioselectivity of these reactions for arenes are dominated by sterics such that the least hindered positions undergo C-H activation. Thus, for monosubstituted arenes statistical

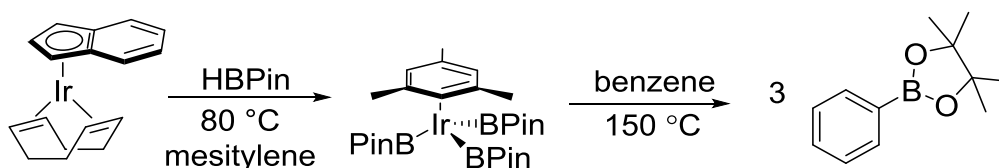
borylation of the meta- and para-positions is generally observed. More importantly, only the 5-position is borylated selectively in 1,3-disubstituted arenes, even for those with ortho-, para-directing groups.<sup>22</sup> These aspects of transition metal C-H activation/ borylation show the great utility of this method for producing arylboronic esters which would otherwise be very difficult to synthesize. The electronics still have a considerable effect on the rates of the reaction, with electron poor arenes reacting much faster than electron rich substrates. The Iridium catalyzed C-H borylation of arenes also shows remarkable chemoselectivity and tolerates a number of functional groups including but not limited to halogens, esters, amides, ethers and benzylic hydrogens.<sup>23</sup>

## Mechanism

The phosphine free  $(\eta^6\text{-C}_6\text{H}_3\text{Me}_3)\text{Ir}(\text{BPin})_3$ , formed in moderate yields from  $(\eta^5\text{-C}_9\text{H}_7)\text{Ir}(\text{COD})$  and excess HBPIn, was found to react with benzene under elevated temperature to yield 3 equivalents of PhBPIn (Figure 1.9) but catalysis with excess HBPIn failed.<sup>18</sup> However, it was shown that addition of a donor ligand such as  $\text{PMe}_3$  to  $(\eta^6\text{-C}_6\text{H}_3\text{Me}_3)\text{Ir}(\text{BPin})_3$  was found to generate an active catalyst for the borylation of arenes. Both  $\text{Ir}(\text{BPin})(\text{PMe}_3)_4$  and  $\text{fac-Ir}(\text{BPin})_3(\text{PMe}_3)_3$  complexes were found to react with benzene to produce PhBPIn at room temperature signifying that both Ir(I) and Ir(III) complexes were capable of C-H activation/borylation. However, the reactivity of these two compounds with iodobenzene were

found to be substantially different. Ir(BPin)(PMe<sub>3</sub>)<sub>4</sub> reacted rapidly with iodobenzene, but no isomers of C<sub>6</sub>H<sub>4</sub>I(BPin) were detected in the product mixture. Conversely, fac-Ir(BPin)<sub>3</sub>(PMe<sub>3</sub>)<sub>3</sub> in iodobenzene gave a mixture of *meta* and *para* isomers of C<sub>6</sub>H<sub>4</sub>I(BPin) as well as a substantial amount of PhBPin.

**Figure 1.9.** Borylation of benzene with (η<sup>6</sup>-C<sub>6</sub>H<sub>3</sub>Me<sub>3</sub>)Ir(BPin)<sub>3</sub>.

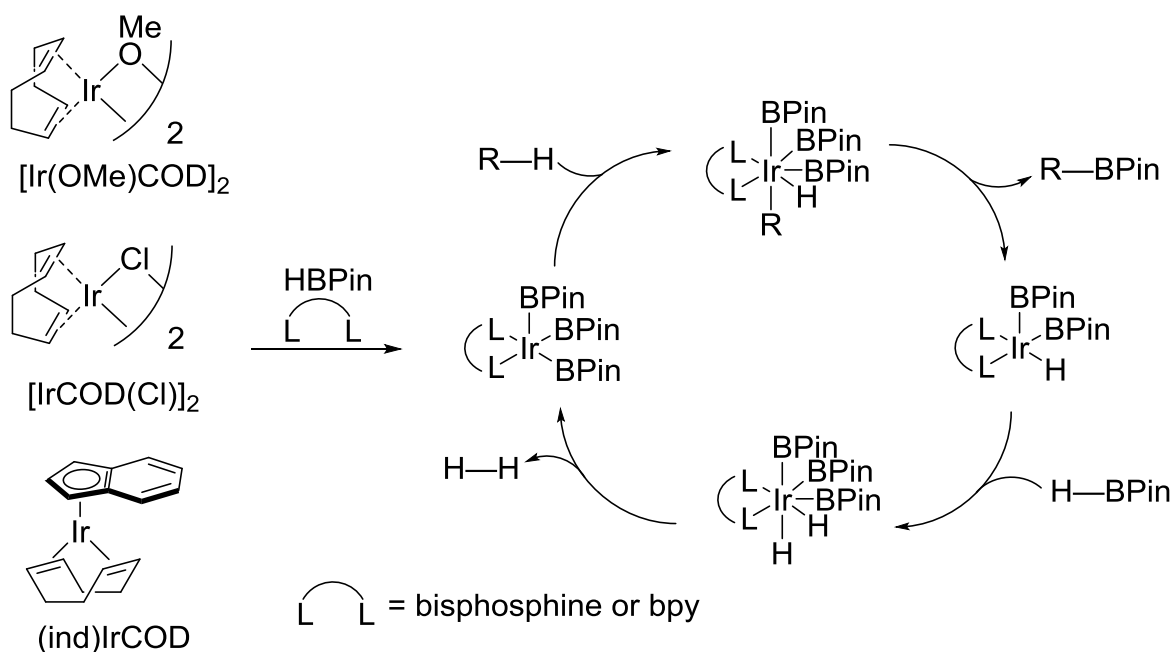


These results favored an Ir(III)/ Ir(IV) catalytic cycle over an Ir(I)/ Ir(II). Isolation of the immediate catalyst precursor (dtbpy)Ir(BPin)<sub>3</sub>(COE)<sup>22b</sup>, (dtbpy = 4,4'-di-*t*-butyl-2,2'-bipyridine), complex and the active 16-electron (dippe)Ir(BPin)<sub>3</sub> and (dcpe)Ir(BPin)<sub>3</sub><sup>24</sup> complexes and subsequent mechanistic studies<sup>25</sup> as well as computational analysis<sup>26</sup> all provide further support for the involvement of an Ir(III)-trisboryl complex as an active component in the catalytic cycle. (dippe is (1,2-bis(diisopropylphosphino)ethane) and dcpe is (1,2-bis(dicyclohexylphosphino)ethane)).

The proposed catalytic cycle operates by oxidative addition of B<sub>2</sub>Pin<sub>2</sub> or HBPin to an Ir(I) species in the presence of a donor ligand, typically bidentate, to generate the active trisboryl Ir(III) catalyst (Figure 1.10). Ir(I) compounds have been found to be proficient precatalysts include (η<sup>5</sup>-C<sub>9</sub>H<sub>7</sub>)Ir(COD), [Ir(COD)Cl]<sub>2</sub> and [Ir(OMe)COD]<sub>2</sub> and bidentate ligands such as

dmpe, dtbpy, or dppe (1,2-bis(diphenylphosphino)ethane) have been employed. The most commonly used system is  $[\text{Ir}(\text{OMe})\text{COD}]_2$  with dtbpy, where the active catalyst is generated in-situ. Oxidative addition of the aromatic substrate to the trisboryl Ir(III) intermediate gives an Ir(V) species. Reductive elimination of the ArBPin product and subsequent oxidative addition by  $\text{B}_2\text{Pin}_2$  or HBPin to the resulting bisboryl Ir(III) complex gives an  $18e^-$  Ir(V) intermediate. Reductive elimination of HBPin or  $\text{H}_2$  regenerates the active trisboryl iridium(III) catalyst.

**Figure 1.10.** Proposed catalytic cycle.

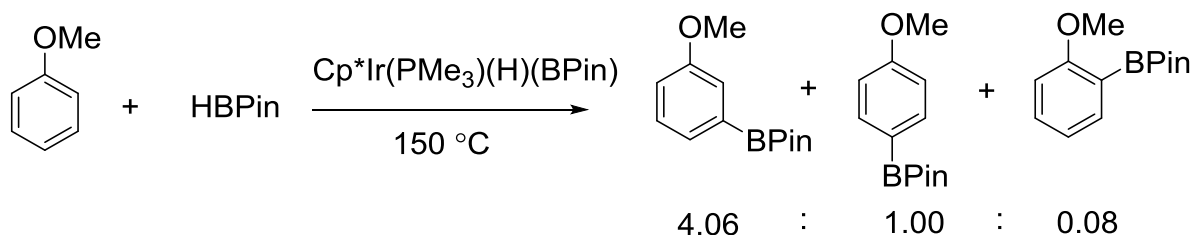


### Deviations From Sterically Directed Regioselectivity via Electronic Bias

As stated early, the regioselectivity of the trisboryl Ir(III) catalysts is largely governed by the sterics of the substrate. In the absence of significant steric bias, subtle electronic effects can

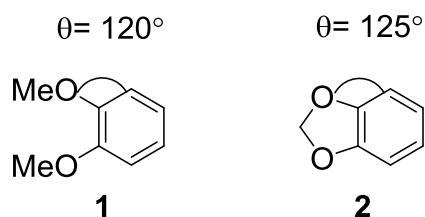
be observed which influence the selectivity as is the case in the reaction below for the borylation of anisole (Figure 1.11).<sup>17</sup> In the absence of electronic effects, one would expect a statistical distribution of products giving a product mixture of 2:1 *meta* to *para* selectivity. The nearly 4:1 selectivity favoring the *meta* position most likely arises from electronic effects originating from the –OMe substituent. These deviations are most likely the result of electronic effects of the aromatic system; either resonance or inductive or both.

**Figure 1.11.** Electronic effects in product distribution.



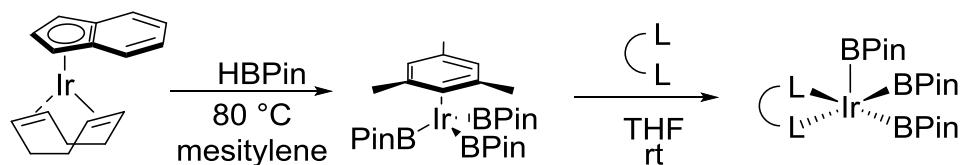
In looking for systems in which to investigate the underlying electronic directing effects of the substrates, ideally one would want a set of substrates with similar electronics, but with reduced steric hinderance. The substrates veratrole (**1**) and benzodioxole (**2**) were chosen for these reasons. By replacing the 1,2-dimethoxy moiety in **1** with a methylene linker in **2**, the steric restraint is greatly reduced *ortho* to the alkoxy functionalizations with minimally perturbing the electronics of the molecule (Figure 1.12).

**Figure 1.12.** Steric hinderance of veratrole (**1**) and benzodioxole (**2**).



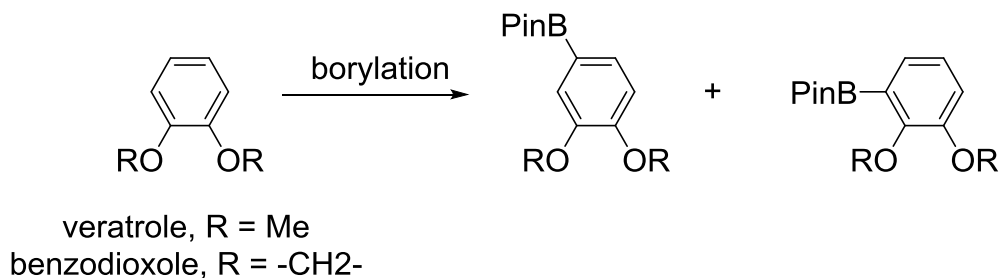
Using an  $(\eta^6\text{-C}_6\text{Me}_3\text{H}_3)\text{Ir}(\text{BPin})_3$  as starting material, five-coordinate bisphosphine complexes can be synthesized by displacement of the  $\eta^6\text{-C}_6\text{Me}_3\text{H}_3$  by the incoming bisphosphine (Figure 1.13). The resulting six-coordinate complex readily loses the  $\eta^2\text{-C}_6\text{Me}_3\text{H}_3$  bond arene yielding the five-coordinate complex.<sup>24</sup>

**Figure 1.13.** 5-coordinate Iridium Catalyst.



Investigating stoichiometric and catalytic reactions of the 5-coordinate complex  $(\text{dippe})\text{Ir}(\text{BPin})_3$ <sup>24</sup> with **1** and **2** it was found that by making the C-H bond *ortho* to oxygen far more accessible in **2**, the regioselectivity of the product distribution was drastically altered going from near exclusive borylation at the 4-position in **1** to near exculsive borylation at the 3-position in **2** (Table 1.1). Stoichiometric and catalytic reactions employing the dipyriddy pre-catalyst  $(\text{dtbpy})\text{Ir}(\text{BPin})_3(\text{COE})$  were also examined with similar results.<sup>27</sup>



**Table 1.1.** Regioselectivity for C-H borylations with veratrole (**1**) and benzodioxole (**2**).

Ir complex	substrate <sup>a</sup>	time	Temp (°C)	meta (%)	ortho (%)
(dippe)Ir(BPin) <sub>3</sub>	<b>1</b>	4 h	100	>99	<1
2 mol % (dippe)Ir(BPin) <sub>3</sub> <sup>b,c</sup>	<b>1</b>	4 h	130	90	2
(dtbpy)Ir(BPin) <sub>3</sub> (COE)	<b>1</b>	1 h	r.t.	99	1
2 mol % (dtbpy)Ir(BPin) <sub>3</sub> (COE)	<b>1</b>	9 h	r.t.	98	2
(dippe)Ir(BPin) <sub>3</sub>	<b>2</b>	1 h	100	2	98
2 mol % (dippe)Ir(BPin) <sub>3</sub>	<b>2</b>	1 h	130	4	96
(dtbpy)Ir(BPin) <sub>3</sub> (COE)	<b>2</b>	15 min	r.t.	5	95
2 mol % (dtbpy)Ir(BPin) <sub>3</sub> (COE) <sup>d</sup>	<b>2</b>	1 h	r.t.	3	91

<sup>a</sup>8 equiv of **1** or **2** were used to minimize diborylation. <sup>b</sup>Generated from 2 mol% (η<sup>5</sup>-C<sub>9</sub>H<sub>7</sub>)Ir(COD) and 2 mol% dippe. <sup>c</sup>8% of the product is 3,5-diborylated. <sup>d</sup>6% of the product is 3,6-diborylated.

Figure 1.14 shows a transition state representing a proton transfer from an aryl substrate to the Ir-Boryl σ-bond (left) and a transition state representing a hydride transfer to an “empty” boron p-orbital of the boryl ligand (right). The actual transition state can be thought to fall between these two extremes. Calculations found a strong correlation between the activation barriers ( $\Delta E^\ddagger$ ) for a number of 5-coordinate Ir complexes and an electronically diverse set of

substrates and the energy difference between the reactants and products ( $\Delta E$ ).<sup>27</sup> This correlation suggested  $\Delta E$  is an excellent predictor of ( $\Delta E^\ddagger$ ) and the transition states responsible for oxidative addition from the 5-coordinate Ir complexes and aryl substrates would mirror **TS1** from figure 1.14. Figure 1.15 shows the correlation of energy difference between reactants and products ( $\Delta E$ ) with the charge developed on the aryl group with linear fits for 6- and 5-membered substrates. Sterically hindered arenes (red) were omitted from the analysis.<sup>27</sup>

**Figure 1.14.** Limiting descriptions of the C-H activation transition states.

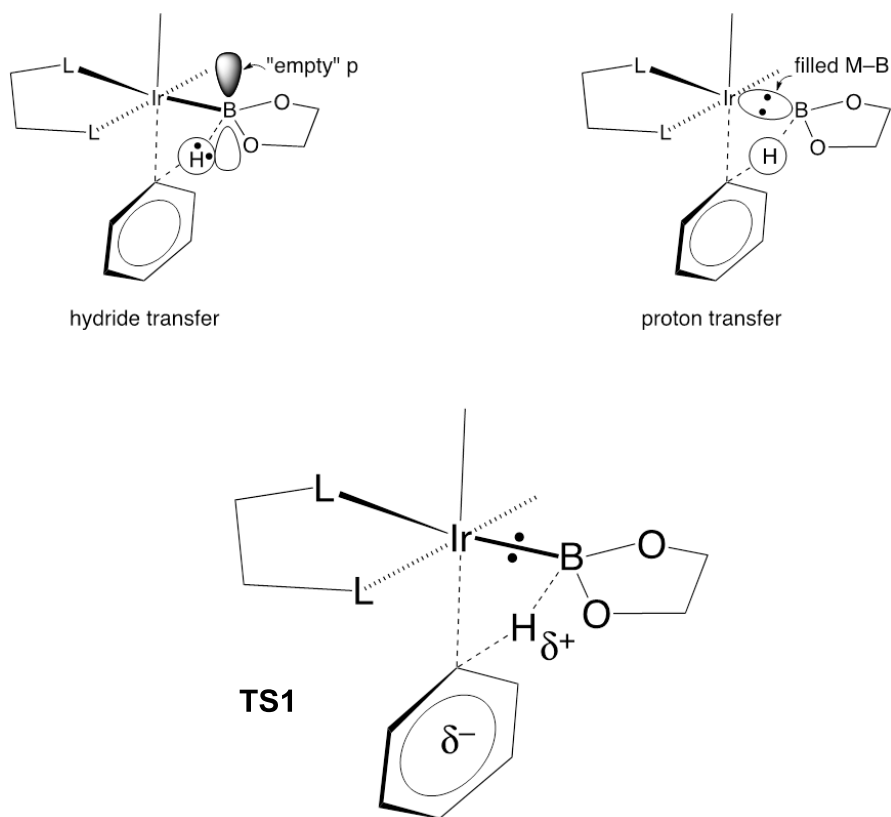
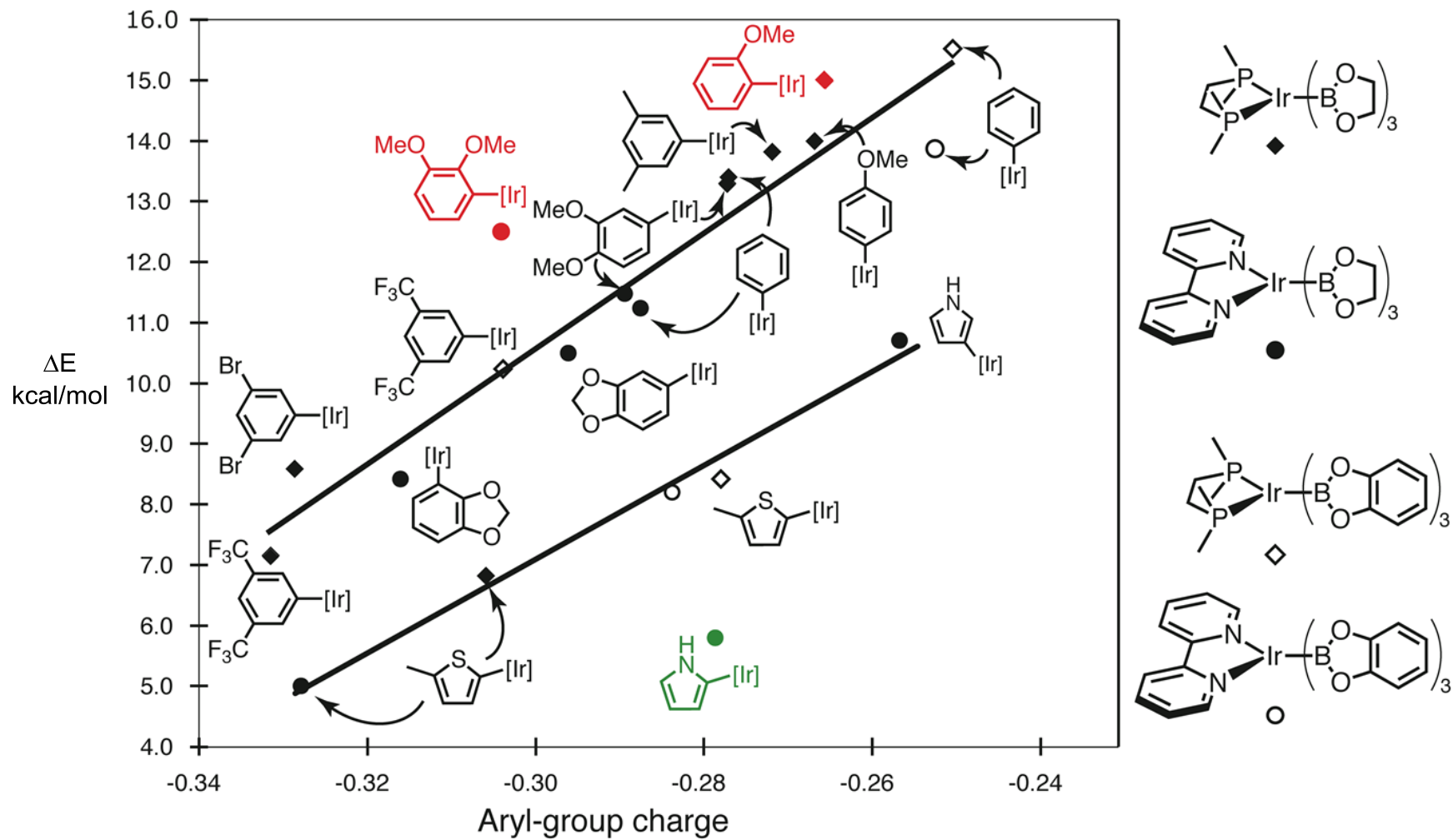
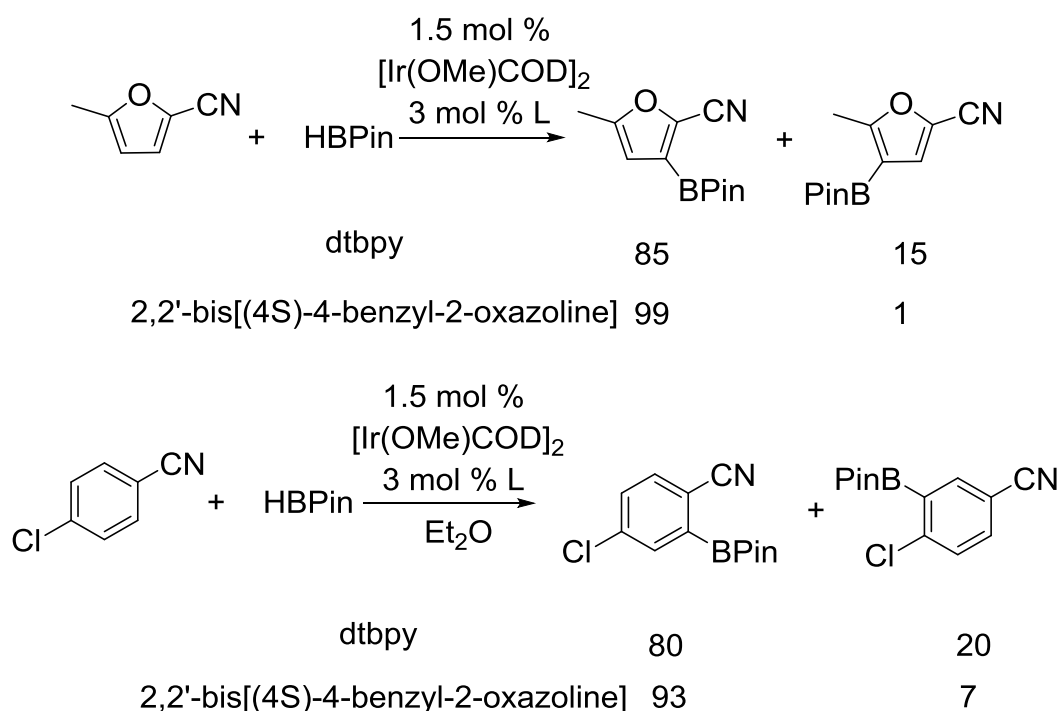


**Figure 1.15.** Correlation of  $\Delta E$  with the charge developed on the aryl group (TS 1 in Figure 1.14). For interpretation of references color in this and all other figures, the reader is referred to the electronic version of this dissertation.



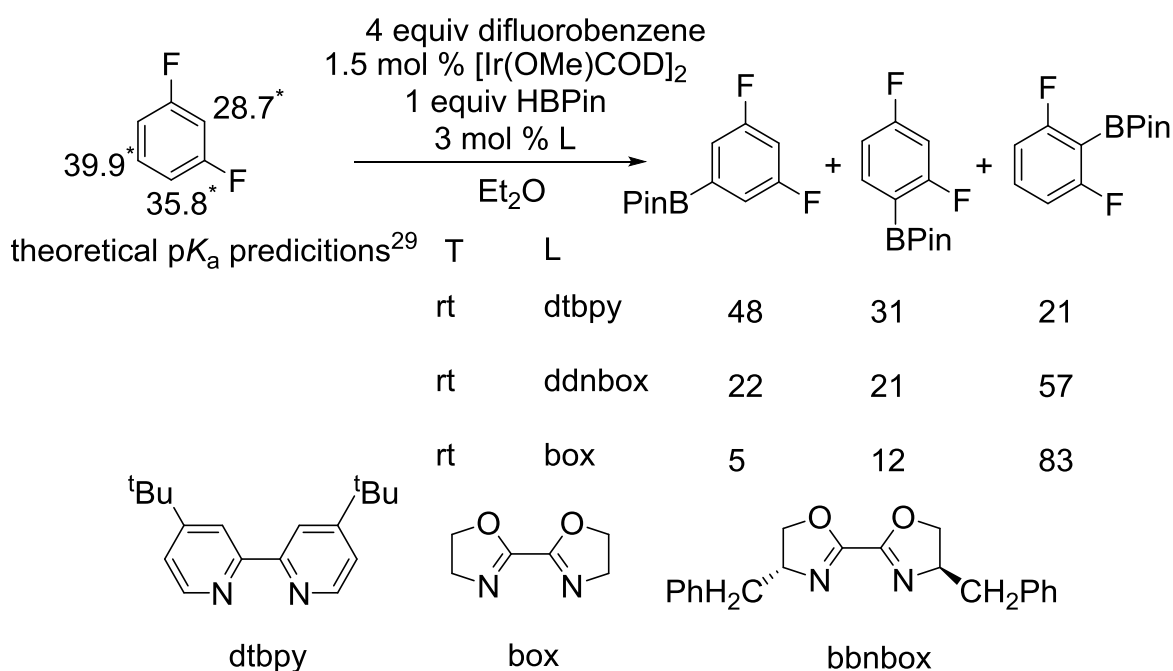
2,2'-bisoxazoline ligands as well as their 4,4'-disubstituted derivatives have been shown to both enhance steric bias in some substrates and conversely favor borylation at the most hindered positions in others.<sup>28</sup> Reactions using the commonly used  $[\text{Ir}(\text{OMe})\text{COD}]_2/\text{dtbpy}$  catalyst system performed on asymmetric 2,5-disubstituted heterocycles and 1,4-disubstituted aromatics containing different substituents of similar steric size led to moderate to poor regioselectivity. Running the reactions under the same conditions with 2,2'-bis[(4*S*)-4-benzyl-2-oxazoline] (bbnbox) as ligand lead to greatly enhanced regioselectivity implying the bbnbox ligand was far more sensitive to steric repulsion (Figure 1.16).

**Figure 1.16.** Ligand design for enhanced regioselectivity.



The sterically small fluorine functionality had also been shown to give a substantial electronic directing effect and it was possible to modify the ligands to obtain a 2-borylated product as the major isomer with a 1,3-difluorobenzene substrate (Figure 1.15). It is very interesting to note that in the previous case the same bbnbox ligand which showed greater regioselectivity now demonstrated regioselective borylation at the most sterically crowded position.

**Figure 1.17.** Regioselective borylations with 1,3-difluorobenzene.



The reversal of regioselectivity based on steric bias vs. electronic bias warrants further investigation and highlights the importance of isolating the bisoxazoline Ir catalysts responsible for C-H activation/borylation to determine what role the bisoxazoline ligands play in altering these regioselectivities.

## REFERENCES

## REFERENCES

- 1) Jones, W. D. *Inorg. Chem.* **2005**, *44*, 4475.
- 2) Kleiman, P. J.; Dubeck, M. *J. Am. Chem. Soc.*, **1963**, *85*, 1544.
- 3) Chatt, J.; Davidson, J. M. *J. Chem. Soc.*, **1965**, 843.
- 4) Tolman, C. A.; Ittel, S. D.; English, A. D.; Jesson, J. P. *J. Am. Chem. Soc.* **1979**, *101*, 1742.
- 5) Jones, W. D.; Kosar, W. P. *J. Am. Chem. Soc.* **1986**, *108*, 5640.
- 6) Ezbiansky, K.; Djurovich, P. I.; LaForest, M.; Sinning, D. J.; Zayes, R.; Berry, D. H. *Organometallics* **1998**, *17*, 1455.
- 7) Crabtree, R. H. *J. Chem. Soc., Dalton, Trans.*, **2001**, 2437.
- 8) Ishiyama, T.; Miyaoura, N. *Pure Appl. Chem.* **2006**, *78*, 1369.
- 9) Zhou, J.; Ru, G. C. *J. Am. Chem. Soc.* **2004**, *126*, 1340.
- 10) Singer, R. D.; Knochel, P. *Chem. Rev.* **1993**, *93*, 2117.
- 11) Ishiyama, T.; Murata, M.; Miyaoura, N. *J. Org. Chem.* **1995**, *60*, 7508.
- 12) Murata, M.; Oyama, T.; Watanabe, S.; Masuda, Y. *J. Org. Chem.* **2000**, *65*, 164.
- 13) Rablen, P. R.; Hartwig, J. F. *J. Am. Chem. Soc.* **1994**, *116*, 4121.
- 14) Henk, P. N.; Blom, H. P.; Westcott, S. A.; Taylor, N. T.; Marder, T. B. *J. Am. Chem. Soc.* **1993**, *115*, 9329.
- 15) Waltz, K. M.; He, X.; Muhoro, C.; Hartwig, J. F. *J. Am. Chem. Soc.* **1995**, *117*, 11357.
- 16) Waltz, K. M.; Hartwig, J. F. *Science* **1997**, *277*, 211.
- 17) Iverson, C. N.; Smith, M. R., III. *J. Am. Chem. Soc.* **1999**, *121*, 7696.

- 18) Cho, J. Y.; Tse, M. K.; Holmes, D.; Maleczka, R. E.; Smith, M. R., III. *Science* **2002**, *295*, 305.
- 19) Chen, H. Schlecht, S. Semple, T. C., Hartwig, J. F. *Science* **2000**, *287*, 1995.
- 20) Chen, H. Hartwig, J. F. *Angew. Chem. Int. Ed.* **1999**, *38*, 3391.
- 21) Cho, J.-Y.; Iverson, C. N.; Smith, M. R., III *J. Am. Chem. Soc.* **2000**, *122*, 12868.
- 22) (a) Shi, F.; Holmes, D.; Maleczka, R. E., Jr.; Smith, M. R., III. *J. Am. Chem. Soc.* **2003**, *125*, 7792. (b) Ishiyama, T.; Takagi, J.; Ishida, K.; Miyaura, N.; Anastasi, N. R.; Hartwig, J. F. *J. Am. Chem. Soc.* **2002**, *124*, 390.
- 23) Mkhaldid, I. A.; Barnard, J. H.; Marder, T. B.; Murph, J. M.; Hartwig, J. F. *Chem. Rev.* **2010**, *110*, 890.
- 24) Chotana, G. C.; Vanchura, B. A., II; Tse, M. K.; Staples, R. J.; Maleczka, R. E., Jr; Smith, M. R., III *Chem. Commun.*, **2009**, 5731.
- 25) Boller, T. M.; Murphy, J. M.; Hapke, M.; Ishiyama, T.; Miyaura, N.; Hartwig, J. F. *J. Am. Chem. Soc.* **2005**, *127*, 14263.
- 26) Tamura, H.; Yamazaki, H.; Sato, H.; Sakaki, S. *J. Am. Chem. Soc.* **2003**, *125*, 16114.
- 27) Vanchura, B. A., II; Preshlock, S. M.; Roosen, P. C.; Kallepalli, V. A.; Staples, R. J.; Maleczka, R. E., Jr; Smith, M. R., III *Chem. Commun.* **2010**, *46*, 7724.
- 28) Chotana, G. A. *Ph. D. Thesis, Mich. State University*, **2008**.
- 29) Shen, K.; Fu, Y.; Li, J.-N.; Liu, L.; Guo, Q.-X. *Tetrahedron*, **2007**, *63*, 1568.



## CHAPTER 2

### OPTIMIZATION OF IRIIDIUM CATALYZED C-H BORYLATIONS

#### Introduction

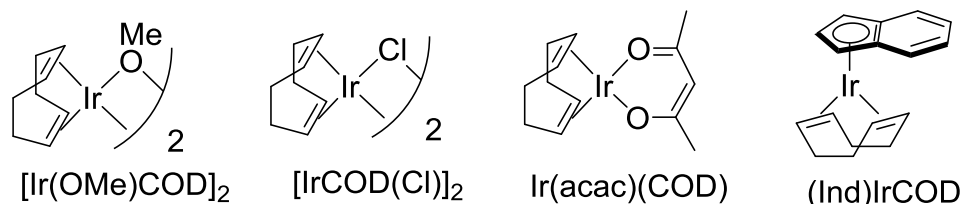
Since the initial inception of Iridium catalyzed C-H borylation, the reaction has been utilized to provide a simple, atom economical route to arylboronate esters from an ever expanding list of aromatic, heteroaromatic and polyaromatic substrates.<sup>1</sup> Throughout the course of its development, many combinations of precatalyst, boron reagent, ligand, and solvent have been used in the literature.<sup>2</sup> Many of these conditions are variants of conditions identified in an early communication by Ishiyama, Takagi, Hartwig, and Miyaura, utilizing [Ir(OMe)COD]<sub>2</sub> as the Ir precatalyst, dtbpy as the ligand, B<sub>2</sub>Pin<sub>2</sub> as the borylating agent, and hexane as the solvent.<sup>3</sup> Since these initial reports, the substrate scope for C–H borylation has expanded considerably and the original set of reaction conditions tended to be optimal for comparatively reactive substrates (e.g. electron deficient arenes). Until recently, there had not been a comprehensive study to look at the roles that solvent, metal precatalyst, boron reagent, reaction time and temperature, orders of addition for catalyst generation, etc. might have on borylations as a function of substrate properties. It is likely that conditions identified as optimal for one substrate class (e.g. electron deficient arenes) maybe far from ideal for other aromatic substrates with high nitrogen content or more electron rich aromatic systems. Moreover, the future success for some substrates may hinge upon factors that have been overlooked. For these reasons, we under took a comprehensive study of the many factors affecting the Ir catalyzed C–H borylation.

## Identification of Reaction Variables.

In an effort to develop optimized conditions that could be applicable for C-H borylation on a wide array of substrates, we focused on the portion of the reaction which is substrate independent, catalyst generation. Varying the precatalyst, ligand, borylating reagent and the order which they are mixed can all have an effect on active catalyst generation. This chemistry has seen a variety of Ir(I) precatalysts and ligands used to access these  $(L_2)Ir(III)BPin_3$  active catalysts. Trends in the effectiveness of various Ir(I)-cyclooctadiene catalyst precursors in a series of  $[Ir(X)(COD)]_2$  complexes has been shown to mirror the basicity of X (i.e.  $OMe > OH > OPh > OAc > Cl > BF_4$ ) for room temperature reactions with electron deficient substrates.<sup>3,4</sup>

The ability of  $[Ir(OMe)(COD)]_2$  and  $[Ir(Cl)(COD)]_2$  catalyst precursors to generate the  $(dtbpy)Ir(COE)BPin_3$  intermediate has also been shown to be greatly affected by the order of addition of the reagents HBPIn or  $B_2Pin_2$  and dtbpy in non-polar solvents at temperatures up to 50 °C.<sup>5</sup> In order to truly determine the most desirable precatalyst for maximum active catalyst generation, we selected a small sample of readily available Ir(I) precatalysts. The four precatalysts used in the screens were the commercially available compounds  $[Ir(OMe)(COD)]_2$ ,  $[Ir(Cl)(COD)]_2$ ,  $Ir(acac)(COD)$ , and  $(Ind)Ir(COD)$  (Figure 2.1).

**Figure 2.1.** Precatalyst Selected for Reaction Screens.

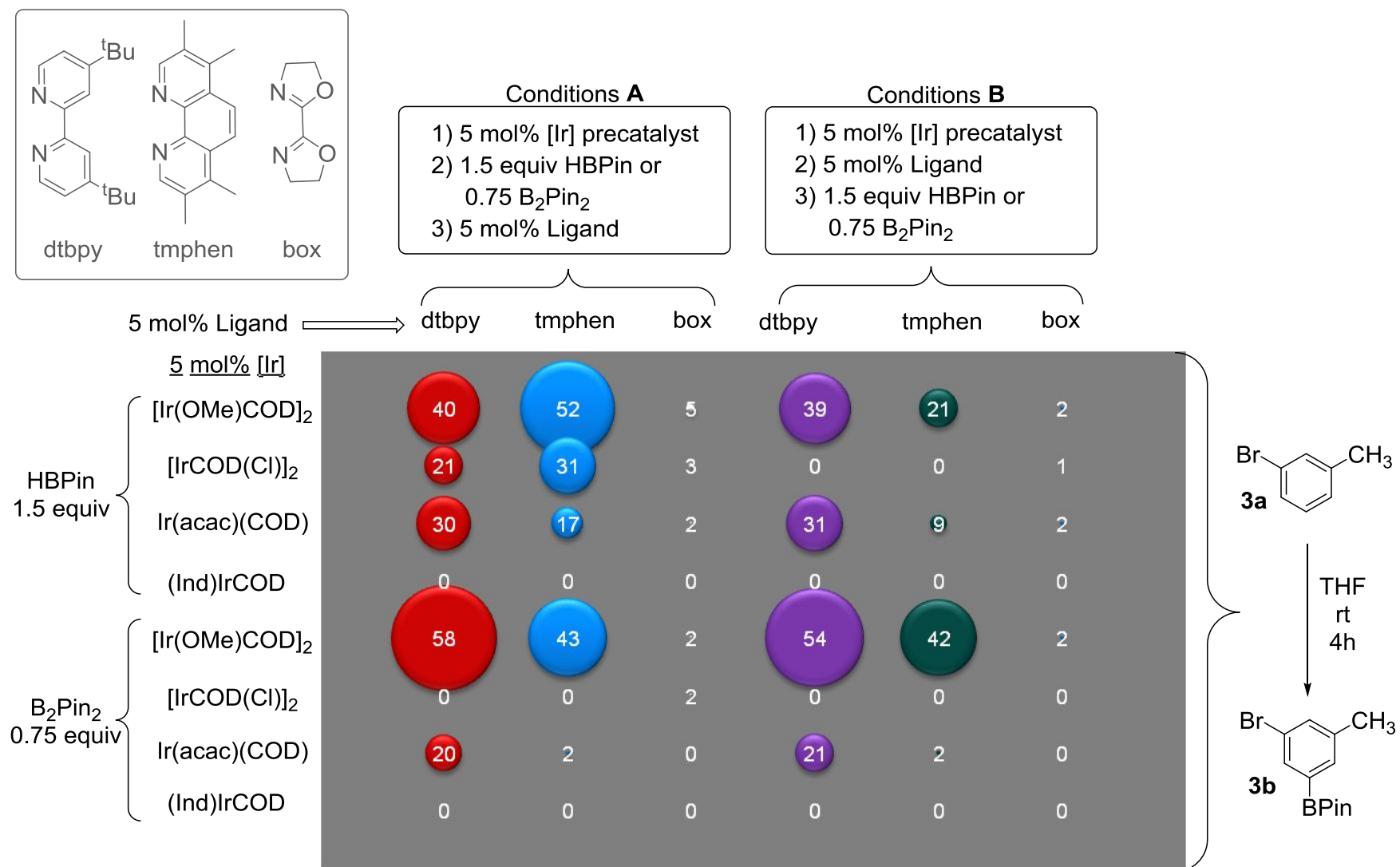


To expedite the process of running the number of reactions required in an encompassing systematic study, reactions were conducted in micro scale 96-well-plate reactors. The ease at which high-throughput experimentation (HTE) allows researchers to set-up large numbers of reactions meant reactions could be run in duplicate and entire reaction screens could be repeated with little effort to certify reproducibility. Reactions conducted in 96-well-plate reactors were set up under two sets of standardized conditions referred to as Conditions **A** or Conditions **B** in the text. Stock solutions were used to dispense material accurately for each well. To facilitate comparisons, the relative effectiveness of reaction conditions was determined by analyzing for the amount of borylated products formed in reactions stopped well before completion.

Microscale Reactions Utilizing **Conditions A**. In a nitrogen filled glovebox, 50  $\mu\text{L}$  of solution containing 0.5  $\mu\text{mol}$  Iridium precatalyst dimer (0.01 M stock solution) or 1.0  $\mu\text{mol}$  Iridium monomer (0.02 M stock solution) in the designated solvent was added to a 1 mL reaction vial containing a magnetic stir bar. To this solution, 50  $\mu\text{L}$  of stock solution containing 30  $\mu\text{mol}$  HBPin (0.6 M) or 15  $\mu\text{mol}$   $\text{B}_2\text{Pin}_2$  (0.3 M) was added to the 1 mL reaction vial. 50  $\mu\text{L}$  of solution containing 1.0  $\mu\text{mol}$  ligand (0.02 M) was added via micro pipette followed by 50  $\mu\text{L}$  of stock solution containing 20  $\mu\text{mol}$  arylsubstrate (0.4 M) and 2  $\mu\text{mol}$  dodecahydrotriphenylene internal standard. The reaction vessel was then sealed and stirred at the desired temperature for an allotted amount of time, at which point the reaction was cooled to room temperature and quenched by exposure to atmospheric  $\text{O}_2$ .

Microscale Reactions Utilizing **Conditions B**. In a nitrogen filled glovebox, 50  $\mu\text{L}$  of solution containing 0.5  $\mu\text{mol}$  Iridium precatalyst dimer (0.01 M stock solution) or 1.0  $\mu\text{mol}$  Iridium monomer (0.02 M stock solution) in the designated solvent was added to a 1 mL reaction

**Figure 2.2.** Room Temperature Reaction Screen With 3-bromotoluene.



Numbers and bubble area size are assay yields of **3b**.

vial containing a magnetic stir bar. To this solution, 50  $\mu\text{L}$  of stock solution containing 1.0  $\mu\text{mol}$  ligand (0.02 M) was added to the 1 mL reaction vial. 50  $\mu\text{L}$  of solution containing 30  $\mu\text{mol}$  HBPin (0.6 M) or 15  $\mu\text{mol}$   $\text{B}_2\text{Pin}_2$  (0.3 M) was added via micro pipette followed by 50  $\mu\text{L}$  of stock solution containing 20  $\mu\text{mol}$  arylsubstrate (0.4 M) and 2  $\mu\text{mol}$  dodecahydrotriphenylene internal standard. The reaction vessel was then sealed and stirred at the desired temperature for an allotted amount of time, at which point the reaction was cooled to room temperature and quenched by exposure to atmospheric  $\text{O}_2$ .

### Orders of Addition Effects for Room Temperature Reactions

Our initial screen utilized the substrate 3-bromotoluene (**3a**) because of its intermediate reactivity at room temperature. The reactions were stopped prior to completion to facilitate comparisons and the reaction time of 4 h was chosen because reactions utilizing the standard literature conditions are at approximately 50% completion at this time. The effects of the order at which HBPin and dtbpy were added to the reaction solution containing one of four precatalysts ( $[\text{Ir}(\text{OMe})(\text{COD})]_2$ ,  $[\text{Ir}(\text{Cl})(\text{COD})]_2$ ,  $\text{Ir}(\text{acac})(\text{COD})$ , or  $(\text{Ind})\text{Ir}(\text{COD})$ ) was screened with the previously mentioned conditions. The differences between reaction conditions **A** and **B**, when HBPin and dtbpy were added to reaction solutions containing  $[\text{Ir}(\text{OMe})(\text{COD})]_2$  proved to be irrelevant (see Figure 2.2). Again with  $[\text{Ir}(\text{OMe})(\text{COD})]_2$  as precatalyst, the same observations were made when  $\text{B}_2\text{Pin}_2$  was used as the borylating reagent under both conditions **A** and **B**. When precatalyst  $[\text{Ir}(\text{Cl})(\text{COD})]_2$ , the immediate synthetic precursor to  $[\text{Ir}(\text{OMe})(\text{COD})]_2$ , was used a marked drop in reactivity was observed relative to reactions with  $[\text{Ir}(\text{OMe})(\text{COD})]_2$ . The

addition of HBPin prior to ligand under these conditions was vital. When dtbpy was added to the reaction mixture before HBPin, or if B<sub>2</sub>Pin<sub>2</sub> was used as borylating reagent, no borylation was observed. Reactions run with Ir(acac)(COD) followed the same trends as [Ir(OMe)(COD)]<sub>2</sub>, all be it with slightly lower conversions. This drop in reactivity was most likely due to a slower rate at which Ir(acac)(COD) generates active catalyst relative to [Ir(OMe)(COD)]<sub>2</sub>, or a lower yield in the formation of active catalyst from catalyst precursor. The coordinately saturated precatalyst (Ind)Ir(COD) was found to be inert under the standard reaction conditions at room temperature.

Order of addition became far more important when the more electron rich 3,4,7,8-tetramethyl-1,10-phenanthroline (tmphen) was used in reactions with HBPin. The combination of [Ir(OMe)(COD)]<sub>2</sub> with tmphen and HBPin produced 2.5 times as much product when conditions **A** were used compared to the identical reaction were order of addition conditions **B** were used. A similar 2.0 fold increase in the amount of product formed was observed with Ir(acac)(COD) using tmphen and HBPin utilizing conditions **A** compared with conditions **B**. No reaction occurred when conditions **B** were used with [Ir(Cl)(COD)]<sub>2</sub> and tmphen with HBPin, mirroring results seen with dtbpy and this precatalyst. Utilizing [Ir(Cl)(COD)]<sub>2</sub>, tmphen and HBPin with order of addition conditions **A** gave fairly good reactivity.

The reactivity of these precatalysts with added ligand provides insight into the effects of order of addition on conversion. <sup>1</sup>H NMR experiments show no complex formation in 1:1 mixtures of either [Ir(OMe)(COD)]<sub>2</sub> and dtbpy or Ir(acac)(COD) and dtbpy in THF<sub>d8</sub> (Figure 2.3). The lack of complexation correlated directly with the absence of any effect on order of

addition. 1:1 mixtures of  $[\text{Ir}(\text{Cl})(\text{COD})]_2$  and dtbpy did, however, form a complex in solution.<sup>6</sup>

This complex can be attributed to the lack of reactivity in reactions when  $[\text{Ir}(\text{Cl})(\text{COD})]_2$  is used as precatalyst. Similar NMR experiments with tmphen led to the formation of insoluble precipitates with precatalysts  $[\text{Ir}(\text{OMe})(\text{COD})]_2$ ,  $[\text{Ir}(\text{Cl})(\text{COD})]_2$  and  $\text{Ir}(\text{acac})(\text{COD})$  in  $\text{THF}_{d8}$ .<sup>7</sup>

In every instance, formation of ligated complexes prior to addition of HBPin corresponds to lower reactivity compared with reactions where the order of addition was reversed. Likewise, under conditions where no complex formation between ligand and precatalyst was observed, the order of addition was found to be irrelevant.

**Figure 2.3.** Precatalyst and ligand complexation.

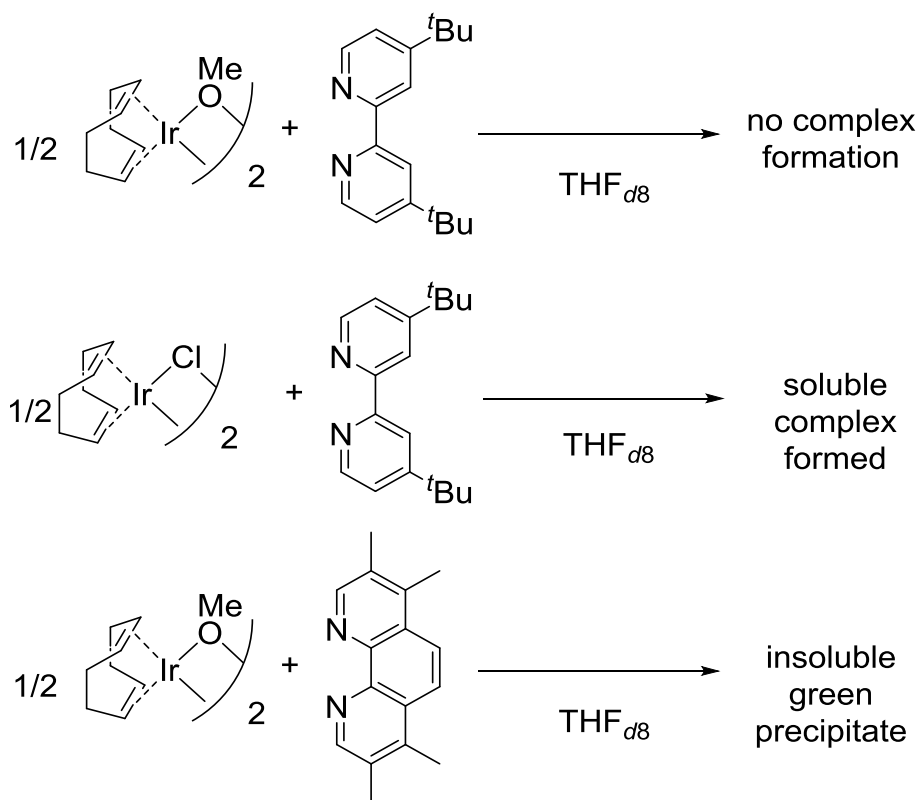


**Figure 2.4.** Rate equation derived from Ref 5.

$$\text{rate} = K_1^{1/2} k_2 [\text{Ir}]^{1/2} [\text{benzene}]$$

$$\text{where } K_1 = [(\text{dtbpy})\text{IrBPin}_3][\text{COE}] / [(\text{dtbpy})\text{Ir}(\text{COE})\text{BPin}_3]$$

### Effects of Borylating Reagent on Relative Reactivity

Although the rate equation for catalytic C-H borylation has been experimentally shown to be zeroth order in borylating reagent (Figure 2.4), the nature of the borylating reagent will still effect the conversion of precatalyst to active catalyst and consequentially affect the relative rates of reactivity.<sup>5</sup> Of the various borylating reagents known to do Ir catalyzed C-H borylation, only HBPIn and B<sub>2</sub>Pin<sub>2</sub> were included in our reaction screen. Borylating reagents such as HBcat (cat = catecholate)<sup>8,9</sup> and HBDan (Dan = 1,8-diaminonaphthyl)<sup>10</sup> were precluded from this study for their relatively lower reactivity and the latter's lack of mechanistic data. Of the reactions screened using the tmphen ligand, HBPIn gave higher conversions than B<sub>2</sub>Pin<sub>2</sub> with every precatalyst screened. For reactions with the dtbpy ligand, B<sub>2</sub>Pin<sub>2</sub> gave nearly 50% higher conversions with [Ir(OMe)COD]<sub>2</sub>, while HBPIn, was nearly 50% better with precatalyst **3**.

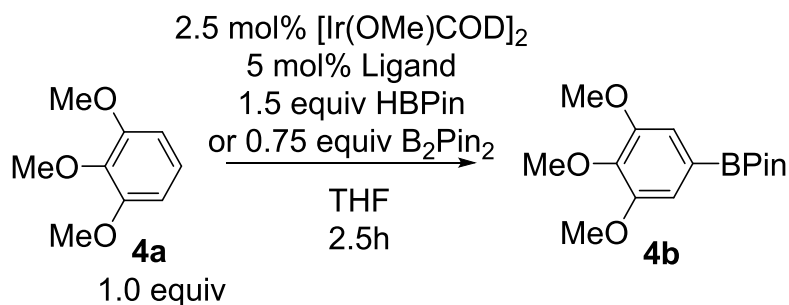
### General Ligand and Precatalyst Trends for Room Temperature Reaction Screen.

A relative ordering a precatalyst activity could be given as [Ir(OMe)(COD)]<sub>2</sub> > Ir(acac)(COD) > [Ir(Cl)(COD)]<sub>2</sub> consistent with the relative ordering of basicity in the precatalyst's counter ions being OMe > acac > Cl. The (η<sup>5</sup>-C<sub>9</sub>H<sub>7</sub>) fragment would obviously be



the most basic counter ion by a large margin, but the lack of reactivity is most likely due to the inability to displace it under these reaction conditions. A 4,4',5,5'-tetrahydro-2,2'-bioxazole (box) ligand was subjected to all screened conditions, however no conditions were found which produced more than trace amounts of product.

**Table 2.1.** Temperature effects on relative conversions for 1,2,3-trimethoxybenzene (**4a**).



entry	cond.	ligand	XBPIn	T (°C)	Yield (%)	T (°C)	Yield (%)
1	<b>A</b>	dtbpy	HBPIn	25	6	80	37
2	<b>A</b>	tmphen	HBPIn	25	10	80	87
3	<b>B</b>	dtbpy	HBPIn	25	7	80	41
4	<b>B</b>	tmphen	HBPIn	25	7	80	90
5	<b>A</b>	dtbpy	B <sub>2</sub> Pin <sub>2</sub>	25	10	80	74
6	<b>A</b>	tmphen	B <sub>2</sub> Pin <sub>2</sub>	25	8	80	88
7	<b>B</b>	dtbpy	B <sub>2</sub> Pin <sub>2</sub>	25	13	80	86
8	<b>B</b>	tmphen	B <sub>2</sub> Pin <sub>2</sub>	25	8	80	93

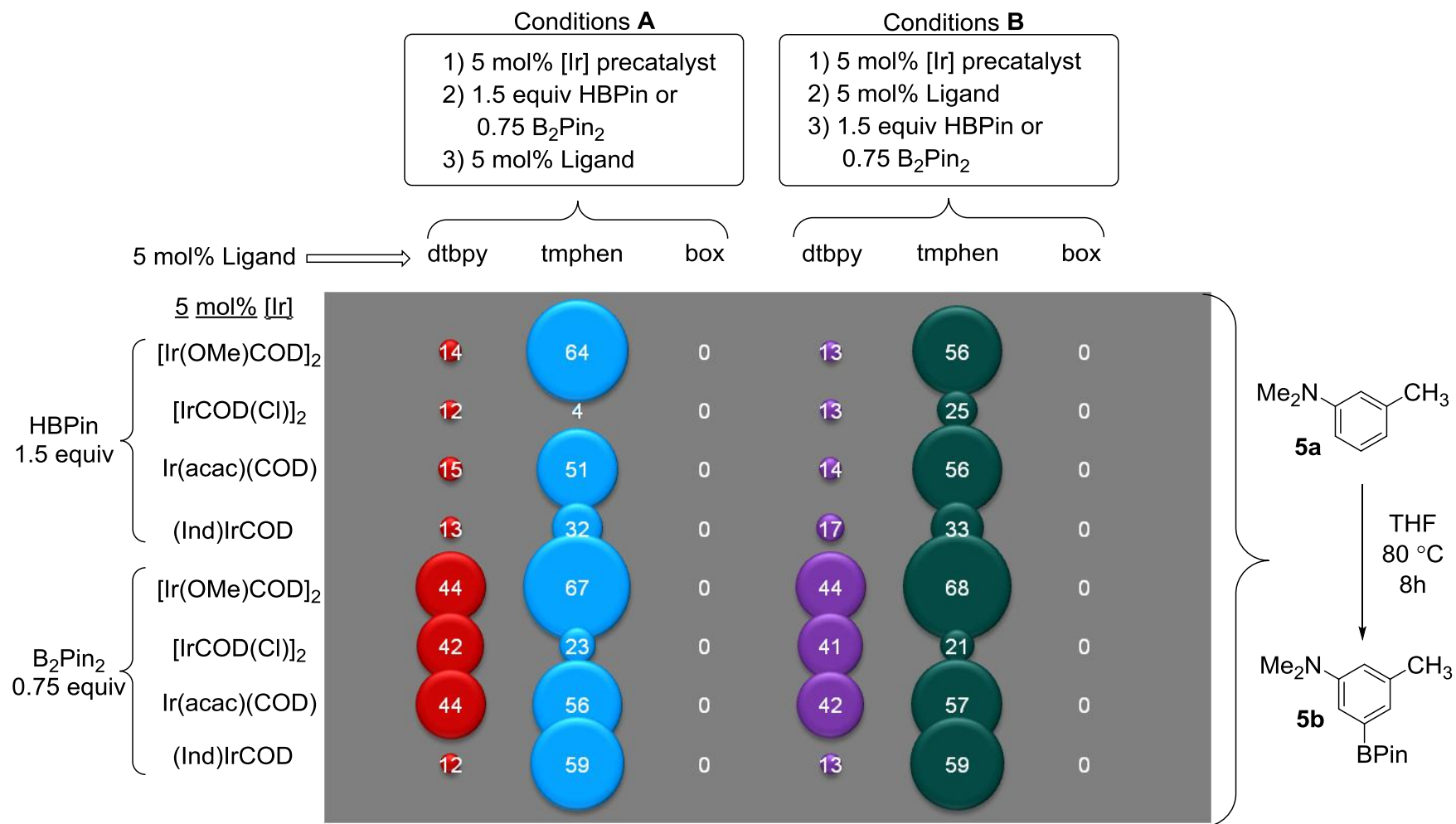
Conditions A: Order of addition 1) 5 mol% [Ir], 2) 1.5 equiv HBPIn or 0.75 equiv B<sub>2</sub>Pin<sub>2</sub>, and 3) 5 mol% Ligand. Conditions B: Order of addition 1) 5 mol% [Ir], 2) 5 mol% Ligand, and 3) 1.5 equiv HBPIn or 0.75 equiv B<sub>2</sub>Pin<sub>2</sub>. Precatalysts used in table 1.

### Temperature effects on optimization screens.

As stated in the introduction, more electron rich aromatics require more forcing conditions to affect borylation, usually in the form of higher reaction temperatures. A preliminary screen with 1,2,3-trimethoxybenzene (**4a**) was performed to determine the effects this common practice has on relative conversions in reactions run at 25 °C and 80 °C. Table 2.1 highlights the results of a set of experiments with precatalyst  $[\text{Ir}(\text{OMe})(\text{COD})]_2$  under various conditions. Optimum conditions for catalyst generation were found to be different at the two reaction temperatures. The order of addition effects observed with tmphen at room temperature (entries 2 and 4), were negligible in comparable entries at 80 °C. In contrast to experiments run at 25 °C, where the borylating reagent and order of addition determined which ligand was more viable, catalysts formed with the tmphen ligand outperformed catalysts with dtbpy under identical conditions in every set of experiments at 80 °C. Also, catalysts formed with the dtbpy ligand displayed a large difference in relative conversions when  $\text{B}_2\text{Pin}_2$  was used compared with HBPIn at both temperatures.

Reactions run with the tmphen ligand and **4a** as substrate, only gave low conversion at 25 °C, while conversion was nearly complete at 80 °C, hindering our ability to draw conclusions about relative rates by observing only set time points. Rather than decreasing reaction times, a more electron rich arene was chosen. Since catalyst formation occurs at the beginning of the reaction, it should be largely substrate independent. For N,N-dimethyltoluidine (**5a**), conversions after 4 h were lower. Thus relative rate information could be gleaned from single time point data. With **5a**, we screened  $[\text{Ir}(\text{OMe})(\text{COD})]_2$ ,  $[\text{Ir}(\text{Cl})(\text{COD})]_2$ ,  $\text{Ir}(\text{acac})(\text{COD})$ , or  $(\text{Ind})\text{Ir}(\text{COD})$ , at 80 °C with identical conditions as was done at room temperature with **3a** (Figure 2.5). Much higher

**Figure 2.5.** Elevated temperature reaction screen preformed on N,N-dimethyltoluidine (**5a**).



Numbers and bubble area size are assay yields of **5b**.

conversions were observed in reactions using tmphen as ligand than with dtbpy. This could be the result of either a more reactive (tmphen)IrBPin<sub>3</sub> catalyst being formed or a much shorter catalyst life time for complexes formed with dtbpy at this temperature. The order of addition effects were nonexistent with all ligands and precatalysts with the sole exception of the combination of HBPin, tmphen and [Ir(Cl)(COD)]<sub>2</sub> (column 2, row 2 and column 5, row 2).

The choice of precatalyst [Ir(OMe)(COD)]<sub>2</sub>, [Ir(Cl)(COD)]<sub>2</sub> or Ir(acac)(COD) was irrelevant with dtbpy ligand. The lower yields with (Ind)Ir(COD) could be the result of an induction period, however, a definitive conclusion cannot be drawn because data was sampled at one data point. Precatalyst [Ir(OMe)(COD)]<sub>2</sub>, performed slightly better than the others with tmphen.

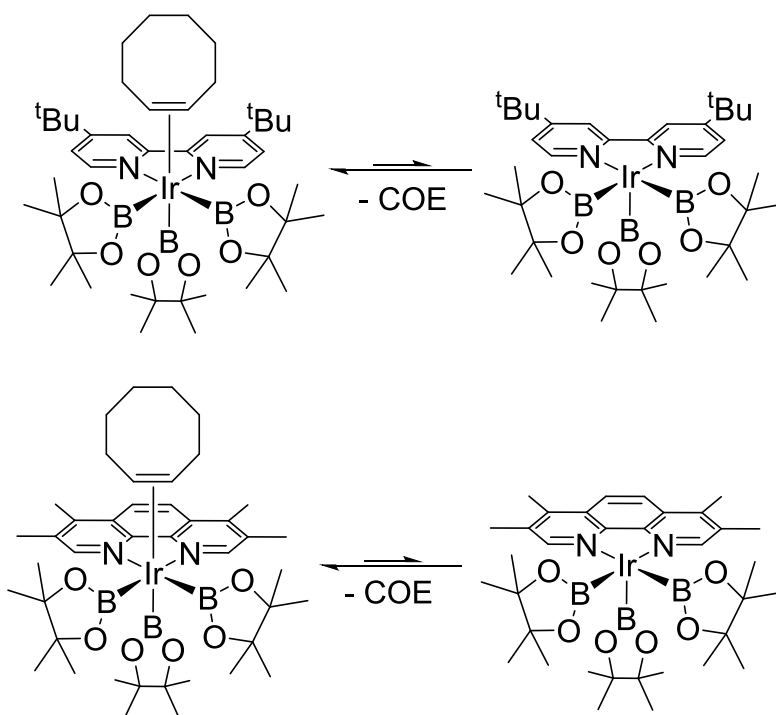
The most distinct systematic difference in reactivities was in the difference in relative conversions for experiments run with HBPin as borylating reagent compared with experiments run with B<sub>2</sub>Pin<sub>2</sub> as borylating reagent. Systems using the dtbpy ligand showed far greater reactivity with B<sub>2</sub>Pin<sub>2</sub> than analogous reactions with HBPin. Reactions with tmphen were much less sensitive to changes to the borylating reagent with the lone exception of higher reactivity occurring with (Ind)Ir(COD), tmphen and B<sub>2</sub>Pin<sub>2</sub> giving nearly 2 times as much borylated product as equivalent reactions with the precatalyst (Ind)Ir(COD), tmphen and HBPin.

### **Solvent Effects on Catalyst Formation at Room Temperature.**

By synthesizing and isolating the six coordinate catalyst precursors (dtbpy)Ir(Bpin)<sub>3</sub>(COE)<sup>5</sup> and (tmphen)Ir(Bpin)<sub>3</sub>(COE) (Figure 2.6), we were able to determine if

the differences in conversions for different ligands resulted from variability in catalyst generation or from intrinsic catalyst potency. The results in Figure 2.7 illustrate the difference in conversion that can be assumed from 100% catalyst generation with (dtbpy)Ir(BPin)<sub>3</sub>(COE) and (tmphen)Ir(BPin)<sub>3</sub>(COE), and from reactions were an unknown amount of active catalyst is formed from [Ir(OMe)(COD)]<sub>2</sub> and respective ligand in-situ.

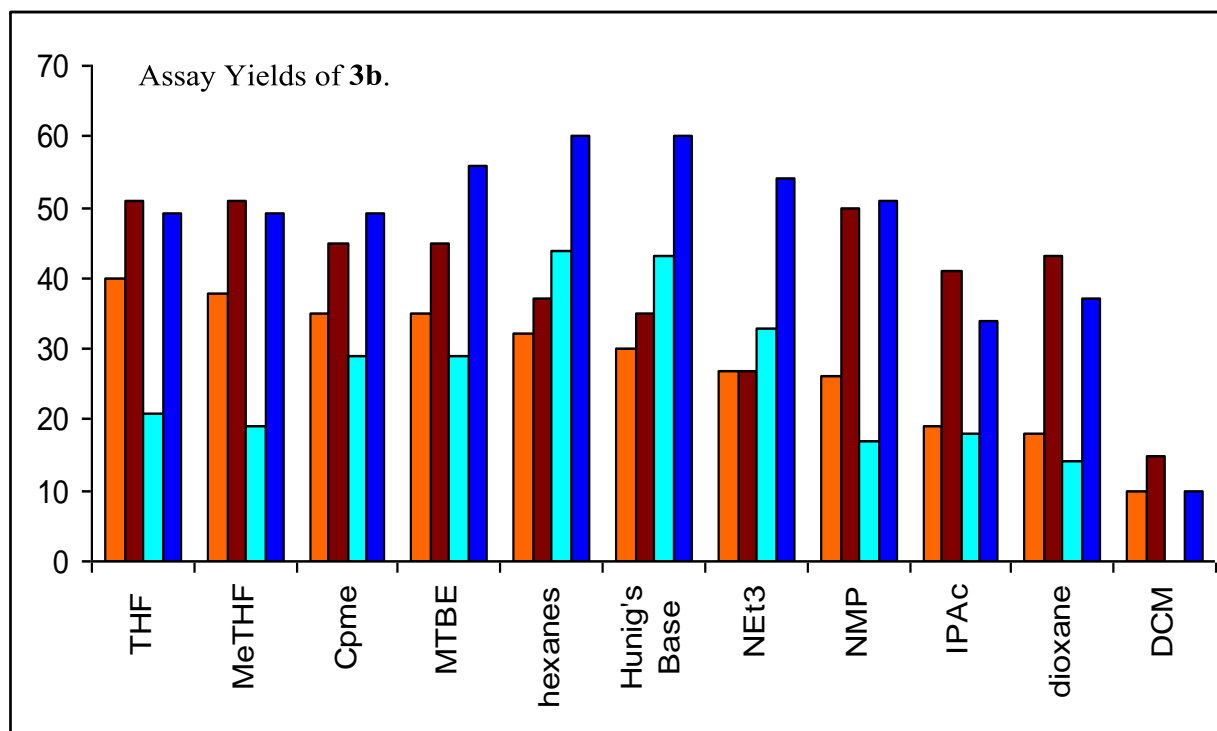
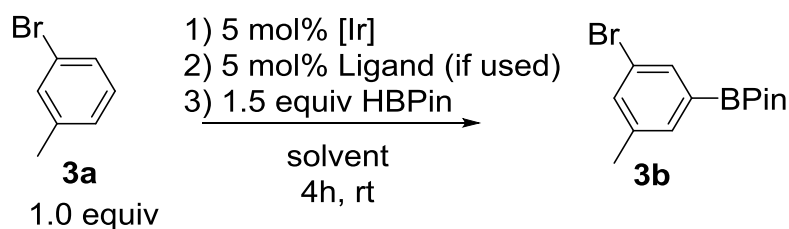
**Figure 2.6.** (dtbpy)Ir(BPin)<sub>3</sub>(COE) and (tmphen)Ir(BPin)<sub>3</sub>(COE).



While the isolated catalyst precursor (tmphen)Ir(BPin)<sub>3</sub>(COE) showed comparable or higher conversions to (dtbpy)Ir(BPin)<sub>3</sub>(COE) in most of the solvents screened, conversions with in-situ generated catalysts formed from tmphen and [Ir(OMe)(COD)]<sub>2</sub> were in most cases lower than those for in-situ generated catalysts from dtbpy and [Ir(OMe)(COD)]<sub>2</sub>. This led us to

conclude that under these reaction conditions, dtbpy and  $[\text{Ir}(\text{OMe})(\text{COD})]_2$  formed active catalysts in much higher yields in both polar and non-polar solvents at 25°C than tmphen and  $[\text{Ir}(\text{OMe})(\text{COD})]_2$  did.

**Figure 2.7.** Solvent Effects on Catalyst Generation at Room Temperature.

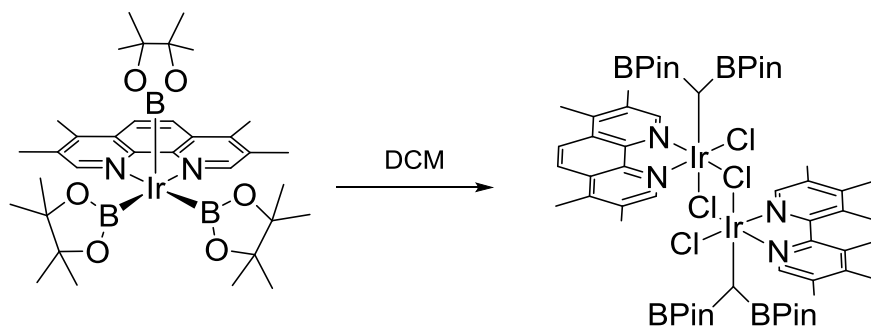


■ 2.5 mol%  $[\text{Ir}(\text{OMe})\text{COD}]_2$  with 5 mol% dtbpy ■ 5 mol% (dtbpy) $\text{Ir}(\text{BPin})_3(\text{COE})$  ■ 2.5 mol%  $[\text{Ir}(\text{OMe})\text{COD}]_2$  with 5 mol% tmphen ■ 5 mol% (tmphen) $\text{Ir}(\text{BPin})_3(\text{COE})$

The worst solvents for generating active catalyst with dtbpy and tmphen appear to be solvents containing carbonyls such as NMP and IPAc, or the very coordinating 1,4-dioxane

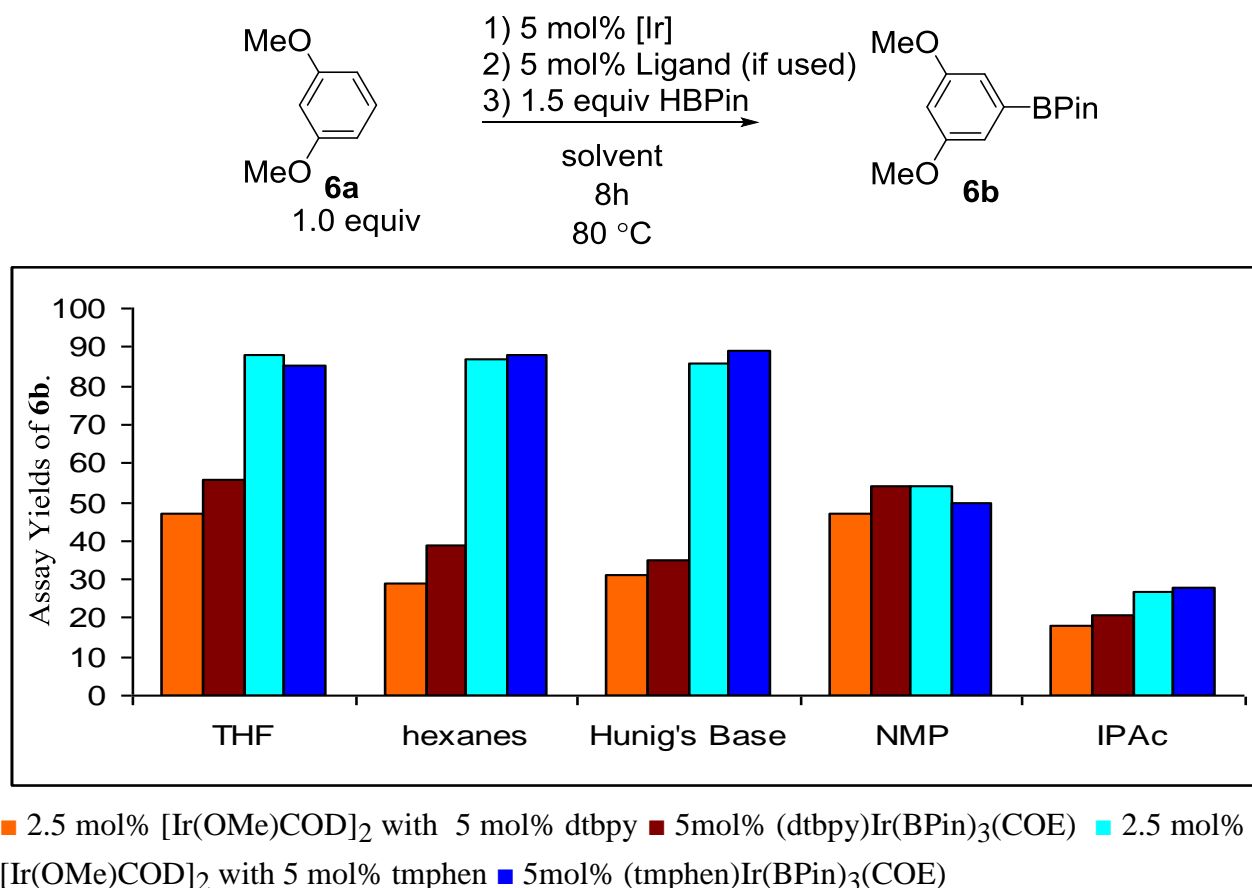
demonstrated by the large difference in reactivities of in-situ generated catalysts with that of the 6-coordinated isolated complex  $(dtbpy)Ir(BPin)_3(COE)$ . Contrary to the popular notion of non-polar solvents being better for borylation reactions, MeTHF, THF and NMP gave the highest conversions when starting from the isolated complex  $(dtbpy)Ir(BPin)_3(COE)$ .  $NEt_3$  appeared to inhibit reactivity of  $(dtbpy)Ir(BPin)_3(COE)$  and catalysts formed in-situ from  $[Ir(OMe)(COD)]_2$  and  $dtbpy$ . The solvents that gave the highest yield for in-situ catalyst generation with  $[Ir(OMe)(COD)]_2$  and  $tmphen$  were hexanes and Hünig's base.

**Figure 2.8.**  $[(tmphen)Ir(CH(BPin)_2)Cl_2]_2$ .



Not all solvents were inert to the Ir catalysts formed during C-H borylation. DCM was observed to react with  $(tmphen)Ir(BPin)_3(COE)$  to form a  $[(tmphen)Ir(CH(BPin)_2)Cl_2]_2$  dimer in quantitative yield when left over night (Figure 2.8). While no structure was isolated, similar reactions of DCM with  $(dtbpy)Ir(BPin)_3(COE)$  could account for the low reactivity. Reactions run with 2.5 mol%  $[Ir(OMe)COD]_2$  and 5 mol%  $dtbpy$  in MeCN and DMF gave only traces of borylated products and reactions in DMSO showed no product formation.

**Figure 2.9.** Solvent effects on catalyst generation with 1,3-dimethoxybenene (**6a**).



### Solvent Effects on Catalyst Formation at Elevated Temperature.

In situ catalyst formation appears to be much more efficient at 80 °C, with isolated complexes and in situ formed catalysts giving nearly equal conversions. IPAc appeared to diminish reactivity with both sets of ligands and NMP appeared to hamper complexes formed with the tmphen ligand (Figure 2.9). The diminished reactivity of NMP at 80 °C is not completely surprising, since the very similar solvent DMF only afforded trace amounts of borylation products at room temperature. Again, the best solvents for borylation with

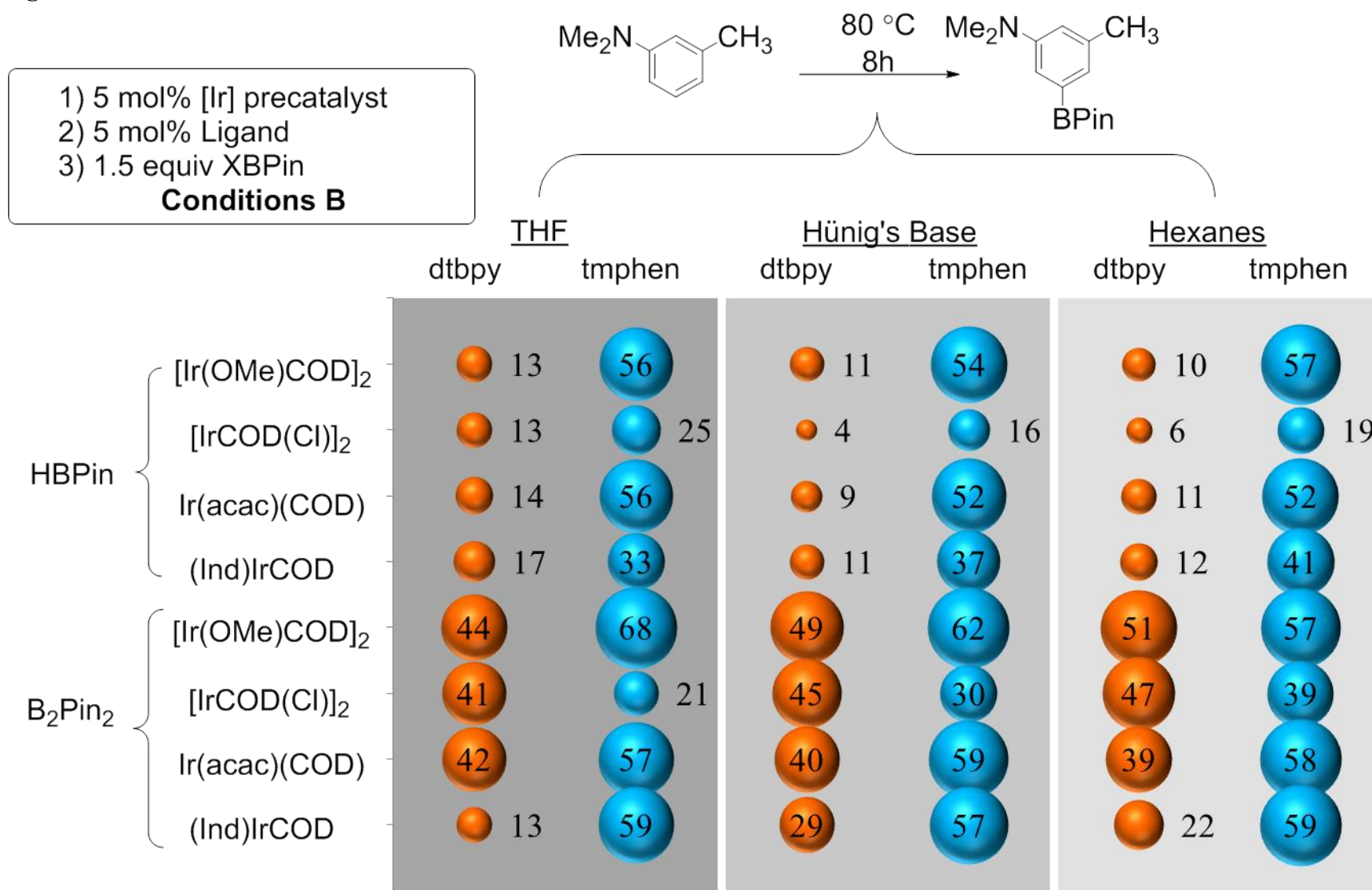


(dtbpy)Ir(BPin)<sub>3</sub>(COE) and catalysts formed in-situ from [Ir(OMe)(COD)]<sub>2</sub> and dtbpy were the polar solvent THF and NMP, outperforming less polar solvents such as hexanes. Catalysts formed from [Ir(OMe)(COD)]<sub>2</sub> and tmphen in-situ and (tmphen)Ir(BPin)<sub>3</sub>(COE) gave comparable conversions in both polar and non-polar solvents ranging from THF to Hünig's base to hexanes. The lower conversions of the in-situ formed catalyst from [Ir(OMe)(COD)]<sub>2</sub> and tmphen in NMP and IPAc and for reactions using (tmphen)Ir(BPin)<sub>3</sub>(COE) in NMP and IPAc maybe the result of side reactions between the active catalyst and the solvent similar to those seen with (tmphen)Ir(BPin)<sub>3</sub>(COE) and DCM at room temperature. Comparing the reactivity of (dtbpy)Ir(BPin)<sub>3</sub>(COE) and (tmphen)Ir(BPin)<sub>3</sub>(COE), we see the latter is much more reactive in THF at higher temperatures. While this was a change from the room temperature results, it did mirror reactivity seen with the elevated temperature reaction screens with **5a**.

### **Elevated Temperature Reaction Screen Performed on 5a in Multiple Solvents.**

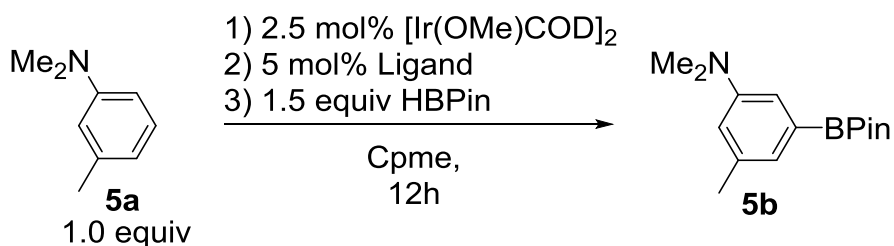
We thought it necessary to observe the effect solvent had on the multiple variables screened in the elevated temperature reaction screen with **5a** so portions of that screen using conditions **B** were run in hexanes and Hünig's base. The data presented in Figure 2.10 shows all precatalysts run with the dtbpy ligand and HBPIn were more reactive in THF than in hexanes or Hünig's base in agreement with the previous elevated solvent screen. However, hexane was the preferred solvent when using B<sub>2</sub>Pin<sub>2</sub> as the borylating reagent out performing the analogous

**Figure 2.10.** Multivariable Solvent Screen.



reactions run with precatalysts  $[\text{Ir}(\text{OMe})(\text{COD})]_2$ ,  $[\text{Ir}(\text{Cl})(\text{COD})]_2$ , and  $(\text{Ind})\text{Ir}(\text{COD})$ . Solvent had very little effect on reactions run with the tmphen ligand giving similar results with both HBPIn and  $\text{B}_2\text{Pin}_2$ . The only significant solvent effect observable with the tmphen catalyst was with  $[\text{Ir}(\text{Cl})(\text{COD})]_2$  and  $\text{B}_2\text{Pin}_2$ , were the more non polar the solvent became, the higher the relative reaction rates became.

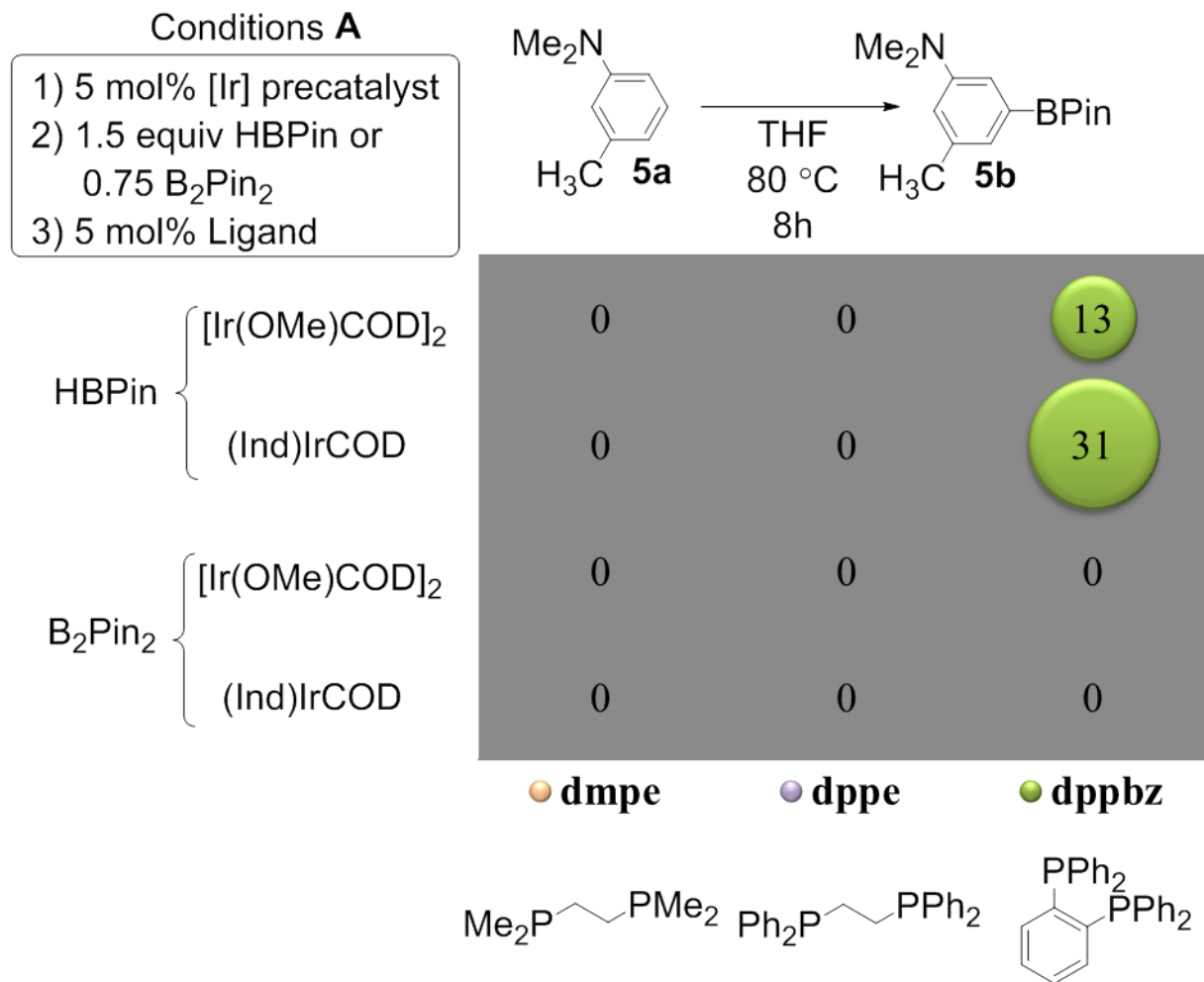
**Table 2.2.** Temperature Effect on Catalyst Stability



Entry	ligand	T (°C)	% yield
1	dtbpy	130	13
2	dtbpy	110	13
3	dtbpy	80	32
4	tmphen	130	38
5	tmphen	110	48
6	tmphen	80	94
7	dppbz	130	52
8	dppbz	110	15 <sup>a</sup>
9	dppbz	80	0

<sup>a</sup>Reaction run in MeTHF.

**Figure 2.11.** Phosphine Ligand Screen.

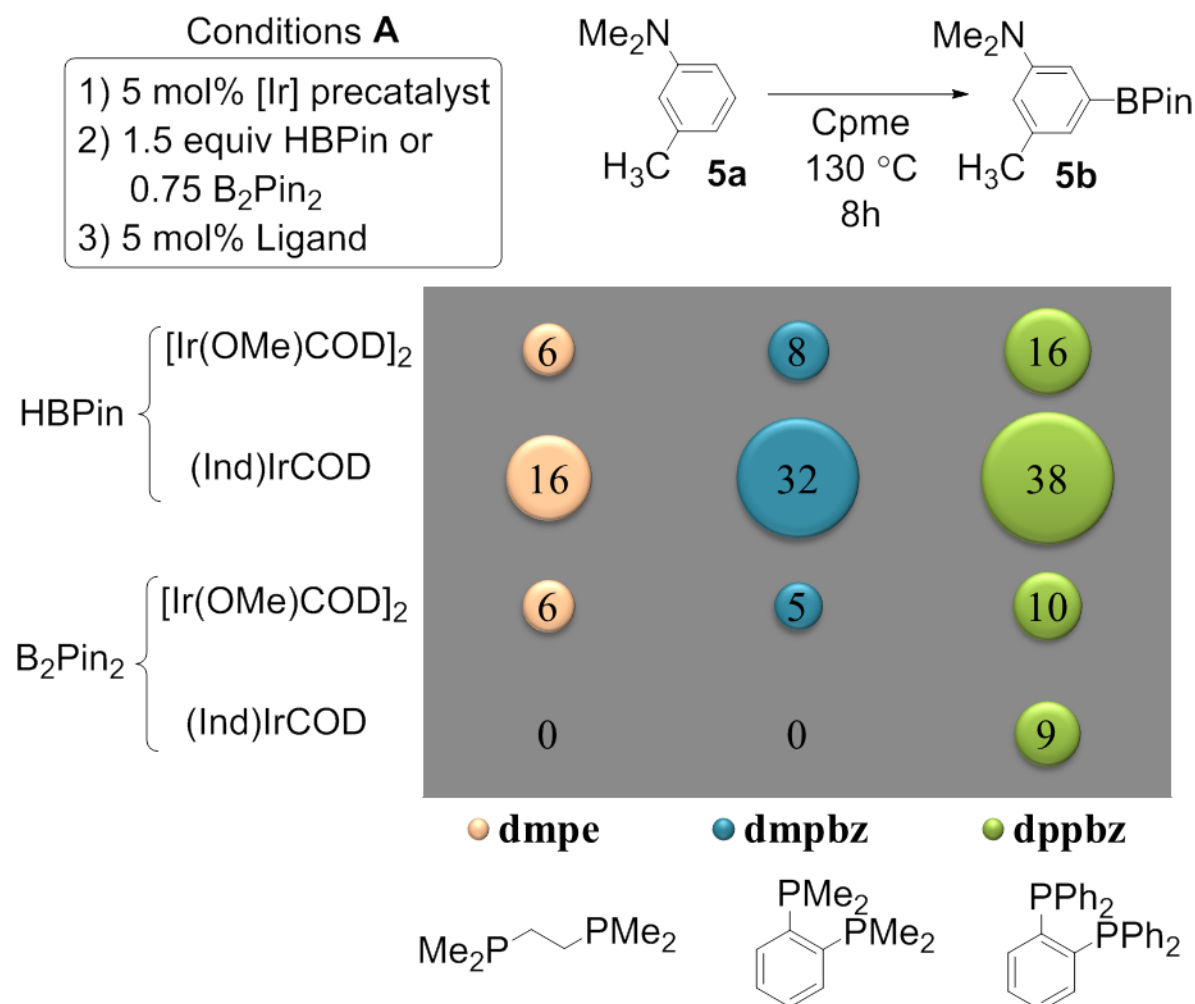


### Phosphine Ligated Iridium Borylation Catalysts.

A number of reports have utilized phosphine ligands for Ir catalyzed borylation reactions. Although we desired to contain within this report, a head to head comparison of Ir catalysts with bidentate phosphine ligands with those of bis nitrogen chelates it was found that the optimum reaction conditions for each were drastically different. While nitrogen chelates such as dtbpy and tmphen soundly outperform phosphine ligated Ir catalysts at temperatures up to 80 °C, phosphine complexes require higher temperatures to become catalytically viable. Table 2.2 shows that as the reaction temperature is increased, reactivity for catalysts derived from dtbpy and tmphen

greatly decreases. Comparing entries 4 and 6 in Table 2.2, we see that as the reaction temperature is raised from 80 °C to 130 °C, reactivity drops from 94% yield to 38% at identical time points. Conversely, comparing Table 2.2 entry 9 with entry 7, reactivity increases from no conversion at 80 °C to 52% conversion at 130 °C with catalysts derived from dppbz (1,2-bis(diphenylphosphino)benzene) and  $[\text{Ir}(\text{OMe})(\text{COD})]_2$ . The effects of heating reactions above 80 °C are not immediately clear but the reduction in catalytic reactivity with dtppy and tmphen Ir complexes is most likely due to catalyst decomposition.

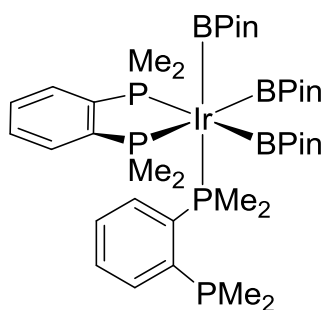
**Figure 2.12.** Elevated Temperature Phosphine Ligand Screen.



## Ligand Effects; Electron Donating Ability and Constrained Geometry.

Reactivity of Ir catalysts has been shown to correlate with increasing donor ability of ligands and Figure 2.11 shows the partial results from a reaction screen using the phosphine ligands dmpe, dppe and dppbz. The lack of reactivity under these reaction conditions is surprising considering that alkyl and aryl phosphines are both significantly strong donor ligands. More so, the sterically smaller and more electron rich dmpe performs much worse than the sterically larger, less electron rich dppbz. The fact that dmpe and dppe are known to form the catalytically incompetent  $(\text{dmpe-}\kappa^2\text{P})\text{Ir}((\text{BPin})_3(\text{dmpe-}\kappa^1\text{P}))$  and  $(\text{dppe-}\kappa^2\text{P})\text{Ir}((\text{BPin})_3(\text{dppe-}\kappa^1\text{P}))$ <sup>11</sup> complexes could account for the lack of reactivity. The constrained benzene backbone in dppbz would prevent the two phosphine coordination sites from orientating themselves trans to each other inhibiting the formation of an analogous  $(\text{dppbz-}\kappa^2\text{P})\text{Ir}((\text{BPin})_3(\text{dppbz-}\kappa^1\text{P}))$  complex.

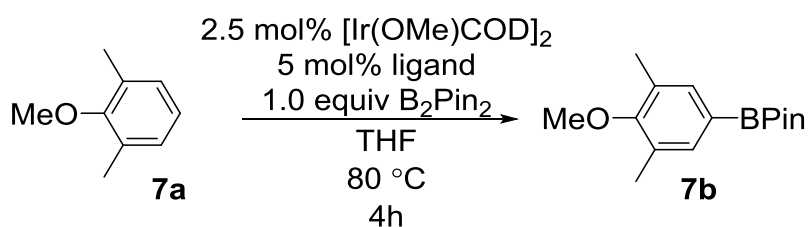
**Figure 2.13.**  $(\text{dmpbz-}\kappa^2\text{P})\text{Ir}((\text{BPin})_3(\text{dmpbz-}\kappa^1\text{P}))$



The results shown in Figure 2.12 of a similar phosphine reaction screen using dmpe, dmpbz (1,2-bis(dimethylphosphino)benzene) and dppbz at 130 °C in Cpme show higher reactivity than those done at 80 °C (Figure 2.10). An additional interesting result is the lower reactivity of the dmpbz ligand relative to the dppbz ligand. As stated previously the lower steric bulk and increased donor ability of ligands lead to more active catalysts. The dmpbz ligand should be both

less sterically hindering and more electron donating than dppbz, but reactions with the dmpbz ligand gave lower yields. An explanation may be that a  $(\text{dmpbz-}\kappa^2\text{P})\text{Ir}((\text{BPin})_3(\text{dmpbz-}\kappa^1\text{P}))$  complex can be formed despite its constrained backbone because of its lower steric bulk (Figure 2.13).

**Table 2.3.** Borylation of 2,6-dimethylanisole (**7a**).

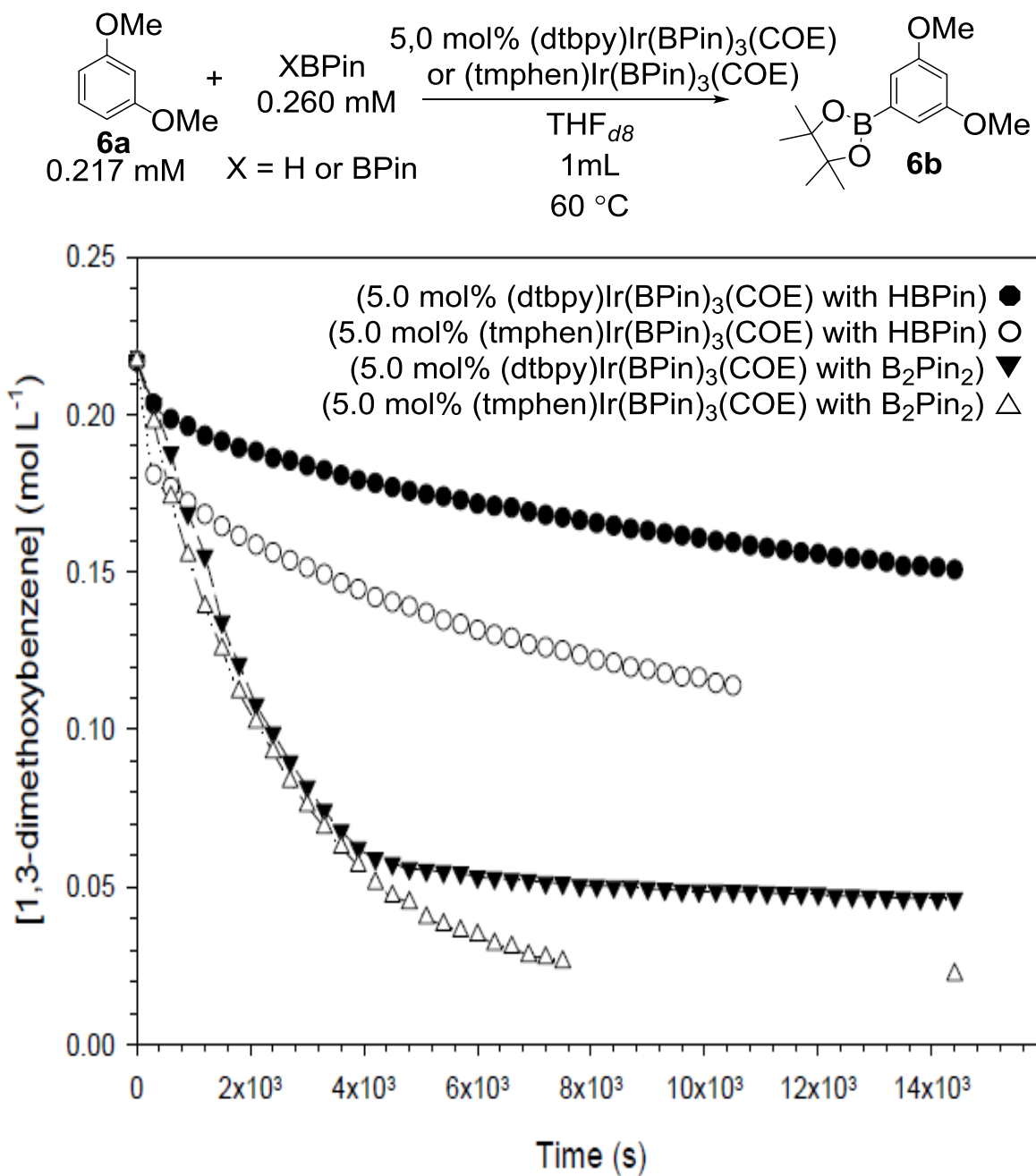


entry	ligand	% yield
1	dtbpy	46
2	dmabpy	55
3	phen	16
4	tmphen	86

In an attempt to probe whether the difference in reactivity of the tmphen ligated complex and the dtbpy ligated complex was due the constrained dihedral angle in the chelate backbone or due to the fact that tmphen is simply a stronger donor ligand than dtbpy, a set of experiments was run with dmabpy (4,4'-bis(dimethylamino)-2,2'-bipyridine) and phen (1,10-phenanthroline) ligands. The results shown in Table 2.3 suggest it is a combination of the two effects. While the dmabpy ligand is more electron rich than the tmphen ligand,<sup>12,13</sup> the importance of the conformational rigidity of tmphen is highlighted by its ability to give higher relative conversions for the borylation of 2,6-dimethylanisole with HBPin. The constrained dihedral angle in the chelate backbone of tmphen is a feature shared with the phen ligand, however, phen gave far

lower relative reaction rates than either the dtbpy or dmabpy ligands, ascribable to phen being comparatively electron deficient.

**Figure 2.14.** Decay of **6a** during the reaction with HBPIn or B<sub>2</sub>pin<sub>2</sub>.





### **Kinetic Experiments with (tmphen)Ir(BPin)<sub>3</sub>(COE) and (dtbpy)Ir(BPin)<sub>3</sub>(COE).**

As was noted in previous sections, the reactivity of reactions run at elevated temperatures showed a clear dependence on the specific borylating reagent used (either HBPIn or B<sub>2</sub>Pin<sub>2</sub>). The (tmphen)Ir(BPin)<sub>3</sub>(COE) also appeared to be much more potent than the (dtbpy)Ir(BPin)<sub>3</sub>(COE) analogue. The increased conversions observed for reactions with (tmphen)Ir(BPin)<sub>3</sub>(COE) and B<sub>2</sub>Pin<sub>2</sub> could be the result of either the complex being much more reactive than the dtbpy analogue or (tmphen)Ir(BPin)<sub>3</sub>(COE) having a longer catalytic lifetime and producing more TONs. Figure 2.14 shows the results of several NMR tube reactions run with 5 mol% (dtbpy)Ir(BPin)<sub>3</sub>(COE) or (tmphen)Ir(BPin)<sub>3</sub>(COE), with either borylating reagent B<sub>2</sub>Pin<sub>2</sub> (0.260 M) or HBPIn (0.260 M) and **6a** (0.217 M) in THF<sub>d8</sub> at 60 °C. For reactions run with B<sub>2</sub>pin<sub>2</sub>, both (dtbpy)Ir(BPin)<sub>3</sub>(COE) and (tmphen)Ir(BPin)<sub>3</sub>(COE) gave comparable initial rates for the initial two half-lives (Figure 2.15). Over this time period, the catalytic resting state could be observed as that of the initial complexes (dtbpy)Ir(BPin)<sub>3</sub>(COE) or (tmphen)Ir(BPin)<sub>3</sub>(COE) respectively. As the reaction progressed toward the inflection point seen in Figure 2.14, HBPIn formed as the byproduct of B<sub>2</sub>Pin<sub>2</sub> and arene and the resting state shifted from that of the 6-coordinate catalyst precursors to that of an unidentified species accompanied by free COE (Figure 2.16). Free COE was observed with a shift in the aromatic resonances in reactions with HBPIn and either (dtbpy)Ir(BPin)<sub>3</sub>(COE) or (tmphen)Ir(BPin)<sub>3</sub>(COE) at room temperature. The observation of different catalytic resting

states with different borylating reagents accounts for how different boron sources could give different reactivity when the reaction has been determined to be zeroth order in borylating reagent (Figure 2.17).<sup>5</sup>

**Figure 2.15.**  $\ln[\text{arene}]$  vs. time over two half-lives.

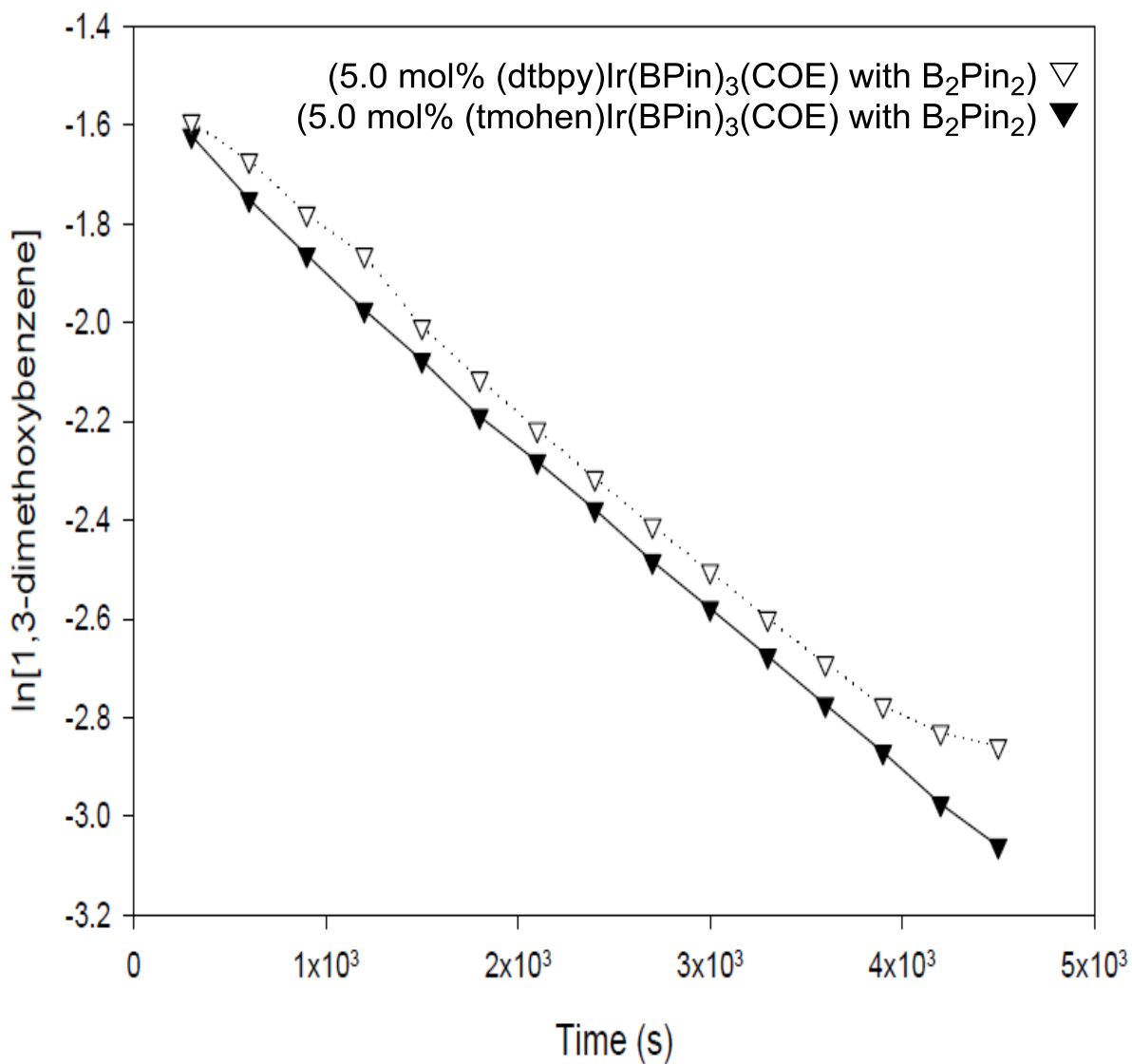
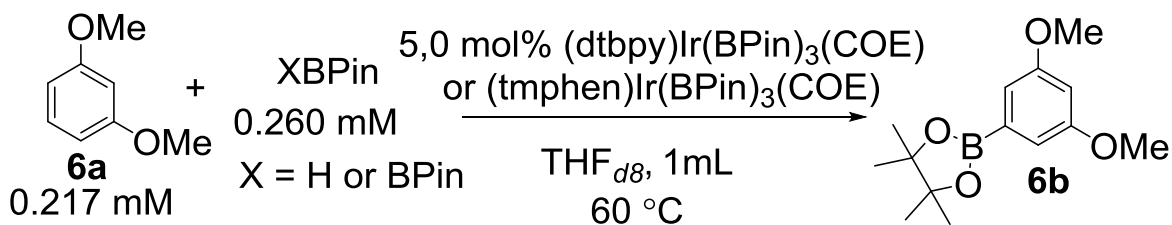


**Figure 2.16.** Catalytic resting states for kinetic experiments with (tmphen)Ir(BPin)<sub>3</sub>(COE) with B<sub>2</sub>Pin<sub>2</sub> (A) and HBPin (B).

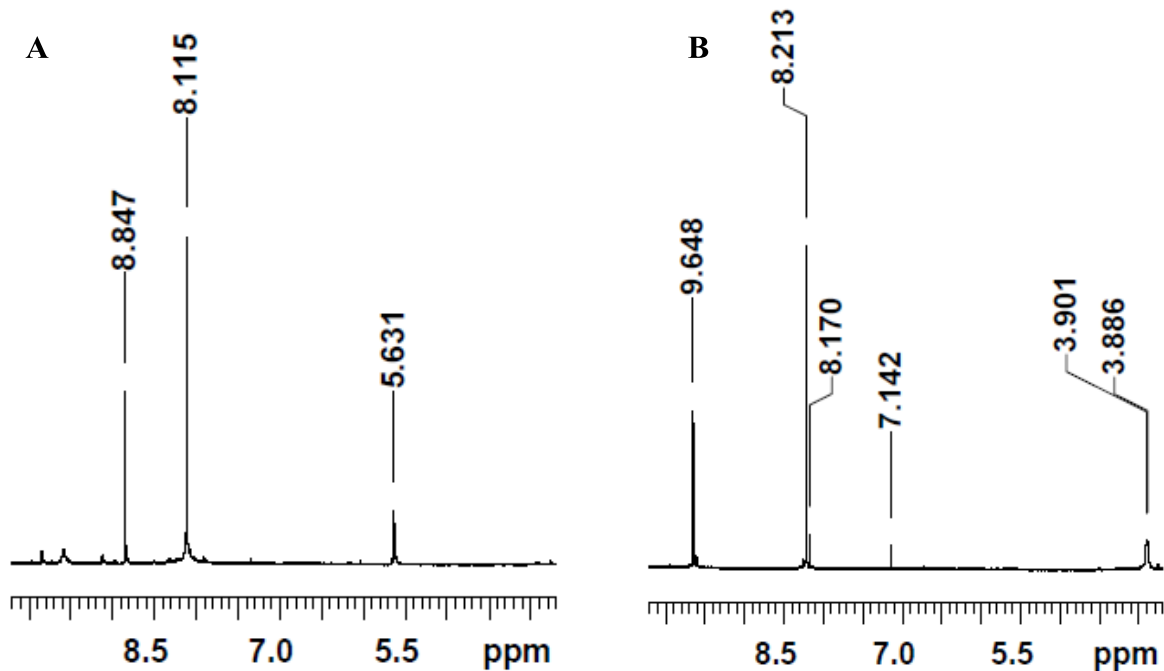


**Figure 2.17.** Proposed catalytic cycle for (dtbpy)Ir(BPin)<sub>3</sub>(COE) from ref. 5.

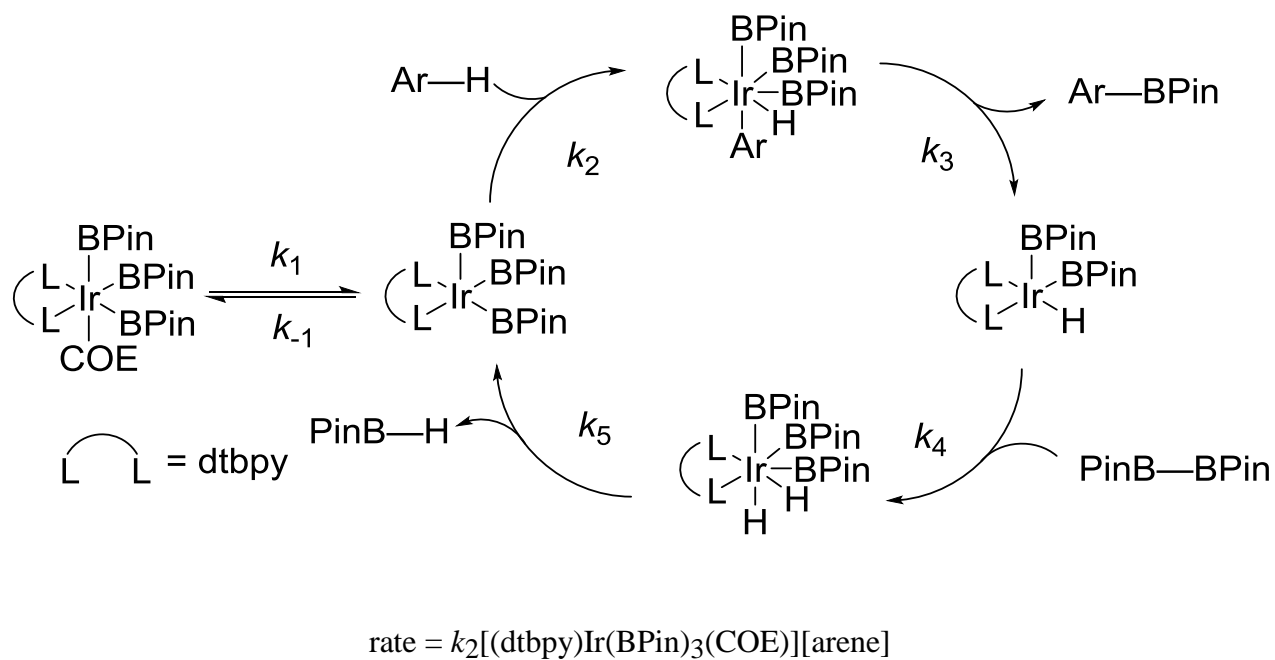
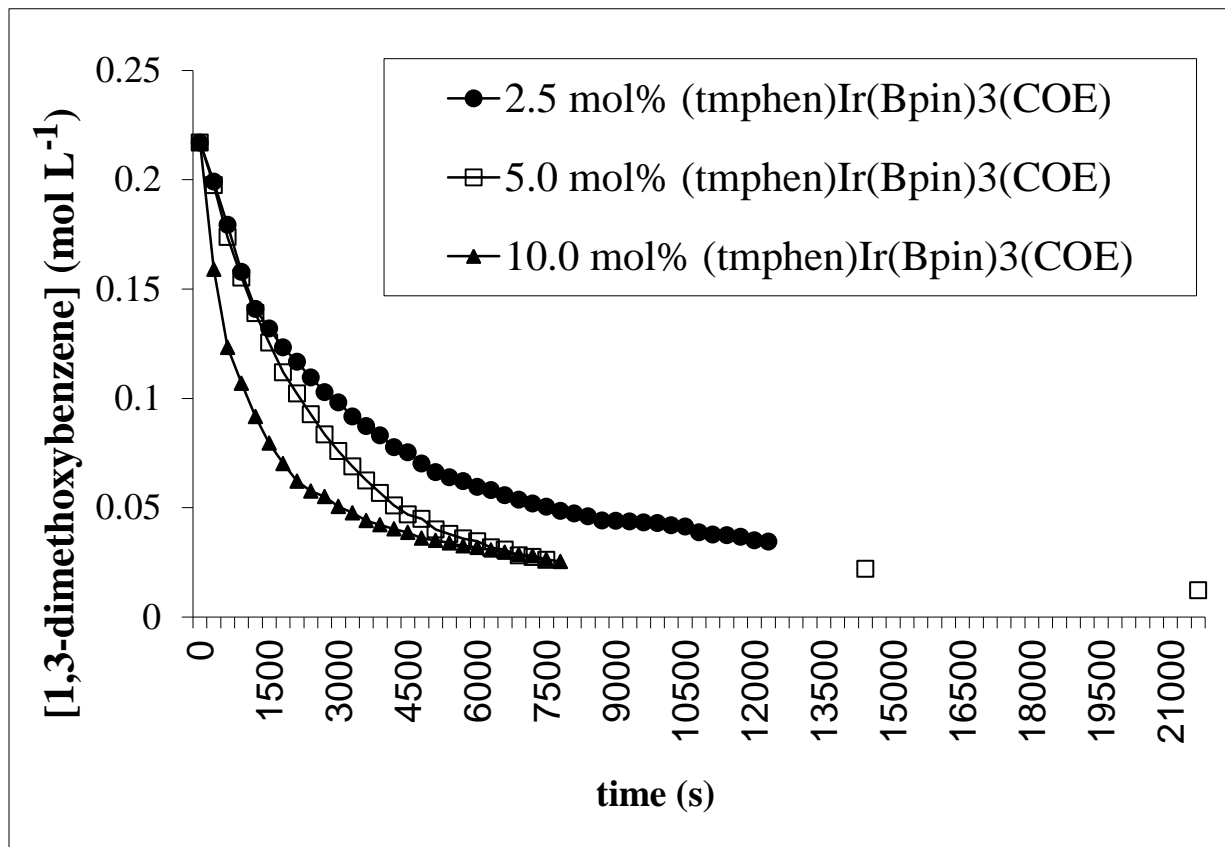
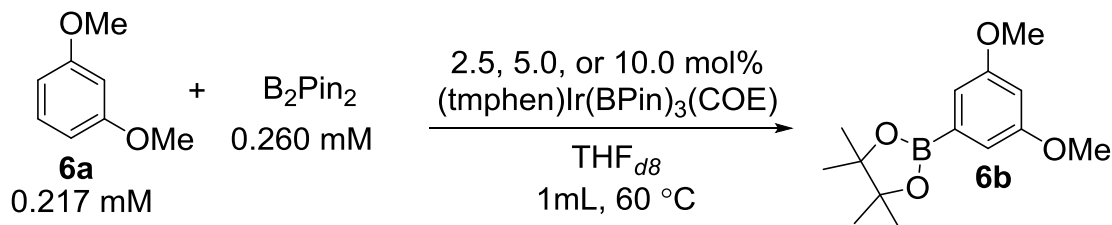


**Figure 2.18.** Kinetic Experiments with (tmphen)Ir(BPin)<sub>3</sub>(COE) at variable catalyst loadings.

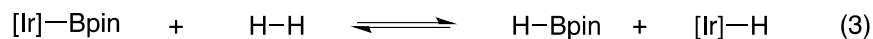
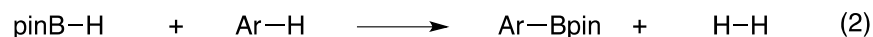
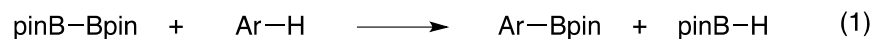


Kinetic experiments done with varying amounts of (tmphen)Ir(BPin)<sub>3</sub>(COE) showed that at higher catalyst loadings (10 mol% (tmphen)Ir(BPin)<sub>3</sub>(COE)), the reaction borylation of **6a** would initially proceed at a faster rate, but would also reach the inflection point quicker than reactions done at lower loadings. Conversely, reactions run with 2.5 mol%

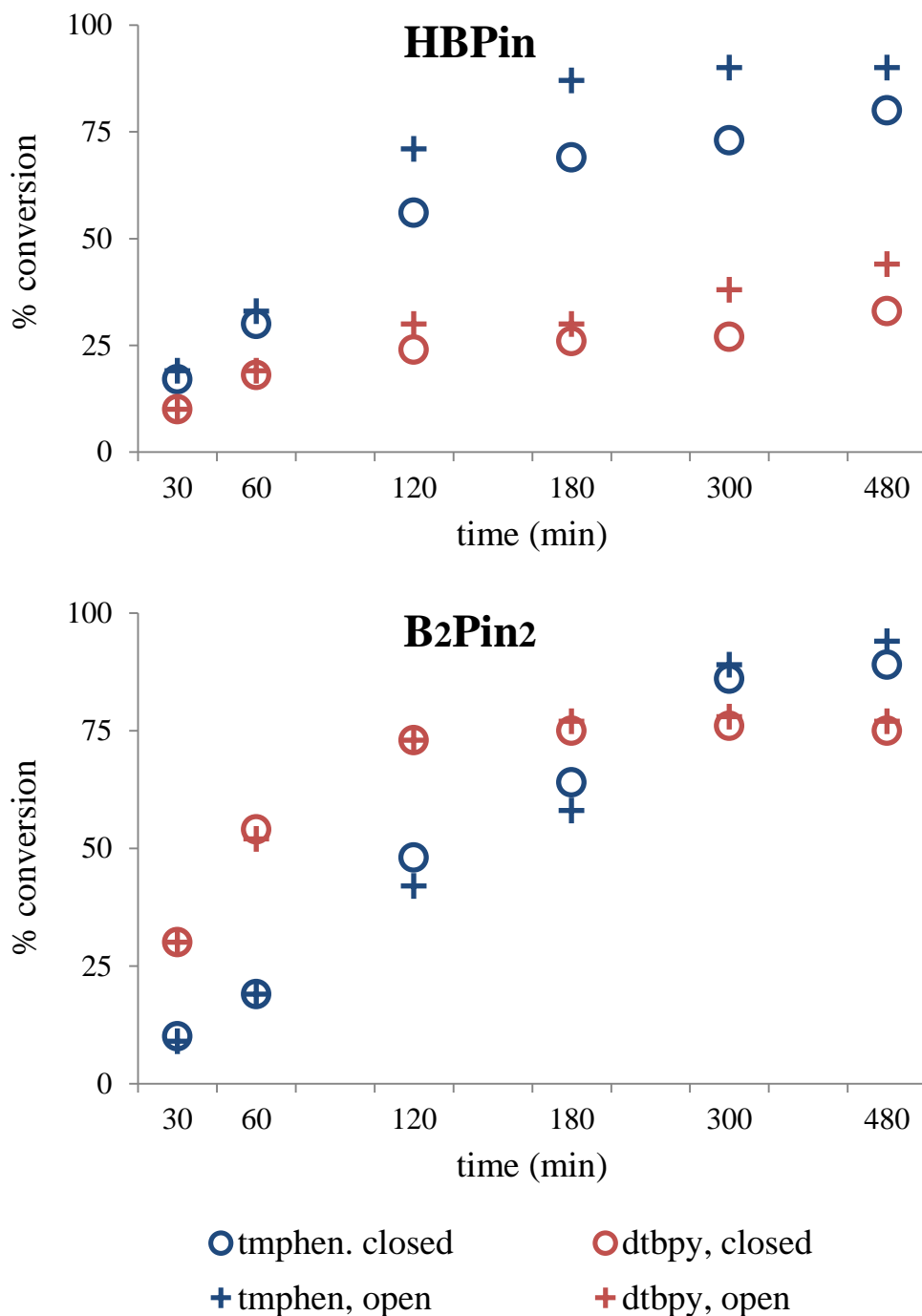
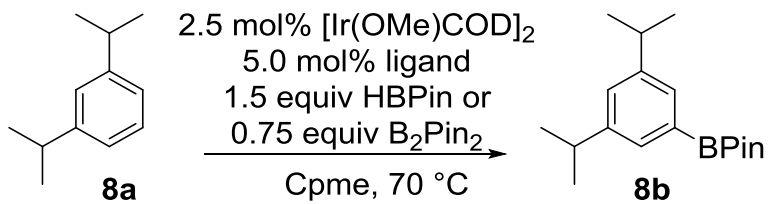
(tmphen)Ir(BPin)<sub>3</sub>(COE) had a slower initial reaction rate but would reach the inflection point at a later time. These results are in agreement with the rate equations determined in ref 5.

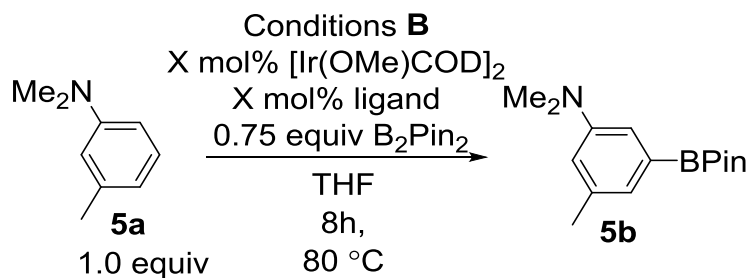
### C-H Borylation in Open vs. Closed Systems.

In this study the reactions were carried out in closed systems to prevent solvent and reagent evaporation. Ir catalyzed C-H borylations with B<sub>2</sub>Pin<sub>2</sub> generate HBPin as shown in Eq 1. HBPin can react further to do a successive borylation and generate one equivalent of H<sub>2</sub> (Eq 2). The H<sub>2</sub> generated can react with Ir-BPin complexes to form hydrides according to Eq 3. Since the effects of Ir-H complexes in the catalytic cycle are not well defined, a comparison between open and closed systems with the borane reagents HBPin and B<sub>2</sub>Pin<sub>2</sub> could offer insight into the effect H<sub>2</sub> concentration has on the reaction. For HBPin, borylations in open systems were slightly more efficient than borylations in closed systems, while borylations with B<sub>2</sub>Pin<sub>2</sub> were essentially the same in open and closed systems (Figure 2.19).



**Figure 2.19.** C-H Borylation in Open vs. Closed Systems with **8a**.



**Table 2.4.** Ligand to Metal Ratios and Catalyst Loading Study.

Ligand equivalents relative to Ir (data in % yield)

Entry	mol% Ir	Ligand	Ligand equivalents relative to Ir (data in % yield)				
			0.8	1.0	1.4	2.0	4.0
1	5.0	dtbpy	<b>55</b>	<b>55</b>	53	54	52
2	2.5	dtbpy	58	57	<b>58</b>	55	53
3	1.0	dtbpy	51	55	54	<b>58</b>	57
4	0.5	dtbpy	32	36	41	47	50
5	5.0	tmphen	<b>75</b>	74	68	61	43
6	2.5	tmphen	72	<b>77</b>	73	68	55
7	1.0	tmphen	57	69	<b>78</b>	<b>78</b>	72
8	0.5	tmphen	40	42	53	<b>79</b>	66

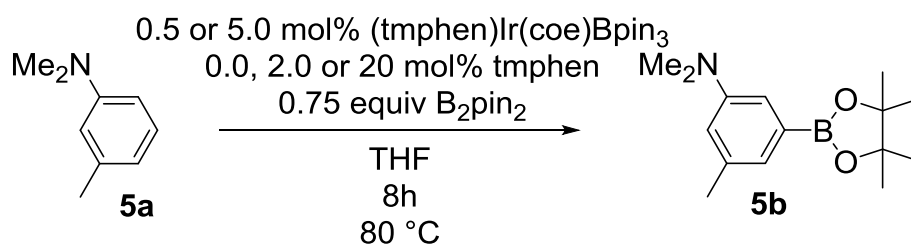
**Ligand to Metal Ratio and Catalyst Loading Study.**

Loading studies were conducted on the catalytic system to determine how concentration, catalyst loadings, and ligand to metal ratios would affect the overall reaction rates. Table 2.4 displays results using [Ir(OMe)(COD)]<sub>2</sub> at four catalyst loadings, with five ligand to Ir ratios ranging from 0.8: 1.0 to 4.0: 1.0, in a 5 M reaction solution with respect to **5a**. The results highlight that reactivity can be maintained as you reduce catalyst loadings up to ten fold by

increasing the ligand to Ir ratio to 2.0: 1.0. This trend was observed for both dtbpy and tmphen ligands, but is more dramatic with tmphen.

Since it is firmly established that mono ligated (dtbpy)IrBPin<sub>3</sub> and (tmphen)IrBPin<sub>3</sub> are the active catalyst species in solution, the increased reactivity at lower concentrations of [Ir(OMe)(COD)]<sub>2</sub> suggest the extra equivalents of ligands aid in catalyst formation under these conditions, which is not unusual for catalyst which require in-situ generation. Further increasing the ligand to metal ratio was found to show diminishing reactivity.

**Table 2.5.** Ligand to Metal Ratio with preformed (tmphen)Ir(COE)BPin<sub>3</sub>.



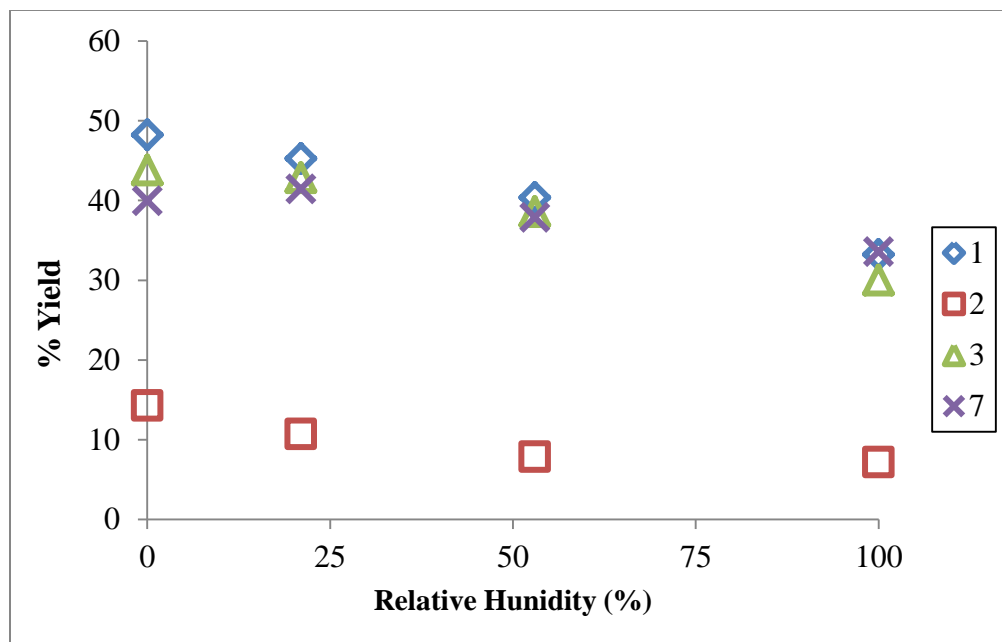
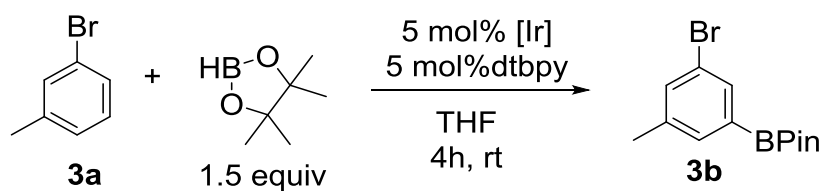
entry	mol % (tmphen)Ir(COE)BPin <sub>3</sub>	mol % tmphen	Yield (%)
1	<b>0.5</b>	--	89
2	<b>0.5</b>	<b>2.0</b>	92
3	<b>5.0</b>	--	82
4	<b>5.0</b>	<b>20</b>	79

Table 2.5 shows the results of a similar ligand to metal ratio and catalyst loading study run with preformed (tmphen)Ir(COE)BPin<sub>3</sub>. Reactions run with additional tmphen gave nearly identical yields as those run without. This supports our hypothesis that the additional ligand aids in active catalyst generation for in-situ generation from precatalyst [Ir(OMe)(COD)]<sub>2</sub>.



Decreasing the catalyst loading with the preformed (tmphen)Ir(COE)BPin<sub>3</sub> gives a less pronounced increase in conversion, similar to what was observed in the in-situ generated catalyst loading studies.

**Figure 2.20.** Precatalyst Stability and Aging Study.

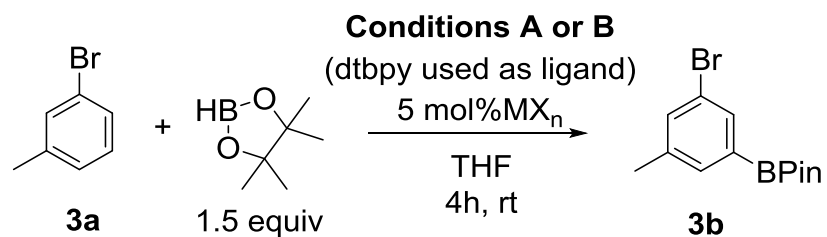


## Precatalyst Stability and Aging Studies.

In an effort to determine the various “shelf-life” of the precatalysts used in our optimization study, we investigated how the reactivity would be effected by varying degrees of humidity over time. Samples of precatalysts  $[\text{Ir}(\text{OMe})(\text{COD})]_2$ ,  $[\text{Ir}(\text{Cl})(\text{COD})]_2$ ,  $\text{Ir}(\text{acac})(\text{COD})$ , and  $(\text{hexafluoroacetylacetonate})\text{Ir}(\text{COD})$  were subdivided and stored in humidity chambers at several humidities for 100 days and then tested against samples that were held in an inert atmosphere ( $\text{N}_2$  filled glove box). The results are shown in Figure 2.20 and precatalysts  $[\text{Ir}(\text{OMe})(\text{COD})]_2$ ,  $\text{Ir}(\text{acac})(\text{COD})$ , and  $(\text{hexafluoroacetylacetonate})\text{Ir}(\text{COD})$  all show a gradual drop in reactivity directly dependent on the conditions in which they were stored, with a more moist environment leading to lower relative rates of reactivity. Precatalyst  $[\text{Ir}(\text{Cl})(\text{COD})]_2$ , while exhibiting a slight drop in reactivity from samples held in a glove box, shows that it is the most “air stable” of the precatalysts commonly used for Ir catalyzed C-H borylation.

Due to  $[\text{Ir}(\text{Cl})(\text{COD})]_2$  superior bench top stability, lower cost and the fact that precatalysts  $[\text{Ir}(\text{OMe})(\text{COD})]_2$ ,  $\text{Ir}(\text{acac})(\text{COD})$ ,  $(\text{Ind})\text{Ir}(\text{COD})$ , and  $(\text{hexafluoroacetylacetonate})\text{Ir}(\text{COD})$  are all prepared from  $[\text{Ir}(\text{Cl})(\text{COD})]_2$ , we investigated the effects various metal salt additives would have on the in-situ formation of these more active precatalysts starting from  $[\text{Ir}(\text{Cl})(\text{COD})]_2$ . Entries 1, 2, and 4 from Table 2.6 show that the relative rates of C-H borylation could be increased by the combination of  $[\text{Ir}(\text{Cl})(\text{COD})]_2$  and K, Na and Ti acetylacetonate salts to the point where they rivaled those seen with  $\text{Ir}(\text{acac})(\text{COD})$  under reaction conditions **B**. Entry 8 demonstrates that  $[\text{Ir}(\text{Cl})(\text{COD})]_2$  with  $\text{KO}t\text{-Bu}$  can show

comparable reactivity to  $[\text{Ir}(\text{OMe})(\text{COD})]_2$  under reaction conditions **B**. Interestingly, the metal salts  $\text{Al}(\text{acac})_3$  and  $\text{Mg}(\text{OMe})_2$  did not improve or inhibit reactivity with  $[\text{Ir}(\text{Cl})(\text{COD})]_2$ , or  $[\text{Ir}(\text{OMe})(\text{COD})]_2$ . Such results raise the possibility that certain metal phenoxide or benzoate salts may be able to undergo C-H borylation. Such a study is beyond the scope of the current optimization work. Under order of addition **A**, when the HBPin is added before the ligand (dtbpy for this experiment), reactions gave similar yields to reactions without metal salt additives (entries 1-6 in Table 2.6).

**Table 2.6.** Metal Additive Screen for In-Situ Precatalyst Generation.

entry	precatalyst	additive	Condition A <sup>a</sup>	Condition B <sup>a</sup>
1	2	K(acac)	14	32
2	2	Na(acac)	13	28
3	2	Al(acac) <sub>3</sub>	13	0
4	2	Ti(O)(acac) <sub>2</sub>	14	27
5	2	--	14	0
6	2	Mg(OMe) <sub>2</sub>	14	2
7	2	KOMe	0	14
8	2	KO <i>t</i> -Bu	20	34
9	1	K(acac)	0	0
10	1	Na(acac)	5	6
11	1	Al(acac) <sub>3</sub>	33	33
12	1	Ti(O)(acac) <sub>2</sub>	30	31
13	1	--	33	33
14	1	Mg(OMe) <sub>2</sub>	33	32
15	1	KOMe	15	9
16	1	KO <i>t</i> -Bu	7	7
17	3	--	31	30

<sup>a</sup>5 mol% metal additive added to reaction vial before all other reagents.

## REFERENCES

## REFERENCES

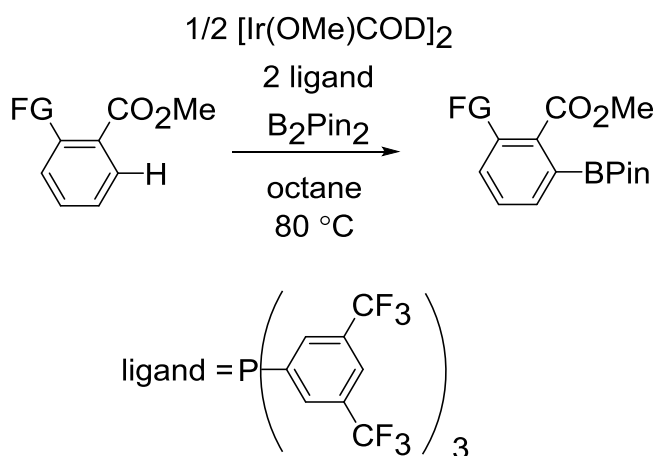
- 1) Mkhallid, I. A. I.; Barnard, J. H.; Marder, T. B.; Murphy, J. M.; Hartwig, J. F. *Chem. Rev.* **2010**, *110*, 890.
- 2) (a) The following articles on C–H borylation have been published since the review article cited in ref. 1: Kallepalli, V. A.; Sanchez, L.; Li, H.; Gesmundo, N. J.; Turton, C. L.; Maleczka, R. E., Jr.; Smith, M. R., III *Heterocycles* **2010**, *80*, 1429; (b) Liskey, C. W.; Liao, X. B.; Hartwig, J. F. *J. Am. Chem. Soc.* **2010**, *132*, 11389; (c) Robbins, D. W.; Boebel, T. A.; Hartwig, J. F. *J. Am. Chem. Soc.* **2010**, *132*, 4068; (d) Itoh, H.; Kikuchi, T.; Ishiyama, T.; Miyaura, N. *Chem. Lett.* **2011**, *40*, 1007; (e) Li, G. Q.; Kiyomura, S.; Yamamoto, Y.; Miyaura, N. *Chem. Lett.* **2011**, *40*, 702; (f) Liao, X. B.; Stanley, L. M.; Hartwig, J. F. *J. Am. Chem. Soc.* **2011**, *133*, 2088; (g) Nguyen, D. H.; Perez-Torrente, J. J.; Lomba, L.; Jimenez, M. V.; Lahoz, F. J.; Oro, L. A. *Dalton Trans.* **2011**, *40*, 8429; (h) Norberg, A. M.; Smith, M. R., III; Maleczka, R. E., Jr. *Synthesis* **2011**, 857; (i) Ozawa, R.; Yoza, K.; Kobayashi, K. *Chem. Lett.* **2011**, *40*, 941; (j) Ros, A.; Estepa, B.; Lopez-Rodriguez, R.; Alvarez, E.; Fernandez, R.; Lassaletta, J. M. *Angew. Chem. Int. Ed.* **2011**, *50*, 11724; (k) Teraoka, T.; Hiroto, S.; Shinokubo, H. *Org. Lett.* **2011**, *13*, 2532; (l) Cheng, J. H.; Yi, C. L.; Liu, T. J.; Lee, C. F. *Chem. Commun.* **2012**, *48*, 8440; (m) Crawford, A. G.; Liu, Z. Q.; Mkhallid, I. A. I.; Thibault, M. H.; Schwarz, N.; Alcaraz, G.; Steffen, A.; Collings, J. C.; Batsanov, A. S.; Howard, J. A. K.; Marder, T. B. *Chem. Eur. J.* **2012**, *18*, 5022; (n) Eliseeva, M. N.; Scott, L. T. *J. Am. Chem. Soc.* **2012**, *134*, 15169; (o) Hartwig, J. F. *Acc. Chem. Res.* **2012**, *45*, 864; (p) Hitosugi, S.; Nakamura, Y.; Matsuno, T.; Nakanishi, W.; Isobe, H. *Tetrahedron Lett.* **2012**, *53*, 1180; (q) Hume, P.; Furkert, D. P.; Brimble, M. A. *Tetrahedron Lett.* **2012**, *53*, 3771; (r) Liskey, C. W.; Hartwig, J. F. *J. Am. Chem. Soc.* **2012**, *134*, 12422; (s) Liu, T. F.; Shao, X. X.; Wu, Y. M.; Shen, Q. L. *Angew. Chem. Int. Ed.* **2012**, *51*, 540; (t) Ohmura, T.; Torigoe, T.; Suginome, M. *J. Am. Chem. Soc.* **2012**, *134*, 17416; (u) Robbins, D. W.; Hartwig, J. F. *Org. Lett.* **2012**, *14*, 4266; (v) Roering, A. J.; Hale, L. V. A.; Squier, P. A.; Ringgold, M. A.; Wiederspan, E. R.; Clark, T. B. *Org. Lett.* **2012**, *14*, 3558; (w) Roosen, P. C.; Kallepalli, V. A.; Chattopadhyay, B.; Singleton, D. A.; Maleczka, R. E., Jr.; Smith, M. R., III *J. Am. Chem. Soc.* **2012**, *134*, 11350; (x) Ros, A.; Lopez-Rodriguez, R.; Estepa, B.; Alvarez, E.; Fernandez, R.; Lassaletta, J. M. *J. Am. Chem. Soc.* **2012**, *134*, 4573; (y) Wang, C.; Sperry, J. *J. Org. Chem.* **2012**, *77*, 2584. (z) Lopez-Rodríguez, R.; Ros, A.; Fernandez, R.; Lassaletta, J. M. *J. Org. Chem.* **2012**, *77*, 9915.
- 3) Ishiyama, T.; Takagi, J.; Hartwig, J. F.; Miyaura, N. *Angew. Chem. Int. Ed.* **2002**, *41*, 3056.
- 4) Kikuchi, T.; Takagi, J.; Isou, H.; Ishiyama, T.; Miyaura, N. *Chem Asian J* **2008**, *3*, 2082-90.
- 5) Boller, T. M.; Murphy, J. M.; Hapke, M.; Ishiyama, T.; Miyaura, N.; Hartwig, J. F. *J Am Chem Soc* **2005**, *127*, 14263-78.
- 6) Mestroni, G.; Camus, A.; Zassinovich, G. *J. Organomet. Chem.* **1974**, *73*, 119.

- 7) Filipuzzi, S.; Farnetti, E. *J. Mol. Catal. A: Chem.* **2005**, 238, 111.
- 8) Liskey, C. W.; Wei, C. S.; Pahls, D. R.; Hartwig, J. F. *Chem Commun* **2009**, 5603-5605.
- 9) Vanchura, B. A., II; Preshlock, S. M.; Roosen, P. C.; Kallepalli, V. A.; Staples, R. J.; Maleczka, R. E., Jr; Smith, M. R., III *Chem. Commun.* **2010**, 46, 7724.
- 10) Iwadate, N.; Suginome, M. *J Organomet Chem* **2009**, 694, 1713-1717.
- 11) Vanchura, B. A., II *Ph. D. Thesis, Mich. State University*, **2010**.
- 12) The electron-donating ability of dipyriddy (dpy) ligands to transition metals can be estimated from relative  $\nu_{\text{CO}}$  frequencies in dpy metal carbonyl complexes or by evaluating their effects on redoxpotentials in dpy complexes. From the average  $\nu_{\text{CO}}$  frequencies in (dpy)Cr(CO)<sub>4</sub> complexes (refs 13a and d) and E° values for Ru<sup>2+/3+</sup> in Ru(dpy)<sub>3</sub><sup>2+</sup> compounds (refs 13b and c), the electron-donor ability increases in the order dtbpy < tmphen << dmabpy.
- 13) (a) Connor, J. A.; Overton, C. *J. Organomet. Chem.* **1983**, 249, 165. (b) Leidner, C. R.; Murray, R. W. *J. Am. Chem. Soc.* **1984**, 106, 1606. (c) Nazeeruddin, M. K.; Zakeeruddin, S. M.; Kalyanasundaram, K. *J. Phys. Chem.* **1993**, 97, 9607. (d) Johnson, R.; Madhani, H.; Bullock, J. P. *Inorg. Chim. Acta* **2007**, 360, 3414.

## CHAPTER 3

### CHELATE DIRECTED C-H BORYLATIONS

**Figure 3.1.** Ester directed C-H borylation.



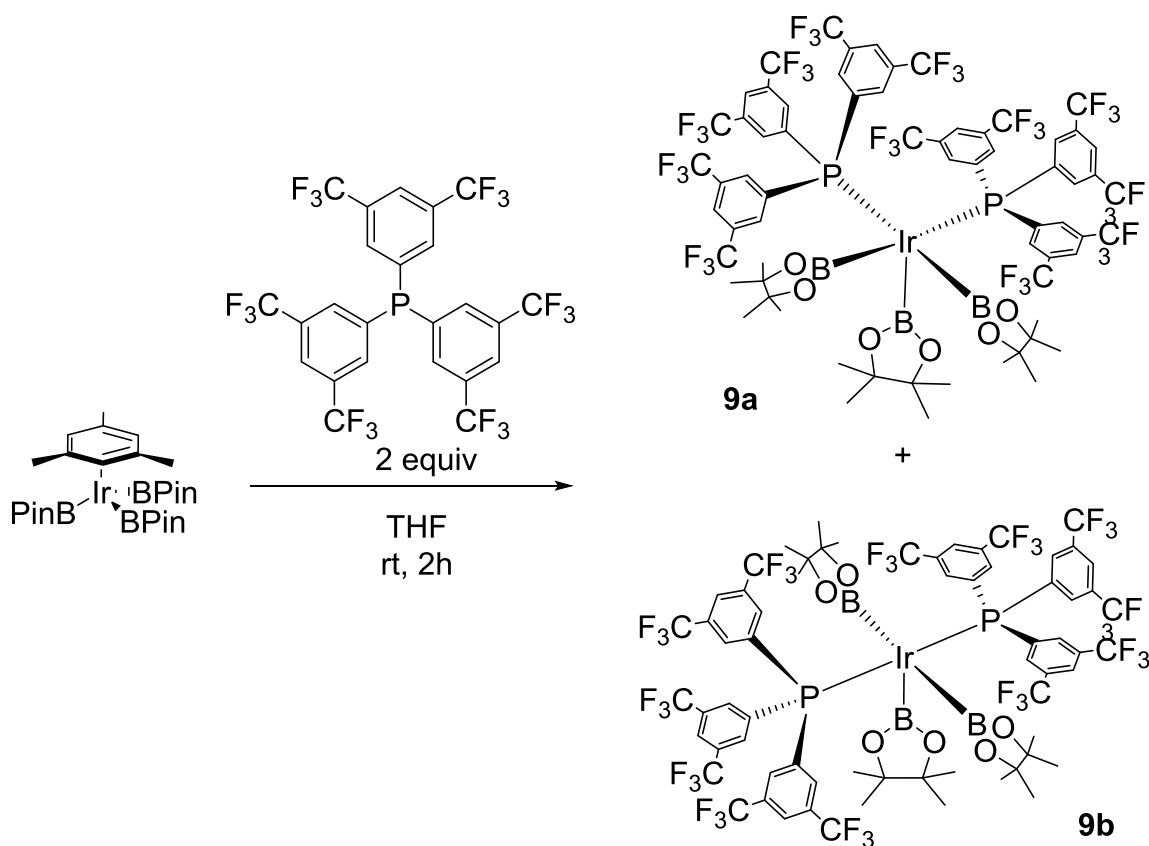
#### Ester directed C-H borylation.

As mentioned in Chapter 1, the regioselectivities of products formed from Ir catalyzed C-H borylation of arenes are primarily controlled by steric effects. We have seen examples in Chapter 1 where substantial electronic effects can influence regioselectivity and in Chapter 4 we will discuss outer sphere directing effects. There have been several examples where borylation occurs *ortho* to a carbonyl via inner sphere chelate directed C-H borylation. In 2008, Miyaura reported the *ortho*-borylation of a number methyl benzoates using the catalyst system  $[\text{Ir}(\text{OMe})\text{COD}]_2$  with 4 equivalents of  $\text{P}(3,5\text{-bis}(\text{CF}_3)_2\text{-C}_6\text{H}_3)_3$  ( $\text{PAr}^{\text{F}}_3$ ) ligand (Figure 3.1).<sup>1</sup> More recently, silica-supported mono(phosphine)-Ir systems have been shown to give similar selectivities with various benzoate derivatives and even great selectivity for borylation *ortho* to chlorine in chlorobenzene.<sup>2</sup> The selectivity of the silica-supported chemistry is believed to occur



as a result of the silica-supported SMAP ligands ability to generate 14 e<sup>-</sup> intermediates. It is of significant note that HBPin was ineffective for catalysis in both cases. Sawamura has since extended the silica-supported phosphine chemistry to *ortho* directed phenol surrogates utilizing HBPin as borylating reagent<sup>3</sup> and primary and secondary bonds in 2-substituted alkyl pyridines.<sup>4</sup>

**Figure 3.2.** *Cis* and *Trans*-(Ar<sup>F</sup><sub>3</sub>P)<sub>2</sub>Ir(BPin)<sub>3</sub>.

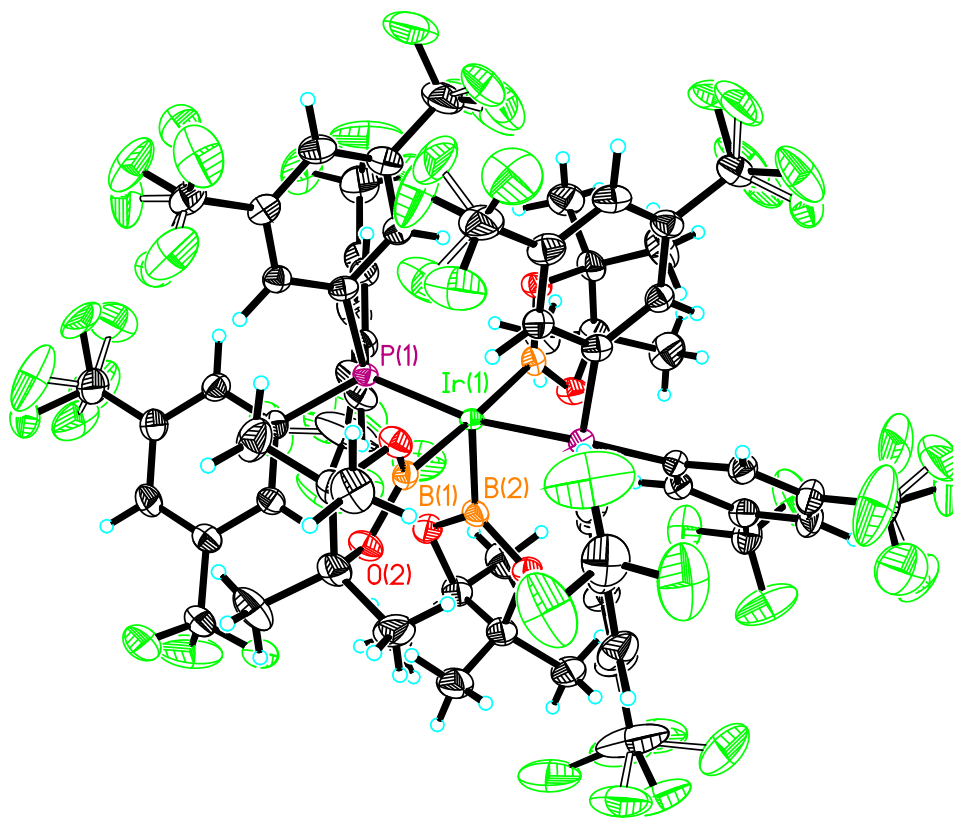


### Synthesis of Discrete 5 Coordinate $(\text{Ar}^{\text{F}}_3\text{P})_2\text{Ir}(\text{BPin})_3$ Trisboryl Complex

Using the procedure first reported by Smith and coworkers,<sup>5</sup> we attempted to isolate Ir complexes relevant to the ester directed C-H borylation reported by Miyaura.<sup>1</sup> Attempts to

isolate  $(\text{Ar}^{\text{F}}_3\text{P})_2\text{Ir}(\text{BPin})_3$  in the reaction between  $(\eta^6\text{-C}_6\text{Me}_3\text{H}_3)\text{Ir}(\text{BPin})_3$  and two equivalents of  $\text{PAr}^{\text{F}}_3$ , the 6 electron arene ligand is displaced to give two products in a 2 : 1 ratio believed to be *cis*- $(\text{Ar}^{\text{F}}_3\text{P})_2\text{Ir}(\text{BPin})_3$  (**9a**) and *trans*- $(\text{Ar}^{\text{F}}_3\text{P})_2\text{Ir}(\text{BPin})_3$  (**9b**), (Figure 3.2).

**Figure 3.3.** *Trans*- $(\text{Ar}^{\text{F}}_3\text{P})_2\text{Ir}(\text{BPin})_3$  (**9b**). The following are 50% thermal ellipsoidal drawings of the molecule in the asymmetric cell with various amount of labeling.

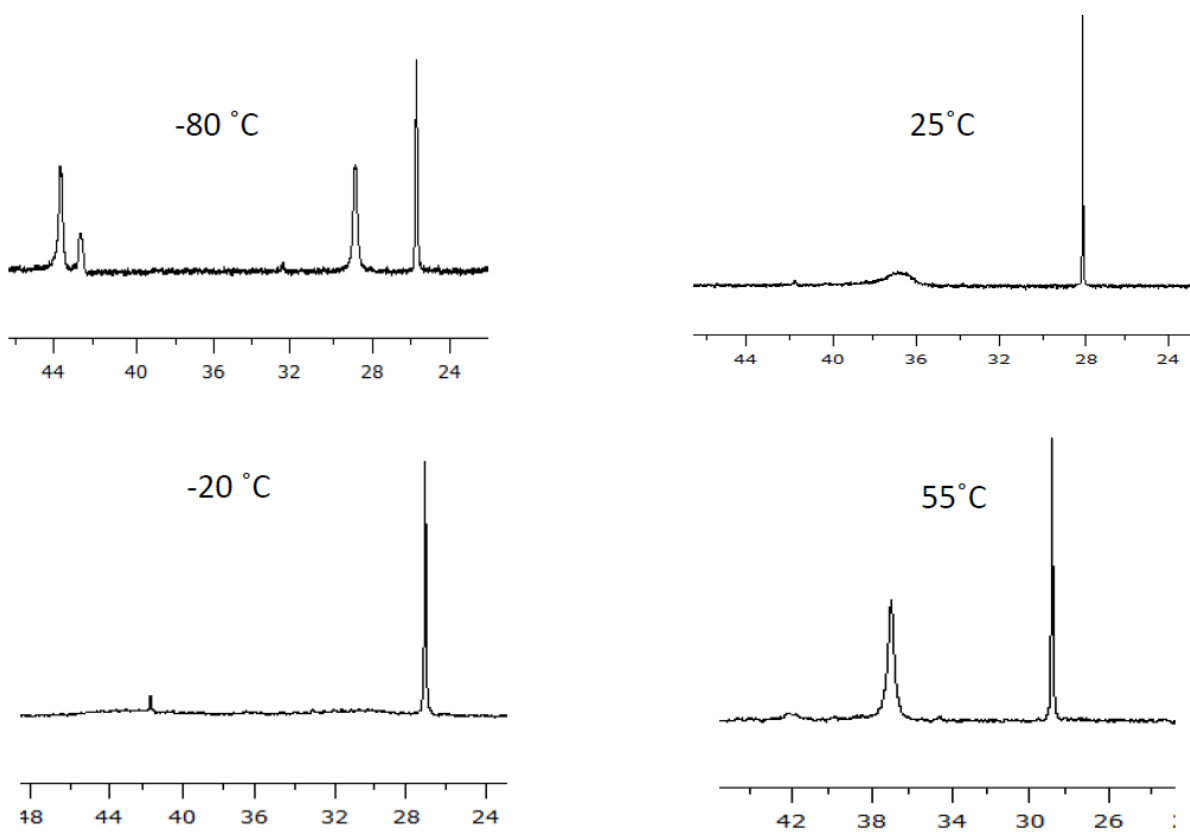


A crystal structure of the **9b** isomer was obtained by recrystallization from THF / pentane at -35 °C (Figure 3.3). The structure of **9b** is of note as being the first and only known example of a metal complex containing *trans* boryl ligands. The *trans* boryl geometry is generally disfavored due to strong ligand-to-metal  $\sigma$ -donation for metal boryl ligands. It is generally expected that for complexes of the type M-B(OR)<sub>2</sub> the metal(d)-to-ligand(p)  $\pi$ -back-bonding is relatively weak compared to the  $\pi$ -interaction between B atom and its diol substituents (pinacol in the case of BPin complexes). The  $\sigma$ -donor strength of the boryl ligands is extremely potent due to boron being even more electropositive than carbon and causes it to have a strong *trans* influence.<sup>6</sup> Ultimately, the *trans*-(Ar<sup>F</sup><sub>3</sub>P)<sub>2</sub>Ir(BPin)<sub>3</sub> geometry of **9b** is most likely the result of the large steric bulk of the two (PAr<sup>F</sup><sub>3</sub>) ligands, while the structure of the *cis*-(Ar<sup>F</sup><sub>3</sub>P)<sub>2</sub>Ir(BPin)<sub>3</sub> isomer **9a** would be the electronically favored product.

The proposed structures of the two isomers were supported by integration from <sup>1</sup>H and <sup>31</sup>P NMR. Addition of excess PAr<sup>F</sup><sub>3</sub> ligand did not perturb the isomer ratio and no coordination of a third PAr<sup>F</sup><sub>3</sub> ligand to form a (Ar<sup>F</sup><sub>3</sub>P)<sub>3</sub>Ir(BPin)<sub>3</sub> species was observed most likely due to the PAr<sup>F</sup><sub>3</sub> ligand's steric bulk. Variable temperature <sup>31</sup>P NMR demonstrated that the major isomer had two inequivalent PAr<sup>F</sup><sub>3</sub> ligands at lower temperatures, broadening into the baseline at 0 °C to -20 °C and sharpening considerably at -80 °C (Figure 3.4). The single peak observed at room temperature suggests that at ambient temperature the phosphine ligands undergo rapid exchange on the NMR time scale. At higher temperatures (55 °C) the signal sharpens substantially.

Unfortunately the complex undergoes decomposition at higher temperatures after prolonged heating.

**Figure 3.4.** Variable temperature  $^{31}\text{P}$  NMR of *Cis* and *Trans*-(Ar<sup>F</sup><sub>3</sub>P)<sub>2</sub>Ir(BPin)<sub>3</sub>.

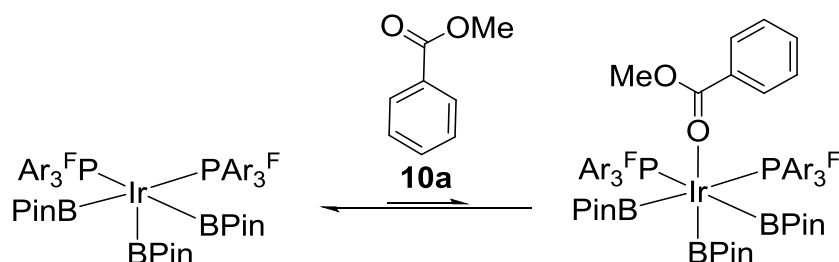


Multiple attempts to crystallize the major isomer have so far proven futile and it appears that the complex may only crystallize as **9b**. Behnaz Ghaffari has shown that samples dissolved at low temperature are of the single isomer **9b** and that they equilibrate over time.

## Mechanistic Insights into $(\text{Ar}^{\text{F}}_3\text{P})_2\text{Ir}(\text{BPin})_3$ Catalytic Cycle

Having isolated and identified the  $^{31}\text{P}$  NMR resonances of the *cis* and *trans*- $(\text{Ar}^{\text{F}}_3\text{P})_2\text{Ir}(\text{BPin})_3$  mixture, we verified that these catalysts were formed using the standard catalytic conditions. Indeed, heating a mixture of  $[\text{Ir}(\text{OMe})\text{COD}]_2$  with 4 equivalents of  $\text{PAr}^{\text{F}}_3$  ligand in the presence of 4 equivalents of  $\text{B}_2\text{Pin}_2$  formed the *cis* and *trans*- $(\text{Ar}^{\text{F}}_3\text{P})_2\text{Ir}(\text{BPin})_3$  mixture as the major products, confirming that the complexes were present during catalysis.

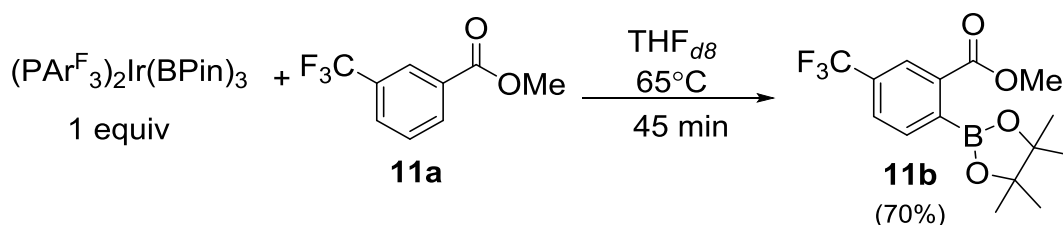
**Figure 3.5.** Ester coordination to  $(\text{Ar}^{\text{F}}_3\text{P})_2\text{Ir}(\text{BPin})_3$  complex.



We next attempted to determine which of the isomers was responsible for ester directed C-H borylation. Dissolving  $(\text{Ar}^{\text{F}}_3\text{P})_2\text{Ir}(\text{BPin})_3$  in  $\text{THF}_{d8}$  with 10 equivalents methyl benzoate (**10a**) did not produce any observable reaction and no free  $\text{PAr}^{\text{F}}_3$  ligand was observed in  $^{31}\text{P}$  NMR at room temperature. We hypothesize that initial ester coordination to the iridium catalyst is the source of the ester directing effect (Figure 3.5). The fact that the resulting intermediate is not observed, suggests ester coordination may be the rate limiting step. However, such experiments have not been done to rule out phosphine dissociation. An NMR tube experiment with  $(\text{Ar}^{\text{F}}_3\text{P})_2\text{Ir}(\text{BPin})_3$  and 10 equivalents of tetrahydrothiophene (THT) did produce free  $\text{PAr}^{\text{F}}_3$

ligand and a new phosphine iridium species at 4 ppm in  $^{31}\text{P}$  NMR in a 1 : 1 ratio. After 30 min, the major isomer **9a** had disappeared while **9b** remained, suggesting the former was the reactive species. After 24h the reaction mixture had gone completely to the new species at 4 ppm and free  $\text{PAr}^{\text{F}}_3$  suggesting **9b** reacts at a much slower rate than **9a** or **9a** must first undergo isomerization to the active isomer and then reacts.

**Figure 3.6.** Stoichiometric borylation of methyl 3-(trifluoromethyl)benzoate (**11a**).



Reacting  $(\text{Ar}^{\text{F}}_3\text{P})_2\text{Ir}(\text{BPin})_3$  directly with methyl 3-(trifluoromethyl)benzoate (**11a**) at  $65^\circ\text{C}$  for 45 min in  $\text{THF}_{d8}$  led to the formation of methyl 2-(4,4,5,5-tetramethyl-1,3,2-dioxaborolan-2-yl)-5-(trifluoromethyl)benzoate (**11b**) in 70% yield (Figure 3.6).  $^{31}\text{P}$  NMR showed two major phosphorous containing compounds, which accounted for a combined 80% of the products formed from the stoichiometric borylation of **11a**. Crystals obtained from the reaction mixture gave the X-Ray structure for a  $\text{trans}-(\text{Ar}^{\text{F}}_3\text{P})_2\text{Ir}(\text{H})(\text{BPin})_2$  (**12**) complex (Figure 3.7) which was in agreement with a minor product with the chemical formula  $\text{Ir}(\text{H})\text{BPin}_2$  and had a  $^{31}\text{P}$  resonance at 33 ppm and pinacol resonances at 0.47 and 0.25 ppm and hydride peak at -7.95 ppm (t,  $J = 18.6$  Hz, 1H).

**Figure 3.7.** *Trans*-(Ar<sup>F</sup><sub>3</sub>P)<sub>2</sub>Ir(H)(BPin)<sub>2</sub> (**12**). The following are 50% thermal ellipsoidal drawings of the molecule in the asymmetric cell with various amount of labeling.

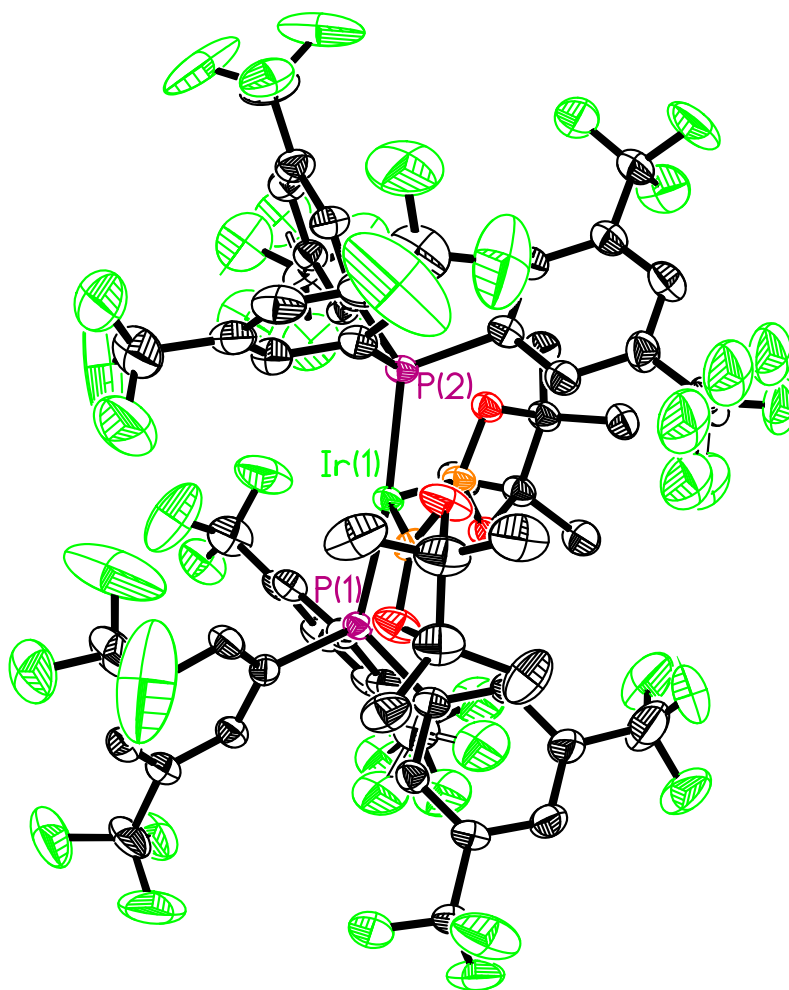
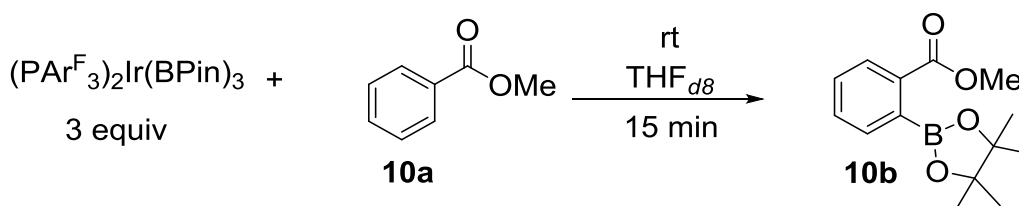


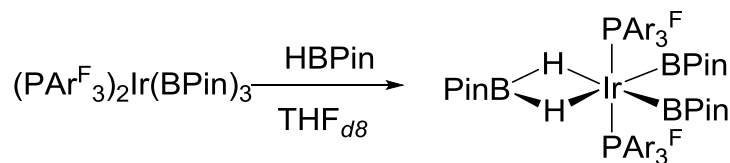
**Figure 3.8.** Borylation of methyl benzoate (**10a**) with excess  $(\text{Ar}^{\text{F}}_3\text{P})_2\text{Ir}(\text{BPin})_3$ .



Reacting  $(\text{Ar}^{\text{F}}_3\text{P})_2\text{Ir}(\text{BPin})_3$  directly with 0.33 equivalents of methyl benzoate (**10a**) at room temperature for 15 min in  $\text{THF}_{d8}$  led to the formation of methyl 2-(4,4,5,5-tetramethyl-1,3,2-dioxaborolan-2-yl)benzoate (**10b**) (Figure 3.8).  $^{31}\text{P}$  NMR showed the formation of three new phosphorous containing compounds, which corresponded to three hydride peaks observed in the  $^1\text{H}$  NMR. A  $^1\text{H}$ - $^{31}\text{P}$  gHMQC experiment determined there was a correlation between the  $^{31}\text{P}$  resonances at 21.6 ppm and a hydride peak at -8.29 ppm (d,  $J = 10.0$  Hz). This compound was the major product formed from reaction of  $(\text{Ar}^{\text{F}}_3\text{P})_2\text{Ir}(\text{BPin})_3$  and **10a**. A second correlation between  $^{31}\text{P}$  resonances at 26.4 ppm and a hydride resonance at -6.55 ppm (dd,  $J = 141.8, 24$  Hz) was identified. This compound was the second most abundant product formed, the major was present in a 2:1 ratio with respect to this species and the hydride without a  $^1\text{H}$ - $^{31}\text{P}$  gHMQC correlation was present in a 1:0.7 ratio. The  $^{31}\text{P}$  resonances at 25.8 ppm and a hydride resonance at -8.49 ppm showed no evidence of coupling in the  $^1\text{H}$ - $^{31}\text{P}$  gHMQC, but their integrations relative to the other  $^{31}\text{P}$  resonances and hydride resonances were roughly equivalent, so there is a possibility they belong to the same species. It should also be noted that none of these were major species observed in the experiment depicted in Figure 3.6.



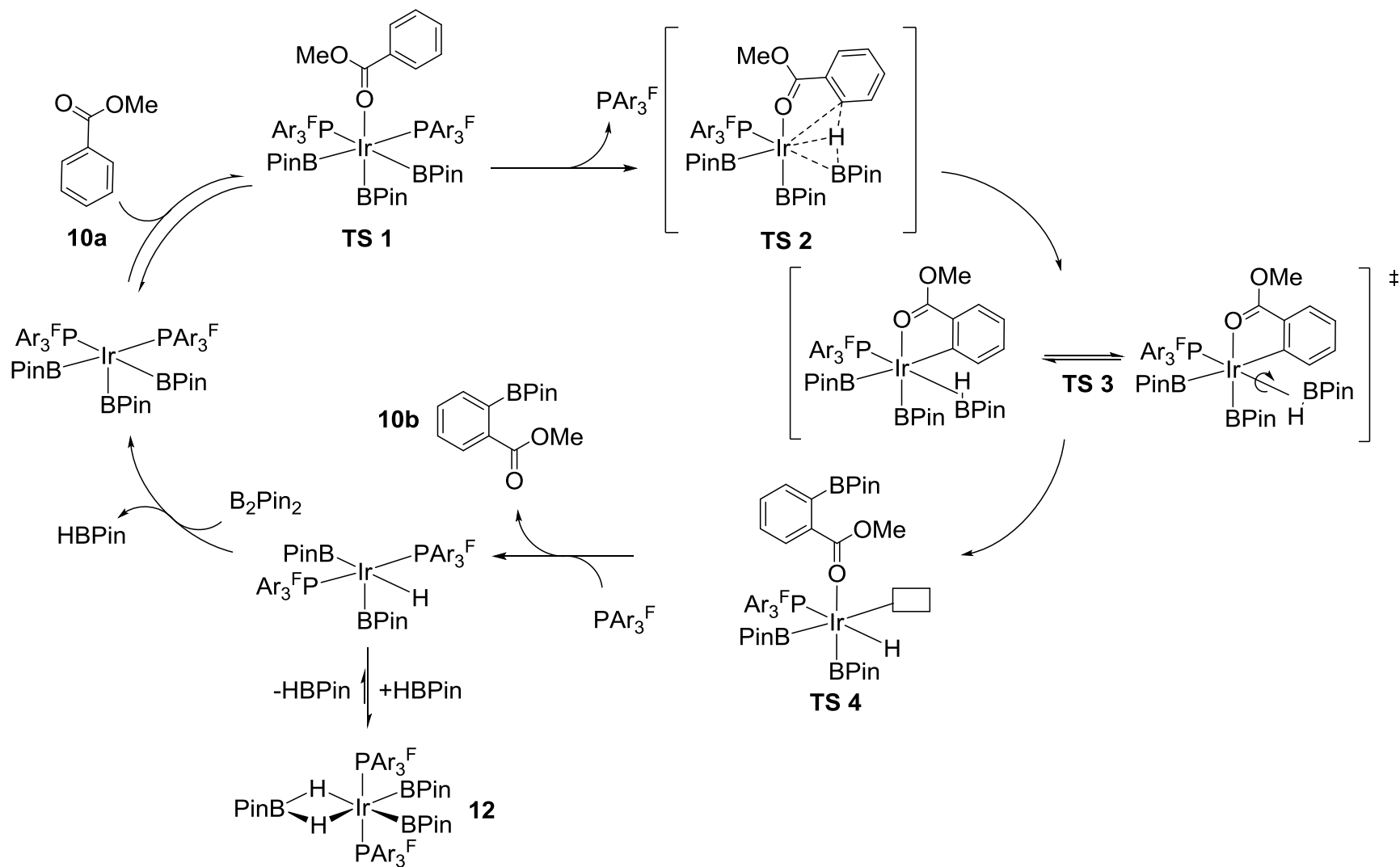
**Figure 3.9.** *Trans*-(Ar<sup>F</sup><sub>3</sub>P)<sub>2</sub>Ir(H<sub>2</sub>BPin)(BPin)<sub>2</sub> (**13**).

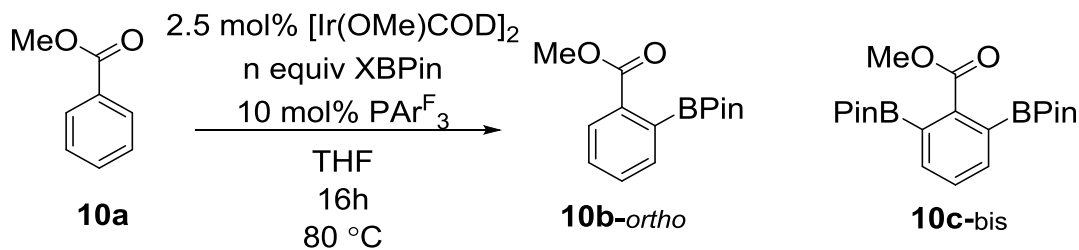


With the aid and hard work of Behnaz Ghaffari we were able to obtain an X-Ray crystal structure of a *trans*-(Ar<sup>F</sup><sub>3</sub>P)<sub>2</sub>Ir(H<sub>2</sub>BPin)(BPin)<sub>2</sub> (**13**) complex (Figure 3.9) formed from the reaction of (Ar<sup>F</sup><sub>3</sub>P)<sub>2</sub>Ir(BPin)<sub>3</sub> with **11a** in THF. This compound was independently synthesized from (Ar<sup>F</sup><sub>3</sub>P)<sub>2</sub>Ir(BPin)<sub>3</sub> and HBPIn in nearly quantitative yields with mild heating. This structure had a single <sup>31</sup>P NMR resonance at 16 ppm and pinacol resonances at 0.62 (s, 12H), 0.54 (br s, 24H) and a hydride resonance at -7.00 ppm (br s, 2H) in the <sup>1</sup>H NMR which were identical to a species formed during the stoichiometric reaction of (Ar<sup>F</sup><sub>3</sub>P)<sub>2</sub>Ir(BPin)<sub>3</sub> and **11a**.

A putative catalytic cycle is shown in Figure 3.10 for the chelate directed borylation of aryl esters with (Ar<sup>F</sup><sub>3</sub>P)<sub>2</sub>Ir(BPin)<sub>3</sub> based on the results from our previous experiments. Initially, the methyl benzoate coordinates to **9a** via its carbonyl. This is proceeded by PAr<sup>F</sup><sub>3</sub> ligand dissociation and directed oxidative addition or sigma bond metathesis of an *ortho* C-H bond, ligand rearrangement and subsequent reductive elimination to give a **TS 4** complex. Ligand displacement by a PAr<sup>F</sup><sub>3</sub> ligand could lead to complex **12** we obtained an X-Ray crystal structure for. This intermediate could react with B<sub>2</sub>Pin<sub>2</sub> to regenerate the (Ar<sup>F</sup><sub>3</sub>P)<sub>2</sub>Ir(BPin)<sub>3</sub> active catalyst or react with HBPIn to form the **13** complex.

**Figure 3.10.** Proposed catalytic cycle for the chelate directed borylation of aryl esters with  $(\text{Ar}^{\text{F}}_3\text{P})_2\text{Ir}(\text{BPin})_3$ .

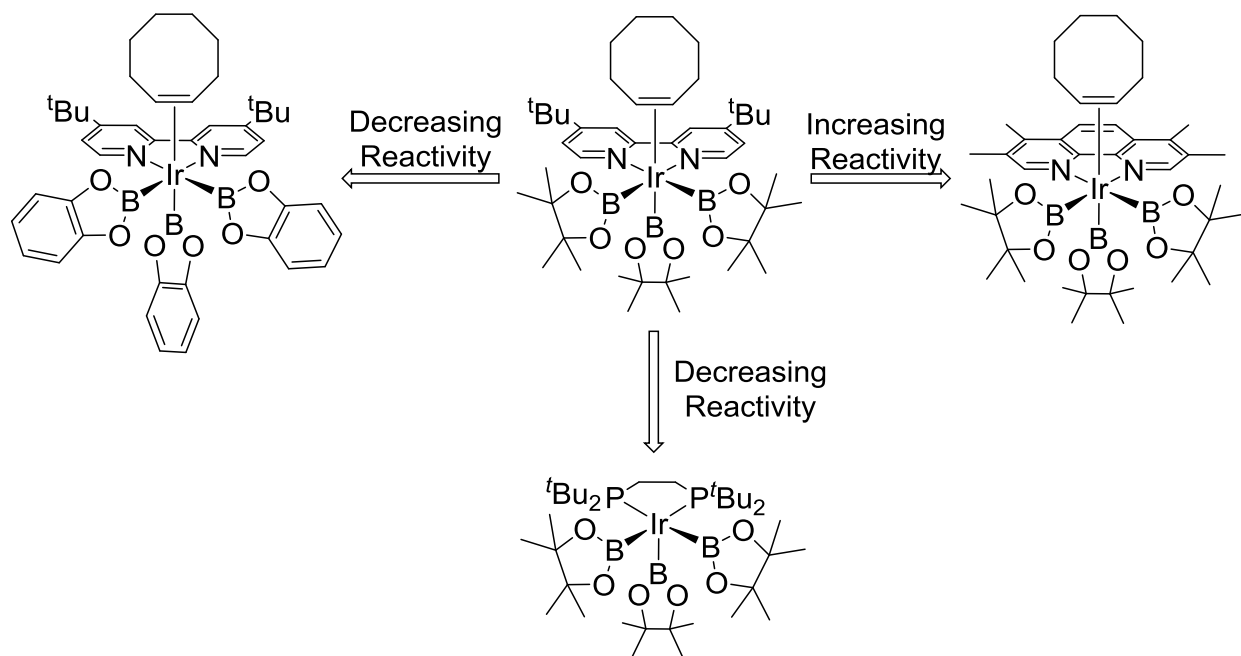


**Table 3.1.** Borane effects on *ortho*-directed borylation of **10a**.

entry	equiv HBpin	equiv $\text{B}_2\text{Pin}_2$	<i>ortho</i> (%)	<i>bis</i> (%)
1	<b>1.0</b>	0.0	0	0
2	<b>1.0</b>	<b>1.0</b>	7	0
3	0.0	<b>1.0</b>	55	8
4	0.0	<b>2.0</b>	56	21

A series of experiments was done to determine the effect borane had on the reactivity of these  $(\text{Ar}^{\text{F}}_3\text{P})_2\text{Ir}(\text{BPIn})_3$  catalysts. Table 3.1 shows that there were no borylation products formed when HBPin was used as borylating reagent and that HBPin had a deleterious effect when  $\text{B}_2\text{Pin}_2$  was used as borylating reagent (entries 2 and 4). These results corroborated what was presented in the initial report by Miyaura<sup>1b</sup> and suggest the **13** complex is a thermodynamic sink, although further experimentation has not been done to confirm this.

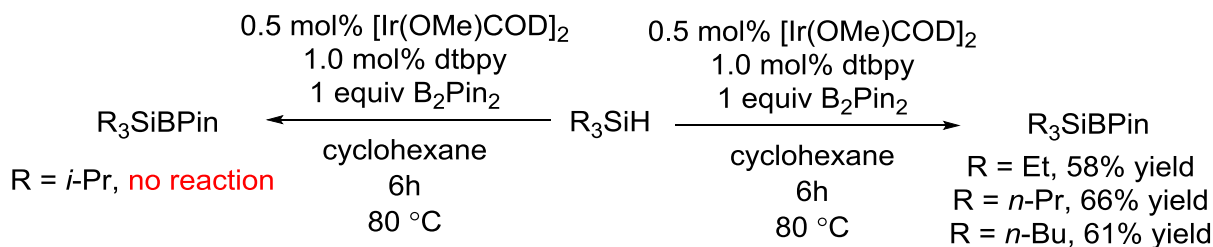
**Figure 3.11.** Designing more reactive Iridium catalysts.



It was identified early in the development of iridium catalyzed C-H borylation chemistry that more electron rich ligands generate catalysts that are more reactive than catalysts containing electron deficient ligands (Figure 3.11). An early example which illustrates this well is the comparison of catalysts derived from  $[\text{Ir}(\text{OMe})\text{COD}]_2$  and 4,4'-di-chloro-2,2'-bipyridine which show far lower reactivity than catalysts utilizing dtbpy and  $[\text{Ir}(\text{OMe})\text{COD}]_2$ .<sup>7</sup> Steric hindrance can also effect a catalysts reactivity as has been demonstrated with the isolated five-coordinate iridium trisboryl complexes,  $(\text{dippe})\text{Ir}(\text{BPin})_3$  and  $(\text{dtbpe})\text{Ir}(\text{BPin})_3$  where dtbpe is (1,2-bis(di-tert-butylphosphino)ethane). A comparison of the stoichiometric borylation of 2-methylthiophene occurred much faster with  $(\text{dippe})\text{Ir}(\text{BPin})_3$  than with  $(\text{dtbpe})\text{Ir}(\text{BPin})_3$  due to the decrease in steric hindrance of the phosphine ligands.<sup>8</sup>

Changing the ancillary boryl ligands proved to have a tremendous effect on the the reactivity of the similar iridium catalysts  $(dtbpy)Ir(BPin)_3(COE)$  and  $(dtbpy)Ir(BCat^*)_3(COE)$  were  $BCat^*$  is 4-*tert*-butylcatecholboryl.<sup>9</sup> Comparisons of the reactivity of those catalyst complexes with benzene highlight the effect the structural changes have on reactivity, with the former reacting at room temperature to produce three equivalents of PhBPin and the latter being stable for several hours at room temperature in a benzene solution. Additionally, the carbonyl analogues were prepared,  $(dtbpy)Ir(BPin)_3(CO)$  and  $(dtbpy)Ir(BCat^*)_3(CO)$ , and the  $U_{CO}$  value corresponding to the CO stretch was 30 wavenumbers greater for the tris- $BCat^*$  complex than that for the tris-BPin complex.

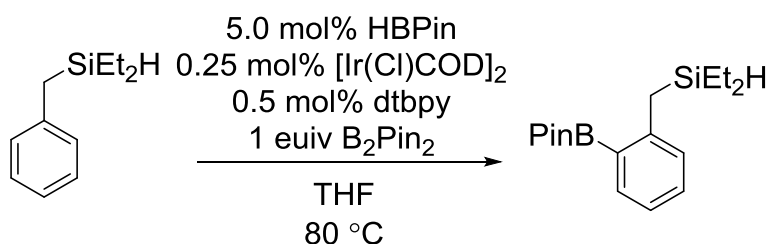
**Figure 3.12.** Synthesis of silylboranes.



Given that the trend of increasing electron density at the iridium center leads to catalysts that are more active towards C-H borylation reactions and silyl ligands are calculated to have even stronger  $\sigma$ -donor abilities than boryl ligands,<sup>6</sup> we sought to design ligands that would incorporate Si-Ir into the catalyst system. The Hartwig group has reported the synthesis of mixed  $R_3SiBPin$  complexes from the reaction of various  $R_3SiH$  and  $B_2Pin_2$  (Figure 3.12)<sup>10</sup> meaning

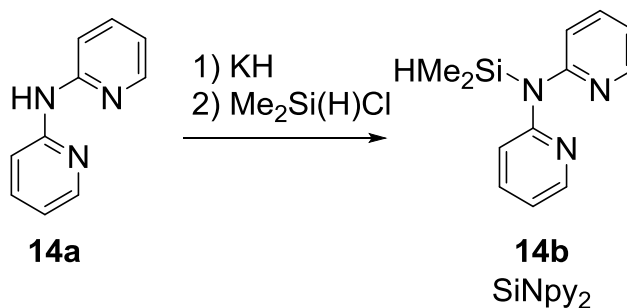
reductive elimination of Si-B compounds could be a potential decomposition pathway. Interestingly, when the bulky  $i\text{Pr}_3\text{SiH}$  are used no silylboranes form. In addition, HBPIn did not yield any silylboranes while identical reactions with  $\text{B}_2\text{Pin}_2$  would produce the corresponding silylboranes.

**Figure 3.13.** Silyl-directed *ortho* borylation of alkylamines.



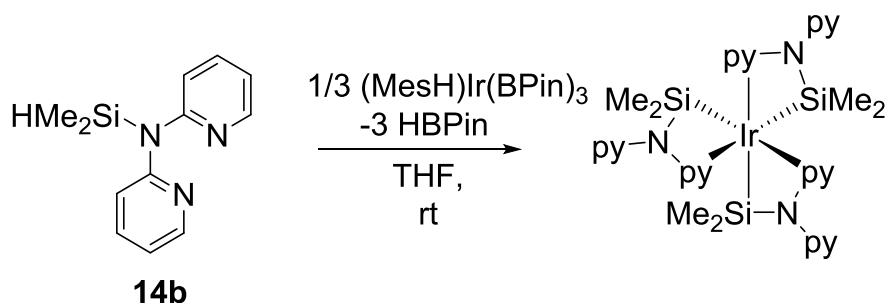
The Hartwig group was then able to do silyl-directed borylations using silylated phenols, arylamines, alkylamines<sup>11,12</sup> and N-H containing heterocycles.<sup>13</sup> In these reactions, the silyl group would serve as a chelating ligand to direct the C-H borylation and then undergo reductive elimination and regenerate the Si-H bond (Figure 3.13). The facile reductive elimination of the  $\text{ArEt}_2\text{Si-H}$  bond by iridium proved useful for catalytic reactions because it allowed for catalytic turnovers. Without such reversibility, the iridium catalyst would become saturated with silyl ligands or it would require additional equivalents of  $\text{B}_2\text{Pin}_2$  to generate  $\text{ArEt}_2\text{Si-BPin}$ .

**Figure 3.14.** N-(dimethylsilyl)-N,N-bis(2-pyridyl)amine (**14b**).



In our initial attempt to create silyl chelate ligands, we synthesized a N-(dimethylsilyl)-N,N-bis(2-pyridyl)-amine (**14b**) from di(2-pyridyl)amine (**14a**) and dimethylchlorosilane (Figure 3.14). We chose **14b** as a target because dipyridine ligands are among the most reactive ligands for iridium catalyzed C-H borylation reactions. We also speculated that the two chelating pyridal ligands would maintain Si-Ir coordination by preventing ligand disassociation since Si-H bond breaking and formation has proven reversible. We also concluded the Me<sub>2</sub>Si(H)Cl was an appropriate silane because excessive steric bulk impedes catalytic reactivity.<sup>8</sup>

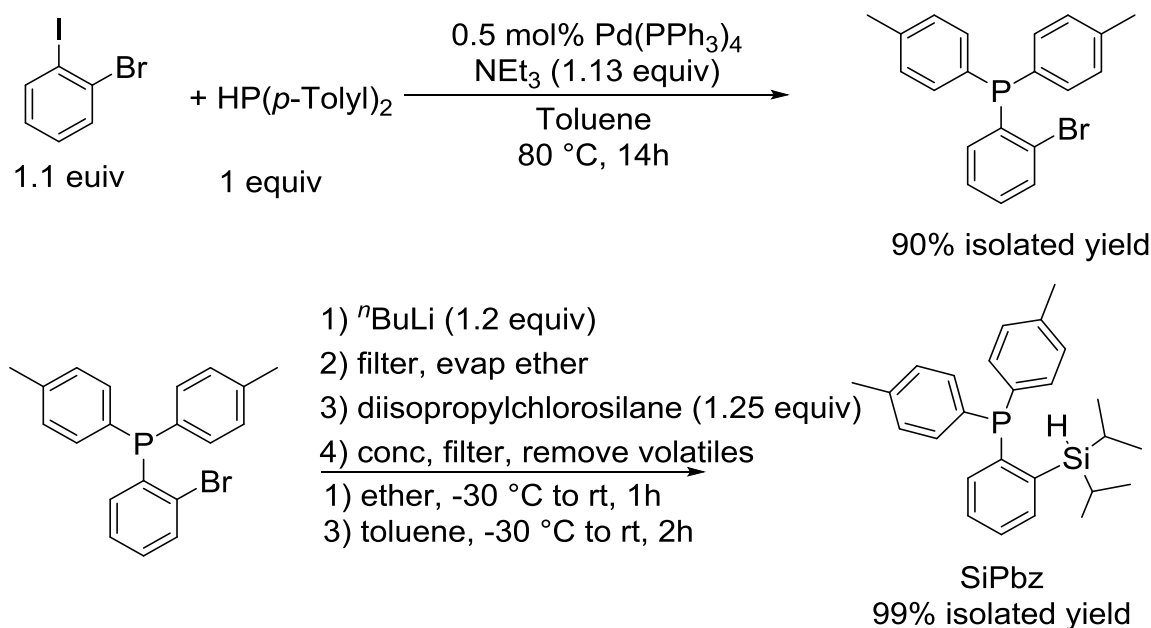
**Figure 3.15.** Synthesis of Ir( $\kappa^2$ -SiNpy<sub>2</sub>)<sub>3</sub>



Work by a co-researcher, Behnaz Ghaffari, showed the **14b** ligand reacted with  $(\text{MesH})\text{Ir}(\text{BPin})_3$  to form a coordinately saturated  $\text{Ir}(\kappa^2\text{-SiNpy}_2)_3$  complex (Figure 3.15).

Catalytic reactions with **14b** and  $[\text{Ir}(\text{OMe})\text{COD}]_2$  showed poor reactivity as well.

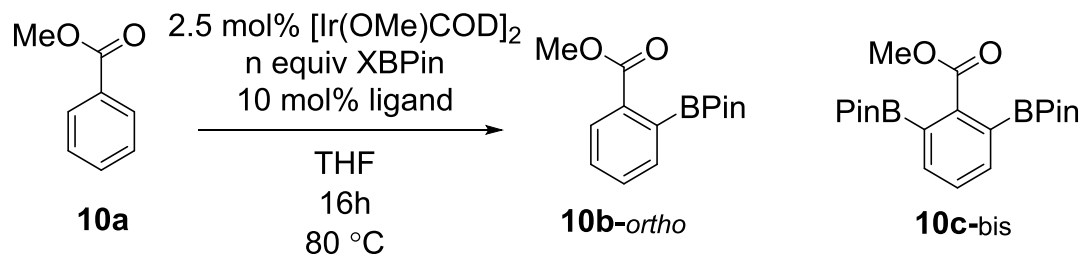
**Figure 3.16.** Synthesis of SiPbz ligands.



Realizing our first attempt at silyl ligands failed because of the dual calamities of being too sterically small, enabling multiple ligands to bond to the iridium center, and the ligands having an unconstrained backbone, allowing the tridentate **14b** to bind as a bidentate ligand. Our next generation of silyl ligands focused on a structural motif that would have a bulky *p*-Tolyl<sub>2</sub>P and <sup>i</sup>Pr<sub>2</sub>Si- coordination sites and a constrained benzene backbone (Figure 3.16). The (2-(diisopropylsilyl)phenyl)di-*p*-tolylphosphane (SiPbz) ligand could be made in two steps from commercially available starting materials and its synthesis (as well as that for the **14b** ligand) allowed for a platform that could be applied to analogues.



**Table 3.2.** Ligand effects on *ortho*-directed borylation of methyl benzoate (**10a**).



entry	ligand	equiv HBpin	equiv B <sub>2</sub> Pin <sub>2</sub>	<i>ortho</i> (%)	<i>bis</i> (%)
1	PAr <sup>F</sup> <sub>3</sub>	<b>1.0</b>	0.0	0	0
2	P(C <sub>6</sub> F <sub>5</sub> ) <sub>3</sub>	<b>1.0</b>	0.0	0	0
3	AsPh <sub>3</sub>	<b>1.0</b>	0.0	0	0
4	SbPh <sub>3</sub>	<b>1.0</b>	0.0	0	0
5	P(OCH(CF <sub>3</sub> ) <sub>2</sub> ) <sub>3</sub>	<b>1.0</b>	0.0	0	0
6	tppp	<b>1.0</b>	0.0	0	0
7	P(odtbz) <sub>3</sub>	<b>1.0</b>	0.0	0	0
8	Me-Verkade	<b>1.0</b>	0.0	0	0
9	SiPBz <sup>a</sup>	<b>1.0</b>	0.0	40 + 27*	0

\* 13% *meta* isomer and 14% *para* isomer. <sup>a</sup> 5 mol% ligand used.

**Ligand Key for Table 3.2.**

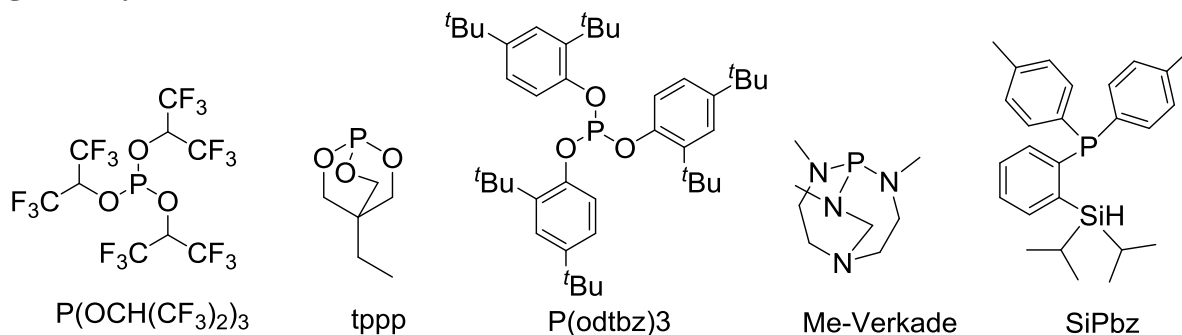
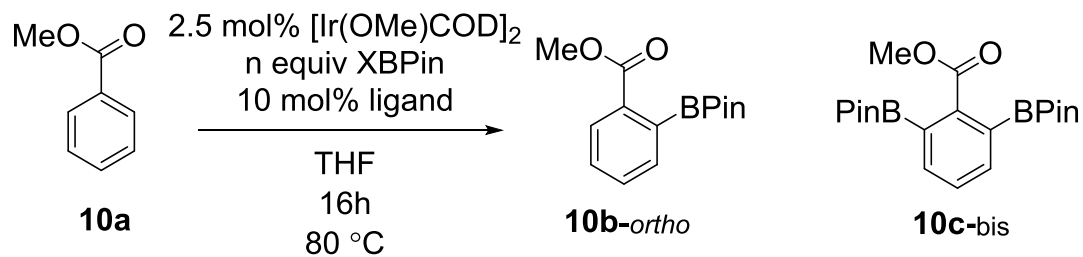


**Table 3.3.** Borane effects on *ortho*-directed borylation of methyl benzoate (**10a**).



entry	ligand	equiv HBpin	equiv B <sub>2</sub> Pin <sub>2</sub>	<i>ortho</i> (%)	<i>bis</i> (%)
1	PAr <sup>F</sup> <sub>3</sub>	<b>1.0</b>	<b>1.0</b>	7	0
2	PAr <sup>F</sup> <sub>3</sub>	0.0	<b>1.0</b>	55	8
3	P(C <sub>6</sub> F <sub>5</sub> ) <sub>3</sub>	<b>1.0</b>	<b>1.0</b>	24	0
4	P(C <sub>6</sub> F <sub>5</sub> ) <sub>3</sub>	0.0	<b>1.0</b>	43	4
5	AsPh <sub>3</sub>	<b>1.0</b>	<b>1.0</b>	6	0
6	AsPh <sub>3</sub>	0.0	<b>1.0</b>	26	0
7	SbPh <sub>3</sub>	<b>1.0</b>	<b>1.0</b>	0	0
8	SbPh <sub>3</sub>	0.0	<b>1.0</b>	0	0
9	P(OCH(CF <sub>3</sub> ) <sub>2</sub> ) <sub>3</sub>	<b>1.0</b>	<b>1.0</b>	7	0
10	P(OCH(CF <sub>3</sub> ) <sub>2</sub> ) <sub>3</sub>	0.0	<b>1.0</b>	30	3
11	tppp	<b>1.0</b>	<b>1.0</b>	0	0
12	tppp	0.0	<b>1.0</b>	0	0
13	P(odtbz) <sub>3</sub>	<b>1.0</b>	<b>1.0</b>	0	0
14	P(odtbz) <sub>3</sub>	0.0	<b>1.0</b>	45	11
15	Me-Verkade	<b>1.0</b>	<b>1.0</b>	0	0

**Table 3.3 (cont'd)**

16	Me-Verkade	0.0	<b>1.0</b>	0	0
17	SiPBz <sup>a</sup>	<b>1.0</b>	<b>1.0</b>	45	55
18	SiPBz <sup>a</sup>	0.0	<b>1.0</b>	58	42

---

<sup>a</sup> 5 mol% ligand used.

An initial reaction screen (Table 3.2) with **10a** showed that the SiPbz ligand outperformed the best ligands reported in the literature for ester directed C-H borylation with homogenous iridium catalysts.<sup>1</sup> It was also the least susceptible to the deleterious effects of HBPIn and was the only ligand screened that produced product with HBPIn as borane source. When reactions run with PAr<sup>F</sup><sub>3</sub> and P(C<sub>6</sub>F<sub>5</sub>)<sub>3</sub> and 1 equivalent B<sub>2</sub>Pin<sub>2</sub> respectable amounts of **10b** were produced (Table 3.3, entry 2 and entry 4 respectively). However, when reactions were run under identical conditions with 1 equivalent HBPIn and 1 equivalent B<sub>2</sub>Pin<sub>2</sub> (Table 3.3, entries 1 and 3) the yields of borylated products dropped substantially. This trend was also seen with AsPh<sub>3</sub> and the phosphite ligands P(OCH(CF<sub>3</sub>)<sub>2</sub>)<sub>3</sub> and P(odtbz)<sub>3</sub>.

SiPbz and **14b** silyl ligands represent a novel approach to designing more reactive iridium catalysts for C-H borylation reactions. Both offer frame works that can be easily modified to optimize the sterics and donor ability of future analogues. I believe these silyl ligands will offer exciting new reactivity for future homogeneous iridium catalyzed C-H borylation reactions.

## REFERENCES

## REFERENCES

- 1) (a) Miyaura, N. *Bull. Chem. Soc. Jpn.* **2008**, *81*, 1535; (b) Ishiyama, T.; Isou, H.; Kikuchi, T.; Miyaura, N. *Chem. Commun.* **2010**, 46, 159.
- 2) (a) Kawamorita, S.; Ohmiya, H.; Hara, K.; Fukuoka, A.; Sawamura, M. *J. Am. Chem. Soc.* **2009**, *131*, 5058; (b) Kawamorita, S.; Ohmiya, H.; Sawamura, M. *J. Org. Chem.* **2010**, *75*, 3855.
- 3) Yamazaki, K.; Kawamorita, S.; Ohmiya, H.; Sawamura, M. *Org. Lett.* **2010**, *12*, 3978.
- 4) Kawamorita, S.; Murakami, R.; Iwai, T.; Sawamura, M. *J. Am. Chem. Soc.* **2013**, *135*, 2947.
- 5) Chotana, G. C.; Vanchura, B. A., II; Tse, M. K.; Staples, R. J.; Maleczka, R. E., Jr; Smith, M. R., III *Chem. Commun.*, **2009**, 5731.
- 6) Dang, L.; Lin, Z.; Marder, T. B. *Chem. Commun.* **2009**, 3987.
- 7) Ishiyama, T.; Takagi, J.; Hartwig, J. F.; Miyaura, N. *Angew. Chem. Int. Ed.* **2002**, *41*, 3056.
- 8) Chotana, G. C.; Vanchura, B. A., II; Tse, M. K.; Staples, R. J.; Maleczka, R. E., Jr; Smith, M. R., III *Chem. Commun.*, **2009**, 5731.
- 9) Liskey, C. W.; Wei, C. S.; Pahls, D. R.; Hartwig, J., F. *Chem. Commun.*, **2009**, 5603.
- 10) Boebel, T. B.; Hartwig, J. F. *Organometallics*, **2008**, *27*, 6013.
- 11) Boebel, T. B.; Hartwig, J. F. *J. Am. Chem. Soc.* **2008**, *130*, 7534.
- 12) Cho, S. H.; Hartwig, J. F. *J. Am. Chem. Soc.* **2013**, *135*, Ahead of Print.
- 13) Robins, D. A.; Boebel, T. B.; Hartwig, J. F. *J. Am. Chem. Soc.* **2010**, *132*, 4068.

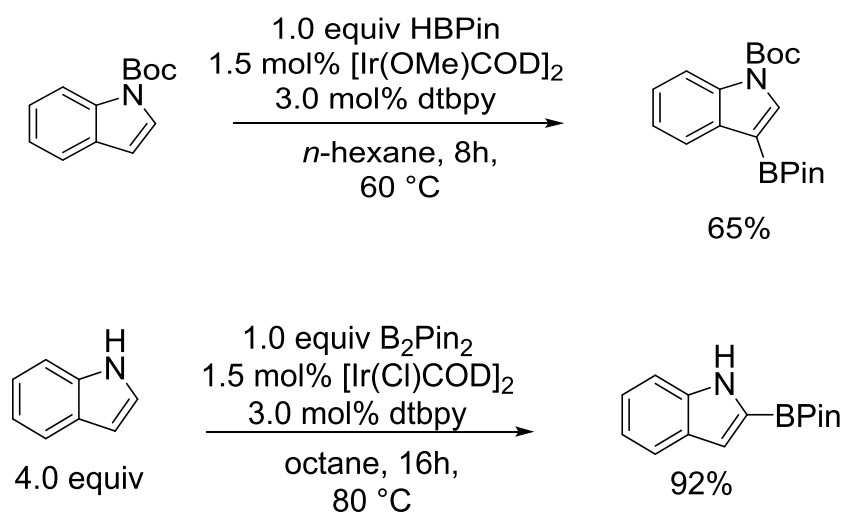
## CHAPTER 4

### BPIN AS A TRACELESS DIRECTING GROUP FOR C-H BORYLATIONS

#### Traceless BPin protected borylation of heterocycles.

It has been demonstrated that *tert*-butoxycarbonyl (Boc) protected heterocycles such as pyrroles and indoles<sup>1</sup> can lead to different borylated regioisomers than their respective unprotected counterparts<sup>2</sup> when subjected to Ir-catalyzed C-H borylation conditions. Figure 4.1 shows that Ir-catalyzed C-H borylation with indole gives the 2-borylated regioisomer. However, NBoc protected indole gives the 3-borylated regioisomer due to the steric bulk of the Boc protecting group when exposed to similar Ir catalyzed C-H borylation conditions.

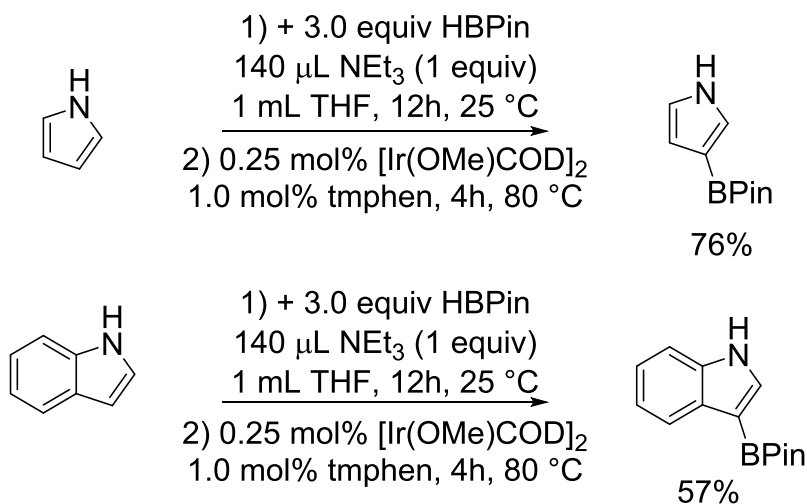
**Figure 4.1.** Borylation of indole.



We envisioned a protocol that would allow for the in-situ protection of heterocycles with HBPIn. The strategy of using N-BPin as a directing group has the advantage of N-BPin bonds being extremely easy to hydrolyze and therefore remove. Unfortunately, pyrrole and indole do

not react with HBPIn to give N-borylation despite the reaction being thermodynamically favored. We hypothesized that the addition of a base such as  $\text{NEt}_3$  or  $\text{NEt}^i\text{Pr}_2$  would make the HBPIn sufficiently hydridic for such a reaction to occur. Indeed, the use of Lewis bases to enhance the hydride transfer character of HBPIn for the reduction of imines has recently been reported.<sup>3</sup> Using this strategy, we were able to do a one pot in-situ protection/ borylation/ deprotection on indole and pyrrole giving the same regiochemistry as the Boc protected compounds (Figure 4.2). It should be noted that borenium cations give the regioselective product by electrophilic arene borylation, however, such chemistry is incompatible with unprotected heteroarenes.<sup>4</sup>

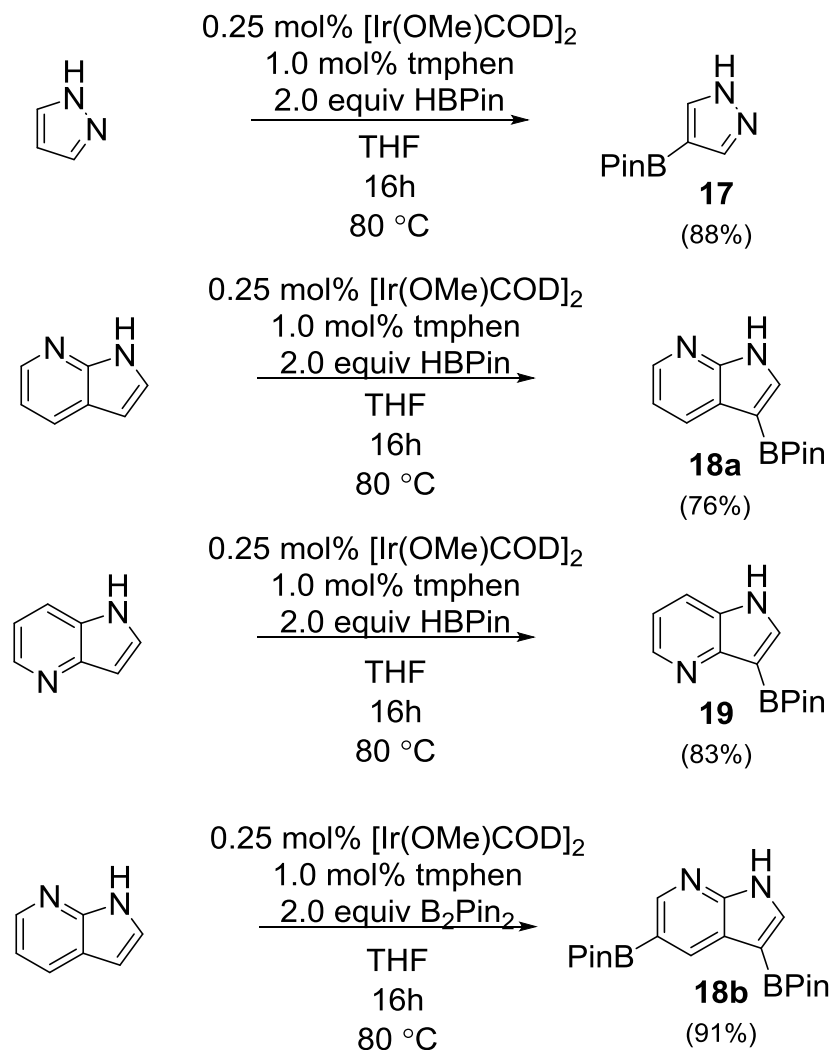
**Figure 4.2.** Base assisted protection of heterocycles with HBPIn.



When a basic functionality is inherent in the heterocyclic substrate, no additional base is needed and we observed a spontaneous reaction between HBPIn and an array of heterocycles including pyrazole, 4-azaindole and 7-azaindoles. It should also be noted that the pKas are lower for pyrazole and azaindoles relative to pyrrole and indole. Application of Ir-catalyzed C-H

borylation conditions gave products identical to those observed with NBoc protected analogues (Figure 4.3). It is noteworthy that for the diborylation of 7-azaindole, that in-situ NBPIn protection occurred with  $B_2Pin_2$ .

**Figure 4.3.** In-situ protection of heterocycles with HBPIn.

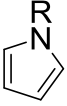
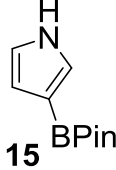
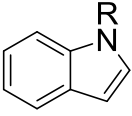
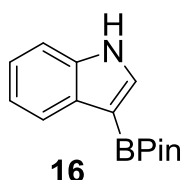
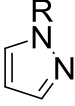
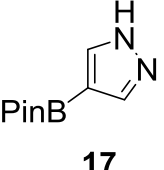
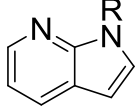
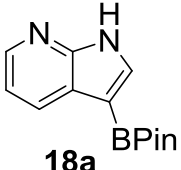
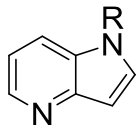
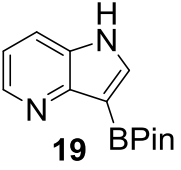


A comparison of isolated yields of borylated products produced via the traceless BPin directing group versus those obtained through NBoc direction/deprotection from reference 2 highlights the efficiency that the traceless BPin directing group provides. Let it be noted that the Boc yields were calculated based on N-Boc protected heterocycles, therefore yields from the



parent heterocycles would be lower for the Boc-directed route. As shown in Figure 4.4, traceless BPin direction offers a distinct advantage, not only in minimizing purification/isolation steps, but also in improving isolated yields of borylated parent heterocycles. For example, the greater than 30% improvement of borylated **17** is found when the traceless route is employed. The case for azaindoles is even more striking as the traceless direction provides **18a** and **19** in good yield, whereas the parent compounds are inaccessible via the Boc-directed route because extensive decomposition to unidentified products occurred during attempted thermal deprotection.

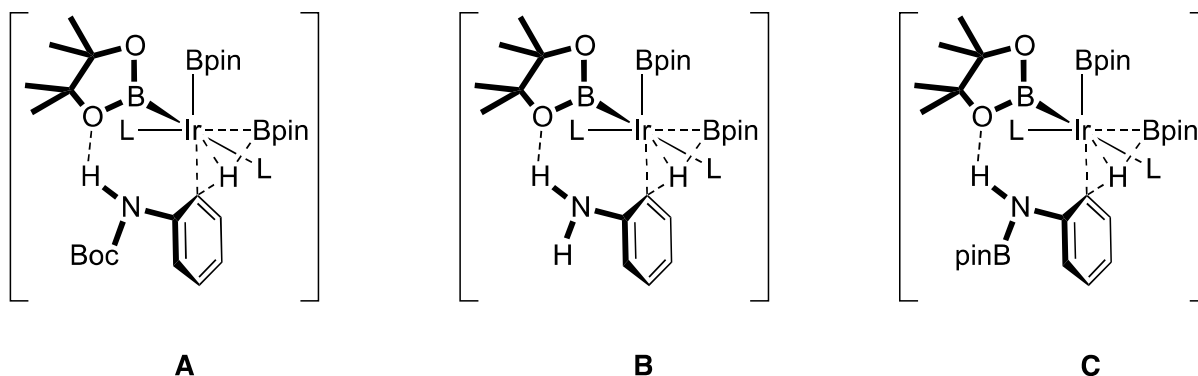
**Figure 4.4.** Comparison of Boc and traceless directed borylation of heterocycles.

Reactant	Product	% Yield R = Boc	% Yield R = H
	 <b>15</b>	64%	76%
	 <b>16</b>	37%	57%
	 <b>17</b>	55%	88%
	 <b>18a</b>	0%	76%
	 <b>19</b>	0%	83%

### Application of BPin as traceless protecting group with primary anilines.

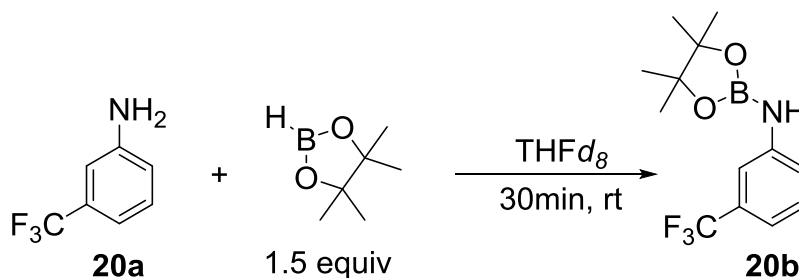
It has recently been shown that N-Boc anilines undergo an outer-sphere directed *ortho*-borylation.<sup>5</sup> Theory and experiment support a mechanism where the selectivity results from transition state stabilization attributed to a hydrogen bonding interaction between the aniline N-H and a BPin oxygen (Figure 4.5A). In principle, unsubstituted anilines could engage in this reaction through a transition state shown as Figure 4.5B or through an N-BPin protected aniline created from the reaction of HBPIn and aniline shown as Figure 4.5C.

**Figure 4.5.** Outer-sphere *ortho* directed iridium catalyzed C-H borylation of aniline.



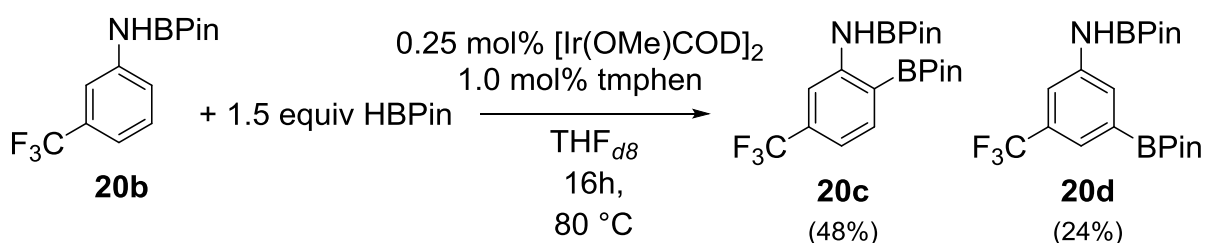
NMR experiments were conducted to determine what species are present in reaction mixtures containing HBPIn and 3-(trifluoromethyl)aniline (**20a**). Vigorous bubbling occurs when HBPIn is added to a solution containing **20a**. <sup>1</sup>H, <sup>11</sup>B and <sup>19</sup>F NMR indicate that a monoborylated N-BPin-3-(trifluoromethyl)aniline (**20b**) forms when **20a** is treated with excess HBPIn (Figure 4.6). No N,N-bis(BPin)-3-(trifluoromethyl)aniline was observed indicating outer-sphere *ortho* directed C-H borylation was feasible in which a polarized N-H bond is needed to function as the directing group. The requirement of only one additional equivalent of HBPIn to serve as a traceless directing group enhances the atom economy of this methodology. Addition of

**Figure 4.6.** Synthesis of N-BPin-3-(trifluoromethyl)aniline (**20b**).



Ir catalyst and additional HBPIn produced a mixture of *ortho* and *meta* borylated products in a 2:1 ratio when heated at 80°C (Figure 4.7). It should be pointed out that no N,N-bis(BPin)-3-(trifluoromethyl)aniline compounds were observed even after prolonged heating. The N-BPin bonds formed in-situ could be easily hydrolyzed with MeOH during work up without degradation of C-BPin bonds formed during catalysis. The net reaction provides a simple one pot procedure where the directing group is installed in-situ and subsequently removed upon work up without requiring any extra steps or isolation.

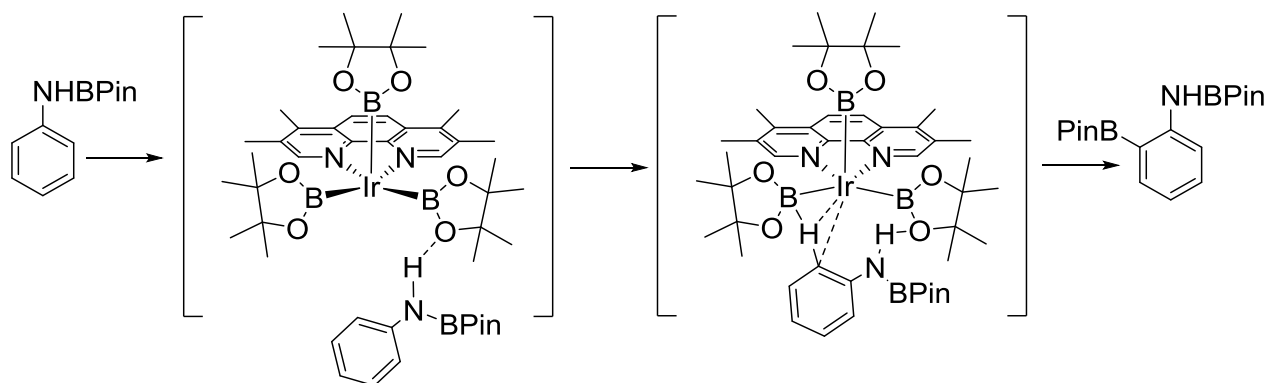
**Figure 4.7.** *Ortho* borylation of N-BPin-3-(trifluoromethyl)aniline (**20b**).



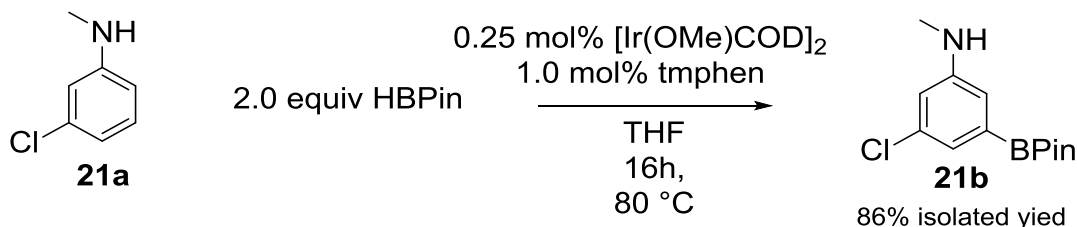
Considering that the reaction is believed to rely on H-bonding between the N-H hydrogen on the substrate and the oxygen of the Ir-boryl ligand (Figure 4.8) this reaction should not be applicable for secondary anilines. This was indeed found to be true when Ir-catalyzed C-H borylation reaction conditions were applied to 3-chloro-N-mehtylaniline (**21a**) only the N-

methyl-3-chloro-5-(4,4,5,5-tetramethyl-1,3,2-dioxaborolan-2-yl)-benzenamine *meta* product was observed (**21b** Figure 4.9).

**Figure 4.8.** Proposed Reaction Mechanism.

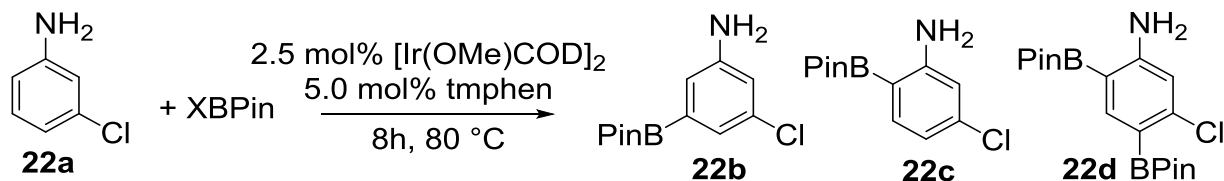


**Figure 4.9.** Borylation of 3-chloro-N-methylaniline (**21a**).

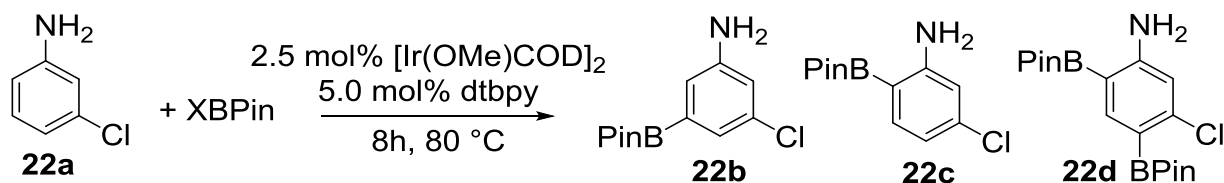


### Optimization.

Solvent, borane and ligand effects were screened in an attempt to optimize regioselectivity and reactivity for the borylation of 3-chloroaniline (**22a**) (Tables 4.1 & 4.2). The general trends that can be drawn from the reaction screen are that as solvent polarity increases from cyclohexane to Hünig's Base to THF to NMP the *ortho* directing effect decreases and more of the *meta* products are formed. Secondly, higher concentrations of B<sub>2</sub>Pin<sub>2</sub> give more *meta* borylated products. This can be significantly blunted by addition of HBPIn. Lastly, the more electron rich tmphen ligand gives more *ortho* directed products in agreement with our

**Table 4.1.** Borane and Solvent Effects on Borylation of 3-chloroaniline (**22a**) with tmphen.

entry	solvent.	equiv borane	yield (%)	<i>meta</i> (%)	<i>ortho</i> (%)	<i>diboryl</i> (%)	<i>meta</i> : <i>ortho</i> + <i>diborylated</i>
1	Cyclohexane	1.1 B <sub>2</sub> Pin <sub>2</sub>	79	23	51	5	1.0 : 2.4
2	Hünig's Base	1.1 B <sub>2</sub> Pin <sub>2</sub>	71	25	45	1	1.0 : 1.8
3	THF	1.1 B <sub>2</sub> Pin <sub>2</sub>	77	32	35	10	1.0 : 1.4
4	NMP	1.1 B <sub>2</sub> Pin <sub>2</sub>	24	16	8	1	1.8 : 1.0
5	Cyclohexane	2.2 B <sub>2</sub> Pin <sub>2</sub>	99	38	29	32	1.0 : 1.6
6	Hünig's Base	2.2 B <sub>2</sub> Pin <sub>2</sub>	99	50	32	18	1.0 : 1.0
7	THF	2.2 B <sub>2</sub> Pin <sub>2</sub>	99	58	21	21	1.4 : 1.0
8	NMP	2.2 B <sub>2</sub> Pin <sub>2</sub>	74	45	22	8	1.5 : 1.0
9	Cyclohexane	1.1 B <sub>2</sub> Pin <sub>2</sub> + 1.1 HBPin	99	26	39	34	1.0 : 2.8
10	Hünig's Base	1.1 B <sub>2</sub> Pin <sub>2</sub> + 1.1 HBPin	99	27	40	31	1.0 : 2.6
11	THF	1.1 B <sub>2</sub> Pin <sub>2</sub> + 1.1 HBPin	99	43	31	25	1.0 : 1.3
12	NMP	1.1 B <sub>2</sub> Pin <sub>2</sub> + 1.1 HBPin	96	56	31	8	1.4 : 1.0

**Table 4.2.** Borane and Solvent Effects on Borylation of 3-chloroaniline (**22a**) with dtbpy.

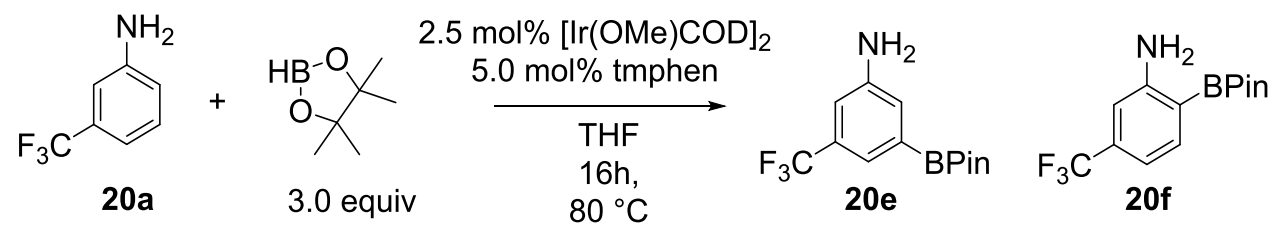
entry	solvent.	equiv borane	yield (%)	<i>meta</i> (%)	<i>ortho</i> (%)	<i>diboryl</i> (%)	<i>meta : ortho + diborylated</i>
1	Cyclohexane	1.1 B <sub>2</sub> Pin <sub>2</sub>	58	27	31	0	1.0 ; 1.2
2	Hünig's Base	1.1 B <sub>2</sub> Pin <sub>2</sub>	34	16	18	0	1.0 : 1.1
3	THF	1.1 B <sub>2</sub> Pin <sub>2</sub>	67	43	23	1	1.8 : 1.0
4	NMP	1.1 B <sub>2</sub> Pin <sub>2</sub>	38	27	11	0	2.6 : 1.0
5	Cyclohexane	2.2 B <sub>2</sub> Pin <sub>2</sub>	99	65	31	3	2.0 : 1.0
6	Hünig's Base	2.2 B <sub>2</sub> Pin <sub>2</sub>	99	65	33	2	1.9 : 1.0
7	THF	2.2 B <sub>2</sub> Pin <sub>2</sub>	99	71	18	10	2.5 : 1.0
8	NMP	2.2 B <sub>2</sub> Pin <sub>2</sub>	84	65	17	2	3.3 : 1.0
9	Cyclohexane	1.1 B <sub>2</sub> Pin <sub>2</sub> + 1.1 HBPin	74	37	36	1	1.0 : 1.0
10	Hünig's Base	1.1 B <sub>2</sub> Pin <sub>2</sub> + 1.1 HBPin	71	33	39	0	1.0 : 1.2
11	THF	1.1 B <sub>2</sub> Pin <sub>2</sub> + 1.1 HBPin	95	57	36	2	1.5 : 1.0
12	NMP	1.1 B <sub>2</sub> Pin <sub>2</sub> + 1.1 HBPin	77	56	19	2	2.6 : 1.0

hypothesized mechanism that increasing the Lewis basicity of the oxygen on the boryl ligand should promote the *ortho* directing effect.

### Solvent Effects on Regioselectivity.

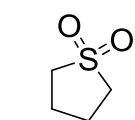
The decreased directing effect in polar solvents can be attributed to suppression of H-bonding between the aniline and the Ir catalyst which proceeds formation of the *ortho* directed products. The rate of formation of the *meta* isomer would not be as susceptible to the change in solvent polarity, therefore you would see a relative increase in the *meta* : *ortho* product ratio.

**Table 4.3.** Solvent Screen for 3-(trifluoromethyl)anilines (**20a**).

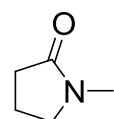


entry	solvent	yield (%)	<i>meta</i> (%)	<i>ortho</i> (%)	<i>meta</i> : <i>ortho</i>
1	Sulfolane	0	--	--	NA
2	NMP	89	62	27	2.3 : 1.0
6	DMA	36	26	10	2.6 : 1.0

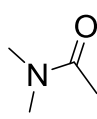
### Solvent Key for Table 4.3.



Sulfolane



NMP



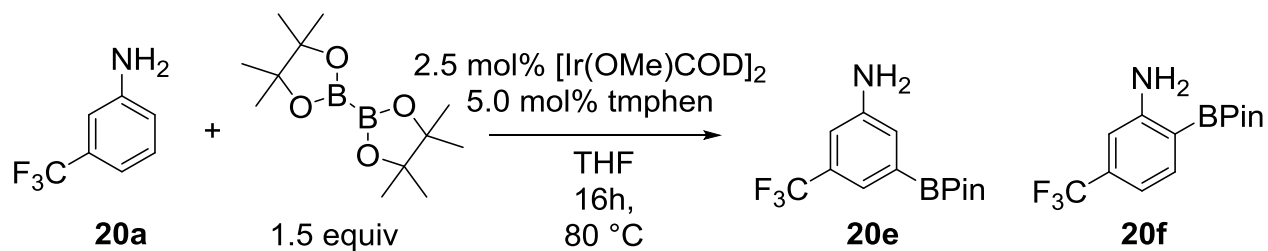
DMA

Further attempts to push the *meta* selectivity in 3-substituted anilines utilizing solvents with even greater dielectric constants met with little success. Table 4.3 shows the results of several experiments carried out on the Ir catalyzed C-H borylation of **20a** in solvents with high dielectric constants ( $\epsilon$ ); sulfolane (43), NMP (33) and DMA (38). While DMA did give greater regioselectivity for the *meta* borylation isomer than NMP, there was a significant drop in yield. Other solvents with high dielectric constants ( $\epsilon$ ), DMSO (47) and DMF (37), were precluded because previous studies showed they are largely incompatible with Ir catalyzed C-H borylation chemistry (see chapter 2).

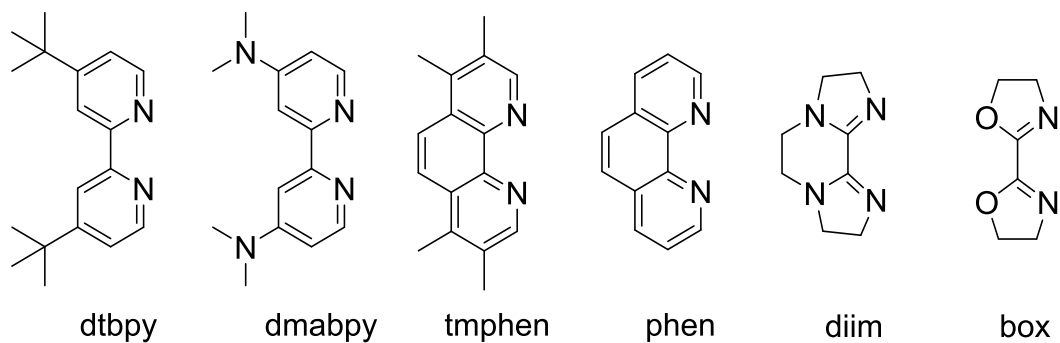
### Ligand Effects on Regioselectivity.

The origin of the ligand effects on selectivity was also observed with the outer-sphere directed borylation of N-Boc protected primary anilines.<sup>5</sup> It was postulated that the basicity on the pinacolate oxygens with more electron-rich ligands attached to the iridium, you favor a stronger NH-O H-bond (Figure 4.5A), which would favor *ortho* borylated products. Several experiments run on **20a** with various ligands (Table 4.4) support what had been seen with the N-Boc directed borylation report. The more electron donating the ancillary ligands became, the greater the *ortho* : *meta* ratio became. The most electron donating ligand screened, dmadpy (4,4'-bis(dimethylamino)-2,2'-bipyridine), gave the greatest *ortho* : *meta* selectivity. The unsubstituted phen (1,10-phenanthroline) ligand showed the lowest *ortho* : *meta* selectivity. The diimine type ligands diim (2,3,5,6,8,9-hexahydrodiimidazo[1,2-a:2',1'-c]pyrazine) and box (4,4',5,5'-tetrahydro-2,2'-bioxazole) ligands showed poor *ortho* : *meta* selectivity as well, however the reaction yields were far lower than all other ligands screened.

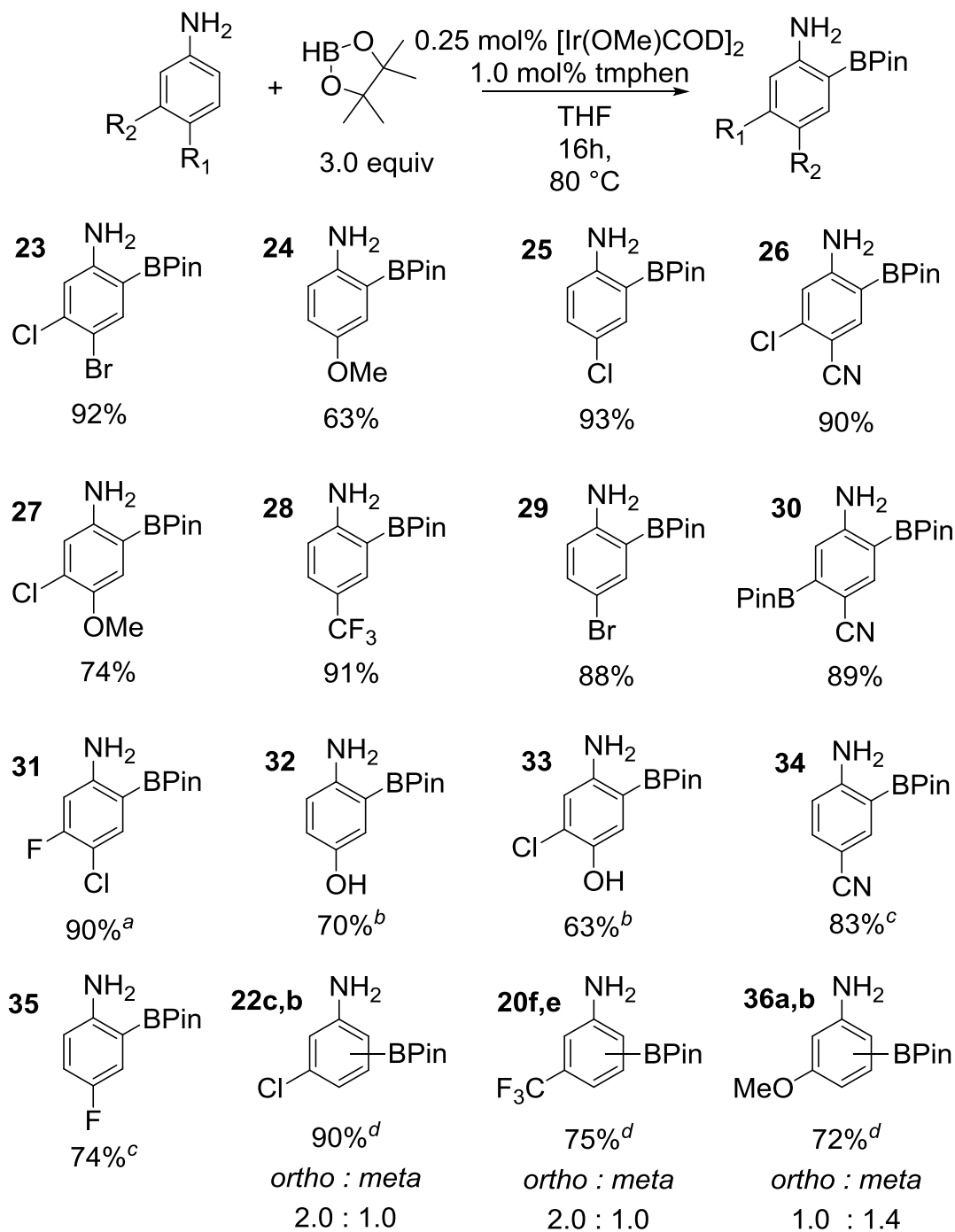


**Table 4.4.** Ligand effects on borylation of 3-(trifluoromethyl)anilines (**20a**).

entry	ligand	yield (%)	<i>meta</i> (%)	<i>ortho</i> (%)	<i>meta</i> : <i>ortho</i>
1	dtbpy	80	38	42	1.0 : 1.1
2	dmabpy	86	33	53	1.0 : 1.6
3	phen	73	42	30	1.4 : 1.0
4	tmphen	86	36	50	1.0 : 1.4
5	diim	17	8	8	1.0 : 1.0
6	box	10	4	6	1.0 : 1.5

**Ligand Key for Table 4.4.**

**Table 4.5.** Traceless BPin protected borylation of anilines.



<sup>a</sup> 8% 2-borylated isomer observed by <sup>1</sup>H NMR. <sup>b</sup> 4.0 equivalents HBPin used. <sup>c</sup> Conditions: 1.5 mol% [Ir(OMe)COD]<sub>2</sub>, 3.0 mol% dmabpy with 2.0 equivalents HBPin in *n*-hexane as reaction solvent. <sup>d</sup> Conditions: 2.5 mol% [Ir(OMe)COD]<sub>2</sub>, 5.0 mol% tmphen.

## Applications.

This methodology was then applied to a number of 4-substituted anilines (Table 4.5). 4-substituted halo anilines provide *ortho* borylated products in excellent isolated yields. 2-borylated products were obtained with 4-chloroaniline, 4-bromoaniline, 4-bromo-5-chloroaniline and 4-(trifluoromethyl)aniline in 93%, 88%, 92%, and 91% isolated yields respectively. Purification and isolation of the unprotected aniline products was achieved by passing the crude material through a short plug of SiO<sub>2</sub> and crystallization from a MeOH/ H<sub>2</sub>O solution. 4-methoxy-2-BPin-benzamine (**24**) and 5-chloro-4-methoxy-2-BPin-benzamine (**27**) were isolated in a similar fashion albeit in lower yields (63% and 74% respectively).

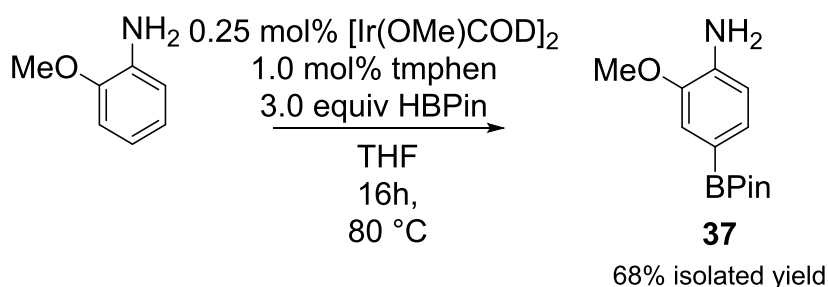
Aminophenols required an additional equivalent of HBPin to undergo O-BPin protection in addition to N-BPin protection. Isolation of analytically pure 4-amino-3-BPin-phenol (**32**) and 4-amino-2-chloro-5-BPin-phenol (**33**) products was achieved by crystallization from DCM/ hexanes in 70% and 63% isolated yields respectively.

When the para-substituent was of low steric bulk, as in 4-amino benzonitrile, standard conditions led to the diborylated products 4-amino-2,5-bisBPin-benzonitrile (**30**). By altering the reaction conditions and using the more electron donating ligand dmabpy, less polar hexanes as solvent and 2.0 equivalents of HBPin, the monoborylated 4-amino-3-BPin-benzonitrile (**34**) could be isolated in 83% yield. The same procedure was used to obtain 4-fluoro-2-BPin-benzamine in 74% isolated yield (**35**). <sup>1</sup>H and <sup>19</sup>F NMR of the crude reaction mixture showed **35** in a 12.5: 1.0 ratio with 4-fluoro-3-BPin-benzamine.

Although borylation of 4-aminobenzonitrile with less equivalents of HBPin gave small amounts of bisborylated products, excellent selectivity could be achieved for 4-amino-2-substituted benzonitriles. The borylation of 4-amino-2-chloro-5-BPin-benzonitrile was achieved using standard conditions in 90% isolated yield with no observable amount of borylation occurring *ortho* to the cyano functionality. Similarly, borylation *ortho* to a fluoro substituent was a nonfactor when the fluoro substituent was *meta* to the amino group in a 4-chloro-3-fluoroaniline. 4-chloro-5-fluoro-2-BPin-benzamine (**31**) was isolated in 90% yield with only trace amounts of the 4-chloro-3-fluoro-2-BPin-benzamine using standard conditions.

The borylation of 3-substituted anilines led to mixtures of *ortho* and *meta* products. The ratio of *ortho* and *meta* products is largely dependent on nature of the 3-substituent with electron withdrawing substituents such as chloro or trifluoromethyl giving **22c** to **22b** and **20f** to **20e** in a 2: 1 ratio from the respective anilines. However, electron donating substituents such as a methoxy group in the *meta* position gave a product ratio of 5-methoxy-2-BPin-aniline (**36a**) to 3-methoxy-5-BPin-aniline (**36b**) of 1.0: 1.4 in favor of the *meta* isomer.

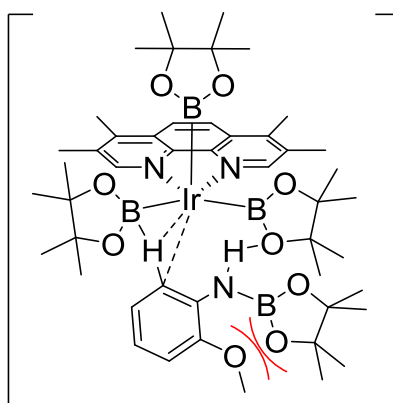
**Figure 4.10.** Borylation of *o*-anisidine.



Unfortunately 2-substituted anilines did not give *ortho* directing borylation products. Nevertheless, borylation of *o*-anisidine gave the 2-methoxy-4-BPin-benzenamine (**37**) isomer with surprisingly high regioselectivity (Figure 4.10). The reason for a lack of directing effect in

2-substituted aniline is most likely the result of steric repulsion between the *ortho* substituent and NBPIn protecting group (Figure 4.11). The regioselectivity of the 2-methoxy-4-BPin-benzenamine over the 2-methoxy-5-BPin-benzenamine (<5% observed in crude  $^1\text{H}$  NMR) was surprising and most likely is the result of electronic effects, albeit non-obvious ones.

**Figure 4.11.** Putative transition state for *ortho*-borylation of 2-substituted anilines.

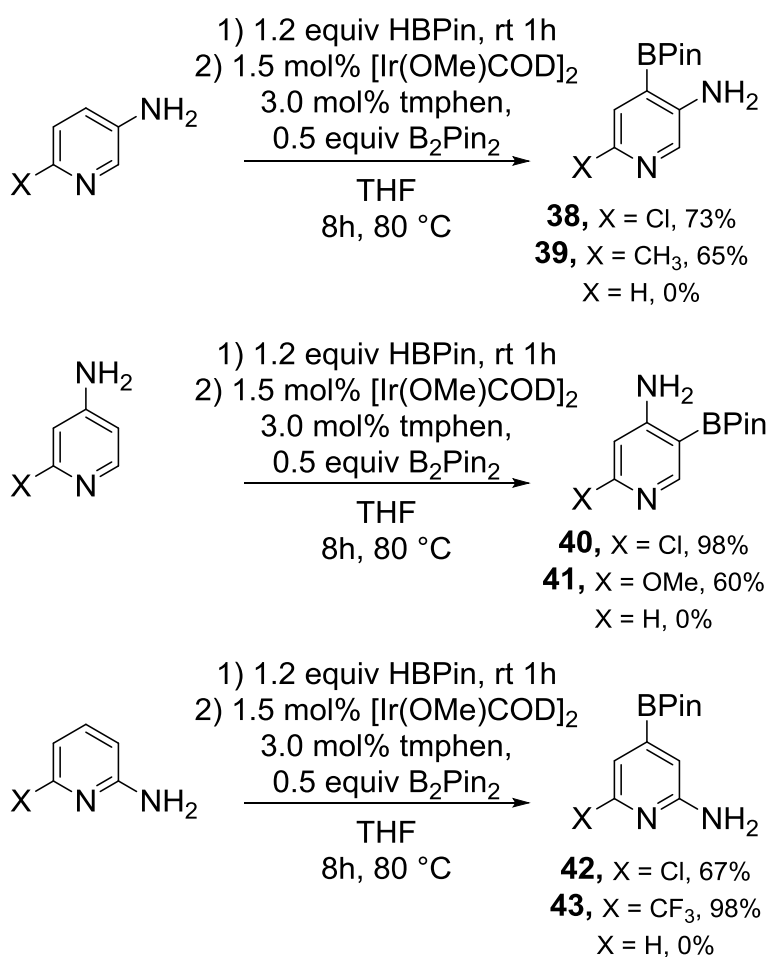


### Borylation of Aminopyridines.

Attempts to borylate aminopyridines were unsuccessful for aminopyridines with an unhindered pyridine N atom. Indeed no products were observed in reactions with 2-aminopyridine, 3-aminopyridine or 4-aminopyridine. Pyridines with substitution *ortho* to the pyridine N did however prove themselves to be compatible with our borylation conditions. Indeed 6-chloropyridin-3-amine and 6-methylpyridin-3-amine and 2-chloropyridin-4-amine and 2-methoxypyridin-4-amine gave *ortho* directed borylation products in moderate to good yields (Figure 4.12). Identical reaction conditions applied to 6-chloropyridin-2-amine and 6-(trifluoromethyl)pyridin-2-amine gave only the sterically determined borylation products. The rationale for this is competing coordination of the H-NBPIn with the pyridine N *ortho* in the 2-

aminopyridines.  $^1\text{H}$  NMR of 6-(trifluoromethyl)pyridine-2-amine and 1.5 equivalents of HBPin showed only mono NHBPin borylated pyridin-2-amine and no  $\text{N}(\text{BPin})_2$  protected pyridine-2-amine.

**Figure 4.12.** Traceless BPin protected borylation of amino pyridines.



## REFERENCES

## REFERENCES

- 1) Kallepalli, V. A.; Shi, F.; Paul, S.; Onyeozili, E. N.; Maleczka, R. E., Jr.; Smith, M. R., III *J. Org. Chem.* **2009**, *74*, 9199.
- 2) Takagi, J.; Sato, J.; Hartwig, J. F.; Ishiyama, T.; Miyaura, N. *Tetrahedron Lett.* **2002**, *43*, 5649.
- 3) Eisenberger, P; Bailey, A. M.; Crudden, C. M. *J. Am. Chem. Soc.* **2012**, *134*, 17384.
- 4) Bagutski, V.; Del Grosso, A.; Carrillo, J. A.; Cade, I. A.; Helm, M. D.; Lawson, J. R.; Singleton, P. J.; Solomon, S. A.; Marcelli, T.; Ingleson, M. J. *J. Am. Chem. Soc.* **2013**, *135*, 474.
- 5) Roosen, P. C.; Kallepalli, V. A.; Chattopadhyay, B.; Singleton, D. A.; Maleczka, R. E., Jr.; Smith, M. R., III *J. Am. Chem. Soc.* **2012**, *134*, 11350.



## CHAPTER 5

### EXPERIMENTAL

#### General Methods.

All reactions were conducted in a nitrogen filled glove-box. THF was distilled from sodium benzophenone solutions. All other solvents were used as received from Sigma-Aldrich (Sure/Seal<sup>TM</sup>) and were stored in the glove-box. All other commercially available materials were used as received. <sup>1</sup>H and <sup>13</sup>C NMR spectra were recorded on a Varian Inova-300 (300.11 and 75.47 MHz respectively), Varian VXR-500 or Varian Unity-500-Plus spectrometer (499.74 and 125.67 MHz respectively) and referenced to residual solvent signals. <sup>11</sup>B spectra were recorded on Varian VXR-500 or Varian Inova-300 operating at 160.41 and 96.29 MHz respectively, and were referenced to neat BF<sub>3</sub>·Et<sub>2</sub>O as the external standard. Elemental analyses were performed at Michigan State University using a Perkin Elmer Series II 2400 CHNS/O Analyzer. Melting points were measured on a MEL-TEMP® capillary melting apparatus and are uncorrected.

#### Stoichiometric borylation of veratrole with (dippe)Ir(BPin)<sub>3</sub>

(dippe)Ir(BPin)<sub>3</sub> (20 mg, 0.024 mmol, 1 equiv) was weighed into a small vial. Veratrole (24.5 μL, 0.19 mmol, 8 equiv) was added to the vial *via* microliter syringe. Cyclohexane (2.4 mL) was added to the vial and the solution was divided four J. Young NMR tubes (600 μL per tube). The tubes were heated in an oil bath at 100 °C and monitored by GC. After 15 min, 0.20 equiv of veratrole were converted to the 4- and 3-substituted boronic esters in a ratio greater than 99:1.

### **Borylation of veratrole (1) with catalysts generated in situ from (Ind)Ir(COD) and dippe**

(Ind)Ir(COD) (2.0 mg, 0.005 mmol, 0.02 equiv) was weighed in a test tube and was transferred to a J. Young NMR tube using C<sub>6</sub>H<sub>12</sub> (100 μL × 4). A standard solution of dippe (13.2 mg, 0.05 mmol, 0.2 equiv) in C<sub>6</sub>H<sub>12</sub> (500 μL) was prepared in a small vial. A 50 μL portion of this solution was then transferred to the J. Young NMR tube (0.02 equiv dippe). Veratrole (255 μL, 2.0 mmol, 8 equiv) and HBPIn (36 μL, 0.25 mmol, 1 equiv) were syringed into the J. Young NMR tube, which was then capped and heated in an oil bath at 130 °C. After 4 h, GC analysis showed that 0.26 equiv. of veratrole were converted to the 4- and 3-substituted boronic esters in a 98:2 ratio.

### **Stoichiometric borylation of veratrole (1) with (dtbpy)Ir(BPin)<sub>3</sub>COE**

(dtbpy)Ir(BPin)<sub>3</sub>COE (30 mg, 0.0315 mmol, 1 equiv) was weighed in a test tube and was dissolved in C<sub>6</sub>D<sub>12</sub> (300 μL). Veratrole (34.8 mg, 0.252 mmol, 8 equiv) was weighed in a test tube and mixed with the solution containing (dtbpy)Ir(BPin)<sub>3</sub>COE. The mixture was then transferred via pipette into a J. Young NMR tube. The J. Young NMR tube was capped and the reaction was monitored by <sup>1</sup>H NMR. The reaction was quenched at 1h (19 % conversion by NMR) with wet EtOAc and the product ratios were determined by GC/FID (99:1 4-isomer to 3-isomer.)

### **Catalytic borylation of veratrole (1) with (dtbpy)Ir(BPin)<sub>3</sub>COE**

(dtbpy)Ir(BPin)<sub>3</sub>COE (19 mg, 0.02 mmol) was weighed in a test tube and was dissolved in C<sub>6</sub>H<sub>12</sub> (2 mL) in a 20 mL scintillation vial containing a magnetic stir bar. 145 μL HBPIn (1 mmol, 1 equiv) was added to the solution via syringe. Veratrole (127 μL, 1 mmol, 1 equiv) was added via syringe to the mixture and the vial was loosely sealed. Reaction was quenched at 9h with wet EtOAc and product ratios determined by GC/FID (98:2 4-isomer to 3-isomer at 26% conversion.)

### **Stoichiometric borylation of 1,3-benzodioxole (2) with (dippe)Ir(BPin)<sub>3</sub>**

(dippe)Ir(BPin)<sub>3</sub> (20 mg, 0.024 mmol, 1 equiv) was weighed into a small vial. 1,3-benzodioxole (22.1 μL, 0.19 mmol, 8 equiv) was added to the vial *via* microliter syringe. Cyclohexane (2.4 mL) was added to the vial and the solution was divided four J. Young NMR tubes (600 μL per tube). The tubes were heated in an oil bath at 100 °C and monitored by GC. After 15 min, 1.3 equiv of 1,3-benzodioxole were converted to the 5- and 4-substituted boronic esters in a 2:98 ratio.

### **Catalytic Borylation of 1,3-benzodioxole (2) with (dippe)Ir(BPin)<sub>3</sub>**

(dippe)Ir(BPin)<sub>3</sub> (4.2 mg, 0.005 mmol, 0.02 equiv) was weighed in a test tube and was transferred to a J. Young NMR tube using C<sub>6</sub>H<sub>12</sub> (100 μL × 4). 1,3-benzodioxole (230 μL, 2.0 mmol, 8 equiv) and HBPin (36 μL, 0.25 mmol, 1 equiv) were syringed into the J. Young NMR tube, which was then capped and heated in an oil bath at 130 °C. After 4 h, GC analysis showed that 0.34 equiv. of 1,3-benzodioxole were converted to the 5- and 4-substituted boronic esters in a 4:96 ratio.

### **Stoichiometric borylation of 1,3-benzodioxole (2) with (dtbpy)Ir(BPin)<sub>3</sub>COE**

(dtbpy)Ir(BPin)<sub>3</sub>COE (30 mg, 0.0315 mmol, 1 equiv) was weighed in a test tube and was dissolved in C<sub>6</sub>D<sub>12</sub> (300 μL). 1,3-benzodioxole (30.8 mg, 0.252 mmol, 8 equiv) was weighed in a test tube and mixed with the solution containing (dtbpy)Ir(BPin)<sub>3</sub>COE. The mixture was then transferred via pipette into a J. Young NMR tube. The J. Young NMR tube was capped and the reaction was monitored by <sup>1</sup>H NMR. The reaction was quenched at 15 min at room temperature (51 % conversion by NMR) with wet EtOAc and the product ratios were determined by GC/FID (95:5 4-isomer to 5-isomer.)

### **Catalytic borylation of 1,3-benzodioxole (2) with (dtbpy)Ir(BPin)<sub>3</sub>COE**

(dtbpy)Ir(BPin)<sub>3</sub>COE (19 mg, 0.02 mmol) was weighed in a test tube and was dissolved in C<sub>6</sub>H<sub>12</sub> (2 mL) in a 20 mL scintillation vial containing a magnetic stir bar. 145  $\mu$ L HBPIn (1 mmol, 1 equiv) was added to the solution via syringe. 1,3-benzodioxole (122 mg, 1 mmol, 1 equiv) was added to the mixture and the vial was loosely sealed. Reaction was quenched at 1h with wet EtOAc and product ratios determined by GC/FID (91:3 4-isomer to 5-isomer with 6% diborylation at 30% conversion.)

### **General Procedures for Screening Iridium Catalyzed C-H Borylation Conditions with Varying Ligands, Iridium Precatalyst, Borane and Order of Addition.**

All reactions were conducted in a nitrogen filled glove-box. THF and MeTHF were distilled from sodium benzophenone solutions. All other solvents were used as received from Sigma-Aldrich (Sure/Seal<sup>TM</sup>) and were stored in the glove-box. All other commercially available materials were used as received. Reactions for high through-put screening were conducted in 8  $\times$  30 mm borosilicate glass shell vials arranged in 96 well metal blocks (Symyx) with magnetic stirring. Materials were dispensed to the vials whenever possible as solutions in the reaction solvent, otherwise in suitable solvents (in which the material was soluble in) via micro pipettors followed by evaporation of the solvent in vacuo in a Genevac<sup>TM</sup> centrifugal evaporator in the glove box. The reactions were heated via the metal 96 well blocks after sealing with a

perfluoroelastomeric backed metal top plate screwed to the metal block. Analysis was accomplished by reversed phase HPLC (Zorbax Eclipse Plus C18, 1.8 micron, 4.6 × 50 mm column eluted with 0.1% aq H<sub>3</sub>PO<sub>4</sub> and acetonitrile) using an internal standard such as dodecahydrotriphenylene to facilitate quantitative HPLC solution assay yield determination.

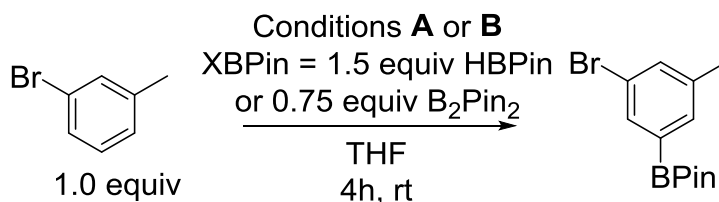
### **General Procedure for Microscale Reactions Utilizing Conditions A.**

In a nitrogen filled glovebox, 50 μL of solution containing 0.5 μmol iridium precatalyst dimer (0.01 M stock solution) or 1.0 μmol iridium monomer (0.02 M stock solution) in the reaction solvent was added to a 1 mL reaction vial containing a magnetic stir bar. To this solution, 50 μL of stock solution containing 30 μmol HBPin (0.6 M) or 15 μmol B<sub>2</sub>Pin<sub>2</sub> (0.3 M) was added to the 1 mL reaction vial. 50 μL of a solution containing 1.0 μmol ligand (0.02 M) was added via micropipette followed by 50 μL of a stock solution containing 20 μmol arylsubstrate (0.4 M) and 2 μmol dodecahydrotriphenylene internal standard. The reaction vessel was then sealed and the reaction mixture stirred at the desired temperature for an allotted amount of time, at which point the reaction was cooled to room temperature and quenched by exposure to atmospheric O<sub>2</sub> and dilution with MeCN.

## General Procedure for Microscale Reactions Utilizing Conditions B.

In a nitrogen filled glovebox, 50  $\mu\text{L}$  of a solution containing 0.5  $\mu\text{mol}$  iridium precatalyst dimer (0.01 M stock solution) or 1.0  $\mu\text{mol}$  iridium monomer (0.02 M stock solution) in the reaction solvent was added to a 1 mL reaction vial containing a magnetic stir bar. To this solution, 50  $\mu\text{L}$  of stock solution containing 1.0  $\mu\text{mol}$  ligand (0.02 M) was added to the 1 mL reaction vial. 50  $\mu\text{L}$  of a solution containing 30  $\mu\text{mol}$  HBPIn (0.6 M) or 15  $\mu\text{mol}$  B<sub>2</sub>Pin<sub>2</sub> (0.3 M) was added via micro pipette followed by 50  $\mu\text{L}$  of stock solution containing 20  $\mu\text{mol}$  arylsubstrate (0.4 M) and 2  $\mu\text{mol}$  dodecahydrotriphenylene internal standard. The reaction vessel was then sealed and stirred at the desired temperature for an allotted amount of time, at which point the reaction was cooled to room temperature and quenched by exposure to atmospheric O<sub>2</sub> and dilution with MeCN.

## Room Temperature Reaction Screen on 3-bromotoluene (3a).

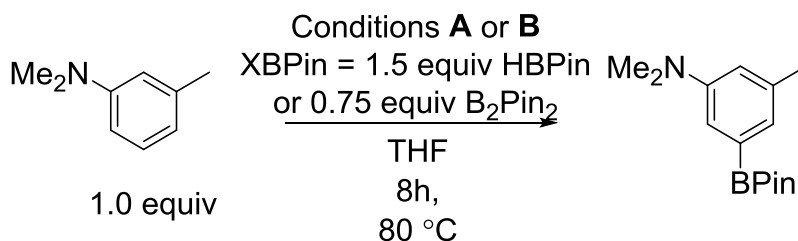


The 96 reactor wells consist of 1mL glass vials equipped with a micro-magnetic stir bar arrayed in a 12x8 reaction plate, 12 columns labeled 1-12 and 8 rows labeled A-H. In a nitrogen filled glove box, 0.01 M stock solutions of [Ir(COD)Cl]<sub>2</sub> in THF and [Ir(OMe)COD]<sub>2</sub> in THF and 0.02 M stock solutions of (Ind)Ir(COD) in THF and Ir(acac)COD in THF were prepared. 50  $\mu\text{L}$  of [Ir(OMe)COD]<sub>2</sub> (0.5  $\mu\text{mol}$ ) stock solution were added to each well across rows A and E (wells

A1-A12 and E1-E12) via micro pipette. 50  $\mu\text{L}$  of  $[\text{Ir}(\text{COD})\text{Cl}]_2$  (0.5  $\mu\text{mol}$ ) stock solution were added to each well across rows B and F (wells B1-B12 and F1-F12) via micro pipette. 50  $\mu\text{L}$  of  $\text{Ir}(\text{acac})\text{COD}$  (1.0  $\mu\text{mol}$ ) stock solution were added to each well across rows C and G (wells C1-C12 and G1-G12) via micro pipette. 50  $\mu\text{L}$  of (Ind)  $\text{Ir}(\text{COD})$  (1.0  $\mu\text{mol}$ ) stock solution were added to each well across rows D and H (wells D1-D12 and H1-H12) via micro pipette. 50  $\mu\text{L}$  of a 0.02 M stock solution of dtbpy (1.0  $\mu\text{mol}$ ) in THF was added down columns 7 and 10 (wells A7-H7 and A10-H10) via micro pipette. 50  $\mu\text{L}$  of a 0.02 M stock solution of tmphen (1.0  $\mu\text{mol}$ ) in THF was added down columns 8 and 11 (wells A8-H8 and A11-H11) via micro pipette. 50  $\mu\text{L}$  of a 0.02 M stock solution of box (1.0  $\mu\text{mol}$ ) in THF was added down columns 9 and 12 (wells A9-H9 and A12-H12) via micro pipette. 50  $\mu\text{L}$  of a 0.6 M stock solution of HBPin (30  $\mu\text{mol}$ ) in THF was added across rows A, B, C, and D (wells A1-D12) via micro pipette. 50  $\mu\text{L}$  of a 0.3 M stock solution of  $\text{B}_2\text{Pin}_2$  (15  $\mu\text{mol}$ ) in THF was added across rows E, F, G, and H (wells E1-H12) via micro pipette. The reaction plate was then capped and stirred for 5 min at room temperature resulting in catalyst generation under **Conditions B** for wells A7-H12. 50  $\mu\text{L}$  of a 0.02 M stock solution of dtbpy (1.0  $\mu\text{mol}$ ) in THF was added down columns 1 and 4 (wells A1-H1 and A4-H4) via micro pipette. 50  $\mu\text{L}$  of a 0.02 M stock solution of tmphen (1.0  $\mu\text{mol}$ ) in THF was added down columns 2 and 5 (wells A2-H2 and A5-H5) via micro pipette. 50  $\mu\text{L}$  of a 0.02 M stock solution of box (1.0  $\mu\text{mol}$ ) in THF was added down columns 3 and 6 (wells A3-H3 and A6-H6) via micro pipette, resulting in catalyst generation under **Conditions A** for wells A7-H12. Finally, 50  $\mu\text{L}$  of a 0.4 M stock solution of 3-bromotoluene containing dodecahydrotriphenylene internal standard (0.04 M) was added to all 96 wells via micro pipette and the reaction plate was sealed and stirred for 4h at room temperature. The reaction was then quenched by exposure to air and dilution with MeCN.



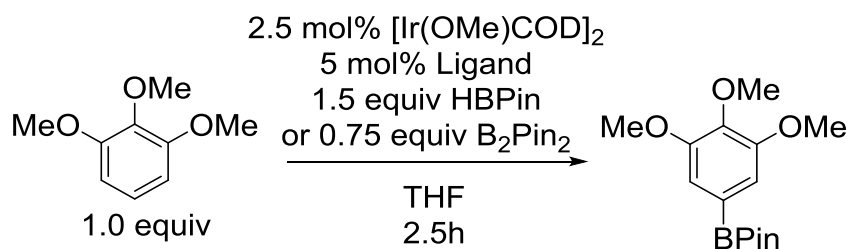
### Elevated Temperature Reaction Screen on *N,N*-dimethyl-*m*-toluidine (5a).



The 96 reactor wells consist of 1mL glass vials equipped with a micro-magnetic stir bar arrayed in a 12x8 reaction plate, 12 columns labeled 1-12 and 8 rows labeled A-H. In a nitrogen filled glove box, 0.01 M stock solutions of [Ir(COD)Cl]<sub>2</sub> in THF and [Ir(OMe)COD]<sub>2</sub> in THF and 0.02 M stock solutions of (Ind)Ir(COD) in THF and Ir(acac)COD in THF were prepared. 50 μL of [Ir(OMe)COD]<sub>2</sub> (0.5 μmol) stock solution were added to each well across rows A and E (wells A1-A12 and E1-E12) via micro pipette. 50 μL of [Ir(COD)Cl]<sub>2</sub> (0.5 μmol) stock solution were added to each well across rows B and F (wells B1-B12 and F1-F12) via micro pipette. 50 μL of Ir(acac)COD (1.0 μmol) stock solution were added to each well across rows C and G (wells C1-C12 and G1-G12) via micro pipette. 50 μL of (Ind) Ir(COD) (1.0 μmol) stock solution were added to each well across rows D and H (wells D1-D12 and H1-H12) via micro pipette. 50 μL of a 0.02 M stock solution of dtbpy (1.0 μmol) in THF was added down columns 7 and 10 (wells A7-H7 and A10-H10) via micro pipette. 50 μL of a 0.02 M stock solution of tmphen (1.0 μmol) in THF was added down columns 8 and 11 (wells A8-H8 and A11-H11) via micro pipette. 50 μL of a 0.02 M stock solution of box (1.0 μmol) in THF was added down columns 9 and 12 (wells A9-H9 and A12-H12) via micro pipette. 50 μL of a 0.6 M stock solution of HBPIn (30 μmol) in THF was added across rows A, B, C, and D (wells A1-D12) via micro pipette. 50 μL of a 0.3 M stock solution of B<sub>2</sub>Pin<sub>2</sub> (15 μmol) in THF was added across rows E, F, G, and H (wells E1-

H12) via micro pipette. The reaction plate was then capped and stirred for 5 min at room temperature resulting in catalyst generation under **Conditions B** for wells A7-H12. 50  $\mu\text{L}$  of a 0.02 M stock solution of dtbpy (1.0  $\mu\text{mol}$ ) in THF was added down columns 1 and 4 (wells A1-H1 and A4-H4) via micro pipette. 50  $\mu\text{L}$  of a 0.02 M stock solution of tmphen (1.0  $\mu\text{mol}$ ) in THF was added down columns 2 and 5 (wells A2-H2 and A5-H5) via micro pipette. 50  $\mu\text{L}$  of a 0.02 M stock solution of box (1.0  $\mu\text{mol}$ ) in THF was added down columns 3 and 6 (wells A3-H3 and A6-H6) via micro pipette, resulting in catalyst generation under **Conditions A** for wells A7-H12. Finally, 50  $\mu\text{L}$  of a 0.4 M stock solution of *N,N*-dimethyl-*m*-toluidine (20  $\mu\text{mol}$ ) in THF, containing dodecahydrotriphenylene internal standard (0.04 M, 2.0  $\mu\text{mol}$ ), was added to all 96 wells via micro pipette and the reaction plate was sealed and stirred for 8h at 80  $^{\circ}\text{C}$ . The reaction was then quenched by exposure to air and dilution with MeCN.

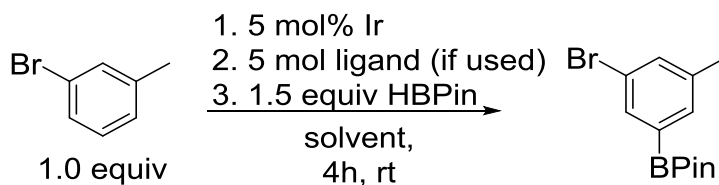
#### General Procedure for Borylation of 1,2,3-trimethoxybenzene (4a).



In a nitrogen filled glovebox, 500  $\mu\text{L}$  of solution containing 5.0  $\mu\text{mol}$  of  $[\text{Ir}(\text{OMe})\text{COD}]_2$  (0.01 M stock solution) in THF was added to a 8 mL scintillation vial containing a magnetic stir bar. To this solution, 500  $\mu\text{L}$  of stock solution containing 10.0  $\mu\text{mol}$  ligand (0.02 M) in THF was added to the 8 mL scintillation vial. 500  $\mu\text{L}$  of solution containing 300  $\mu\text{mol}$  HBPin (0.6 M) in THF or 150  $\mu\text{mol}$   $\text{B}_2\text{Pin}_2$  (0.3 M) in THF was added via micro pipette followed by 500  $\mu\text{L}$  of

stock solution containing 200  $\mu\text{mol}$  arylsubstrate (0.4 M) in THF and 20  $\mu\text{mol}$  dodecahydrotriphenylene internal standard. The reaction vessel was then sealed and stirred at the desired temperature for 2.5h, at which point the reaction was cooled to room temperature and quenched by exposure to atmospheric  $\text{O}_2$  and dilution with MeCN.

### Solvent Effects on Catalyst Formation at Room Temperature (3a).

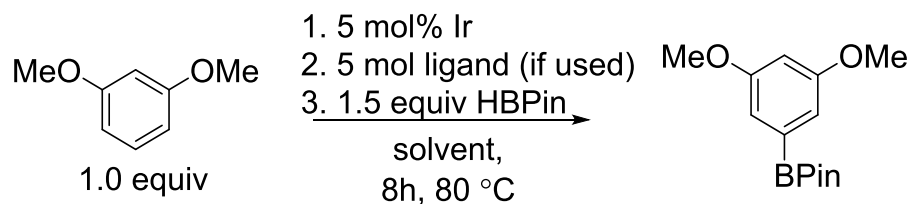


The 96 reactor wells consist of 1mL glass vials equipped with a micro-magnetic stir bar arrayed in a 12x8 reaction plate, 12 columns labeled 1-12 and 8 rows labeled A-H. In a nitrogen filled glove box, 0.01 M stock solutions of  $[\text{Ir}(\text{OMe})\text{COD}]_2$  in THF and 0.02 M stock solutions of  $(\text{dtbpy})\text{Ir}(\text{BPin})_3\text{COE}$  in THF and  $(\text{tmphen})\text{Ir}(\text{BPin})_3\text{COE}$  in THF were prepared. 50  $\mu\text{L}$  of  $[\text{Ir}(\text{OMe})\text{COD}]_2$  (0.5  $\mu\text{mol}$ ) stock solution were added to each well across rows A, C, E and G (wells A1-A12, C1-C12, E1-E12 and G1-G12) via micro pipette. 50  $\mu\text{L}$  of  $(\text{dtbpy})\text{Ir}(\text{BPin})_3\text{COE}$  (1.0  $\mu\text{mol}$ ) stock solution were added to each well across rows B and F (wells B1-B12 and F1-F12) via micro pipette. 50  $\mu\text{L}$  of  $(\text{tmphen})\text{Ir}(\text{BPin})_3\text{COE}$  (1.0  $\mu\text{mol}$ ) stock solution were added to each well across rows D and H (wells D1-D12 and H1-H12) via micro pipette. 50  $\mu\text{L}$  of a 0.02 M stock solution of dtbpy (1.0  $\mu\text{mol}$ ) in THF was added to each well across rows A and E (wells A1-A12 and E1-E12) via micro pipette. 50  $\mu\text{L}$  of a 0.02 M stock solution of tmphen (1.0  $\mu\text{mol}$ )

in THF was to each well across rows C and G (wells C1-C12 and G1-G12) via micro pipette. Volatile solvent were removed under reduced pressure. 100  $\mu\text{L}$  of a 0.3 M stock solution of HBPIn (30  $\mu\text{mol}$ ) in THF was added down column 1 (wells A1 through H1) via micro pipette. 100  $\mu\text{L}$  of a 0.3 M stock solution of HBPIn (30  $\mu\text{mol}$ ) in MeTHF was added down column 2 (wells A2-H2) via micro pipette. 100  $\mu\text{L}$  of a 0.3 M stock solution of HBPIn (30  $\mu\text{mol}$ ) in Cpme was added down column 3 (wells A3-H3) via micro pipette. 100  $\mu\text{L}$  of a 0.3 M stock solution of HBPIn (30  $\mu\text{mol}$ ) in MTBE was added down column 4 (wells A4-H4) via micro pipette. 100  $\mu\text{L}$  of a 0.3 M stock solution of HBPIn (30  $\mu\text{mol}$ ) in hexanes was added down column 5 (wells A5-H5) via micro pipette. 100  $\mu\text{L}$  of a 0.3 M stock solution of HBPIn (30  $\mu\text{mol}$ ) in Hünig's base was added down column 6 (wells A6-H6) via micro pipette. 100  $\mu\text{L}$  of a 0.3 M stock solution of HBPIn (30  $\mu\text{mol}$ ) in  $\text{NEt}_3$  was added down column 7 (wells A7-H7) via micro pipette. 100  $\mu\text{L}$  of a 0.3 M stock solution of HBPIn (30  $\mu\text{mol}$ ) in NMP was added down column 8 (wells A8-H8) via micro pipette. 100  $\mu\text{L}$  of a 0.3 M stock solution of HBPIn (30  $\mu\text{mol}$ ) in IPAc was added down column 9 (wells A9-H9) via micro pipette. 100  $\mu\text{L}$  of a 0.3 M stock solution of HBPIn (30  $\mu\text{mol}$ ) in 1,4-dioxane was added down column 10 (wells A10-H10) via micro pipette. 100  $\mu\text{L}$  of a 0.3 M stock solution of HBPIn (30  $\mu\text{mol}$ ) in DCM was added down column 11 (wells A11-H11) via micro pipette. 100  $\mu\text{L}$  of a 0.3 M stock solution of HBPIn (30  $\mu\text{mol}$ ) in MeCN was added down column 12 (wells A12-H12) via micro pipette. 100  $\mu\text{L}$  of a 0.2 M stock solution of 3-bromotoluene (20  $\mu\text{mol}$ ) with 2.0  $\mu\text{mol}$  dodecahydrotriphenylene internal standard in THF was added down column 1 (wells A1 through H1) via micro pipette. 100  $\mu\text{L}$  of a 0.2 M stock solution of 3-bromotoluene (20  $\mu\text{mol}$ ) with 2.0  $\mu\text{mol}$  dodecahydrotriphenylene internal standard in MeTHF was added down column 2 (wells A2-H2) via micro pipette. 100  $\mu\text{L}$  of 0.2 M stock solution of 3-bromotoluene (20  $\mu\text{mol}$ ) with 2.0  $\mu\text{mol}$  dodecahydrotriphenylene internal standard

in Cpme was added down column 3 (wells A3-H3) via micro pipette. 100  $\mu\text{L}$  of a 0.2 M stock solution of 3-bromotoluene (20  $\mu\text{mol}$ ) with 2.0  $\mu\text{mol}$  dodecahydrotriphenylene internal standard in MTBE was added down column 4 (wells A4-H4) via micro pipette. 100  $\mu\text{L}$  of 0.2 M stock solution of 3-bromotoluene (20  $\mu\text{mol}$ ) with 2.0  $\mu\text{mol}$  dodecahydrotriphenylene internal standard in hexanes was added down column 5 (wells A5-H5) via micro pipette. 100  $\mu\text{L}$  of a 0.2 M stock solution of 3-bromotoluene (20  $\mu\text{mol}$ ) with 2.0  $\mu\text{mol}$  dodecahydrotriphenylene internal standard in Hünig's base was added down column 6 (wells A6-H6) via micro pipette. 100  $\mu\text{L}$  of a 0.2 M stock solution of 3-bromotoluene (20  $\mu\text{mol}$ ) with 2.0  $\mu\text{mol}$  dodecahydrotriphenylene internal standard in  $\text{NEt}_3$  was added down column 7 (wells A7-H7) via micro pipette. 100  $\mu\text{L}$  of a 0.2 M stock solution of 3-bromotoluene (20  $\mu\text{mol}$ ) with 2.0  $\mu\text{mol}$  dodecahydrotriphenylene internal standard in NMP was added down column 8 (wells A8-H8) via micro pipette. 100  $\mu\text{L}$  of a 0.2 M stock solution of 3-bromotoluene (20  $\mu\text{mol}$ ) with 2.0  $\mu\text{mol}$  dodecahydrotriphenylene internal standard in IPAc was added down column 9 (wells A9-H9) via micro pipette. 100  $\mu\text{L}$  of a 0.2 M stock solution of 3-bromotoluene (20  $\mu\text{mol}$ ) with 2.0  $\mu\text{mol}$  dodecahydrotriphenylene internal standard in 1,4-dioxane was added down column 10 (wells A10-H10) via micro pipette. 100  $\mu\text{L}$  of a 0.2 M stock solution of 3-bromotoluene (20  $\mu\text{mol}$ ) with 2.0  $\mu\text{mol}$  dodecahydrotriphenylene internal standard in DCM was added down column 11 (wells A11-H11) via micro pipette. 100  $\mu\text{L}$  of a 0.2 M stock solution of 3-bromotoluene (20  $\mu\text{mol}$ ) with 2.0  $\mu\text{mol}$  dodecahydrotriphenylene internal standard in MeCN was added down column 12 (wells A12-H12) via micro pipette. The reaction plate was then sealed and stirred for 4h at room temperature. The reaction was then quenched by exposure to air and dilution with MeCN.

### Solvent Effects on Catalyst Formation at Elevated Temperature (6a).



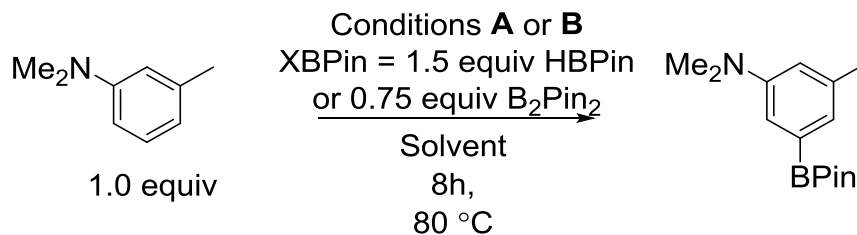
The 96 reactor wells consist of 1mL glass vials equipped with a micro-magnetic stir bar arrayed in a 12x8 reaction plate, 12 columns labeled 1-12 and 8 rows labeled A-H. In a nitrogen filled glove box, 0.01 M stock solutions of  $[\text{Ir}(\text{OMe})\text{COD}]_2$  in THF and 0.02 M stock solutions of  $(\text{dtbpy})\text{Ir}(\text{BPin})_3\text{COE}$  in THF and  $(\text{tmphen})\text{Ir}(\text{BPin})_3\text{COE}$  in THF were prepared. 50  $\mu\text{L}$  of  $[\text{Ir}(\text{OMe})\text{COD}]_2$  (0.5  $\mu\text{mol}$ ) stock solution were added to each well across rows A, C, E and G (wells A1-A6, C1-C6, E1-E6 and G1-G6) via micro pipette. 50  $\mu\text{L}$  of  $(\text{dtbpy})\text{Ir}(\text{BPin})_3\text{COE}$  (1.0  $\mu\text{mol}$ ) stock solution were added to each well across rows B and F (wells B1-B6 and F1-F6) via micro pipette. 50  $\mu\text{L}$  of  $(\text{tmphen})\text{Ir}(\text{BPin})_3\text{COE}$  (1.0  $\mu\text{mol}$ ) stock solution were added to each well across rows D and H (wells D1-D6 and H1-H6) via micro pipette. 50  $\mu\text{L}$  of a 0.02 M stock solution of dtbpy (1.0  $\mu\text{mol}$ ) in THF was added to each well across rows A and E (wells A1-A6 and E1-E6) via micro pipette. 50  $\mu\text{L}$  of a 0.02 M stock solution of tmphen (1.0  $\mu\text{mol}$ ) in THF was to each well across rows C and G (wells C1-C6 and G1-G6) via micro pipette. Volatile solvent were removed under reduced pressure. 100  $\mu\text{L}$  of a 0.3 M stock solution of HBPIn (30  $\mu\text{mol}$ ) in THF was added down column 1 (wells A1 through H1) via micro pipette. 100  $\mu\text{L}$  of a 0.3 M stock solution of HBPIn (30  $\mu\text{mol}$ ) in hexanes was added down column 2 (wells A2-H2) via micro pipette. 100  $\mu\text{L}$  of a 0.3 M stock solution of HBPIn (30  $\mu\text{mol}$ ) in Hünig's base was added down column 3 (wells A3-H3) via micro pipette. 100  $\mu\text{L}$  of a 0.3 M stock solution of

HBPIn (30  $\mu\text{mol}$ ) in NMP was added down column 4 (wells A4-H4) via micro pipette. 100  $\mu\text{L}$  of a 0.3 M stock solution of HBPIn (30  $\mu\text{mol}$ ) in IPAc was added down column 5 (wells A5-H5) via micro pipette. 100  $\mu\text{L}$  of a 0.3 M stock solution of HBPIn (30  $\mu\text{mol}$ ) in MeCN was added down column 6 (wells A6-H6) via micro pipette. 100  $\mu\text{L}$  of a 0.2 M stock solution of N,N-dimethyl-*m*-toluidine (20  $\mu\text{mol}$ ) with 2.0  $\mu\text{mol}$  dodecahydrotriphenylene internal standard in THF was added down column 1 (wells A1 through H1) via micro pipette. 100  $\mu\text{L}$  of a 0.2 M stock solution of N,N-dimethyl-*m*-toluidine (20  $\mu\text{mol}$ ) with 2.0  $\mu\text{mol}$  dodecahydrotriphenylene internal standard in hexanes was added down column 2 (wells A2-H2) via micro pipette. 100  $\mu\text{L}$  of 0.2 M stock solution of N,N-dimethyl-*m*-toluidine (20  $\mu\text{mol}$ ) with 2.0  $\mu\text{mol}$  dodecahydrotriphenylene internal standard in Hünig's base was added down column 3 (wells A3-H3) via micro pipette. 100  $\mu\text{L}$  of a 0.2 M stock solution of N,N-dimethyl-*m*-toluidine (20  $\mu\text{mol}$ ) with 2.0  $\mu\text{mol}$  dodecahydrotriphenylene internal standard in NMP was added down column 4 (wells A4-H4) via micro pipette. 100  $\mu\text{L}$  of 0.2 M stock solution of N,N-dimethyl-*m*-toluidine (20  $\mu\text{mol}$ ) with 2.0  $\mu\text{mol}$  dodecahydrotriphenylene internal standard in IPAc was added down column 5 (wells A5-H5) via micro pipette. 100  $\mu\text{L}$  of a 0.2 M stock solution of N,N-dimethyl-*m*-toluidine (20  $\mu\text{mol}$ ) with 2.0  $\mu\text{mol}$  dodecahydrotriphenylene internal standard in MeCN was added down column 6 (wells A6-H6) via micro pipette. The reaction plate was then sealed and stirred for 8h at 80 °C. The reaction was then quenched by exposure to air and dilution with MeCN.

### Extended Solvent Screen at Room Temperature.

In a nitrogen filled glovebox, 16.6 mg  $[\text{Ir}(\text{OMe})\text{COD}]_2$  (2.5  $\mu\text{mol}$ , 2.5 mol%) and 13.3 mg 4,4'-di-tert-butyl-2,2'-bipyridine (5.0  $\mu\text{mol}$ , 5.0 mol%) was dissolved in 1 mL reaction solvent in a 15 mL pressure tube containing a magnetic stir bar. 1.5 equiv HBPIn (1.5 mmol, 218  $\mu\text{L}$ ), 1.0 equiv 3-bromotoluene (1.0 mol, 121  $\mu\text{L}$ ) and 0.1 equiv dodecahydrotriphenylene (0.1 mmol, 24 mg) internal standard were added to the reaction vessel. The reaction vessel was then sealed and allowed to stir at room temp for 4h, at which point the reaction was cooled to room temperature and the reaction mixture quenched by exposure to atmospheric  $\text{O}_2$ . Volatiles were removed under reduced pressure and product yields were determined by  $^1\text{H}$  NMR in  $\text{CDCl}_3$  with respect to dodecahydrotriphenylene internal standard. For DMSO as solvent, 0% product was observed. For DMF as solvent, 4% product was observed.

### Elevated Temperature Reaction Screen Performed on N,N-dimethyltoluidine (5a) in Multiple Solvents.



The 96 reactor wells consist of 1mL glass vials equipped with a micro-magnetic stir bar arrayed in a 12x8 reaction plate, 12 columns labeled 1-12 and 8 rows labeled A-H. In a nitrogen filled



glove box, 0.01 M stock solutions of  $[\text{Ir}(\text{COD})\text{Cl}]_2$  in THF and  $[\text{Ir}(\text{OMe})\text{COD}]_2$  in THF and 0.02 M stock solutions of  $(\text{Ind})\text{Ir}(\text{COD})$  in THF and  $\text{Ir}(\text{acac})\text{COD}$  in THF were prepared. 50  $\mu\text{L}$  of  $[\text{Ir}(\text{OMe})\text{COD}]_2$  (0.5  $\mu\text{mol}$ ) stock solution were added to wells across rows A and E (wells A1-A2, A7-A8 and E1-E2, E7-E8) via micro pipette. 50  $\mu\text{L}$  of  $[\text{Ir}(\text{COD})\text{Cl}]_2$  (0.5  $\mu\text{mol}$ ) stock solution were added to wells across rows B and F (wells B1-B2, B7-B8 and F1-F2, F7-F8) via micro pipette. 50  $\mu\text{L}$  of  $\text{Ir}(\text{acac})\text{COD}$  (1.0  $\mu\text{mol}$ ) stock solution were added to wells across rows C and G (wells C1-C2, C7-C8 and G1-G2, G7-G8) via micro pipette. 50  $\mu\text{L}$  of  $(\text{Ind})\text{Ir}(\text{COD})$  (1.0  $\mu\text{mol}$ ) stock solution were added to wells across rows D and H (wells D1-D2, D7-D8 and H1-H2, H7-H8) via micro pipette. 0.01 M stock solutions of  $[\text{Ir}(\text{COD})\text{Cl}]_2$  in hexanes and  $[\text{Ir}(\text{OMe})\text{COD}]_2$  in hexanes and 0.02 M stock solutions of  $(\text{Ind})\text{Ir}(\text{COD})$  in hexanes and  $\text{Ir}(\text{acac})\text{COD}$  in hexanes were prepared. 50  $\mu\text{L}$  of  $[\text{Ir}(\text{OMe})\text{COD}]_2$  (0.5  $\mu\text{mol}$ ) stock solution were added to wells across rows A and E (wells A3-A4, A9-A10 and E3-E4, E9-E10) via micro pipette. 50  $\mu\text{L}$  of  $[\text{Ir}(\text{COD})\text{Cl}]_2$  (0.5  $\mu\text{mol}$ ) stock solution were added to wells across rows B and F (wells B3-B4, B9-B10 and F3-F4, F9-F10) via micro pipette. 50  $\mu\text{L}$  of  $\text{Ir}(\text{acac})\text{COD}$  (1.0  $\mu\text{mol}$ ) stock solution were added to wells across rows C and G (wells C3-C4, C9-C10 and G3-G4, G9-G10) via micro pipette. 50  $\mu\text{L}$  of  $(\text{Ind})\text{Ir}(\text{COD})$  (1.0  $\mu\text{mol}$ ) stock solution were added to wells across rows D and H (wells D3-D4, D9-D10 and H3-H4, H9-H10) via micro pipette. 0.01 M stock solutions of  $[\text{Ir}(\text{COD})\text{Cl}]_2$  in Hünig's base and  $[\text{Ir}(\text{OMe})\text{COD}]_2$  in Hünig's base and 0.02 M stock solutions of  $(\text{Ind})\text{Ir}(\text{COD})$  in Hünig's base and  $\text{Ir}(\text{acac})\text{COD}$  in Hünig's base were prepared. 50  $\mu\text{L}$  of  $[\text{Ir}(\text{OMe})\text{COD}]_2$  (0.5  $\mu\text{mol}$ ) stock solution were added to wells across rows A

and E (wells A5-A6, A11-A12 and E5-E6, E11-E12) via micro pipette. 50  $\mu\text{L}$  of  $[\text{Ir}(\text{COD})\text{Cl}]_2$  (0.5  $\mu\text{mol}$ ) stock solution were added to wells across rows B and (wells B5-B6, B11-B12 and F5-F6, F11-F12) via micro pipette. 50  $\mu\text{L}$  of  $\text{Ir}(\text{acac})\text{COD}$  (1.0  $\mu\text{mol}$ ) stock solution were added to wells across rows C and G (wells C5-C6, C11-C12 and G5-G6, G11-G12) via micro pipette. 50  $\mu\text{L}$  of (Ind)  $\text{Ir}(\text{COD})$  (1.0  $\mu\text{mol}$ ) stock solution were added to wells across rows D and H (wells D5-D6, D11-D12 and H5-H6, H11-H12) via micro pipette. 50  $\mu\text{L}$  of a 0.02 M stock solution of dtbpy (1.0  $\mu\text{mol}$ ) in THF was added down columns 1 and 7 (wells A1-H1 and A7-H7) via micro pipette. 50  $\mu\text{L}$  of a 0.02 M stock solution of tmphen (1.0  $\mu\text{mol}$ ) in THF was added down columns 2 and 8 (wells A2-H2 and A8-H8) via micro pipette. 50  $\mu\text{L}$  of a 0.02 M stock solution of dtbpy (1.0  $\mu\text{mol}$ ) in hexanes was added down columns 3 and 9 (wells A3-H3 and A9-H9) via micro pipette. 50  $\mu\text{L}$  of a 0.02 M stock solution of tmphen (1.0  $\mu\text{mol}$ ) in hexanes was added down columns 4 and 10 (wells A4-H4 and A10-H10) via micro pipette. 50  $\mu\text{L}$  of a 0.02 M stock solution of dtbpy (1.0  $\mu\text{mol}$ ) in Hünig's base was added down columns 5 and 11 (wells A5-H5 and A11-H11) via micro pipette. 50  $\mu\text{L}$  of a 0.02 M stock solution of tmphen (1.0  $\mu\text{mol}$ ) in Hünig's base was added down columns 6 and 12 (wells A6-H6 and A12-H12) via micro pipette. 50  $\mu\text{L}$  of a 0.6 M stock solution of HBPin (30  $\mu\text{mol}$ ) in THF was added to wells A1-D2 and A7-D8 via micro pipette. 50  $\mu\text{L}$  of a 0.3 M stock solution of  $\text{B}_2\text{Pin}_2$  (15  $\mu\text{mol}$ ) in THF was added to wells E1-H2 and E7-H8 via micro pipette. 50  $\mu\text{L}$  of a 0.6 M stock solution of HBPin (30  $\mu\text{mol}$ ) in hexanes was added to wells A3-D4 and A9-D10 via micro pipette. 50  $\mu\text{L}$  of a 0.3 M stock solution of  $\text{B}_2\text{Pin}_2$  (15  $\mu\text{mol}$ ) in hexanes was added to wells E3-H4 and E9-H10 via micro pipette. 50  $\mu\text{L}$  of a 0.6 M stock solution of HBPin (30  $\mu\text{mol}$ ) in Hünig's base was added across to wells A5-D6 and A11-D12 via micro pipette. 50  $\mu\text{L}$  of a 0.3 M stock solution of  $\text{B}_2\text{Pin}_2$  (15

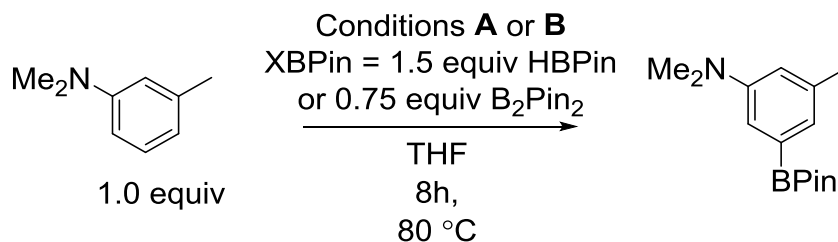
$\mu\text{mol}$ ) in Hünig's base was added to wells E5-H6 and E11-H12 via micro pipette. The reaction plate was then capped and stirred for 5 min at room temperature resulting in catalyst generation under **Conditions B**. Finally, 50  $\mu\text{L}$  of a 0.4 M stock solution of N,N-dimethyl-*m*-toluidine (20  $\mu\text{mol}$ ) in THF, containing dodecahydrotriphenylene internal standard (0.04 M, 2.0  $\mu\text{mol}$ ), was added to wells A1-H2 and A7-H8 via micro pipette. 50  $\mu\text{L}$  of a 0.4 M stock solution of N,N-dimethyl-*m*-toluidine (20  $\mu\text{mol}$ ) in hexanes, containing dodecahydrotriphenylene internal standard (0.04 M, 2.0  $\mu\text{mol}$ ), was added to wells A3-H4 and A9-H10 via micro pipette. 50  $\mu\text{L}$  of a 0.4 M stock solution of N,N-dimethyl-*m*-toluidine (20  $\mu\text{mol}$ ) in Hünig's base, containing dodecahydrotriphenylene internal standard (0.04 M, 2.0  $\mu\text{mol}$ ), was added to wells A5-H6 and A11-H12 via micro pipette and the reaction plate was sealed and stirred for 8h at 80 °C. The reaction was then quenched by exposure to air and dilution with MeCN.

### Temperature Effect on Catalyst Stability

In a nitrogen filled glovebox, 16.6 mg  $[\text{Ir}(\text{OMe})\text{COD}]_2$  (2.5  $\mu\text{mol}$ , 2.5 mol%) and 5.0  $\mu\text{mol}$  dtbpy, tmphen or dppbz, (5.0 mol%) of ligand was dissolved in 1 mL Cpme in a 15 mL pressure tube containing a magnetic stir bar. 1.5 equiv HBPIn (1.5 mmol, 218  $\mu\text{L}$ ), 1.0 equiv N,N-dimethyl-*m*-toluidine (1.0 mol, 145  $\mu\text{L}$ ) and 0.1 equiv dodecahydrotriphenylene (0.1 mmol, 24 mg) internal standard were added to the reaction vessel. The reaction vessel was then sealed and allowed to stir at the indicated temperature (80, 110 or 130 °C) for 12h, at which point the reaction was cooled to room temperature and the reaction mixture quenched by exposure to atmospheric  $\text{O}_2$ . Volatiles were removed under reduced pressure and product yields were determined by  $^1\text{H}$  NMR in  $\text{CDCl}_3$  with respect to dodecahydrotriphenylene internal standard.

## Elevated Temperature Reaction Screen on *N,N*-dimethyl-*m*-toluidine (5a) with Phosphine

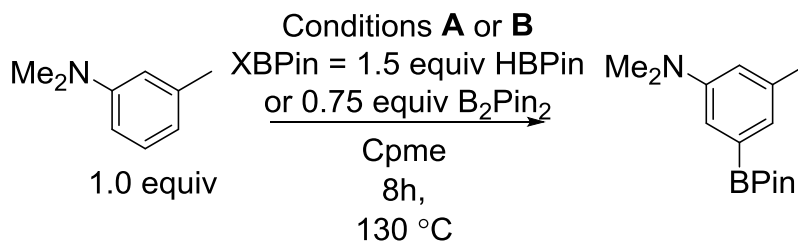
### Ligands



The 96 reactor wells consist of 1mL glass vials equipped with a micro-magnetic stir bar arrayed in a 12x8 reaction plate, 12 columns labeled 1-12 and 8 rows labeled A-H. In a nitrogen filled glove box, 0.01 M stock solutions of [Ir(COD)Cl]<sub>2</sub> in THF and [Ir(OMe)COD]<sub>2</sub> in THF and 0.02 M stock solutions of (Ind)Ir(COD) in THF and Ir(acac)COD in THF were prepared. 50 μL of [Ir(OMe)COD]<sub>2</sub> (0.5 μmol) stock solution were added to each well across rows A and E (wells A1-A12 and E1-E12) via micro pipette. 50 μL of [Ir(COD)Cl]<sub>2</sub> (0.5 μmol) stock solution were added to each well across rows B and F (wells B1-B12 and F1-F12) via micro pipette. 50 μL of Ir(acac)COD (1.0 μmol) stock solution were added to each well across rows C and G (wells C1-C12 and G1-G12) via micro pipette. 50 μL of (Ind) Ir(COD) (1.0 μmol) stock solution were added to each well across rows D and H (wells D1-D12 and H1-H12) via micro pipette. 50 μL of a 0.02 M stock solution of dmpe (1.0 μmol) in THF was added down columns 7 and 10 (wells A7-H7 and A10-H10) via micro pipette. 50 μL of a 0.02 M stock solution of dppe (1.0 μmol) in THF was added down columns 8 and 11 (wells A8-H8 and A11-H11) via micro pipette. 50 μL of a 0.02 M stock solution of dppbz (1.0 μmol) in THF was added down columns 9 and 12 (wells A9-H9 and A12-H12) via micro pipette. 50 μL of a 0.6 M stock solution of HBPIn (30 μmol) in THF was added across rows A, B, C, and D (wells A1-D12) via micro pipette. 50 μL of a 0.3 M

stock solution of B<sub>2</sub>Pin<sub>2</sub> (15 μmol) in THF was added across rows E, F, G, and H (wells E1-H12) via micro pipette. The reaction plate was then capped and stirred for 5 min at room temperature resulting in catalyst generation under **Conditions B** for wells A7-H12. 50 μL of a 0.02 M stock solution of dmpe (1.0 μmol) in THF was added down columns 1 and 4 (wells A1-H1 and A4-H4) via micro pipette. 50 μL of a 0.02 M stock solution of dppe (1.0 μmol) in THF was added down columns 2 and 5 (wells A2-H2 and A5-H5) via micro pipette. 50 μL of a 0.02 M stock solution of dppbz (1.0 μmol) in THF was added down columns 3 and 6 (wells A3-H3 and A6-H6) via micro pipette, resulting in catalyst generation under **Conditions A** for wells A7-H12. Finally, 50 μL of a 0.4 M stock solution of N,N-dimethyl-*m*-toluidine (20 μmol) in THF, containing dodecahydrotriphenylene internal standard (0.04 M, 2.0 μmol), was added to all 96 wells via micro pipette and the reaction plate was sealed and stirred for 8h at 80 °C. The reaction was then quenched by exposure to air and dilution with MeCN.

### 130 °C Reaction Screen on N,N-dimethyl-*m*-toluidine (5a) with Phosphine Ligands



The 96 reactor wells consist of 1mL glass vials equipped with a micro-magnetic stir bar arrayed in a 12x8 reaction plate, 12 columns labeled 1-12 and 8 rows labeled A-H. In a nitrogen filled glove box, 0.01 M stock solutions of [Ir(COD)Cl]<sub>2</sub> in Cpme and [Ir(OMe)COD]<sub>2</sub> in Cpme and 0.02 M stock solutions of (Ind)Ir(COD) in Cpme and Ir(acac)COD in Cpme were prepared. 50 μL

of  $[\text{Ir}(\text{OMe})\text{COD}]_2$  (0.5  $\mu\text{mol}$ ) stock solution were added to each well across rows A and E (wells A1-A12 and E1-E12) via micro pipette. 50  $\mu\text{L}$  of  $[\text{Ir}(\text{COD})\text{Cl}]_2$  (0.5  $\mu\text{mol}$ ) stock solution were added to each well across rows B and F (wells B1-B12 and F1-F12) via micro pipette. 50  $\mu\text{L}$  of  $\text{Ir}(\text{acac})\text{COD}$  (1.0  $\mu\text{mol}$ ) stock solution were added to each well across rows C and G (wells C1-C12 and G1-G12) via micro pipette. 50  $\mu\text{L}$  of (Ind)  $\text{Ir}(\text{COD})$  (1.0  $\mu\text{mol}$ ) stock solution were added to each well across rows D and H (wells D1-D12 and H1-H12) via micro pipette. 50  $\mu\text{L}$  of a 0.02 M stock solution of dmpe (1.0  $\mu\text{mol}$ ) in Cpme was added down columns 7 and 10 (wells A7-H7 and A10-H10) via micro pipette. 50  $\mu\text{L}$  of a 0.02 M stock solution of dmpbz (1.0  $\mu\text{mol}$ ) in Cpme was added down columns 8 and 11 (wells A8-H8 and A11-H11) via micro pipette. 50  $\mu\text{L}$  of a 0.02 M stock solution of dppbz (1.0  $\mu\text{mol}$ ) in Cpme was added down columns 9 and 12 (wells A9-H9 and A12-H12) via micro pipette. 50  $\mu\text{L}$  of a 0.6 M stock solution of HBPin (30  $\mu\text{mol}$ ) in Cpme was added across rows A, B, C, and D (wells A1-D12) via micro pipette. 50  $\mu\text{L}$  of a 0.3 M stock solution of  $\text{B}_2\text{Pin}_2$  (15  $\mu\text{mol}$ ) in Cpme was added across rows E, F, G, and H (wells E1-H12) via micro pipette. The reaction plate was then capped and stirred for 5 min at room temperature resulting in catalyst generation under **Conditions B** for wells A7-H12. 50  $\mu\text{L}$  of a 0.02 M stock solution of dmpe (1.0  $\mu\text{mol}$ ) in Cpme was added down columns 1 and 4 (wells A1-H1 and A4-H4) via micro pipette. 50  $\mu\text{L}$  of a 0.02 M stock solution of dmpbz (1.0  $\mu\text{mol}$ ) in Cpme was added down columns 2 and 5 (wells A2-H2 and A5-H5) via micro pipette. 50  $\mu\text{L}$  of a 0.02 M stock solution of dppbz (1.0  $\mu\text{mol}$ ) in Cpme was added down columns 3 and 6 (wells A3-H3 and A6-H6) via micro pipette, resulting in catalyst generation under **Conditions A** for wells A7-H12. Finally, 50  $\mu\text{L}$  of a 0.4 M stock solution of *N,N*-dimethyl-*m*-toluidine (20  $\mu\text{mol}$ ) in Cpme, containing dodecahydrotriphenylene internal standard (0.04 M,

2.0  $\mu\text{mol}$ ), was added to all 96 wells via micro pipette and the reaction plate was sealed and stirred for 8h at 130 °C. The reaction was then quenched by exposure to air and dilution with MeCN.

### **Borylation of 2,6-dimethylanisole (7a).**

In a nitrogen filled glovebox, 16.6 mg  $[\text{Ir}(\text{OMe})\text{COD}]_2$  (2.5  $\mu\text{mol}$ , 2.5 mol%) and 5.0  $\mu\text{mol}$  dtbpy, dmabpy, phen or tmphen, (5.0 mol%) of ligand was dissolved in 1 mL THF in a 15 mL pressure tube containing a magnetic stir bar. 1.0 equiv  $\text{B}_2\text{Pin}_2$  (1.0 mmol, 254 mg), 1.0 equiv 2,6-dimethylanisole (1.0 mol, 141  $\mu\text{L}$ ) and 0.1 equiv dodecahydrotriphenylene (0.1 mmol, 24 mg) internal standard were added to the reaction vessel. The reaction vessel was then sealed and allowed to stir at 80 °C for 4h, at which point the reaction was cooled to room temperature and the reaction mixture quenched by exposure to atmospheric  $\text{O}_2$ . Volatiles were removed under reduced pressure and product yields were determined by  $^1\text{H}$  NMR in  $\text{CDCl}_3$  with respect to dodecahydrotriphenylene internal standard.

### **Kinetic Experiments with (tmphen)Ir(BPin)<sub>3</sub>(COE) and (dtbpy)Ir(BPin)<sub>3</sub>(COE).**

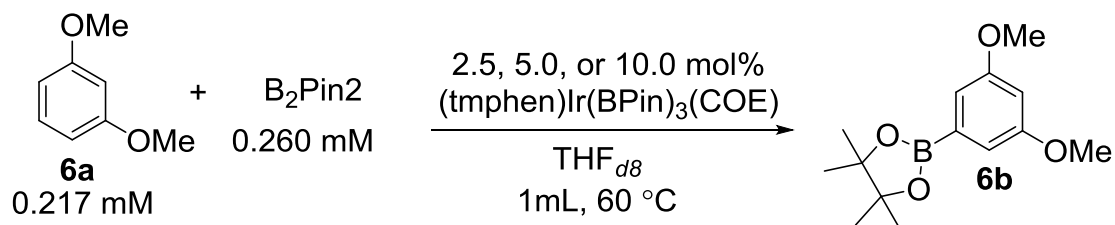
37  $\mu\text{L}$  of HBPIn or 66 mg B<sub>2</sub>Pin<sub>2</sub> (0.260 mmol, 1.2 equiv) was weighed into a test tube and dissolved in 1 mL THF<sub>d8</sub>. This solution was then transferred to a test tube containing 5.84 mg of (tmphen)Ir(BPin)<sub>3</sub>(COE) or 6.04 mg of (dtbpy)Ir(BPin)<sub>3</sub>(COE) (6.35  $\mu\text{mol}$ , 5.0 mol%) and 10.68 mg 1,3,5-tri-*tert*-butylbenzene (43  $\mu\text{mol}$ , 0.20 equiv). 1,3-dimethoxybenzene (27.8  $\mu\text{L}$ , 0.217 mmol, 1 equiv) was added to the vial *via* microliter syringe. The solution was then transferred to a screw cap NMR tube. The tubes were heated in the NMR probe and monitored by <sup>1</sup>H NMR.

### **Precatalyst Aging Study**

Batches of [Ir(OMe)COD]<sub>2</sub>, [Ir(Cl)COD]<sub>2</sub>, Ir(acac)COD, and Ir(1,1,1,3,3,3-hexafluoroacetylacetonate)COD were bought from multiple commercial suppliers, subdivided and stored in closed containers over solid Mg(SO<sub>4</sub>) (21% relative humidity), saturated aqueous Mg(NO<sub>3</sub>) (51% relative humidity) and deionized H<sub>2</sub>O (100% relative humidity) for 100 days and then tested with **General Procedure for Microscale Reactions Utilizing Conditions A**. The relative humidities were determined by an internal hydrometer.



**Kinetic Experiments with (tmphen)Ir(BPin)<sub>3</sub>(COE) at higher and lower catalyst loadings.**

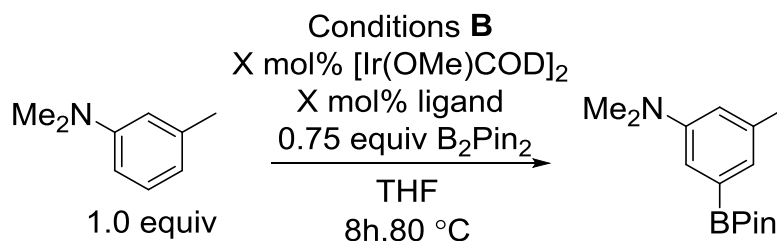


66 mg B<sub>2</sub>Pin<sub>2</sub> (0.260 mmol, 1.2 equiv) was weighed into a test tube and dissolved in 1 mL THF<sub>d8</sub>. This solution was then transferred to a test tube containing 2.92 or 11.68 mg of (tmphen)Ir(BPin)<sub>3</sub>(COE) (3.18 μmol, 2.5 mol% or 12.7 μmol, 10.0 mol%) and 10.68 mg 1,3,5-tri-*tert*-butylbenzene (43 μmol, 0.20 equiv) internal standard. 1,3-dimethoxybenzene (27.8 μL, 0.217 mmol, 1 equiv) was added to the vial *via* microliter syringe. The solution was then transferred to a screw cap NMR tube. The tubes were heated in the NMR probe and monitored by <sup>1</sup>H NMR.

### **Open and Closed System C-H Borylation of 1,3-diisopropylbenzene (8a).**

In a nitrogen filled glovebox, a 250  $\mu\text{L}$  of a 0.010 M stock solution containing  $[\text{Ir}(\text{OMe})\text{COD}]_2$  in THF was dispensed into an 8 mL scintillation vial equipped with a magnetic stir bar. To this solution, 250  $\mu\text{L}$  of a 0.020 M stock solution containing tmphen in THF, followed by 250  $\mu\text{L}$  of a 0.60 M stock solution containing HBPin in THF. Finally, 250  $\mu\text{L}$  of a 0.40 M stock solution containing 1,3-diisopropylbenzene substrate and dodecahydrotriphenylene (0.040 M with respect to DHT) as internal standard in THF was added to the reaction vial and the vial was sealed with an open top screw cap fitted with a Teflon seal. 12 such reaction vials were made of which six were fitted with an 18<sub>G</sub> 1½ PrecisionGlide® Needle. 12 additional reaction vials were made with a 0.30 M stock solution containing B<sub>2</sub>Pin<sub>2</sub> in THF in place of the 0.60 M HBPin/THF solutions. Again 6 of these were fitted with an 18<sub>G</sub> 1½ PrecisionGlide® Needle. 24 reaction vials identical to those previously described with the exception of a 0.020 M stock solution containing dtbpy instead of tmphen were prepared, again 12 made with a 0.60 M stock solution containing HBPin in THF and 12 with a 0.30 M stock solution containing B<sub>2</sub>Pin<sub>2</sub> in THF. Half of each 12 were likewise, fitted with an 18<sub>G</sub> 1½ PrecisionGlide® Needle. The reaction vials were then placed on to two 4x6 reactor well plates and heated to 70 °C in the glove box. At each of the six time points (30 min, 1, 2, 3, 5, and 8h) 8 reaction vials (1 of each ligand, borylating reagent and open vs. closed combination) were removed and quenched by exposure to atmospheric O<sub>2</sub> and conversions were determined by HPLC. The weight of the reaction mixture was then measured to determine if there was any significant loss of solvent. In all cases the weight of the reaction mixtures was the same showing there was no appreciable loss of solvent.

## Catalyst Loading Study

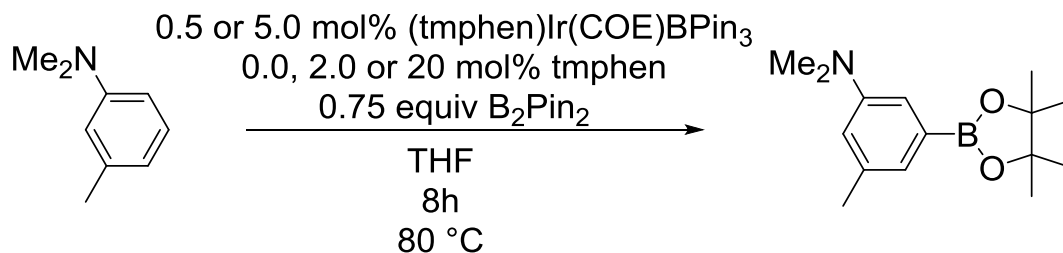


Reaction was set-up in a nitrogen filled glove box, in a 96 reactor well plate consisting of 1mL glass vials equipped with a micro-magnetic stir bar arrayed in a 12x8 reaction plate, 12 columns labeled 1-12 and 8 rows labeled A-H. A 0.02 M stock solution of dtbpy in THF was prepared and 40  $\mu\text{L}$  (0.8  $\mu\text{mol}$ ) was added to wells A1 and A7, 50  $\mu\text{L}$  (1.0  $\mu\text{mol}$ ) was added to wells A2 and A8, 70  $\mu\text{L}$  (1.4  $\mu\text{mol}$ ) was added to wells A3 and A9, 100  $\mu\text{L}$  (2.0  $\mu\text{mol}$ ) was added to wells A4 and A10, 200  $\mu\text{L}$  (4.0  $\mu\text{mol}$ ) was added to wells A5 and A11, and 400  $\mu\text{L}$  (8.0  $\mu\text{mol}$ ) was added to wells A6 and A12 via micro pipette. A 0.01 M stock solution of dtbpy in THF was prepared and 40  $\mu\text{L}$  (0.4  $\mu\text{mol}$ ) was added to wells B1 and B7, 50  $\mu\text{L}$  (0.5  $\mu\text{mol}$ ) was added to wells B2 and B8, 70  $\mu\text{L}$  (0.7  $\mu\text{mol}$ ) was added to wells B3 and B9, 100  $\mu\text{L}$  (1.0  $\mu\text{mol}$ ) was added to wells B4 and B10, 200  $\mu\text{L}$  (2.0  $\mu\text{mol}$ ) was added to wells B5 and B11, and 400  $\mu\text{L}$  (4.0  $\mu\text{mol}$ ) was added to wells B6 and B12 via micro pipette. A 0.004 M stock solution of dtbpy in THF was prepared and 40  $\mu\text{L}$  (0.16  $\mu\text{mol}$ ) was added to wells C1 and C7, 50  $\mu\text{L}$  (0.2  $\mu\text{mol}$ ) was added to wells C2 and C8, 70  $\mu\text{L}$  (0.28  $\mu\text{mol}$ ) was added to wells C3 and C9, 100  $\mu\text{L}$  (0.4  $\mu\text{mol}$ ) was added to wells C4 and C10, 200  $\mu\text{L}$  (0.8  $\mu\text{mol}$ ) was added to wells C5 and C11, and 400  $\mu\text{L}$  (1.6  $\mu\text{mol}$ ) was added to wells C6 and C12 via micro pipette. A 0.002 M stock solution of dtbpy in THF was prepared and 40  $\mu\text{L}$  (0.08  $\mu\text{mol}$ ) was added to wells D1 and D7, 50  $\mu\text{L}$  (0.1  $\mu\text{mol}$ ) was added to wells D2 and D8, 70  $\mu\text{L}$  (0.14  $\mu\text{mol}$ ) was added to wells D3 and D9, 100  $\mu\text{L}$  (0.2  $\mu\text{mol}$ ) was added to wells D4 and D10, 200  $\mu\text{L}$  (0.4  $\mu\text{mol}$ ) was added to wells D5 and D11, and 400  $\mu\text{L}$  (0.8  $\mu\text{mol}$ ) was added to wells D6 and D12 via micro pipette. A 0.02 M stock solution of tmphen

in THF was prepared and 40  $\mu\text{L}$  (0.8  $\mu\text{mol}$ ) was added to wells E1 and E7, 50  $\mu\text{L}$  (1.0  $\mu\text{mol}$ ) was added to wells E2 and E8, 70  $\mu\text{L}$  (1.4  $\mu\text{mol}$ ) was added to wells E3 and E9, 100  $\mu\text{L}$  (2.0  $\mu\text{mol}$ ) was added to wells E4 and E10, 200  $\mu\text{L}$  (4.0  $\mu\text{mol}$ ) was added to wells E5 and E11, and 400  $\mu\text{L}$  (8.0  $\mu\text{mol}$ ) was added to wells E6 and E12 via micro pipette. A 0.01 M stock solution of tmphen in THF was prepared and 40  $\mu\text{L}$  (0.4  $\mu\text{mol}$ ) was added to wells F1 and F7, 50  $\mu\text{L}$  (0.5  $\mu\text{mol}$ ) was added to wells F2 and F8, 70  $\mu\text{L}$  (0.7  $\mu\text{mol}$ ) was added to wells F3 and F9, 100  $\mu\text{L}$  (1.0  $\mu\text{mol}$ ) was added to wells F4 and F10, 200  $\mu\text{L}$  (2.0  $\mu\text{mol}$ ) was added to wells F5 and F11, and 400  $\mu\text{L}$  (4.0  $\mu\text{mol}$ ) was added to wells F6 and F12 via micro pipette. A 0.004 M stock solution of tmphen in THF was prepared and 40  $\mu\text{L}$  (0.16  $\mu\text{mol}$ ) was added to wells G1 and G7, 50  $\mu\text{L}$  (0.2  $\mu\text{mol}$ ) was added to wells G2 and G8, 70  $\mu\text{L}$  (0.28  $\mu\text{mol}$ ) was added to wells G3 and G9, 100  $\mu\text{L}$  (0.4  $\mu\text{mol}$ ) was added to wells G4 and G10, 200  $\mu\text{L}$  (0.8  $\mu\text{mol}$ ) was added to wells G5 and G11, and 400  $\mu\text{L}$  (1.6  $\mu\text{mol}$ ) was added to wells G6 and G12 via micro pipette. A 0.002 M stock solution of tmphen in THF was prepared and 40  $\mu\text{L}$  (0.08  $\mu\text{mol}$ ) was added to wells H1 and H7, 50  $\mu\text{L}$  (0.1  $\mu\text{mol}$ ) was added to wells H2 and H8, 70  $\mu\text{L}$  (0.14  $\mu\text{mol}$ ) was added to wells H3 and H9, 100  $\mu\text{L}$  (0.2  $\mu\text{mol}$ ) was added to wells H4 and H10, 200  $\mu\text{L}$  (0.4  $\mu\text{mol}$ ) was added to wells H5 and H11, and 400  $\mu\text{L}$  (0.8  $\mu\text{mol}$ ) was added to wells H6 and H12 via micro pipette. The THF was then removed under reduced pressure. 500  $\mu\text{L}$  of a 0.001 M stock solution of  $[\text{Ir}(\text{OMe})\text{COD}]_2$  (0.5  $\mu\text{mol}$ ) in THF was added to each well across rows A and E (wells A1-A12 and E1-E12) via micro pipette. 250  $\mu\text{L}$  of a 0.001 M stock solution of  $[\text{Ir}(\text{OMe})\text{COD}]_2$  (0.25  $\mu\text{mol}$ ) in THF was added to each well across rows A and E (wells B1-B12 and F1-F12) via micro pipette. 100  $\mu\text{L}$  of a 0.001 M stock solution of  $[\text{Ir}(\text{OMe})\text{COD}]_2$  (0.1  $\mu\text{mol}$ ) in THF was added to each well across rows C and G (wells C1-C12 and G1-G12) via micro pipette. 50  $\mu\text{L}$  of a 0.001

M stock solution of  $[\text{Ir}(\text{OMe})\text{COD}]_2$  (0.05  $\mu\text{mol}$ ) in THF was added to each well across rows D and H (wells D1-D12 and H1-H12) via micro pipette. The THF was then removed under reduced pressure. 100  $\mu\text{L}$  of 0.75 M stock solution of  $\text{B}_2\text{Pin}_2$  (0.75  $\mu\text{mol}$ ) in THF was added to all 96 wells. 100  $\mu\text{L}$  of 1.0 M stock solution of *N,N*-dimethyl-*m*-toluidine (100  $\mu\text{mol}$ ) and 10  $\mu\text{mol}$  dodecahydrotriphenylene internal standard in THF was added to all 96 wells. The well plate was sealed and heated to 80  $^\circ\text{C}$  for 8h, at which point the reaction was cooled to room temperature and quenched by exposure to atmospheric  $\text{O}_2$  and dilution with MeCN.

#### Ligand to Metal Ratio with preformed $(\text{tmphen})\text{Ir}(\text{COE})\text{BPin}_3$



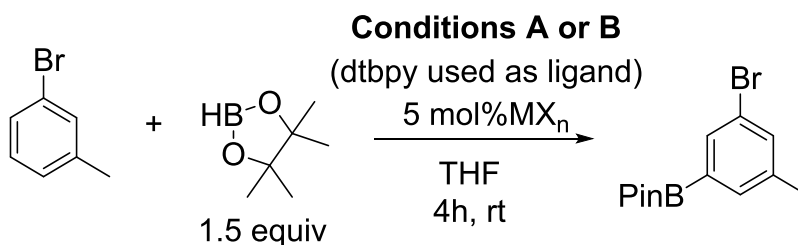
In a nitrogen filled glovebox, 190 mg (0.75 mmol)  $\text{B}_2\text{Pin}_2$ , 24 mg (0.10 mmol) dodecahydrotriphenylene, 4.6 or 46 mg (0.005 or 0.05 mmol)  $(\text{tmphen})\text{Ir}(\text{COE})\text{BPin}_3$ , and 4.7 or 47 mg (0.02 or 0.2 mmol) *tmphen* (if used) were weighed into test tubes and then dissolved in 1 mL THF and transferred to a 15 mL pressure tube containing a magnetic stir bar. 145  $\mu\text{L}$  (1.0 mmol) of *N,N*-dimethyl-*m*-toluidine was added to the pressure tube. The reaction vessel was sealed and the reaction mixture heated to 80  $^\circ\text{C}$  for 8h, at which point the reaction was cooled to

room temperature and quenched by exposure to atmospheric O<sub>2</sub> and MeOH. Volatiles were removed under reduced pressure and reaction yields were determined by <sup>1</sup>H NMR.

**Table 5.1.** Ligand to Metal Ratio with preformed (tmphen)Ir(COE)BPin<sub>3</sub>.

entry	mol % (tmphen)Ir(COE)BPin <sub>3</sub>	mol % tmphen	Yield (%)
1	<b>0.5</b>	--	89
2	<b>0.5</b>	<b>2.0</b>	92
3	<b>5.0</b>	--	82
4	<b>5.0</b>	<b>20</b>	79

#### Additive Screen.

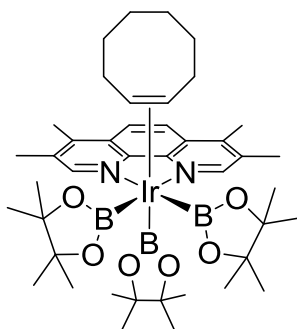


The 96 reactor wells consist of 1mL glass vials equipped with a micro-magnetic stir bar arrayed in a 12x8 reaction plate, 12 columns labeled 1-12 and 8 rows labeled A-H. In a nitrogen filled glove box, 0.02 M stock solutions of K(acac) in MeOH, Na(acac) in MeOH, KOMe in MeOH and K<sup>t</sup>BuO in THF and 0.01 M stock solutions of Ti(acac)<sub>2</sub>(O) in MeOH and Mg(acac)<sub>2</sub> in MeOH and 0.66 M stock solution of Al(acac)<sub>3</sub> in MeOH were prepared. Volatile solvent were

removed under reduced pressure. 50  $\mu\text{L}$  of  $[\text{Ir}(\text{COD})\text{Cl}]_2$  (0.5  $\mu\text{mol}$ ) stock solution were added to each well down columns 1, 2, 5, 6, 9, and 10 (wells A1-H2, A5-H6, and A9-H10) via micro pipette. 50  $\mu\text{L}$  of  $[\text{Ir}(\text{OMe})\text{COD}]_2$  (0.5  $\mu\text{mol}$ ) stock solution were added to each well down columns 3, 4, 7, 8, 11, and 12 (wells A3-H4, A7-H8, and A11-H12) via micro pipette. 50  $\mu\text{L}$  of  $(\text{dtbpy})\text{Ir}(\text{BPin})_3\text{COE}$  (1.0  $\mu\text{mol}$ ) stock solution were added to each well across rows B and F (wells B1-B12 and F1-F12) via micro pipette. 50  $\mu\text{L}$  of a 0.02 M stock solution of dtbpy (1.0  $\mu\text{mol}$ ) in THF was added down columns 1, 3, 5, 7, 9, and 11 (wells A1-H1, A3-H3, A5-H5, A7-H7, A9-H9 and A11-H11) via micro pipette. 50  $\mu\text{L}$  of a 0.6 M stock solution of HBPin (30  $\mu\text{mol}$ ) in THF was added to all 96 reaction wells. 50  $\mu\text{L}$  of a 0.02 M stock solution of dtbpy (1.0  $\mu\text{mol}$ ) in THF was added down columns 2, 4, 6, 8, 10, and 12 (wells A2-H2, A4-H4, A6-H6, A8-H8, A10-H10 and A12-H12) via micro pipette. Finally, 50  $\mu\text{L}$  of a 0.4 M stock solution of 3-bromotoluene containing dodecahydrotriphenylene internal standard (0.04 M) was added to all 96 wells via micro pipette and the reaction plate was sealed and stirred for 4h at room temperature. The reaction was then quenched by exposure to air and dilution with MeCN.

**Precatalyst and Ligand NMR reactions.** In a nitrogen filled glovebox, 25  $\mu\text{mol}$  iridium precatalyst dimer or 50  $\mu\text{mol}$  Iridium monomer was dissolved in 750  $\mu\text{L}$  in  $\text{THF}_{d8}$  in a test tube. This solution was then transferred to a test tube containing 50  $\mu\text{mol}$  ligand and 5  $\mu\text{mol}$  1,3,5-tri-*t*-butylbenzene via pipette. The resulting mixture was then transferred to a screw cap NMR tube and sealed.

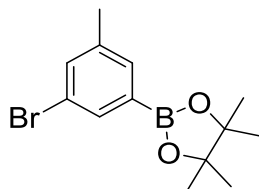
## Synthesis of (tmphen)Ir(BPin)<sub>3</sub>(COE)



In a 100 mL flask, equipped with a magnetic stir bar, 500 mg [Ir(OMe)COD]<sub>2</sub> (0.75 mmol) was dissolved in 80 mL cyclohexane. 1.2 mL *cis*-cyclooctene (9 mmol) was added via micropipette. 1.3 mL of HBPIn (9 mmol) was added dropwise by syringe to a vigorously stirred solution. A solution of 3,4,7,8-tetramethyl-1,10-phenanthroline (354 mg, 1.5 mmol) dissolved in DCM (10 mL) was added via pipette and the solution was stirred for 30 min. Volatiles were removed by evaporation and (tmphen)Ir(BPin)<sub>3</sub>(COE) was purified by trituration with petroleum ether as a yellow solid (yield 510 mg, 37% yield); decomposition 114-120 °C. <sup>1</sup>H NMR (500 MHz, THF<sub>d8</sub>, -35 °C) δ 9.62 (s, 2H), 8.18 (s, 2H), 3.86 (d, *J* = 7 Hz, 2H), 2.76 (s, 6H) 2.55 (s, 6H), 1.27 (br m, 12H), 1.22 (s, 12H), 1.19 (s, 12H), 0.54 (s, 12H); <sup>13</sup>C NMR (125 MHz, THF<sub>d8</sub>, -35 °C) δ 154.2, 146.9, 140.5, 131.2, 128.3, 122.3, 79.0, 78.6, 75.4, 31.1, 26.3, 24.9, 24.2, 23.9; <sup>11</sup>B NMR (160 MHz, THF<sub>d8</sub>) δ 37 (br s); Anal. Calcd for C<sub>44</sub>H<sub>66</sub>IrB<sub>3</sub>N<sub>2</sub>O<sub>6</sub>: C, 54.85; H, 7.23; N, 3.05. Found: C, 54.63; H, 6.98; N, 2.99.

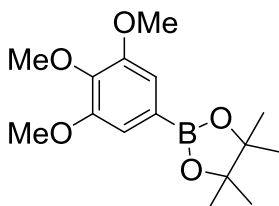


**3-Bromo-5-(4,4,5,5-tetramethyl-1,3,2-dioxaborolan-2-yl)toluene (3b)**



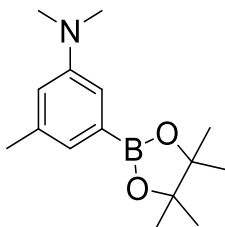
General procedure A was scaled up to the 1.0 mmol scale for isolation using  $[\text{Ir}(\text{OMe})\text{COD}]_2$  as catalyst, dtbpy as ligand and 0.75 equiv  $\text{B}_2\text{Pin}_2$  as borylating reagent. Product was isolated by passing the reaction mixture through  $\text{SiO}_2$  and evaporation of the volatiles. Off-white solid; 217 mg, 73% yield; mp 74-76 °C. NMR data reported matched that in ref 1.  $^1\text{H}$  NMR (500 MHz,  $\text{CDCl}_3$ )  $\delta$  7.73 (s, 1H), 7.53 (s, 1H), 7.41 (s, 1H), 2.32 (s, 3H), 1.34 (s, 12H);  $^{13}\text{C}$  NMR (125 MHz,  $\text{CDCl}_3$ )  $\delta$  140.1, 133.8, 133.3, 121.5, 84.0, 24.5, 20.3;  $^{11}\text{B}$  NMR (160 MHz,  $\text{CDCl}_3$ )  $\delta$  30 (br s).

**1,2,3-Trimethoxy-5-(4,4,5,5-tetramethyl-1,3,2-dioxaborolan-2-yl)benzene (4b)**



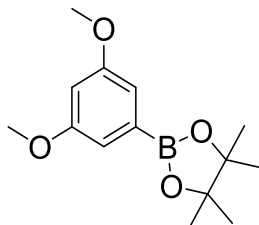
General procedure A was scaled up to the 1.0 mmol scale for isolation using  $[\text{Ir}(\text{OMe})\text{COD}]_2$  as catalyst, dtbpy as ligand and 0.75 equiv  $\text{B}_2\text{Pin}_2$  as borylating reagent. Product was isolated by passing the reaction mixture through  $\text{SiO}_2$  and evaporation of the volatiles, followed by recrystallization from 1:1 MeOH:H<sub>2</sub>O. White solid; 270 mg, 92% yield; mp 104-106 °C. NMR data reported matched that in ref 2. <sup>1</sup>H NMR (500 MHz, CDCl<sub>3</sub>) δ 7.03 (s, 2H), 3.90 (s, 6H), 3.87 (s, 3H), 1.34 (s, 12H); <sup>13</sup>C NMR (125 MHz, CDCl<sub>3</sub>) δ 152.9, 140.9, 111.3, 83.9, 60.8, 56.1, 24.8; <sup>11</sup>B NMR (160 MHz, CDCl<sub>3</sub>) δ 30 (br s).

**N,N-Dimethyl-3-(4,4,5,5-tetramethyl-1,3,2-dioxaborolan-2-yl)-5-methyl benzamine (5b)**



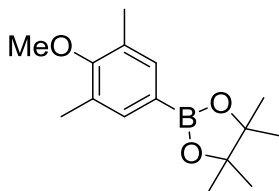
General procedure A was scaled up to the 1.0 mmol scale for isolation using  $[\text{Ir}(\text{OMe})\text{COD}]_2$  as catalyst, dtbpy as ligand and 0.75 equiv  $\text{B}_2\text{Pin}_2$  as borylating reagent. Product was isolated by passing the reaction mixture through  $\text{SiO}_2$  and evaporation of the volatiles. Off-white solid; 245 mg, 94% yield; mp 82-84 °C.  $^1\text{H}$  NMR (500 MHz,  $\text{CDCl}_3$ )  $\delta$  7.03 (s, 1H), 7.02 (s, 1H), 6.68 (s, 1H), 2.95 (s, 6H), 2.32 (s, 3H), 1.34 (s, 12H);  $^{13}\text{C}$  NMR (125 MHz,  $\text{CDCl}_3$ )  $\delta$  150.4, 138.0, 124.1, 116.7, 116.0, 83.5, 40.8, 24.8, 21.6;  $^{11}\text{B}$  NMR (160 MHz,  $\text{CDCl}_3$ )  $\delta$  31 (br s). Anal. Calcd for  $\text{C}_{15}\text{H}_{24}\text{BNO}_2$ : C, 68.98; H, 9.26; N, 5.36. Found: C, 69.18; H, 9.26; N, 5.36.

**1,3-Dimethoxy-5-(4,4,5,5-tetramethyl-1,3,2-dioxaborolan-2-yl) benzene (6b)**



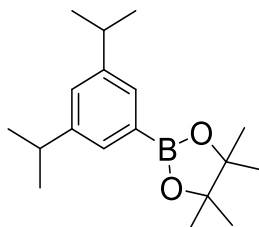
General procedure A was scaled up to the 1.0 mmol scale for isolation using  $[\text{Ir}(\text{OMe})\text{COD}]_2$  as catalyst, dtbpy as ligand and 0.75 equiv  $\text{B}_2\text{Pin}_2$  as borylating reagent. Product was isolated by passing the reaction mixture through  $\text{SiO}_2$  and evaporation of the volatiles. White solid; 216 mg, 82% yield; mp 87-88 °C. NMR data matched that reported in ref 1.  $^1\text{H}$  NMR (500 MHz,  $\text{CDCl}_3$ )  $\delta$  6.95 (d,  $J = 2.4$  Hz, 2H), 6.56 (t,  $J = 2.4$  Hz, 1H), 3.81 (s, 6H), 1.34 (s, 12H);  $^{13}\text{C}$  NMR (125 MHz,  $\text{CDCl}_3$ )  $\delta$  160.4, 111.6, 104.5, 83.9, 55.4, 24.8;  $^{11}\text{B}$  NMR (160 MHz,  $\text{CDCl}_3$ )  $\delta$  30 (br s).

**2,5-Dimethyl-4-(4,4,5,5-tetramethyl-1,3,2-dioxaborolan-2-yl) anisole (7b)**



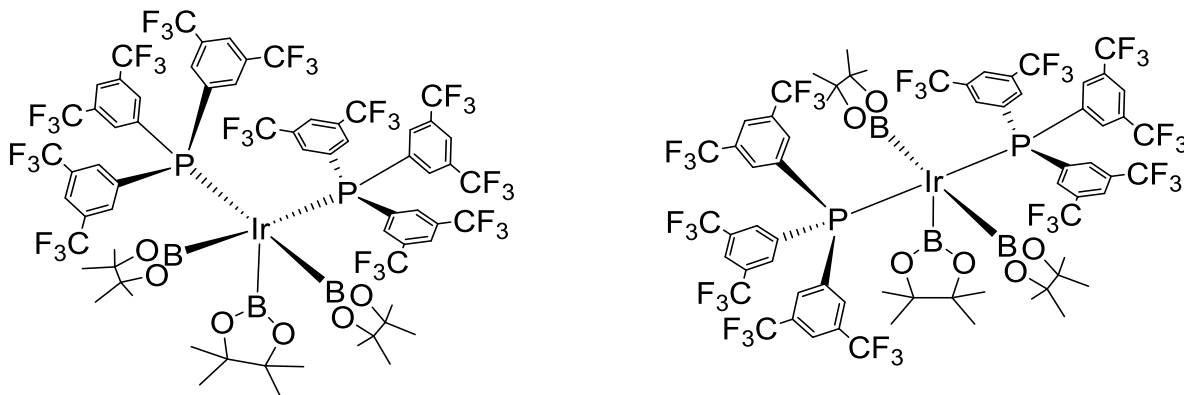
General procedure A was scaled up to the 1.0 mmol scale for isolation using  $[\text{Ir}(\text{OMe})\text{COD}]_2$  as catalyst, dtbpy as ligand and 0.75 equiv  $\text{B}_2\text{Pin}_2$  as borylating reagent. Product was isolated by passing the reaction mixture through  $\text{SiO}_2$  and evaporation of the volatiles. White solid; 230 mg, 88% yield; mp 84-86 °C. NMR data matched that reported in ref 3.  $^1\text{H}$  NMR (500 MHz,  $\text{CDCl}_3$ )  $\delta$  7.49 (s, 2H), 3.73 (s, 3H), 2.29 (s, 6H), 1.33 (s, 12H);  $^{13}\text{C}$  NMR (125 MHz,  $\text{CDCl}_3$ )  $\delta$  159.8, 135.6, 130.3, 83.6, 59.6, 24.8, 15.8;  $^{11}\text{B}$  NMR (160 MHz,  $\text{CDCl}_3$ )  $\delta$  31 (br s).

**1,3-Diisopropyl-5-(4,4,5,5-tetramethyl-1,3,2-dioxaborolan-2-yl) benzene (8b)**



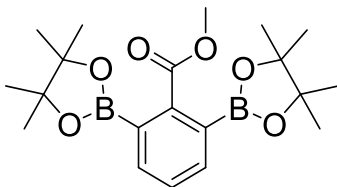
General procedure A was scaled up to the 1.0 mmol scale for isolation using  $[\text{Ir}(\text{OMe})\text{COD}]_2$  as catalyst, dtbpy as ligand and 0.75 equiv  $\text{B}_2\text{Pin}_2$  as borylating reagent. Product was isolated by passing the reaction mixture through  $\text{SiO}_2$  and evaporation of the volatiles. White solid; 239 mg, 83% yield; mp 118-120 °C. NMR data matched that reported in ref 4.  $^1\text{H}$  NMR (500 MHz,  $\text{CDCl}_3$ )  $\delta$  7.51 (d,  $J = 1.5$  Hz, 2H), 7.19 (t,  $J = 1.5$  Hz, 1H), 2.93 (m, 2H), 1.35 (s, 12H), 1.28 (m, 12 H);  $^{13}\text{C}$  NMR (125 MHz,  $\text{CDCl}_3$ )  $\delta$  148.1, 132.6, 130.4, 127.7, 83.6, 34.2, 24.8, 24.0;  $^{11}\text{B}$  NMR (160 MHz,  $\text{CDCl}_3$ )  $\delta$  31 (br s).

**Synthesis of *cis*- and *trans*-((3,5-bis(trifluoromethyl)benzene)<sub>3</sub>P)<sub>2</sub>Ir(BPin)<sub>3</sub> (9a) and (9b).**



In a 20 mL vial, equipped with a magnetic stirring bar, ( $\eta^6$ -MesH)Ir(BPin)<sub>3</sub> (280 mg, 0.40 mmol, 1 equiv) was dissolved in THF (4 mL). Tris(3,5-bis(trifluoromethyl)benzene)<sub>3</sub>phosphine (PAr<sup>F</sup><sub>3</sub>) (570 mg, 0.81 mmol, 2 equiv) was weighed out in a test tube and was transferred to the reaction vial by dissolving in THF (2 mL). The reaction was stirred at room temperature for 4 h. The crude reaction mixture was pumped down under high vacuum to give a mixture of the desired complex and its *cis* isomer as a light yellow solid (yield 580 mg, 76%). *cis*-(Ar<sup>F</sup><sub>3</sub>P)<sub>2</sub>Ir(BPin)<sub>3</sub> <sup>1</sup>H NMR (THF<sub>d8</sub>, 500 MHz):  $\delta$  8.37 (s, 6H), 8.04 (br, 12H), 1.02 (s, 36H); <sup>11</sup>B NMR (THF<sub>d8</sub>, 160 MHz):  $\delta$  39; <sup>31</sup>P NMR (THF<sub>d8</sub>, 202 MHz):  $\delta$  36.86; <sup>19</sup>F NMR (THF<sub>d8</sub>, 470 MHz)  $\delta$  -58.72. *trans*-(Ar<sup>F</sup><sub>3</sub>P)<sub>2</sub>Ir(BPin)<sub>3</sub> <sup>1</sup>H NMR (THF<sub>d8</sub>, 500 MHz):  $\delta$  8.19 (s, 6H), 8.13 (s, 12H), 0.78 (s, 36H); <sup>11</sup>B NMR (THF<sub>d8</sub>, 160 MHz):  $\delta$  39; <sup>31</sup>P NMR (THF<sub>d8</sub>, 202 MHz):  $\delta$  28.81; <sup>19</sup>F NMR (THF<sub>d8</sub>, 470 MHz)  $\delta$  -58.53.

**methyl 2,6-bis(4,4,5,5-tetramethyl-1,3,2-dioxaborolan-2-yl)benzoate (10c)**



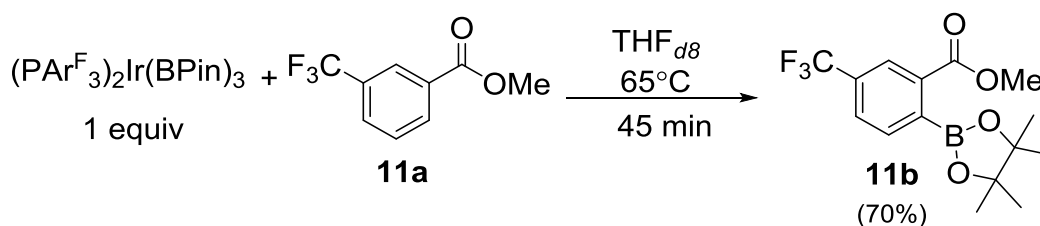
In a nitrogen filled glovebox, 126  $\mu\text{L}$  methyl benzoate (1.0 mmol, 1.0 equiv) was dissolved in 1 mL THF in a 15 mL pressure tube containing a magnetic stir bar. 2.0 equiv  $\text{B}_2\text{Pin}_2$  (218  $\mu\text{L}$ ) was added and the reaction vessel was sealed and stirred at room temperature for 1h. 2.5  $\mu\text{mol}$   $[\text{Ir}(\text{OMe})\text{COD}]_2$  (2.5 mol%) and 5.0  $\mu\text{mol}$   $\text{SiPbz}$  (5.0 mol%) were added and the reaction vessel was sealed and heated at 80  $^\circ\text{C}$  for 16h. The reaction mixture was allowed to return to room temperature and the reaction mixture was exposed to air and diluted with 1 mL MeOH. The volatiles were then removed under reduced pressure and the product was purified by passing it through a short plug of  $\text{SiO}_2$  in MTBE. The product was isolated by recrystallization from MeOH/ $\text{H}_2\text{O}$ . White solid (244 mg);  $^1\text{H}$  NMR (500 MHz,  $\text{CDCl}_3$ )  $\delta$  7.70 (d,  $J = 7.4$  Hz, 2H), 7.43 (d,  $J = 7.3$  Hz, 1H), 3.89 (s, 3H), 1.35 (s, 24H);  $^{13}\text{C}$  NMR (125 MHz,  $\text{CDCl}_3$ )  $\delta$  170.6, 141.7, 135.4, 128.9, 84.0, 52.0, 24.8;  $^{11}\text{B}$  NMR (160 MHz,  $\text{CDCl}_3$ )  $\delta$  31 (br s). ; HRMS (ESI)  $m/z$  calcd for  $\text{C}_{20}\text{H}_{31}\text{B}_2\text{O}_6$   $[\text{M} + \text{H}]^+$  389.2307, found 389.2307.



### **Ligand and Borane Effects Screen on the Borylation of methyl benzoate (10a).**

Reaction was conducted in  $8 \times 30$  mm borosilicate glass shell vials arranged in 96 well metal blocks (Symyx) with magnetic stirring. In a nitrogen filled glove box, a 50  $\mu$ L of 0.01 M stock solutions of  $[\text{Ir}(\text{OMe})\text{COD}]_2$  (0.5  $\mu$ mol) in THF were added to a 1 mL reaction vial containing a magnetic stir bar. 50  $\mu$ L of a 0.04 M stock solution of ligand (2.0  $\mu$ mol) in THF was added to reaction vials containing  $[\text{Ir}(\text{OMe})\text{COD}]_2$ . 50  $\mu$ L of a solution of either 30  $\mu$ mol HBPIn (0.6 M), 30  $\mu$ mol  $\text{B}_2\text{Pin}_2$  (0.6 M), 30  $\mu$ mol HBPIn and 30  $\mu$ mol  $\text{B}_2\text{Pin}_2$  (0.6 M), or 60  $\mu$ mol  $\text{B}_2\text{Pin}_2$  (1.2 M) in THF was added via micropipette. Finally, 50  $\mu$ L of a 0.2 M stock solution containing methyl benzoate (20  $\mu$ mol) and 2.0  $\mu$ mol dodecahydrotriphenylene internal standard in THF was added to the reaction mixture. The reaction vessel was then sealed and stirred at 80  $^\circ\text{C}$  for 16h. The reaction was then cooled to room temperature and quenched by exposure to atmospheric  $\text{O}_2$  and dilution with MeCN. Volatiles were removed and assay yields were determined by  $^1\text{H}$  NMR.

### Stoichiometric borylation of (11a) with $(\text{Ar}^{\text{F}}_3\text{P})_2\text{Ir}(\text{BPin})_3$

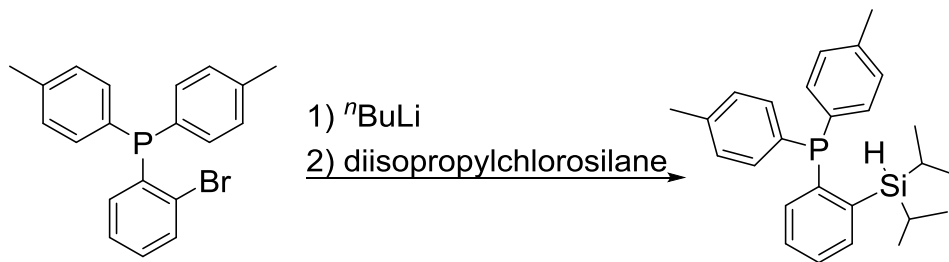


$(\text{Ar}^{\text{F}}_3\text{P})_2\text{Ir}(\text{BPin})_3$  (80 mg, 0.0418 mmol, 1 equiv) was weighed in a test tube and was dissolved in  $\text{THF}_{d8}$  (750  $\mu\text{L}$ ). Methyl 3-trifluoromethylbenzoate (6.5 mg, 0.0418 mmol, 1 equiv) was weighed in a test tube and mixed with the solution containing  $(\text{Ar}^{\text{F}}_3\text{P})_2\text{Ir}(\text{BPin})_3$ . The mixture was then transferred via pipette into a J. Young NMR tube. The J. Young NMR tube was capped and the reaction was monitored by  $^1\text{H}$  and  $^{31}\text{P}$  NMR.

### NMR reaction of $(\text{Ar}^{\text{F}}_3\text{P})_2\text{Ir}(\text{BPin})_3$ with excess THT.

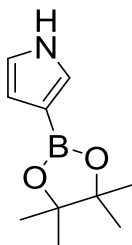
$(\text{Ar}^{\text{F}}_3\text{P})_2\text{Ir}(\text{BPin})_3$  (40 mg, 0.0209 mmol, 1 equiv) was weighed in a test tube and was dissolved in THF (1.0 mL). THT (18  $\mu\text{L}$ , 0.209 mmol, 10 equiv) was added to the solution containing  $(\text{Ar}^{\text{F}}_3\text{P})_2\text{Ir}(\text{BPin})_3$  via micro syringe. The mixture was then transferred via pipette into a J. Young NMR tube. The J. Young NMR tube was capped and the reaction was monitored  $^{31}\text{P}$  NMR.

### Synthesis of (2-(diisopropylsilyl)phenyl)di-p-tolylphosphane (SiPbz).



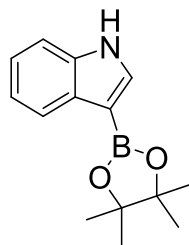
In a nitrogen filled glovebox, 333 mg (2-bromophenyl)di-p-tolylphosphine (0.9 mmol) was dissolved in 10 mL ether in a 20 mL scintillation vial and cooled to  $-30\text{ }^{\circ}\text{C}$ . 396  $\mu\text{L}$  of  $n\text{BuLi}$  (2.5M in hexanes, 1.1 equiv) was further diluted in 5 mL ether and added to the solution containing (2-bromophenyl)di-p-tolylphosphine drop wise. The reaction was sealed and stirred for 30 min while it was allowed to come to room temperature. Volatiles were removed under reduced pressure and the residue was dissolved in 10 mL toluene. 162 mg diisopropylchlorosilane (1.08 mmol, 1.2 equiv) was added to the solution and the reaction was sealed and stirred at room temperature for 4 h. The mixture was then filtered and the precipitate washed with toluene. Volatiles were removed under reduced pressure and the product was isolated as a pure white solid (365 mg, 99% yield). );  $^1\text{H}$  NMR (500 MHz,  $\text{C}_6\text{D}_6$ )  $\delta$  7.62-7.58 (m, 1H), 7.36-7.33 (m, 1H), 7.31 (t,  $J = 7.8, 7.4$  Hz, 4H), 7.08-7.02 (m, 2H), 6.90 (d,  $J = 7.8$  Hz, 4H), 4.57 (m, 1H), 1.98 (s, 6H), 1.47 (m, 2H), 1.17 (d,  $J = 7.3$  Hz, 6H), 1.01 (d,  $J = 7.4$  Hz, 6H);  $^{13}\text{C}$  NMR (125 MHz,  $\text{C}_6\text{D}_6$ )  $\delta$  144.7 (d,  $J = 11.5$  Hz), 143.3, 142.9, 137.9, 136.9 (d,  $J = 5.3$  Hz), 134.9 (s,  $J = 10.5$  Hz), 134.3, 133.7 (d,  $J = 19.1$  Hz), 129.3, 129.2, 20.7, 19.4, 12.3 (d,  $J = 5.7$  Hz);  $^{31}\text{P}$  NMR (202 MHz,  $\text{C}_6\text{D}_6$ )  $\delta$  -9.74 (s).

### 3-(4,4,5,5-tetramethyl-1,3,2-dioxaborolan-2-yl)-1H-pyrrole (15)



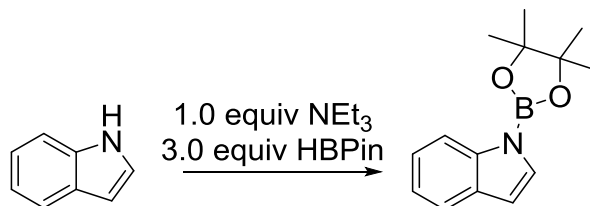
In a nitrogen filled glovebox, 69  $\mu\text{L}$  pyrrole (1 mmol) was dissolved in 1 mL THF in a 15 mL pressure tube containing a magnetic stir bar. 3.0 equiv HBPIn (435  $\mu\text{L}$ ) and 1.0 equiv  $\text{NEt}_3$  (140  $\mu\text{L}$ ) was added and the reaction vessel was sealed and stirred at room temperature for 12h. 0.25  $\mu\text{mol}$   $[\text{Ir}(\text{OMe})\text{COD}]_2$  (0.25 mol%) and 1.0  $\mu\text{mol}$  3,4,7,8-tetramethyl-1,10-phenanthroline (1.0 mol%) were added and the reaction vessel was sealed and heated at 80  $^\circ\text{C}$  for 4h. The reaction mixture was allowed to return to room temperature and the reaction mixture was exposed to air and diluted with 5 mL MeOH. The volatiles were then removed under reduced pressure and the product was purified by passing it through a short plug of  $\text{SiO}_2$  in MTBE. The product was isolated by recrystallization from MeOH/ $\text{H}_2\text{O}$ . White solid (185 mg, 76% isolated yield);  $^1\text{H}$  NMR (500 MHz,  $\text{CDCl}_3$ )  $\delta$  8.62 (br s, 1H), 7.24 (d, 2H), 6.85 (dd,  $J = 4.4, 2.5$  Hz, 1H), 6.57 (d,  $J = 1.4$  Hz, 1H), 1.33 (s, 12H);  $^{13}\text{C}$  NMR (125 MHz,  $\text{CDCl}_3$ )  $\delta$  127.0, 118.5, 113.8, 83.0, 24.9;  $^{11}\text{B}$  NMR (160 MHz,  $\text{CDCl}_3$ )  $\delta$  29 (br s).<sup>5,6</sup>

### 3-(4,4,5,5-tetramethyl-1,3,2-dioxaborolan-2-yl)-indole (16)



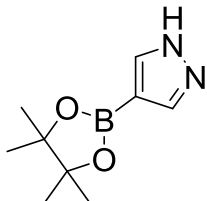
In a nitrogen filled glovebox, 117 mg indole (1 mmol) was dissolved in 1 mL THF in a 15 mL pressure tube containing a magnetic stir bar. 2.0 equiv HBPIn (290  $\mu$ L) and 1.0 equiv  $\text{NEt}_3$  (140  $\mu$ L) was added and the reaction vessel was sealed and heated at 80  $^\circ\text{C}$  for 10 min. 0.25  $\mu$ mol  $[\text{Ir}(\text{OMe})\text{COD}]_2$  (0.25 mol%) and 1.0  $\mu$ mol 3,4,7,8-tetramethyl-1,10-phenanthroline (1.0 mol%) were added and the reaction vessel was sealed and heated at 80  $^\circ\text{C}$  for 4h. The reaction mixture was allowed to return to room temperature and the reaction mixture was exposed to air and diluted with 5 mL MeOH. The volatiles were then removed under reduced pressure and the product was purified by passing it through a short plug of  $\text{SiO}_2$  in MTBE. The product was isolated by recrystallization from MeOH/ $\text{H}_2\text{O}$ . White solid (139 mg, 57% isolated yield);  $^1\text{H}$  NMR (500 MHz,  $\text{CDCl}_3$ )  $\delta$  8.47 (br s, 1H), 8.08 (dd,  $J = 7.3, 2.4$  Hz, 2H), 7.65 (d,  $J = 2.4$  Hz, 1H), 7.40 (dd,  $J = 7.4, 1.9$  Hz, 1H), 7.23-7.18 (m, 2H), 1.37 (s, 12H);  $^{13}\text{C}$  NMR (125 MHz,  $\text{CDCl}_3$ )  $\delta$  136.0, 133.5, 131.9, 122.8, 83.0, 24.9;  $^{11}\text{B}$  NMR (160 MHz,  $\text{CDCl}_3$ )  $\delta$  30 (br s).<sup>5</sup>

**In Situ generation of 1-(4,4,5,5-tetramethyl-1,3,2-dioxaborolan-2-yl)-1H-indole**



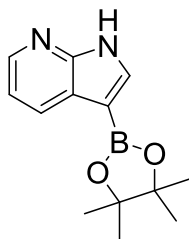
In a nitrogen filled glovebox 117 mg indole (1 mmol) was dissolved in 1 mL  $C_6D_6$  in a screw cap NMR tube. 2.0 equiv HBpin (290  $\mu$ L) and 1.0 equiv  $NEt_3$  (140  $\mu$ L) was added and the tube was sealed and heated at 80  $^\circ$ C for 30 min. Quantitative conversion was observed by NMR.  $^1H$  NMR (500 MHz,  $C_6D_6$ )  $\delta$  8.24 (d,  $J = 8.4$  Hz, 1H), 7.56 (d,  $J = 7.8$  Hz, 1H), 7.48 (d,  $J = 3.5$  Hz, 1H), 7.25 (dd,  $J = 8.4, 6.8$  Hz, 1H), 7.15 (dd,  $J = 7.8, 6.8$  Hz, 1H), 0.96 (s, 12H);  $^{11}B$  NMR (160 MHz,  $C_6D_6$ )  $\delta$  24 (br s).

**4-(4,4,5,5-tetramethyl-1,3,2-dioxaborolan-2-yl)-pyrazole (17)**



In a nitrogen filled glovebox, 68 mg pyrazole (1 mmol) was dissolved in 1 mL THF in a 15 mL pressure tube containing a magnetic stir bar. 0.25  $\mu\text{mol}$   $[\text{Ir}(\text{OMe})\text{COD}]_2$  (0.25 mol%), 1.0  $\mu\text{mol}$  3,4,7,8-tetramethyl-1,10-phenanthroline (1.0 mol%) and 2.0 equiv HBPIn (290  $\mu\text{L}$ ) were added and the reaction vessel was sealed and heated at 80  $^{\circ}\text{C}$  for 4h. The reaction mixture was allowed to return to room temperature and the reaction mixture was exposed to air and diluted with 5 mL MeOH. The volatiles were then removed under reduced pressure and the product was purified by passing it through a short plug of  $\text{SiO}_2$  in MTBE. The product was isolated by recrystallization from MeOH/ $\text{H}_2\text{O}$ . White solid (171 mg, 88% isolated yield);  $^1\text{H}$  NMR (500 MHz,  $\text{CDCl}_3$ )  $\delta$  7.90 (s, 1H), 7.81 (s, 1H), 4.75 (br s, 1H), 1.35 (s, 12H);  $^{13}\text{C}$  NMR (125 MHz,  $\text{CDCl}_3$ )  $\delta$  133.9, 83.8, 24.9;  $^{11}\text{B}$  NMR (160 MHz,  $\text{CDCl}_3$ )  $\delta$  30 (br s).<sup>5</sup>

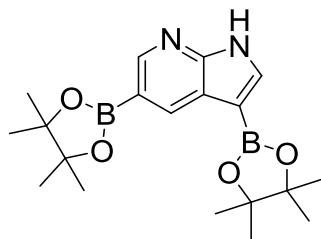
### 3-(4,4,5,5-tetramethyl-1,3,2-dioxaborolan-2-yl)-7-azaindole (18a)



In a nitrogen filled glovebox, 188 mg 7-azaindole (1 mmol) was dissolved in 1 mL THF in a 15 mL pressure tube containing a magnetic stir bar. 0.25  $\mu\text{mol}$   $[\text{Ir}(\text{OMe})\text{COD}]_2$  (0.25 mol%), 1.0  $\mu\text{mol}$  3,4,7,8-tetramethyl-1,10-phenanthroline (1.0 mol%) and 2.0 equiv HBPin (290  $\mu\text{L}$ ) were added and the reaction vessel was sealed and heated at 80  $^\circ\text{C}$  for 4h. The reaction mixture was allowed to return to room temperature and the reaction mixture was exposed to air and diluted with 5 mL MeOH. The volatiles were then removed under reduced pressure and the product was purified by passing it through a short plug of  $\text{SiO}_2$  in MTBE. The product was isolated by recrystallization from MeOH/ $\text{H}_2\text{O}$ . White solid (185 mg, 76% isolated yield);  $^1\text{H}$  NMR (500 MHz,  $\text{CDCl}_3$ )  $\delta$  11.36 (br s, 1H), 8.32 (m, 2H), 7.84 (s, 1H), 7.14 (dd,  $J = 7.3, 4.9$  Hz, 1H), 1.37 (s, 12H);  $^{13}\text{C}$  NMR (125 MHz,  $\text{CDCl}_3$ )  $\delta$  149.9, 142.5, 134.8, 130.9, 124.4, 116.5, 83.0, 24.9;  $^{11}\text{B}$  NMR (160 MHz,  $\text{CDCl}_3$ )  $\delta$  29 (br s).

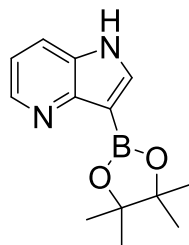


**3,5-bis(4,4,5,5-tetramethyl-1,3,2-dioxaborolan-2-yl)-7-azaindole (18b)**



In a nitrogen filled glovebox, 188 mg 7-azaindole (1 mmol) was dissolved in 1 mL THF in a 15 mL pressure tube containing a magnetic stir bar. 0.25  $\mu\text{mol}$   $[\text{Ir}(\text{OMe})\text{COD}]_2$  (0.25 mol%), 1.0  $\mu\text{mol}$  3,4,7,8-tetramethyl-1,10-phenanthroline (1.0 mol%) and 2.0 equiv  $\text{B}_2\text{Pin}_2$  (508 mg) were added and the reaction vessel was sealed and heated at 80  $^\circ\text{C}$  for 4h. The reaction mixture was allowed to return to room temperature and the reaction mixture was exposed to air and diluted with 5 mL MeOH. The volatiles were then removed under reduced pressure and the product was purified by passing it through a short plug of  $\text{SiO}_2$  in MTBE. The product was isolated by recrystallization from MeOH/ $\text{H}_2\text{O}$ . White solid (332 mg, 91% isolated yield); mp: 209-210  $^\circ\text{C}$ ;  $^1\text{H}$  NMR (500 MHz,  $\text{CDCl}_3$ )  $\delta$  11.7 (s, 1H), 8.73 (d,  $J = 1.5$  Hz, 1H), 8.68 (d,  $J = 1.5$  Hz, 1H), 7.83 (s, 1H), 1.40 (s, 12H), 1.38 (s, 12H);  $^{13}\text{C}$  NMR (125 MHz,  $\text{CDCl}_3$ )  $\delta$  151.5, 149.3, 137.6, 134.9, 123.4, 83.8, 83.1, 24.9;  $^{11}\text{B}$  NMR (160 MHz,  $\text{CDCl}_3$ )  $\delta$  31; HRMS (ESI)  $m/z$  calcd for  $\text{C}_{19}\text{H}_{28}\text{B}_2\text{N}_2\text{O}_4$   $[\text{M} + \text{H}]^+$  371.2320, found 371.2509.

### 3-(4,4,5,5-tetramethyl-1,3,2-dioxaborolan-2-yl)-4-azaindole (19)



In a nitrogen filled glovebox, 188 mg 4-azaindole (1 mmol) was dissolved in 1 mL THF in a 15 mL pressure tube containing a magnetic stir bar. 0.25  $\mu\text{mol}$   $[\text{Ir}(\text{OMe})\text{COD}]_2$  (0.25 mol%), 1.0  $\mu\text{mol}$  3,4,7,8-tetramethyl-1,10-phenanthroline (1.0 mol%) and 2.0 equiv HBPIn (290  $\mu\text{L}$ ) were added and the reaction vessel was sealed and heated at 80  $^\circ\text{C}$  for 4h. The reaction mixture was allowed to return to room temperature and the reaction mixture was exposed to air and diluted with 5 mL MeOH. The volatiles were then removed under reduced pressure and the product was purified by passing it through a short plug of  $\text{SiO}_2$  in MTBE. The product was isolated by recrystallization from MeOH/ $\text{H}_2\text{O}$ . White solid (202 mg, 83% isolated yield);  $^1\text{H}$  NMR (500 MHz,  $\text{DMSO-d}_6$ )  $\delta$  11.39 (br s, 1H), 8.51 (s, 1H), 7.97 (s, 1H), 7.71 (dd,  $J = 5.9, 3.0$  Hz, 1H), 6.54 (s, 1H), 1.30 (s, 12H);  $^{13}\text{C}$  NMR (125 MHz,  $\text{DMSO-d}_6$ )  $\delta$  148.5, 148.0, 131.3, 128.3, 124.8, 102.2, 84.0, 25.1; HRMS (ESI)  $m/z$  calcd for  $\text{C}_{13}\text{H}_{17}\text{BN}_2\text{O}_2$   $[\text{M} + \text{H}]^+$  245.1461, found 245.1456.

**Borane and Solvent Effects Screen on Borylation of 3-chloroaniline (22a).** In a nitrogen filled glove box, a 50  $\mu\text{L}$  of 0.01 M stock solutions of  $[\text{Ir}(\text{OMe})\text{COD}]_2$  in THF were added to a 1 mL reaction vial containing a magnetic stir bar. 50  $\mu\text{L}$  of a 0.02 M stock solution of dtbpy (1.0  $\mu\text{mol}$ ) or tmphen (1.0  $\mu\text{mol}$ ) in DCM was added to reaction vials containing  $[\text{Ir}(\text{OMe})\text{COD}]_2$ . Volatiles were removed under reduced pressure. The reaction vials were then subjected to one set of three following conditions using stock solutions made up in THF, cyclohexane, N,N-diisopropylethylamine, or NMP:

1) 100  $\mu\text{L}$  of a solution of 22  $\mu\text{mol}$   $\text{B}_2\text{Pin}_2$  (0.22 M) in the reaction solvent was added via micropipette.

2) 100  $\mu\text{L}$  of a solution of 44  $\mu\text{mol}$   $\text{B}_2\text{Pin}_2$  (0.44 M) in the reaction solvent was added via micropipette.

3) 100  $\mu\text{L}$  of a solution containing 22  $\mu\text{mol}$  HBPin (0.22 M) and 22  $\mu\text{mol}$   $\text{B}_2\text{Pin}_2$  (0.22 M) in the reaction solvent was added via micropipette.

Then, 100  $\mu\text{L}$  of a 0.2 M stock solution containing 3-chloroaniline (20  $\mu\text{mol}$ ) and 2.0  $\mu\text{mol}$  dodecahydrotriphenylene internal standard in reaction solvent was added to the reaction mixture. The reaction vessel was then sealed and the reaction mixture stirred at 80  $^\circ\text{C}$  for 8h. The reaction was then cooled to room temperature and quenched by exposure to atmospheric  $\text{O}_2$  and dilution with MeOH. Volatiles were removed and assay yields were determined by  $^1\text{H}$  NMR.

**Extended Solvent Screen for 3-(trifluoromethyl)anilines (20a).** In a nitrogen filled glove box, 1 mmol 3-(trifluoromethyl)aniline was dissolved in 1 mL NMP, DMA or 1.26 g sulfolane in a 15 mL pressure tube containing a magnetic stir bar. 1.5 equiv HBPin (218  $\mu$ L) was added and the reaction vessel was sealed and stirred at room temperature for 1h. 0.25  $\mu$ mol [Ir(OMe)COD]<sub>2</sub> (0.25 mol%), 1.0  $\mu$ mol 3,4,7,8-tetramethyl-1,10-phenanthroline (1.0 mol%), and 100  $\mu$ mol dodecahydrotriphenylene (24 mg) internal standard and an additional 1.5 mmol HBPin (218  $\mu$ L) and the reaction vessel was sealed and heated at 80 °C for 16h. The reaction mixture was allowed to return to room temperature and the reaction mixture was exposed to air and diluted with 5 mL H<sub>2</sub>O. The product was extracted with DCM and dried under reduced pressure and the product was purified by passing it through a short plug of SiO<sub>2</sub> in MTBE.

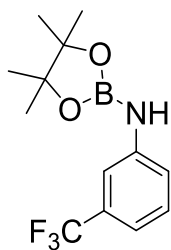
**Table 5.2.** Solvent Screen for 3-(trifluoromethyl)anilines (20)

entry	solvent	yield (%)	<i>meta</i> (%)	<i>ortho</i> (%)	<i>meta</i> : <i>ortho</i>
1	Sulfolane	0	--	--	NA
2	NMP	89	62	27	2.3 : 1.0
6	DMA	36	26	10	2.6 : 1.0

**Ligand Effects Screen on Borylation of 3-(trifluoromethyl)aniline (20).** Reaction was conducted in 8 × 30 mm borosilicate glass shell vials arranged in 24 well metal blocks (Symyx) with magnetic stirring. In a nitrogen filled glove box, a 50 μL of 0.01 M stock solutions of [Ir(OMe)COD]<sub>2</sub> (0.5 μmol) in THF were added to a 1 mL reaction vial containing a magnetic stir bar. 50 μL of a 0.02 M stock solution of ligand (1.0 μmol) in THF was added to reaction vials containing [Ir(OMe)COD]<sub>2</sub>. 50 μL of a solution of 30 μmol B<sub>2</sub>Pin<sub>2</sub> (0.6 M) in THF was added via micropipette. Finally, 50 μL of a 0.2 M stock solution containing 3-(trifluoromethyl)aniline (20 μmol) and 2.0 μmol dodecahydrotriphenylene internal standard in THF was added to the reaction mixture. The reaction vessel was then sealed and stirred at 80 °C for 16h. The reaction was then cooled to room temperature and quenched by exposure to atmospheric O<sub>2</sub> and dilution with MeOH. Volatiles were removed and assay yields were determined by <sup>1</sup>H NMR.

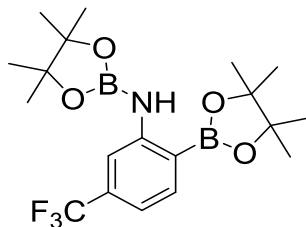
**In Situ generation and borylation of 4,4,5,5-tetramethyl-N-(3-(trifluoromethyl)phenyl)-1,3,2-dioxaborolan-2-amine.** In a nitrogen filled glovebox, 62  $\mu\text{L}$  3-(trifluoromethyl)aniline (0.5 mmol) and 21 mg 1,4-bis(trifluoromethyl)-benzene (0.1 mmol) was dissolved in 1 mL  $\text{THF}_{d8}$  and transferred to a screw cap NMR tube. 109  $\mu\text{L}$  HBPIn (0.75 mmol) was added via micro pipette and the tube was loosely sealed. After 30 min, the cap was firmly tightened and  $^1\text{H}$  and  $^{19}\text{F}$  NMR were recorded. The NMR tube was returned to the glove box and 1.7 mg  $[\text{Ir}(\text{OMe})\text{COD}]_2$  (0.25 mol%), 2.4 mg 3,4,7,8-tetramethyl-1,10-phenanthroline (1.0 mol%) and an additional 109  $\mu\text{L}$  HBPIn (0.75 mmol 1.5 equiv HBPIn (218  $\mu\text{L}$ ) was added and the reaction vessel was sealed and heated at 80  $^\circ\text{C}$  for 8h.

**$^1\text{H}$  and  $^{19}\text{F}$  NMR of 4,4,5,5-tetramethyl-N-(3-(trifluoromethyl)phenyl)-1,3,2-dioxaborolan-2-amine (20b)**



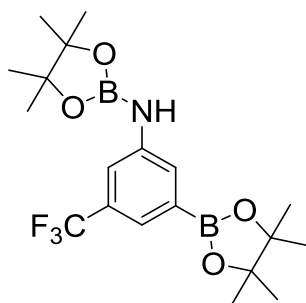
$^1\text{H}$  NMR (500 MHz,  $\text{THF}_{d8}$ )  $\delta$  7.39 (s, 1H), 7.33 (d,  $J = 8.3$  Hz, 1H), 7.24 (t,  $J = 8.3, 7.8$  Hz, 1H), 7.00 (d,  $J = 7.8$  Hz, 1H), 6.32 (br s, 1H), 1.27 (s, 12H);  $^{19}\text{F}$  NMR (470 MHz,  $\text{THF}_{d8}$ )  $\delta$  63.6 (s).

**<sup>1</sup>H and <sup>19</sup>F NMR of 4,4,5,5-tetramethyl-N-(2-(4,4,5,5-tetramethyl-1,3,2-dioxaborolan-2-yl)-5-(trifluoromethyl)phenyl)-1,3,2-dioxaborolan-2-amine (20c)**



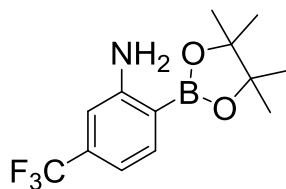
<sup>1</sup>H NMR (500 MHz, THF<sub>d8</sub>) δ 7.96 (s, 1H), 7.73 (d, *J* = 7.8 Hz, 1H), 7.00 (d, *J* = 8.3 Hz, 1H), 6.88 (s, 1H), 1.35 (s, 12H), 1.29 (s, 12H); <sup>19</sup>F NMR (470 MHz, THF<sub>d8</sub>) δ 64.1 (s).

**<sup>1</sup>H and <sup>19</sup>F NMR of 4,4,5,5-tetramethyl-N-(3-(4,4,5,5-tetramethyl-1,3,2-dioxaborolan-2-yl)-5-(trifluoromethyl)phenyl)-1,3,2-dioxaborolan-2-amine (20d)**



<sup>1</sup>H NMR (500 MHz, THF<sub>d8</sub>) δ 7.67 (s, 1H), 7.57 (s, 1H), 7.42 (s, 1H), 6.26 (s, 1H), 1.31 (s, 12H), 1.27 (s, 12H); <sup>19</sup>F NMR (470 MHz, THF<sub>d8</sub>) δ 63.4 (s).

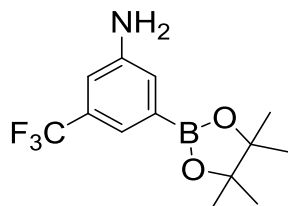
**2-(4,4,5,5-tetramethyl-1,3,2-dioxaborolan-2-yl)-5-(trifluoromethyl)-benzenamine (20f)**



In a nitrogen filled glovebox, 124  $\mu\text{L}$  3-(trifluoromethyl)aniline (1.0 mmol, 1.0 equiv) was dissolved in 1 mL THF in a 15 mL pressure tube containing a magnetic stir bar. 1.5 equiv HBPIn (218  $\mu\text{L}$ ) was added and the reaction vessel was sealed and stirred at room temperature for 1h. 2.5  $\mu\text{mol}$   $[\text{Ir}(\text{OMe})\text{COD}]_2$  (2.5 mol%) and 5.0  $\mu\text{mol}$  3,4,7,8-tetramethyl-1,10-phenanthroline (5.0 mol%) were added followed by an additional 1.5 equiv HBPIn (218  $\mu\text{L}$ ) and the reaction vessel was sealed and heated at 80  $^\circ\text{C}$  for 16h. The reaction mixture was allowed to return to room temperature and the reaction mixture was exposed to air and diluted with 5 mL MeOH. The volatiles were then removed under reduced pressure and the product was purified by passing it through a short plug of  $\text{SiO}_2$  in MTBE. Purified by column chromatography; heptane: MTBE (90: 10). White solid (153 mg); mp: 64-65  $^\circ\text{C}$ ;  $^1\text{H}$  NMR (500 MHz,  $\text{CDCl}_3$ )  $\delta$  7.70 (d,  $J = 7.9$  Hz, 1H), 6.88 (d,  $J = 7.9$  Hz, 1H), 6.80 (s, 1H), 4.92 (br s, 2H), 1.35 (s, 12H);  $^{13}\text{C}$  NMR (125 MHz,  $\text{CDCl}_3$ )  $\delta$  153.6, 137.4, 134.4 (q,  $J = 31.5$  Hz), 125.2 (q,  $J = 272.8$  Hz), 112.8 (q,  $J = 3.8$  Hz), 110.9 (q,  $J = 3.8$  Hz), 84.0, 24.9;  $^{19}\text{F}$  NMR (470 MHz,  $\text{CDCl}_3$ )  $\delta$  63.6;  $^{11}\text{B}$  NMR (160 MHz,  $\text{CDCl}_3$ )  $\delta$  30 (br s); HRMS (ESI)  $m/z$  calcd for  $\text{C}_{13}\text{H}_{17}\text{BF}_3\text{NO}_2$   $[\text{M} + \text{H}]^+$  288.1383, found 288.1378.<sup>7</sup>

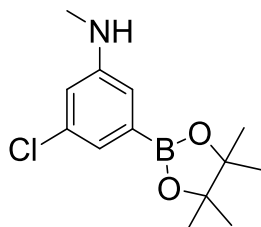


**3-(4,4,5,5-tetramethyl-1,3,2-dioxaborolan-2-yl)-5-(trifluoromethyl)-benzenamine (20e)**



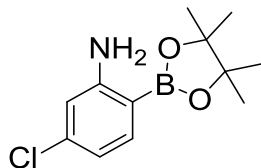
Purified by column chromatography; heptane: MTBE (90: 10). White solid (62 mg); mp: 61-62 °C;  $^1\text{H}$  NMR (500 MHz,  $\text{CDCl}_3$ )  $\delta$  7.43 (s, 1H), 7.26 (s, 1H), 6.96 (s, 1H), 3.82 (br s, 2H), 1.34 (s, 12H);  $^{13}\text{C}$  NMR (125 MHz,  $\text{CDCl}_3$ )  $\delta$  146.1, 131.2 (q,  $J = 31.5$  Hz), 125.3 (q,  $J = 272.7$  Hz), 124.1, 121.1 (q,  $J = 3.8$  Hz), 113.8 (q,  $J = 3.8$  Hz), 84.2, 24.9;  $^{19}\text{F}$  NMR (470 MHz,  $\text{CDCl}_3$ )  $\delta$  62.8;  $^{11}\text{B}$  NMR (160 MHz,  $\text{CDCl}_3$ )  $\delta$  31 (br s); HRMS (ESI)  $m/z$  calcd for  $\text{C}_{13}\text{H}_{17}\text{BF}_3\text{NO}_2$  [ $\text{M} + \text{H}$ ] $^+$  288.1383, found 288.1376.

**N-methyl-3-chloro-5-(4,4,5,5-tetramethyl-1,3,2-dioxaborolan-2-yl)-benzenamine (21b)**



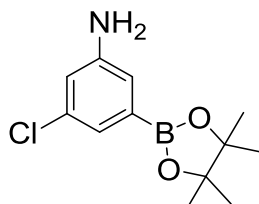
In a nitrogen filled glovebox, 122  $\mu\text{L}$  3-chloro-*N*-methylaniline (1.0 mmol, 1.0 equiv) was dissolved in 1 mL THF in a 15 mL pressure tube containing a magnetic stir bar. 2.0 equiv HBPIn (290  $\mu\text{L}$ ) was added and the reaction vessel was sealed and stirred at room temperature for 1h. 0.25  $\mu\text{mol}$   $[\text{Ir}(\text{OMe})\text{COD}]_2$  (0.25 mol%) and 1.0  $\mu\text{mol}$  3,4,7,8-tetramethyl-1,10-phenanthroline (1.0 mol%) was added and the reaction vessel was sealed and heated at 80  $^\circ\text{C}$  for 16h. The reaction mixture was allowed to return to room temperature and the reaction mixture was exposed to air and diluted with 5 mL MeOH. The volatiles were then removed under reduced pressure and the product was purified by passing it through a short plug of  $\text{SiO}_2$  in MTBE. Product isolated by recrystallization from MeOH/ $\text{H}_2\text{O}$ . White solid (230 mg, 86% isolated yield); mp: 75-76  $^\circ\text{C}$ ;  $^1\text{H}$  NMR (500 MHz,  $\text{CDCl}_3$ )  $\delta$  7.11 (d,  $J = 2.0$  Hz, 1H), 6.90 (d,  $J = 2.5$  Hz, 1H), 6.66 (t,  $J = 2.4, 2.0$  Hz, 1H), 3.77 (br s, 1H), 2.82 (s, 3H), 1.33 (s, 12H);  $^{13}\text{C}$  NMR (125 MHz,  $\text{CDCl}_3$ )  $\delta$  133.9, 122.9, 117.0, 114.4, 84.0, 30.6, 24.9;  $^{11}\text{B}$  NMR (160 MHz,  $\text{CDCl}_3$ )  $\delta$  30 (br s); HRMS (ESI)  $m/z$  calcd for  $\text{C}_{13}\text{H}_{19}\text{BClNO}_2$   $[\text{M} + \text{H}]^+$  268.1276, found 268.1270.

**5-chloro-2-(4,4,5,5-tetramethyl-1,3,2-dioxaborolan-2-yl)-benzenamine (22c)**



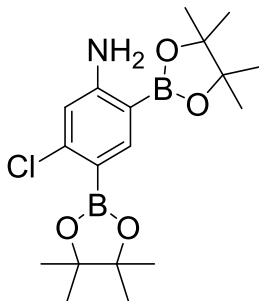
In a nitrogen filled glovebox, 106  $\mu\text{L}$  3-(chloro)aniline (1.0 mmol, 1.0 equiv) was dissolved in 1 mL THF in a 15 mL pressure tube containing a magnetic stir bar. 1.5 equiv HBPIn (218  $\mu\text{L}$ ) was added and the reaction vessel was sealed and stirred at room temperature for 1h. 2.5  $\mu\text{mol}$   $[\text{Ir}(\text{OMe})\text{COD}]_2$  (2.5 mol%) and 5.0  $\mu\text{mol}$  3,4,7,8-tetramethyl-1,10-phenanthroline (5.0 mol%) were added followed by an additional 1.5 equiv HBPIn (218  $\mu\text{L}$ ) and the reaction vessel was sealed and heated at 80  $^\circ\text{C}$  for 16h. The reaction mixture was allowed to return to room temperature and the reaction mixture was exposed to air and diluted with 5 mL MeOH. The volatiles were then removed under reduced pressure and the product was purified by passing it through a short plug of  $\text{SiO}_2$  in MTBE. Purified by column chromatography; heptane: MTBE (90: 10). White solid (105 mg, 42% isolated yield); mp: 64-65  $^\circ\text{C}$ ;  $^1\text{H}$  NMR (500 MHz,  $\text{CDCl}_3$ )  $\delta$  7.50 (d,  $J = 7.8$  Hz, 1H), 6.63 (dd,  $J = 7.8, 1.9$  Hz, 1H), 6.58 (d,  $J = 2.0$  Hz, 1H), 4.80 (br s, 2H), 1.35 (s, 12H);  $^{13}\text{C}$  NMR (125 MHz,  $\text{CDCl}_3$ )  $\delta$  154.6, 138.6, 138.0, 117.1, 114.2, 83.6, 24.9;  $^{11}\text{B}$  NMR (160 MHz,  $\text{CDCl}_3$ )  $\delta$  30 (br s); HRMS (ESI)  $m/z$  calcd for  $\text{C}_{12}\text{H}_{17}\text{BClNO}_2$  [ $\text{M} + \text{H}$ ] $^+$  254.1121, found 254.1129.

**3-chloro-5-(4,4,5,5-tetramethyl-1,3,2-dioxaborolan-2-yl)aniline (22b)**



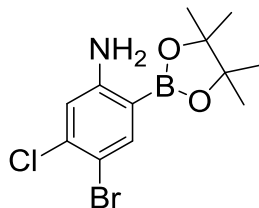
Purified by column chromatography; heptane: MTBE (90: 10). Yellow solid (43 mg, 17% isolated yield); mp: 54-55 °C;  $^1\text{H}$  NMR (500 MHz,  $\text{CDCl}_3$ )  $\delta$  7.17 (d,  $J = 1.0$  Hz, 1H), 6.98 (d,  $J = 1.9$  Hz, 1H) 6.76 (dd,  $J = 1.9, 1.0$  Hz, 1H), 3.70 (br s, 2H), 1.34 (s, 12H);  $^{13}\text{C}$  NMR (125 MHz,  $\text{CDCl}_3$ )  $\delta$  147.1, 146.3, 124.4, 119.2, 115.4, 84.0, 24.8;  $^{11}\text{B}$  NMR (160 MHz,  $\text{CDCl}_3$ )  $\delta$  30 (br s); HRMS (ESI)  $m/z$  calcd for  $\text{C}_{12}\text{H}_{17}\text{BClNO}_2$  [ $\text{M} + \text{H}$ ] $^+$  254.1121, found 254.1134.

**$^1\text{H}$  and  $^{13}\text{C}$  NMR of 5-chloro-2,4-bis(4,4,5,5-tetramethyl-1,3,2-dioxaborolan-2-yl)aniline (22d)**



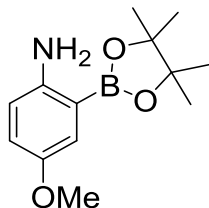
$^1\text{H}$  NMR (500 MHz,  $\text{CDCl}_3$ )  $\delta$  7.96 (s, 1H), 6.56 (s, 1H), 4.97 (br s, 2H), 1.34 (s, 12H), 1.33 (s, 12H);  $^{13}\text{C}$  NMR (125 MHz,  $\text{CDCl}_3$ )  $\delta$  156.5, 146.3, 144.6, 114.9, 83.6, 83.4, 24.9, 24.8.

**4-bromo-5-chloro-2-(4,4,5,5-tetramethyl-1,3,2-dioxaborolan-2-yl)-benzamine (23)**



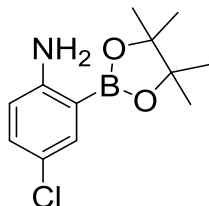
In a nitrogen filled glovebox, 206 mg 4-bromo-3-chloroaniline (1.0 mmol, 1.0 equiv) was dissolved in 1 mL THF in a 15 mL pressure tube containing a magnetic stir bar. 1.5 equiv HBPin (218  $\mu$ L) was added and the reaction vessel was sealed and stirred at room temperature for 1h. 0.25  $\mu$ mol [Ir(OMe)COD]<sub>2</sub> (0.25 mol%) and 1.0  $\mu$ mol 3,4,7,8-tetramethyl-1,10-phenanthroline (1.0 mol%) were added followed by an additional 1.5 equiv HBPin (218  $\mu$ L) and the reaction vessel was sealed and heated at 80 °C for 16h. The reaction mixture was allowed to return to room temperature and the reaction mixture was exposed to air and diluted with 5 mL MeOH. The volatiles were then removed under reduced pressure and the product was purified by passing it through a short plug of SiO<sub>2</sub> in MTBE. Product isolated by recrystallization from MeOH/H<sub>2</sub>O. White solid (305 mg, 92% isolated yield); mp: 79-81 °C; <sup>1</sup>H NMR (500 MHz, CDCl<sub>3</sub>)  $\delta$  7.76 (s, 1H), 6.70 (s, 1H), 4.80 (br s, 2H), 1.33 (s, 12H); <sup>13</sup>C NMR (125 MHz, CDCl<sub>3</sub>)  $\delta$  153.3, 141.0, 138.0, 116.0, 108.4, 84.0, 24.9; <sup>11</sup>B NMR (160 MHz, CDCl<sub>3</sub>)  $\delta$  30 (br s); HRMS (ESI) m/z calcd for C<sub>12</sub>H<sub>17</sub>BBrClNO<sub>2</sub> [M + H]<sup>+</sup> 332.0224, found 332.0222.

**4-methoxy-2-(4,4,5,5-tetramethyl-1,3,2-dioxaborolan-2-yl)-benzenamine (24)**



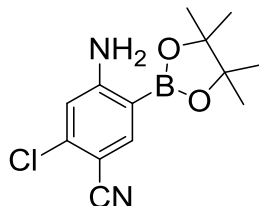
In a nitrogen filled glovebox, 115  $\mu\text{L}$  *p*-anisidine (1.0 mmol, 1.0 equiv) was dissolved in 1 mL THF in a 15 mL pressure tube containing a magnetic stir bar. 1.5 equiv HBPIn (218  $\mu\text{L}$ ) was added and the reaction vessel was sealed and stirred at room temperature for 1h. 0.25  $\mu\text{mol}$   $[\text{Ir}(\text{OMe})\text{COD}]_2$  (0.25 mol%) and 1.0  $\mu\text{mol}$  3,4,7,8-tetramethyl-1,10-phenanthroline (1.0 mol%) were added followed by an additional 1.5 equiv HBPIn (218  $\mu\text{L}$ ) and the reaction vessel was sealed and heated at 80  $^\circ\text{C}$  for 16h. The reaction mixture was allowed to return to room temperature and the reaction mixture was exposed to air and diluted with 5 mL MeOH. The volatiles were then removed under reduced pressure and the product was purified by passing it through a short plug of  $\text{SiO}_2$  in MTBE. Product isolated by recrystallization from MeOH/ $\text{H}_2\text{O}$ . Pale red solid (157 mg, 63% isolated yield); mp: 73-74  $^\circ\text{C}$ ;  $^1\text{H}$  NMR (500 MHz,  $\text{C}_6\text{D}_6$ )  $\delta$  7.60 (d,  $J = 2.9$  Hz, 1H), 6.94 (dd,  $J = 8.3, 2.9$  Hz, 1H), 6.53 (d,  $J = 8.8$  Hz, 1H), 4.31 (br s, 2H), 3.37 (s, 3H), 1.03 (s, 12H);  $^{13}\text{C}$  NMR (125 MHz,  $\text{CDCl}_3$ )  $\delta$  147.9, 133.9, 120.6, 119.6, 116.5, 83.8, 56.0, 24.9;  $^{11}\text{B}$  NMR (160 MHz,  $\text{CDCl}_3$ )  $\delta$  31 (br s); HRMS (ESI)  $m/z$  calcd for  $\text{C}_{13}\text{H}_{20}\text{BNO}_3$   $[\text{M} + \text{H}]^+$  250.1617, found 250.1616.

**4-chloro-2-(4,4,5,5-tetramethyl-1,3,2-dioxaborolan-2-yl)-benzenamine (25)**



In a nitrogen filled glovebox, 128 mg 4-chloroaniline (1.0 mmol, 1.0 equiv) was dissolved in 1 mL THF in a 15 mL pressure tube containing a magnetic stir bar. 1.5 equiv HBPin (218  $\mu$ L) was added and the reaction vessel was sealed and stirred at room temperature for 1h. 0.25  $\mu$ mol [Ir(OMe)COD]<sub>2</sub> (0.25 mol%) and 1.0  $\mu$ mol 3,4,7,8-tetramethyl-1,10-phenanthroline (1.0 mol%) were added followed by an additional 1.5 equiv HBPin (218  $\mu$ L) and the reaction vessel was sealed and heated at 80 °C for 16h. The reaction mixture was allowed to return to room temperature and the reaction mixture was exposed to air and diluted with 5 mL MeOH. The volatiles were then removed under reduced pressure and the product was purified by passing it through a short plug of SiO<sub>2</sub> in MTBE. Product isolated by recrystallization from MeOH/H<sub>2</sub>O. White solid (236 mg, 93% isolated yield); mp: 91-93 °C; <sup>1</sup>H NMR (500 MHz, CDCl<sub>3</sub>)  $\delta$  7.54 (d, *J* = 2.5 Hz, 1H), 7.14 (dd, *J* = 8.8, 2.5 Hz, 1H), 6.53 (d, *J* = 8.8 Hz, 1H), 4.69 (br s, 2H), 1.33 (s, 12H); <sup>13</sup>C NMR (125 MHz, CDCl<sub>3</sub>)  $\delta$  152.0, 135.8, 132.4, 121.6, 116.2, 83.9, 24.9; <sup>11</sup>B NMR (160 MHz, CDCl<sub>3</sub>)  $\delta$  30 (br s); HRMS (ESI) *m/z* calcd for C<sub>12</sub>H<sub>17</sub>BCINO<sub>2</sub> [M + H]<sup>+</sup> 254.1119, found 254.1116.

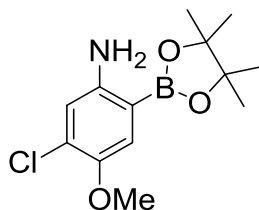
**4-amino-2-chloro-5-(4,4,5,5-tetramethyl-1,3,2-dioxaborolan-2-yl)-benzonitrile (26)**



In a nitrogen filled glovebox, 152 mg 4-amino-2-chlorobenzonitrile (1.0 mmol, 1.0 equiv) was dissolved in 1 mL THF in a 15 mL pressure tube containing a magnetic stir bar. 1.5 equiv HBPIn (218  $\mu$ L) was added and the reaction vessel was sealed and stirred at room temperature for 1h. 0.25  $\mu$ mol [Ir(OMe)COD]<sub>2</sub> (0.25 mol%) and 1.0  $\mu$ mol 3,4,7,8-tetramethyl-1,10-phenanthroline (1.0 mol%) were added followed by an additional 1.5 equiv HBPIn (218  $\mu$ L) and the reaction vessel was sealed and heated at 80 °C for 16h. The reaction mixture was allowed to return to room temperature and the reaction mixture was exposed to air and diluted with 5 mL MeOH. The volatiles were then removed under reduced pressure and the product was purified by passing it through a short plug of SiO<sub>2</sub> in MTBE. Product isolated by recrystallization from MeOH/H<sub>2</sub>O. White solid (250 mg, 90% isolated yield); mp: 123-125 °C; <sup>1</sup>H NMR (500 MHz, CDCl<sub>3</sub>)  $\delta$  7.87 (s, 1H), 6.61 (s, 1H), 5.32 (br s, 2H), 1.34 (s, 12H); <sup>13</sup>C NMR (125 MHz, CDCl<sub>3</sub>)  $\delta$  157.1, 143.37, 140.4, 117.3, 114.5, 100.1, 84.4, 24.9; <sup>11</sup>B NMR (160 MHz, CDCl<sub>3</sub>)  $\delta$  30 (br s); HRMS (ESI) m/z calcd for C<sub>13</sub>H<sub>16</sub>BClN<sub>2</sub>O<sub>2</sub> [M + H]<sup>+</sup> 279.1072, found 279.1068.



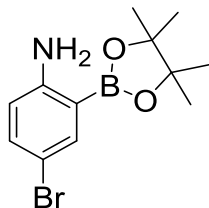
**5-chloro-4-methoxy-2-(4,4,5,5-tetramethyl-1,3,2-dioxaborolan-2-yl)-benzamine (27)**



In a nitrogen filled glovebox, 154 mg 3-chloro-4-methoxyaniline (1.0 mmol, 1.0 equiv) was dissolved in 1 mL THF in a 15 mL pressure tube containing a magnetic stir bar. 1.5 equiv HBPin (218  $\mu$ L) was added and the reaction vessel was sealed and stirred at room temperature for 1h. 0.25  $\mu$ mol [Ir(OMe)COD]<sub>2</sub> (0.25 mol%) and 1.0  $\mu$ mol 3,4,7,8-tetramethyl-1,10-phenanthroline (1.0 mol%) were added followed by an additional 1.5 equiv HBPin (218  $\mu$ L) and the reaction vessel was sealed and heated at 80 °C for 16h. The reaction mixture was allowed to return to room temperature and the reaction mixture was exposed to air and diluted with 5 mL MeOH. The volatiles were then removed under reduced pressure and the product was purified by passing it through a short plug of SiO<sub>2</sub> in MTBE. Product isolated by recrystallization from MeOH/H<sub>2</sub>O.

White solid (210 mg, 74% isolated yield); mp: 133-134 °C; <sup>1</sup>H NMR (500 MHz, CDCl<sub>3</sub>)  $\delta$  7.15 (s, 1H), 6.67 (s, 1H), 4.49 (br s, 2H), 3.84 (s, 3H), 1.34 (s, 12H); <sup>13</sup>C NMR (125 MHz, CDCl<sub>3</sub>)  $\delta$  148.4, 146.8, 127.6, 119.9, 116.9, 83.8, 57.0, 24.9; <sup>11</sup>B NMR (160 MHz, CDCl<sub>3</sub>)  $\delta$  31 (br s); HRMS (ESI) m/z calcd for C<sub>13</sub>H<sub>19</sub>BClNO<sub>3</sub> [M + H]<sup>+</sup> 284.1225, found 284.1220.

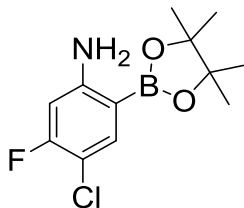
#### 4-bromo-2-(4,4,5,5-tetramethyl-1,3,2-dioxaborolan-2-yl)-benzenamine (29)



In a nitrogen filled glovebox, 170 mg 4-bromoaniline (1.0 mmol, 1.0 equiv) was dissolved in 1 mL THF in a 15 mL pressure tube containing a magnetic stir bar. 1.5 equiv HBPIn (218  $\mu$ L) was added and the reaction vessel was sealed and stirred at room temperature for 1h. 0.25  $\mu$ mol [Ir(OMe)COD]<sub>2</sub> (0.25 mol%) and 1.0  $\mu$ mol 3,4,7,8-tetramethyl-1,10-phenanthroline (1.0 mol%) were added followed by an additional 1.5 equiv HBPIn (218  $\mu$ L) and the reaction vessel was sealed and heated at 80 °C for 16h. The reaction mixture was allowed to return to room temperature and the reaction mixture was exposed to air and diluted with 5 mL MeOH. The volatiles were then removed under reduced pressure and the product was purified by passing it through a short plug of SiO<sub>2</sub> in MTBE. Product isolated by recrystallization from MeOH/H<sub>2</sub>O.

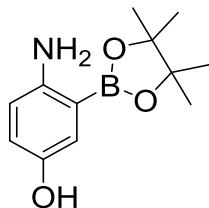
White solid (246 mg, 88% isolated yield); mp: 101-102 °C; <sup>1</sup>H NMR (500 MHz, CD<sub>2</sub>Cl<sub>2</sub>)  $\delta$  7.62 (d, *J* = 2.5 Hz, 1H), 7.27 (dd, *J* = 8.8, 2.5 Hz, 1H), 6.53 (d, *J* = 8.3 Hz, 1H), 4.85 (br s, 2H), 1.34 (s, 12H); <sup>13</sup>C NMR (125 MHz, CD<sub>2</sub>Cl<sub>2</sub>)  $\delta$  152.5, 138.5, 135.0, 116.5, 108.1, 83.9, 24.6; <sup>11</sup>B NMR (160 MHz, CD<sub>2</sub>Cl<sub>2</sub>)  $\delta$  30 (br s); HRMS (ESI) *m/z* calcd for C<sub>12</sub>H<sub>17</sub>BBrNO<sub>2</sub> [M + H]<sup>+</sup> 298.0614, found 298.0609.

**4-chloro-5-fluoro-2-(4,4,5,5-tetramethyl-1,3,2-dioxaborolan-2-yl)-benzamine (31)**



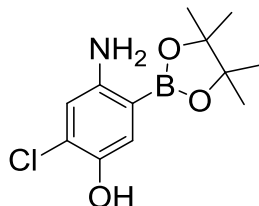
In a nitrogen filled glovebox, 145 mg 4-chloro-3-fluoroaniline (1.0 mmol, 1.0 equiv) was dissolved in 1 mL THF in a 15 mL pressure tube containing a magnetic stir bar. 1.5 equiv HBPIn (218  $\mu$ L) was added and the reaction vessel was sealed and stirred at room temperature for 1h. 0.25  $\mu$ mol [Ir(OMe)COD]<sub>2</sub> (0.25 mol%) and 1.0  $\mu$ mol 3,4,7,8-tetramethyl-1,10-phenanthroline (1.0 mol%) were added followed by an additional 1.5 equiv HBPIn (218  $\mu$ L) and the reaction vessel was sealed and heated at 80 °C for 16h. The reaction mixture was allowed to return to room temperature and the reaction mixture was exposed to air and diluted with 5 mL MeOH. The volatiles were then removed under reduced pressure and the product was purified by passing it through a short plug of SiO<sub>2</sub> in MTBE. 8% 2-borylated isomer was observed by <sup>1</sup>H NMR but not isolated. Product isolated by recrystallization from MeOH/H<sub>2</sub>O. White solid (244 mg, 90% isolated yield); mp: 95-96 °C; <sup>1</sup>H NMR (500 MHz, CDCl<sub>3</sub>)  $\delta$  7.58 (d, *J* = 9.3 Hz, 1H), 6.36 (d, *J* = 11.2 Hz, 1H), 4.84 (br s, 2H), 1.33 (s, 12H); <sup>13</sup>C NMR (125 MHz, CDCl<sub>3</sub>)  $\delta$  161.9 (d, *J* = 249.8 Hz), 154.0 (d, *J* = 10.5 Hz), 138.4 (d, *J* = 2.9 Hz), 125.5, 102.4 (d, *J* = 23.9 Hz), 83.9, 24.9; <sup>19</sup>F NMR (470 MHz, CDCl<sub>3</sub>)  $\delta$  110.9 (t, *J* = 10 Hz); <sup>11</sup>B NMR (160 MHz, CDCl<sub>3</sub>)  $\delta$  30 (br s); HRMS (ESI) *m/z* calcd for C<sub>12</sub>H<sub>16</sub>BClFNO<sub>2</sub> [M + H]<sup>+</sup> 272.1025, found 272.1019.

**4-amino-3-(4,4,5,5-tetramethyl-1,3,2-dioxaborolan-2-yl)-phenol (32)**



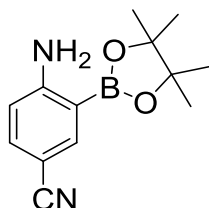
In a nitrogen filled glovebox, 109 mg 4-aminophenol (1.0 mmol, 1.0 equiv) was dissolved in 1 mL THF in a 15 mL pressure tube containing a magnetic stir bar. 4.0 equiv HBPIn (580  $\mu$ L) was added and the reaction vessel was sealed and stirred at room temperature for 1h. 0.25  $\mu$ mol [Ir(OMe)COD]<sub>2</sub> (0.25 mol%) and 1.0  $\mu$ mol 3,4,7,8-tetramethyl-1,10-phenanthroline (1.0 mol%) were added and the reaction vessel was sealed and heated at 80 °C for 16h. The reaction mixture was allowed to return to room temperature and the reaction mixture was exposed to air and diluted with 5 mL MeOH. The volatiles were then removed under reduced pressure and the product was purified by passing it through a short plug of SiO<sub>2</sub> in DCM. Compound was purified by recrystallized from DCM: hexanes. White solid (165 mg, 70% isolated yield); <sup>1</sup>H NMR (500 MHz, CDCl<sub>3</sub>)  $\delta$  7.06 (d, *J* = 2.9 Hz, 1H), 6.78 (dd, *J* = 8.3, 3.0 Hz, 1H), 6.53 (d, *J* = 8.3 Hz, 1H), 4.44 (br s, 3H), 1.33 (s, 12H); <sup>13</sup>C NMR (125 MHz, CDCl<sub>3</sub>)  $\delta$  147.6, 147.0, 121.9, 120.6, 116.5, 83.7, 24.9; <sup>11</sup>B NMR (160 MHz, CDCl<sub>3</sub>)  $\delta$  30 (br s); HRMS (ESI) *m/z* calcd for C<sub>12</sub>H<sub>18</sub>BNO<sub>3</sub> [M + H]<sup>+</sup> 236.1414, found 236.1413.

**4-amino-2-chloro-5-(4,4,5,5-tetramethyl-1,3,2-dioxaborolan-2-yl)-phenol (33)**



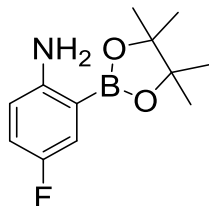
In a nitrogen filled glovebox, 143 mg 4-amino-2-chlorophenol (1.0 mmol, 1.0 equiv) was dissolved in 1 mL THF in a 15 mL pressure tube containing a magnetic stir bar. 4.0 equiv HBPIn (580  $\mu$ L) was added and the reaction vessel was sealed and stirred at room temperature for 1h. 0.25  $\mu$ mol [Ir(OMe)COD]<sub>2</sub> (0.25 mol%) and 1.0  $\mu$ mol 3,4,7,8-tetramethyl-1,10-phenanthroline (1.0 mol%) were added and the reaction vessel was sealed and heated at 80 °C for 16h. The reaction mixture was allowed to return to room temperature and the reaction mixture was exposed to air and diluted with 5 mL MeOH. The volatiles were then removed under reduced pressure and the product was purified by passing it through a short plug of SiO<sub>2</sub> in DCM. Compound was purified by recrystallization from DCM / hexanes. White solid (170 mg, 63% isolated yield); <sup>1</sup>H NMR (500 MHz, CDCl<sub>3</sub>)  $\delta$  7.36 (s, H), 6.61 (s, 1H), 4.84 (br s, 1H), 4.40 (br s, 2H), 1.33 (s, 12H); <sup>13</sup>C NMR (125 MHz, CDCl<sub>3</sub>)  $\delta$  147.8, 142.8, 124.5, 123.1, 115.0, 83.8, 24.9; <sup>11</sup>B NMR (160 MHz, CDCl<sub>3</sub>)  $\delta$  30 (br s); HRMS (ESI) m/z calcd for C<sub>12</sub>H<sub>17</sub>BClNO<sub>3</sub> [M + H]<sup>+</sup> 270.1068, found 270.1066.

**4-amino-3-(4,4,5,5-tetramethyl-1,3,2-dioxaborolan-2-yl)benzonitrile (34)**



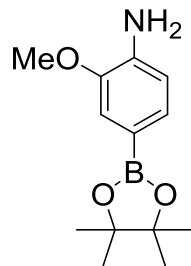
In a nitrogen filled glovebox, 118 mg 4-aminobenzonitrile (1.0 mmol, 1.0 equiv) was dissolved in 1 mL *n*-hexane in a 15 mL pressure tube containing a magnetic stir bar. 2.0 equiv HBPIn (290  $\mu$ L) was added and the reaction vessel was sealed and stirred at room temperature for 1h. 1.5  $\mu$ mol [Ir(OMe)COD]<sub>2</sub> (1.5 mol%) and 3.0  $\mu$ mol N<sup>4</sup>,N<sup>4</sup>,N<sup>4'</sup>,N<sup>4'</sup>-tetramethyl-[2,2'-bipyridine]-4,4'-diamine (3.0 mol%) were added and the reaction vessel was sealed and heated at 80 °C for 16h. The reaction mixture was allowed to return to room temperature and the reaction mixture was exposed to air and diluted with 5 mL MeOH. The volatiles were then removed under reduced pressure and the product was purified by passing it through a short plug of SiO<sub>2</sub> in MTBE. Product isolated by recrystallization from MeOH/H<sub>2</sub>O. White solid (146 mg, 60% isolated yield, (83% assay yield by <sup>1</sup>H NMR); mp: 96-97 °C; <sup>1</sup>H NMR (500 MHz, CDCl<sub>3</sub>)  $\delta$  7.92 (d, *J* = 2.0 Hz, 1H), 7.43 (dd, *J* = 8.8, 2.0 Hz, 1H), 6.57 (d, *J* = 8.8 Hz, 1H), 5.27 (br s, 2H), 1.37 (s, 12H); <sup>13</sup>C NMR (125 MHz, CDCl<sub>3</sub>)  $\delta$  156.5, 141.9, 135.9, 120.2, 114.5, 99.0, 84.2, 24.9; <sup>11</sup>B NMR (160 MHz, CDCl<sub>3</sub>)  $\delta$  30 (br s); HRMS (ESI) *m/z* calcd for C<sub>13</sub>H<sub>17</sub>BN<sub>2</sub>O<sub>2</sub> [M + H]<sup>+</sup> 245.1464, found 245.1594.

**4-fluoro-2-(4,4,5,5-tetramethyl-1,3,2-dioxaborolan-2-yl)-benzamine (35)**



In a nitrogen filled glovebox, 95  $\mu\text{L}$  4-fluoroaniline (1.0 mmol, 1.0 equiv) was dissolved in 1 mL *n*-hexane in a 15 mL pressure tube containing a magnetic stir bar. 2.0 equiv HBPIn (290  $\mu\text{L}$ ) was added and the reaction vessel was sealed and stirred at room temperature for 1h. 1.5  $\mu\text{mol}$   $[\text{Ir}(\text{OMe})\text{COD}]_2$  (1.5 mol%) and 3.0  $\mu\text{mol}$   $\text{N}^4, \text{N}^4, \text{N}^{4'}, \text{N}^{4'}$ -tetramethyl-[2,2'-bipyridine]-4,4'-diamine (3.0 mol%) were added and the reaction vessel was sealed and heated at 80  $^\circ\text{C}$  for 16h. The reaction mixture was allowed to return to room temperature and the reaction mixture was exposed to air and diluted with 5 mL MeOH. The volatiles were then removed under reduced pressure and the product was purified by passing it through a short plug of  $\text{SiO}_2$  in MTBE. Compound was purified by recrystallization from DCM / hexanes. Yellow oil (102 mg, 43% isolated yield (74% assay yield by  $^1\text{H}$  NMR));  $^1\text{H}$  NMR (500 MHz,  $\text{CD}_2\text{Cl}_2$ )  $\delta$  7.20 (dd,  $J = 9.3, 3.0$  Hz, 1H), 6.91 (td,  $J = 17.1, 8.8, 3.5$  Hz, 1H), 6.54 (q,  $J = 4.4$  Hz, 1H), 4.46 (br s, 2 H), 1.33 (s, 12H);  $^{13}\text{C}$  NMR (125 MHz,  $\text{CD}_2\text{Cl}_2$ )  $\delta$  155.9 (d  $J = 276.2$  Hz), 150.1, 121.2 (d,  $J = 20$  Hz), 119.4 (d,  $J = 23$  Hz), 115.7 (d,  $J = 6.7$  Hz), 84.0, 24.6;  $^{19}\text{F}$  NMR (470 MHz,  $\text{CD}_2\text{Cl}_2$ )  $\delta$  130.2 (td,  $J = 21.6, 13.2, 5.0$  Hz);  $^{11}\text{B}$  NMR (160 MHz,  $\text{CD}_2\text{Cl}_2$ )  $\delta$  30 (br s); HRMS (ESI)  $m/z$  calcd for  $\text{C}_{12}\text{H}_{17}\text{BFNO}_2$   $[\text{M} + \text{H}]^+$  238.1417, found 238.1540.

**2-methoxy-4-(4,4,5,5-tetramethyl-1,3,2-dioxaborolan-2-yl)-benzenamine (37)**

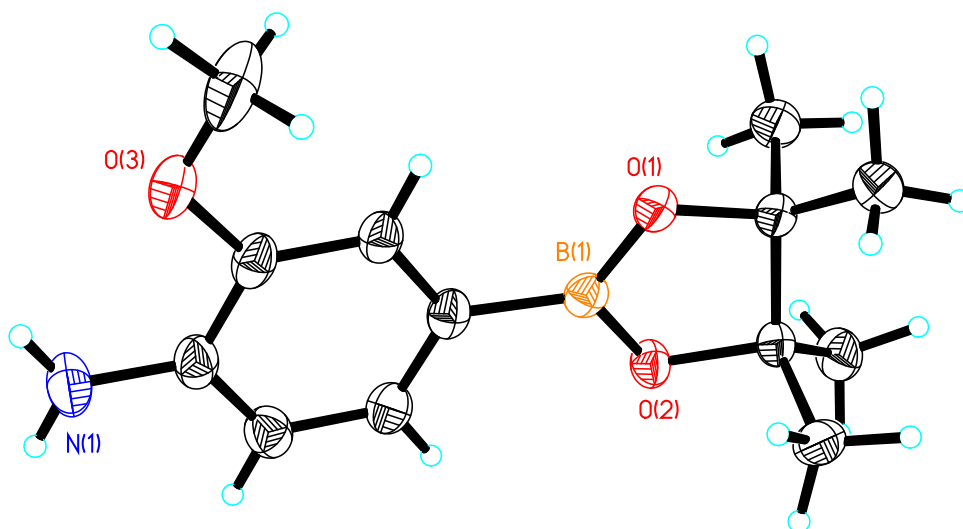


In a nitrogen filled glovebox, 113  $\mu\text{L}$  *o*-anisidine (1.0 mmol, 1.0 equiv) was dissolved in 1 mL THF in a 15 mL pressure tube containing a magnetic stir bar. 1.5 equiv HBPin (218  $\mu\text{L}$ ) was added and the reaction vessel was sealed and stirred at room temperature for 1h. 0.25  $\mu\text{mol}$   $[\text{Ir}(\text{OMe})\text{COD}]_2$  (0.25 mol%) and 1.0  $\mu\text{mol}$  3,4,7,8-tetramethyl-1,10-phenanthroline (1.0 mol%) were added followed by an additional 1.5 equiv HBPin (218  $\mu\text{L}$ ) and the reaction vessel was sealed and heated at 80  $^{\circ}\text{C}$  for 16h. The reaction mixture was allowed to return to room temperature and the reaction mixture was exposed to air and diluted with 5 mL MeOH. The volatiles were then removed under reduced pressure and the product was purified by passing it through a short plug of  $\text{SiO}_2$  in MTBE. Product isolated by recrystallization from MeOH/ $\text{H}_2\text{O}$ . White solid (152 mg, 61% isolated yield); mp: 68-70  $^{\circ}\text{C}$ ;  $^1\text{H}$  NMR (500 MHz,  $\text{CDCl}_3$ )  $\delta$  7.30 (dd,  $J = 7.8, 1.5$  Hz, 1H), 7.20 (d,  $J = 1.5$  Hz, 1H), 6.71 (d,  $J = 7.5$  Hz, 1H), 4.08 (br s, 2H), 3.89 (s, 3H), 1.33 (s, 12H);  $^{13}\text{C}$  NMR (125 MHz,  $\text{CDCl}_3$ )  $\delta$  146.5, 139.3, 128.8, 115.9, 114.1, 83.3, 55.5, 24.8;  $^{11}\text{B}$  NMR (160 MHz,  $\text{CDCl}_3$ )  $\delta$  31 (br s); HRMS (ESI)  $m/z$  calcd for  $\text{C}_{13}\text{H}_{20}\text{BNO}_3$   $[\text{M} + \text{H}]^+$  250.1614, found 250.1612.



**Figure 5.1. 2-methoxy-4-(4,4,5,5-tetramethyl-1,3,2-dioxaborolan-2-yl)-benzenamine (37).**

The following are 50% thermal ellipsoidal drawings of the molecule in the asymmetric cell with various amount of labeling.



**Crystal structure determination of 2-methoxy-4-(4,4,5,5-tetramethyl-1,3,2-dioxaborolan-**

**2yl)-benzenamine. Crystal Data.**  $C_{13}H_{20}BNO_3$ ,  $M = 249.11$ , orthorhombic,  $a = 7.76150(10)$

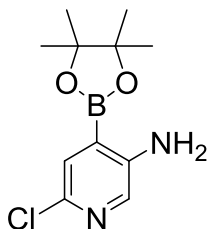
$\text{\AA}$ ,  $b = 9.78630(10) \text{\AA}$ ,  $c = 17.9222(2) \text{\AA}$ ,  $V = 1371.31(3) \text{\AA}^3$ ,  $T = 173(2) \text{K}$ , space group  $P2_12_12_1$

(# 19),  $Z = 4$ ,  $\mu(\text{Cu K}\alpha) = 0.678 \text{ mm}^{-1}$ , 9806 reflections measured, 2457 unique ( $R_{\text{int}} = 0.0258$ )

which were used in all calculations. The final  $wR_2$  was 0.0842 (all data) an  $R_1$  was 0.0319

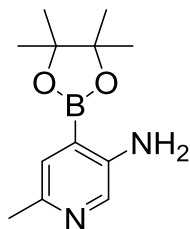
(> $2\sigma(I)$ ).

**5-amino-2-chloro-4-(4,4,5,5-tetramethyl-1,3,2-dioxaborolan-2-yl)-pyridine (38)**



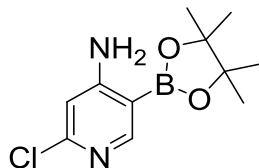
In a nitrogen filled glovebox, 128 mg 6-chloropyridin-3-amine (1.0 mmol, 1.0 equiv) was dissolved in 1 mL THF in a 15 mL pressure tube containing a magnetic stir bar. 1.2 equiv HBPIn (173  $\mu$ L) was added and the reaction vessel was sealed and stirred at room temperature for 1h. 1.5  $\mu$ mol [Ir(OMe)COD]<sub>2</sub> (1.5 mol%), 3.0  $\mu$ mol 3,4,7,8-tetramethyl-1,10-phenanthroline (3.0 mol%) and 0.5 equiv B<sub>2</sub>Pin<sub>2</sub> (127 mg) were added and the reaction vessel was sealed and heated at 80 °C for 8h. The reaction mixture was allowed to return to room temperature and the reaction mixture was exposed to air and diluted with 5 mL MeOH. The volatiles were then removed under reduced pressure and the product was purified by passing it through a short plug of SiO<sub>2</sub> in DCM. Compound was purified by recrystallization from DCM / hexanes. White solid (224 mg, 88% isolated yield); mp: 116-117 °C; <sup>1</sup>H NMR (500 MHz, CDCl<sub>3</sub>)  $\delta$  7.81 (s, 1H), 7.41 (s, 1H), 4.68 (br s, 2H), 1.34 (s, 12H); <sup>13</sup>C NMR (125 MHz, CDCl<sub>3</sub>)  $\delta$  147.3, 138.7, 136.8, 129.4, 84.6, 24.9; <sup>11</sup>B NMR (160 MHz, CDCl<sub>3</sub>)  $\delta$  30 (br s); HRMS (ESI) m/z calcd for C<sub>11</sub>H<sub>16</sub>BClN<sub>2</sub>O<sub>2</sub> [M + H]<sup>+</sup> 255.1016, found 255.0990.

**5-amino-4-(4,4,5,5-tetramethyl-1,3,2-dioxaborolan-2-yl)-2-methyl pyridine (39)**



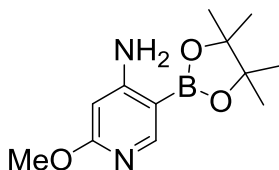
In a nitrogen filled glovebox, 108 mg 6-methylpyridin-3-amine (1.0 mmol, 1.0 equiv) was dissolved in 1 mL THF in a 15 mL pressure tube containing a magnetic stir bar. 1.2 equiv HBPIn (173  $\mu$ L) was added and the reaction vessel was sealed and stirred at room temperature for 1h. 1.5  $\mu$ mol [Ir(OMe)COD]<sub>2</sub> (1.5 mol%), 3.0  $\mu$ mol 3,4,7,8-tetramethyl-1,10-phenanthroline (3.0 mol%) and 0.5 equiv B<sub>2</sub>Pin<sub>2</sub> (127 mg) were added and the reaction vessel was sealed and heated at 80 °C for 8h. The reaction mixture was allowed to return to room temperature and the reaction mixture was exposed to air and diluted with 5 mL MeOH. The volatiles were then removed under reduced pressure and the product was purified by passing it through a short plug of SiO<sub>2</sub> in MTBE. Compound was purified by recrystallization from hexanes / EtOAc. White solid (152 mg, 63% isolated yield); mp: 68-70 °C; <sup>1</sup>H NMR (500 MHz, CD<sub>2</sub>Cl<sub>2</sub>)  $\delta$  7.95 (s, H), 7.23 (s, 1H), 4.55 (br s, 2H), 2.37 (s, 3H), 1.36 (s, 12H); <sup>13</sup>C NMR (125 MHz, CD<sub>2</sub>Cl<sub>2</sub>)  $\delta$  146.2, 145.6, 136.7, 128.2, 84.2, 24.7, 22.5; <sup>11</sup>B NMR (160 MHz, CD<sub>2</sub>Cl<sub>2</sub>)  $\delta$  30 (br s); HRMS (ESI) m/z calcd for C<sub>12</sub>H<sub>19</sub>BN<sub>2</sub>O<sub>2</sub> [M + H]<sup>+</sup> 235.1620, found 235.1387.

**2-chloro-5-(4,4,5,5-tetramethyl-1,3,2-dioxaborolan-2-yl)pyridin-4-amine (40)**



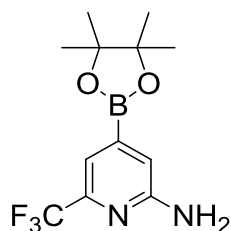
In a nitrogen filled glovebox, 128 mg 2-chloropyridin-4-amine (1.0 mmol, 1.0 equiv) was dissolved in 1 mL THF in a 15 mL pressure tube containing a magnetic stir bar. 1.2 equiv HBPin (173  $\mu$ L) was added and the reaction vessel was sealed and stirred at room temperature for 1h. 1.5  $\mu$ mol [Ir(OMe)COD]<sub>2</sub> (1.5 mol%), 3.0  $\mu$ mol 3,4,7,8-tetramethyl-1,10-phenanthroline (3.0 mol%) and 0.5 equiv B<sub>2</sub>Pin<sub>2</sub> (127 mg) were added and the reaction vessel was sealed and heated at 80 °C for 8h. The reaction mixture was allowed to return to room temperature and the reaction mixture was exposed to air and diluted with 5 mL MeOH. The volatiles were then removed under reduced pressure and the product was purified by passing it through a short plug of SiO<sub>2</sub> in DCM. Product isolated by recrystallized from MeOH/ H<sub>2</sub>O. White solid (249 mg, 98% isolated yield); mp: 170-171 °C; <sup>1</sup>H NMR (500 MHz, CDCl<sub>3</sub>)  $\delta$  8.34 (s, 1H), 6.46 (s, 1H), 5.29 (br s, 2H), 1.34 (s, 12H); <sup>13</sup>C NMR (125 MHz, CDCl<sub>3</sub>)  $\delta$  160.3, 157.5, 154.8, 107.7, 84.1, 24.9; <sup>11</sup>B NMR (160 MHz, CDCl<sub>3</sub>)  $\delta$  30 (br s); HRMS (ESI) m/z calcd for C<sub>11</sub>H<sub>16</sub>BClN<sub>2</sub>O<sub>2</sub> [M + H]<sup>+</sup> 255.1074, found 255.1206.

**2-methoxy-5-(4,4,5,5-tetramethyl-1,3,2-dioxaborolan-2-yl)pyridin-4-amine (41)**



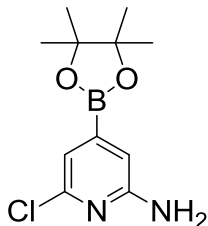
In a nitrogen filled glovebox, 124 mg 2-methoxypyridin-4-amine (1.0 mmol, 1.0 equiv) was dissolved in 1 mL THF in a 15 mL pressure tube containing a magnetic stir bar. 1.2 equiv HBPIn (173  $\mu$ L) was added and the reaction vessel was sealed and stirred at room temperature for 1h. 1.5  $\mu$ mol [Ir(OMe)COD]<sub>2</sub> (1.5 mol%), 3.0  $\mu$ mol 3,4,7,8-tetramethyl-1,10-phenanthroline (3.0 mol%) and 0.5 equiv B<sub>2</sub>Pin<sub>2</sub> (127 mg) were added and the reaction vessel was sealed and heated at 80 °C for 8h. The reaction mixture was allowed to return to room temperature and the reaction mixture was exposed to air and diluted with 5 mL MeOH. The volatiles were then removed under reduced pressure and the product was purified by passing it through a short plug of SiO<sub>2</sub> in DCM. Product isolated by recrystallized from MeOH/ H<sub>2</sub>O. White solid (150 mg, 60% isolated yield); mp: 91-94 °C; ; <sup>1</sup>H NMR (500 MHz, CDCl<sub>3</sub>)  $\delta$  8.27 (s, 1H), 5.83 (s, 1H), 5.10 (br s, 2H), 3.89 (s, 3H), 1.34 (s, 12H); <sup>13</sup>C NMR (125 MHz, CDCl<sub>3</sub>)  $\delta$  160.7, 156.3, 148.5, 92.0, 83.5, 53.3, 24.9; <sup>11</sup>B NMR (160 MHz, CDCl<sub>3</sub>)  $\delta$  30 (br s); HRMS (ESI) m/z calcd for C<sub>12</sub>H<sub>19</sub>BN<sub>2</sub>O<sub>3</sub> [M + H]<sup>+</sup> 251.1569, found 251.1700.

**4-(4,4,5,5-tetramethyl-1,3,2-dioxaborolan-2-yl)-6-(trifluoromethyl)pyridin-2-amine (42)**



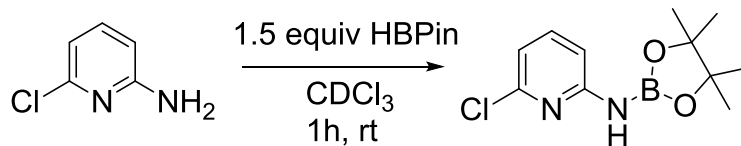
In a nitrogen filled glovebox, 162 mg 6-(trifluoromethyl)pyridin-2-amine (1.0 mmol, 1.0 equiv) was dissolved in 1 mL THF in a 15 mL pressure tube containing a magnetic stir bar. 1.2 equiv HBPIn (173  $\mu$ L) was added and the reaction vessel was sealed and stirred at room temperature for 1h. 1.5  $\mu$ mol [Ir(OMe)COD]<sub>2</sub> (1.5 mol%), 3.0  $\mu$ mol 3,4,7,8-tetramethyl-1,10-phenanthroline (3.0 mol%) and 0.5 equiv B<sub>2</sub>Pin<sub>2</sub> (127 mg) were added and the reaction vessel was sealed and heated at 80 °C for 8h. The reaction mixture was allowed to return to room temperature and the reaction mixture was exposed to air and diluted with 5 mL MeOH. The volatiles were then removed under reduced pressure and the product was purified by passing it through a short plug of SiO<sub>2</sub> in DCM. Product isolated by recrystallized from MeOH/ H<sub>2</sub>O. White solid (282 mg, 98% isolated yield); mp: 97-98 °C; <sup>1</sup>H NMR (500 MHz, CDCl<sub>3</sub>)  $\delta$  7.32 (s, 1H), 7.03 (s, 1H), 4.74 (br s, 2H), 1.34 (s, 12H); <sup>13</sup>C NMR (125 MHz, CDCl<sub>3</sub>)  $\delta$  158.0, 145.9 (q, *J* = 33 Hz), 122.8 (q, *J* = 273 Hz), 117.8, 114.5 (q, *J* = 3 Hz), 84.7, 24.8; <sup>19</sup>F NMR (470 MHz, CDCl<sub>3</sub>)  $\delta$  68.5; <sup>11</sup>B NMR (160 MHz, CDCl<sub>3</sub>)  $\delta$  30 (br s); HRMS (ESI) *m/z* calcd for C<sub>12</sub>H<sub>16</sub>BF<sub>3</sub>N<sub>2</sub>O<sub>2</sub> [M + H]<sup>+</sup> 289.1337, found 289.1680.

**6-chloro-4-(4,4,5,5-tetramethyl-1,3,2-dioxaborolan-2-yl)pyridin-2-amine (43)**



In a nitrogen filled glovebox, 128 mg 6-chloropyridin-2-amine (1.0 mmol, 1.0 equiv) was dissolved in 1 mL THF in a 15 mL pressure tube containing a magnetic stir bar. 1.2 equiv HBPin (173  $\mu$ L) was added and the reaction vessel was sealed and stirred at room temperature for 1h. 1.5  $\mu$ mol [Ir(OMe)COD]<sub>2</sub> (1.5 mol%), 3.0  $\mu$ mol 3,4,7,8-tetramethyl-1,10-phenanthroline (3.0 mol%) and 0.5 equiv B<sub>2</sub>Pin<sub>2</sub> (127 mg) were added and the reaction vessel was sealed and heated at 80 °C for 8h. The reaction mixture was allowed to return to room temperature and the reaction mixture was exposed to air and diluted with 5 mL MeOH. The volatiles were then removed under reduced pressure and the product was purified by passing it through a short plug of SiO<sub>2</sub> in DCM. Product isolated by recrystallized from MeOH/ H<sub>2</sub>O. White solid (170 mg, 67% isolated yield); mp: 160-163 °C; <sup>1</sup>H NMR (500 MHz, CDCl<sub>3</sub>)  $\delta$  6.99 (s, 1H), 6.75 (s, 1H), 4.54 (br s, 2H), 1.34 (s, 12H); <sup>13</sup>C NMR (125 MHz, CDCl<sub>3</sub>)  $\delta$  158.1, 149.4, 117.8, 112.0, 84.6, 24.8; <sup>11</sup>B NMR (160 MHz, CDCl<sub>3</sub>)  $\delta$  30 (br s); HRMS (ESI) m/z calcd for C<sub>11</sub>H<sub>16</sub>BClN<sub>2</sub>O<sub>2</sub> [M + H]<sup>+</sup> 255.1074, found 255.1205.

**In Situ generation of 6-chloro-N-(4,4,5,5-tetramethyl-1,3,2-dioxaborolan-2-yl)pyridin-2-amine**



In a nitrogen filled glovebox 128 mg 6-chloropyridin-2-amine (1 mmol) was dissolved in 1 mL CDCl<sub>3</sub> in a screw cap NMR tube. 1.5 equiv HBpin (218  $\mu$ L) was added and the tube was sealed and kept at room temperature for 1h. Quantitative conversion was observed by NMR. <sup>1</sup>H NMR (500 MHz, CDCl<sub>3</sub>)  $\delta$  7.40 (t,  $J$  = 7.8, 7.3 Hz, 1H), 7.24 (d,  $J$  = 8.3 Hz, 1H), 6.72 (d,  $J$  = 7.3 Hz, 1H), 5.55 (s, 1H), 1.26 (s, 12H); <sup>11</sup>B NMR (160 MHz, CDCl<sub>3</sub>)  $\delta$  24 (br s).



**Table 5.3.** Crystal data and structure refinement for **37**.

Identification code	<b>37</b>	
Empirical formula	C <sub>13</sub> H <sub>20</sub> B N O <sub>3</sub>	
Formula weight	249.11	
Temperature	173(2) K	
Wavelength	1.54178 Å	
Crystal system	Orthorhombic	
Space group	P 21 21 21	
Unit cell dimensions	a = 7.76150(10) Å	α = 90°.
	b = 9.78630(10) Å	β = 90°.
	c = 17.9222(2) Å	γ = 90°.
Volume	1361.31(3) Å <sup>3</sup>	
Z	4	
Density (calculated)	1.215 Mg/m <sup>3</sup>	
Absorption coefficient	0.678 mm <sup>-1</sup>	
F(000)	536	
Crystal size	0.44 x 0.35 x 0.35 mm <sup>3</sup>	
Theta range for data collection	4.94 to 67.99°.	
Index ranges	-9<=h<=9, -11<=k<=11, -19<=l<=21	
Reflections collected	9806	
Independent reflections	2457 [R(int) = 0.0258]	
Completeness to theta = 67.99°	99.4 %	
Absorption correction	Semi-empirical from equivalents	
Max. and min. transmission	0.7967 and 0.7555	
Refinement method	Full-matrix least-squares on F <sup>2</sup>	
Data / restraints / parameters	2457 / 0 / 168	
Goodness-of-fit on F <sup>2</sup>	1.123	
Final R indices [I>2sigma(I)]	R1 = 0.0317, wR2 = 0.0839	
R indices (all data)	R1 = 0.0319, wR2 = 0.0842	
Absolute structure parameter	0.03(17)	
Largest diff. peak and hole	0.156 and -0.214 e.Å <sup>-3</sup>	

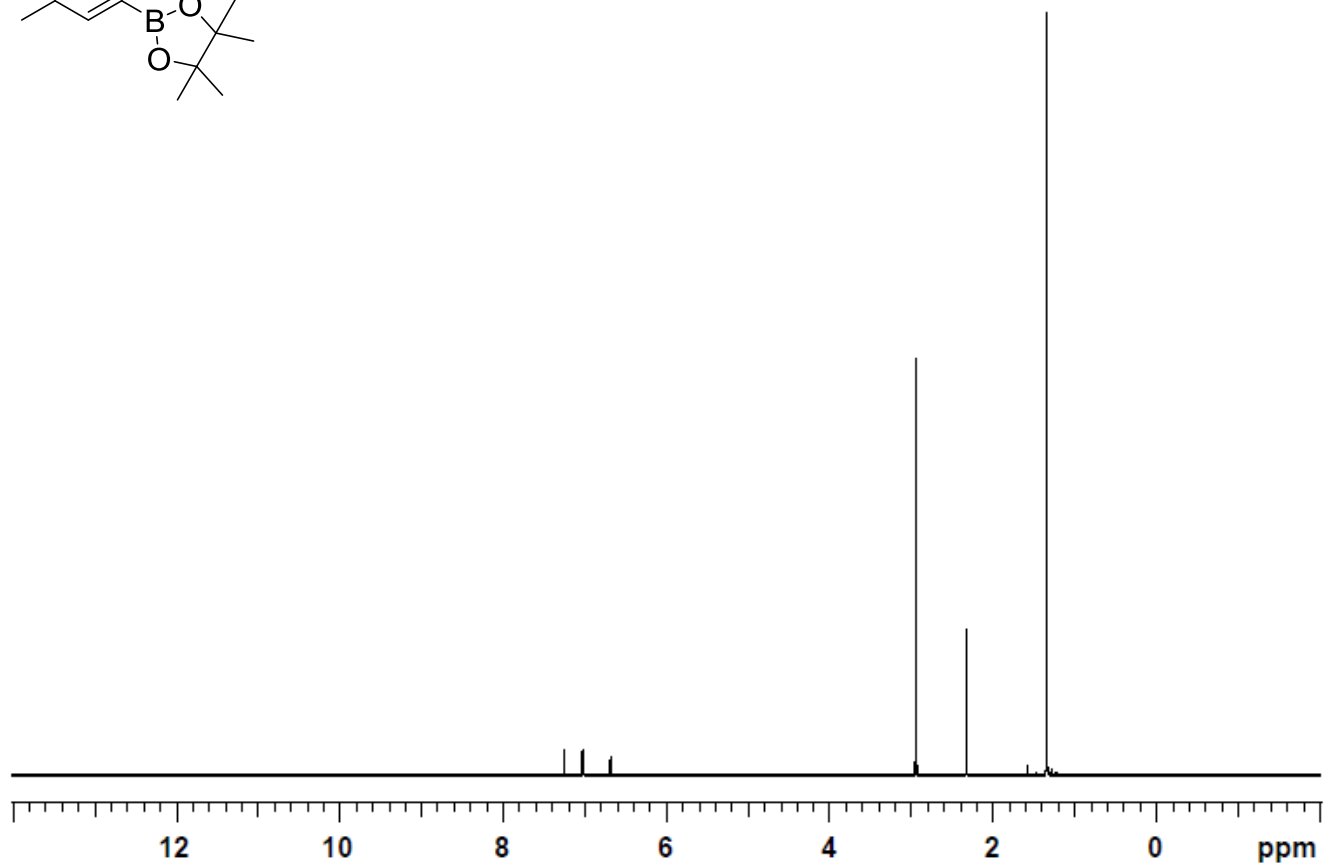
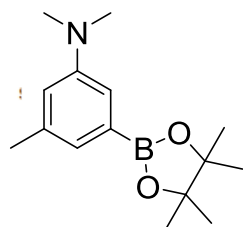
**Table 5.4.** Crystal data and structure refinement for *Trans*-(Ar<sup>F</sup><sub>3</sub>P)<sub>2</sub>Ir(BPin)<sub>3</sub> (**12**).

Identification code	<i>Trans</i> -(Ar <sup>F</sup> <sub>3</sub> P) <sub>2</sub> Ir(BPin) <sub>3</sub> ( <b>12</b> ).	
Empirical formula	C <sub>66</sub> H <sub>54</sub> B <sub>3</sub> F <sub>36</sub> Ir O <sub>6</sub> P <sub>2</sub>	
Formula weight	1913.66	
Temperature	173(2) K	
Wavelength	0.71073 Å	
Crystal system	Monoclinic	
Space group	C 2/c	
Unit cell dimensions	a = 24.853(2) Å	α = 90°.
	b = 13.8099(10) Å	β = 105.221(2)°.
	c = 22.283(2) Å	γ = 90°.
Volume	7379.7(11) Å <sup>3</sup>	
Z	4	
Density (calculated)	1.722 Mg/m <sup>3</sup>	
Absorption coefficient	1.994 mm <sup>-1</sup>	
F(000)	3776	
Crystal size	0.21 x 0.11 x 0.07 mm <sup>3</sup>	
Theta range for data collection	1.70 to 25.36°.	
Index ranges	-29 ≤ h ≤ 29, -16 ≤ k ≤ 16, -26 ≤ l ≤ 26	
Reflections collected	53170	
Independent reflections	6768 [R(int) = 0.0526]	
Completeness to theta = 25.00°	100.0 %	
Absorption correction	Semi-empirical from equivalents	
Max. and min. transmission	0.8665 and 0.6773	
Refinement method	Full-matrix least-squares on F <sup>2</sup>	
Data / restraints / parameters	6768 / 177 / 620	
Goodness-of-fit on F <sup>2</sup>	1.043	
Final R indices [I > 2σ(I)]	R1 = 0.0279, wR2 = 0.0665	
R indices (all data)	R1 = 0.0320, wR2 = 0.0687	
Largest diff. peak and hole	0.903 and -0.638 e.Å <sup>-3</sup>	

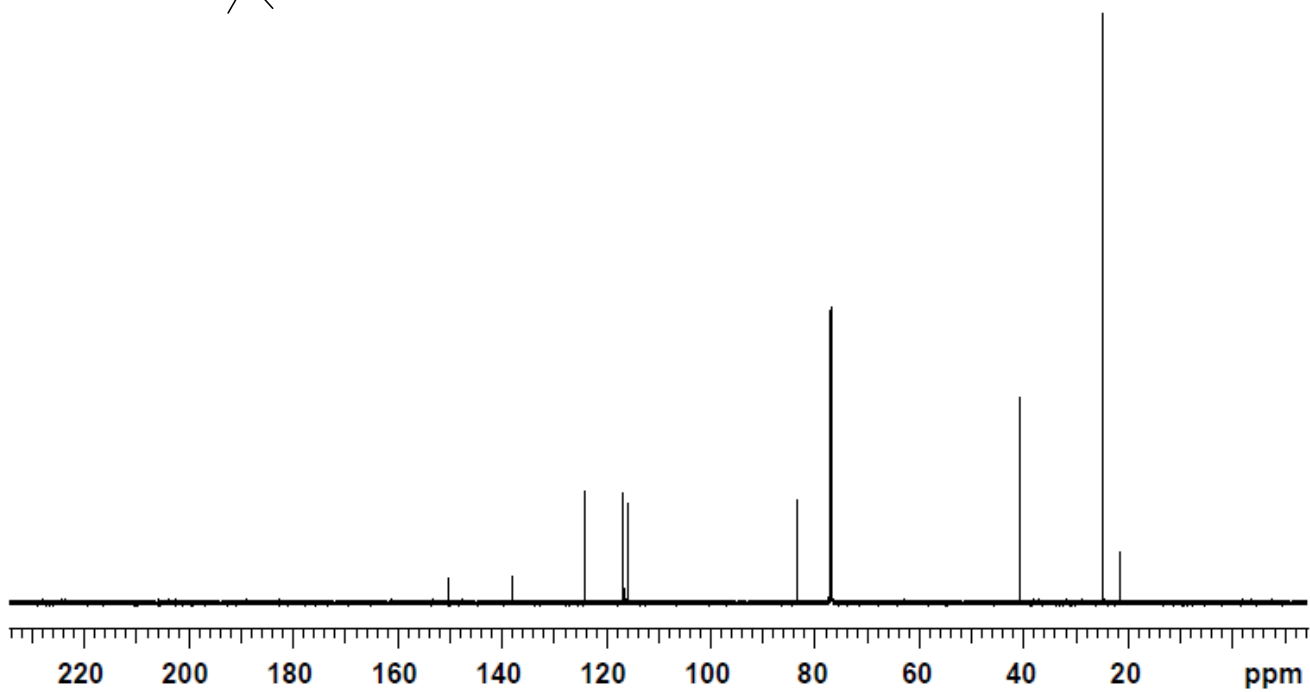
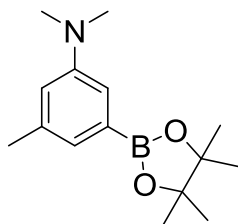
**Table 5.5.** Crystal data and structure refinement for *Trans*-(Ar<sup>F</sup><sub>3</sub>P)<sub>2</sub>Ir(H)(BPin)<sub>2</sub> (**13**).

Identification code	<i>Trans</i> -(Ar <sup>F</sup> <sub>3</sub> P) <sub>2</sub> Ir(H)(BPin) <sub>2</sub> ( <b>13</b> ).	
Empirical formula	C <sub>60</sub> H <sub>42</sub> B <sub>2</sub> F <sub>36</sub> Ir O <sub>4</sub> P <sub>2</sub>	
Formula weight	1786.70	
Temperature	120(2) K	
Wavelength	1.54178 Å	
Crystal system	Triclinic	
Space group	P -1	
Unit cell dimensions	a = 10.6867(4) Å	α = 79.792(4)°.
	b = 14.1473(6) Å	β = 88.238(3)°.
	c = 24.3165(10) Å	γ = 74.490(3)°.
Volume	3485.9(2) Å <sup>3</sup>	
Z	2	
Density (calculated)	1.702 Mg/m <sup>3</sup>	
Absorption coefficient	5.440 mm <sup>-1</sup>	
F(000)	1750	
Crystal size	0.295 x 0.215 x 0.074 mm <sup>3</sup>	
Theta range for data collection	3.29 to 68.53°.	
Index ranges	-12 ≤ h ≤ 12, -16 ≤ k ≤ 17, 0 ≤ l ≤ 29	
Reflections collected	24742	
Independent reflections	24742 [R(int) = 0.0000]	
Completeness to theta = 68.53°	98.3 %	
Absorption correction	Semi-empirical from equivalents	
Max. and min. transmission	0.753056 and 0.529282	
Refinement method	Full-matrix least-squares on F <sup>2</sup>	
Data / restraints / parameters	24742 / 147 / 1036	
Goodness-of-fit on F <sup>2</sup>	1.100	
Final R indices [I > 2σ(I)]	R1 = 0.0903, wR2 = 0.2198	
R indices (all data)	R1 = 0.1106, wR2 = 0.2377	
Largest diff. peak and hole	1.632 and -2.387 e.Å <sup>-3</sup>	

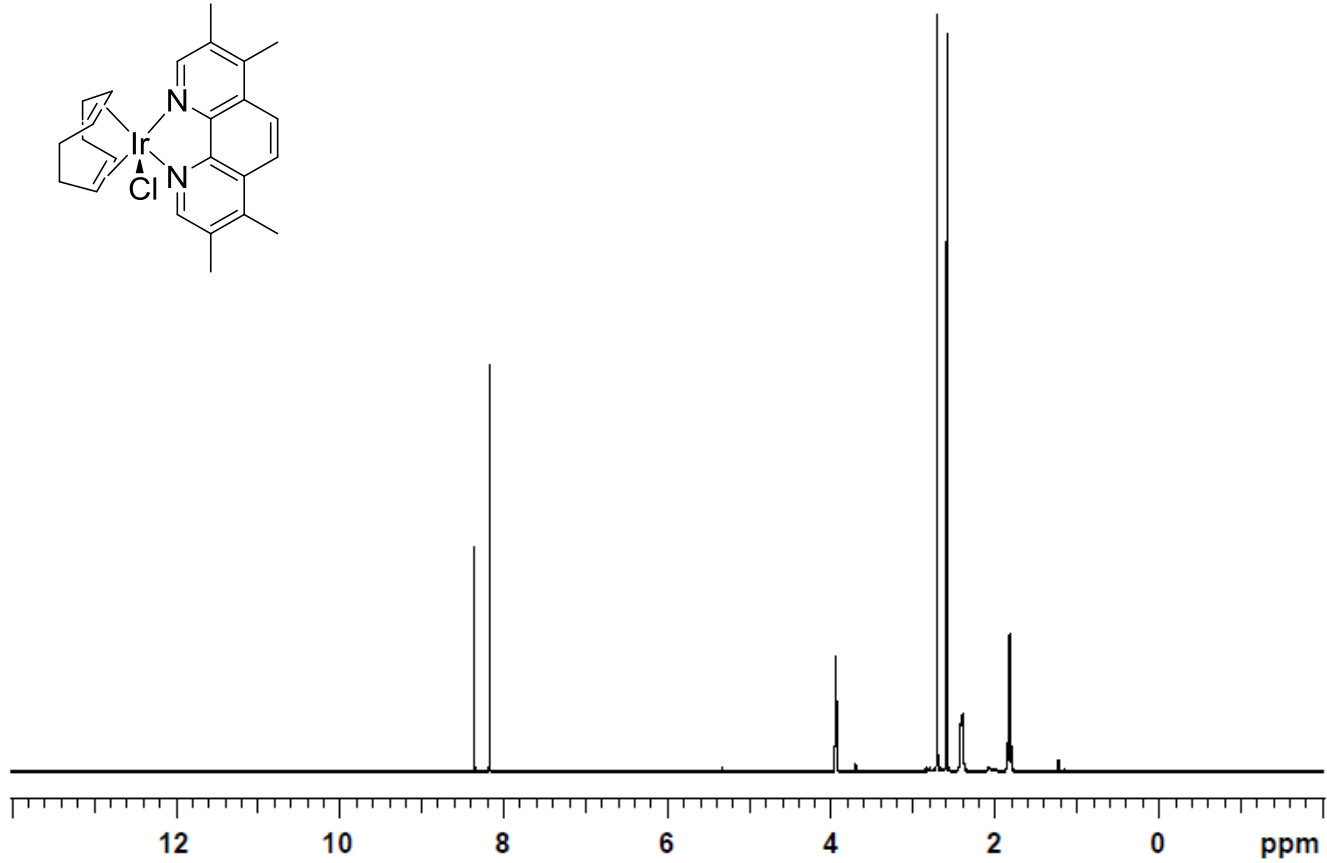
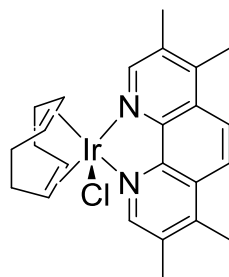
$^1\text{H}$  NMR (500 MHz,  $\text{CDCl}_3$ ) N,N-Dimethyl-3-(4,4,5,5-tetramethyl-1,3,2-dioxaborolan-2-yl)-5-methyl benzamine (5b)



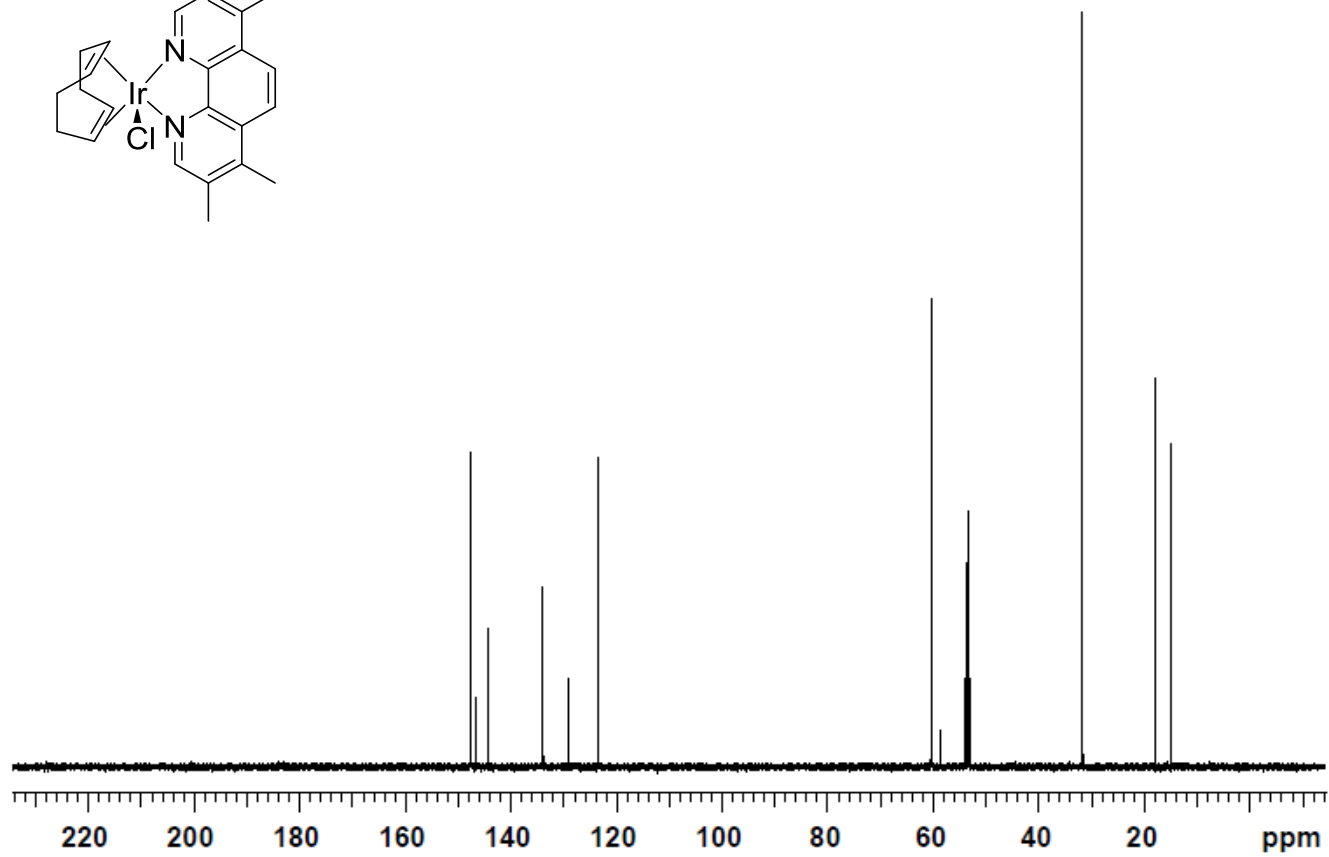
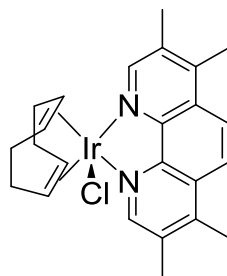
$^{13}\text{C}$  NMR (125 MHz,  $\text{CDCl}_3$ ) N,N-Dimethyl-3-(4,4,5,5-tetramethyl-1,3,2-dioxaborolan-2-yl)-5-methyl benzamine (5b)



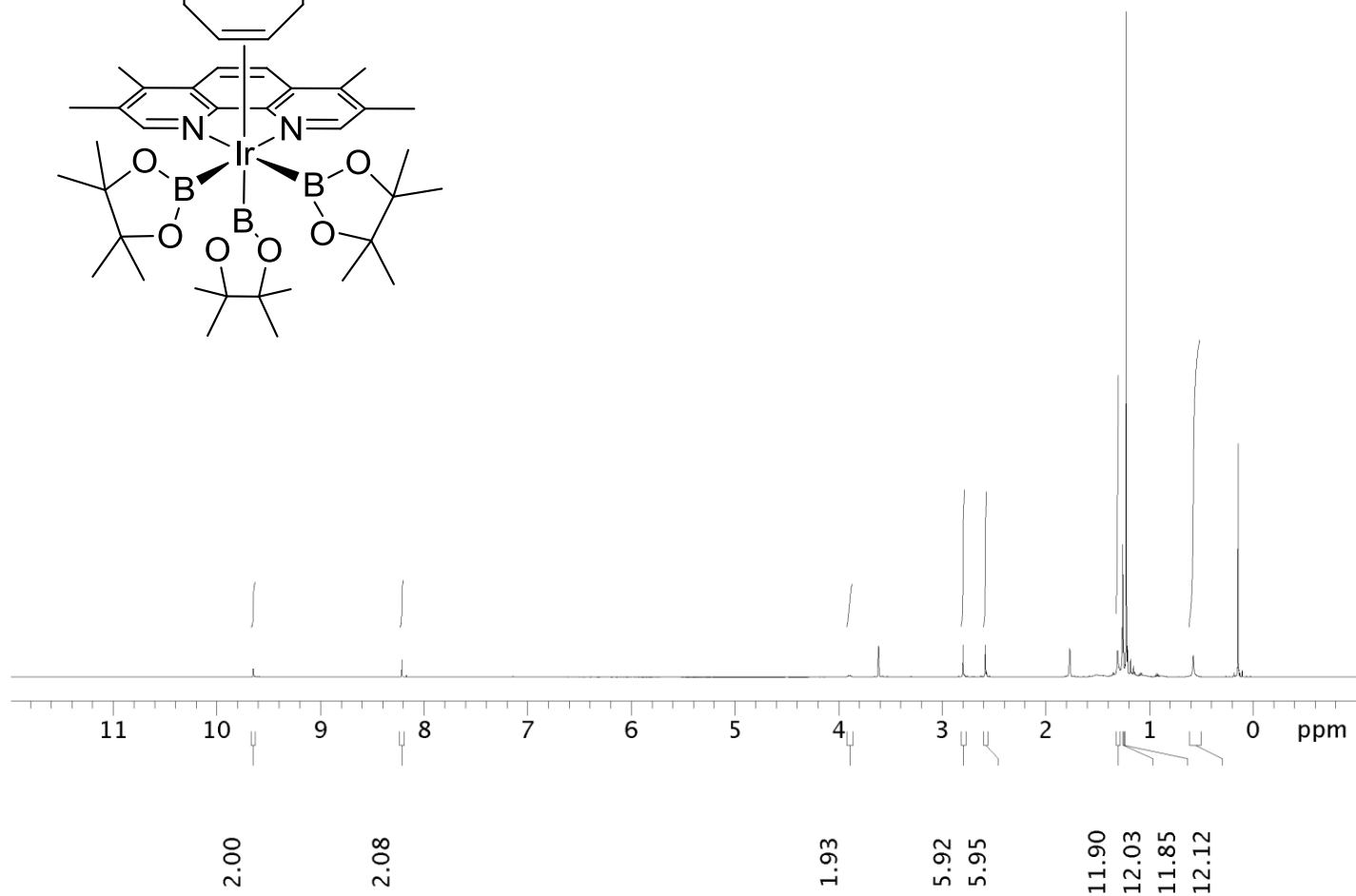
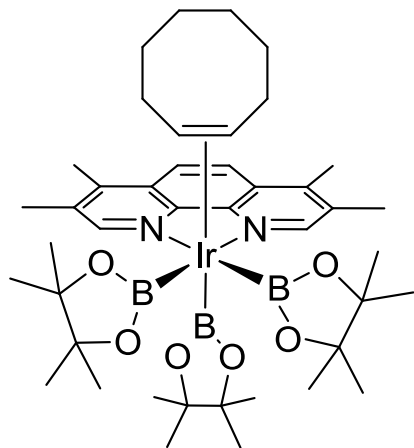
$^1\text{H}$  NMR (500 MHz,  $\text{CD}_2\text{Cl}_2$ ) (tmphen)Ir(COD)(Cl)



$^{13}\text{C}$  NMR (125 MHz,  $\text{CD}_2\text{Cl}_2$ ) (tmphen)Ir(COD)(Cl)

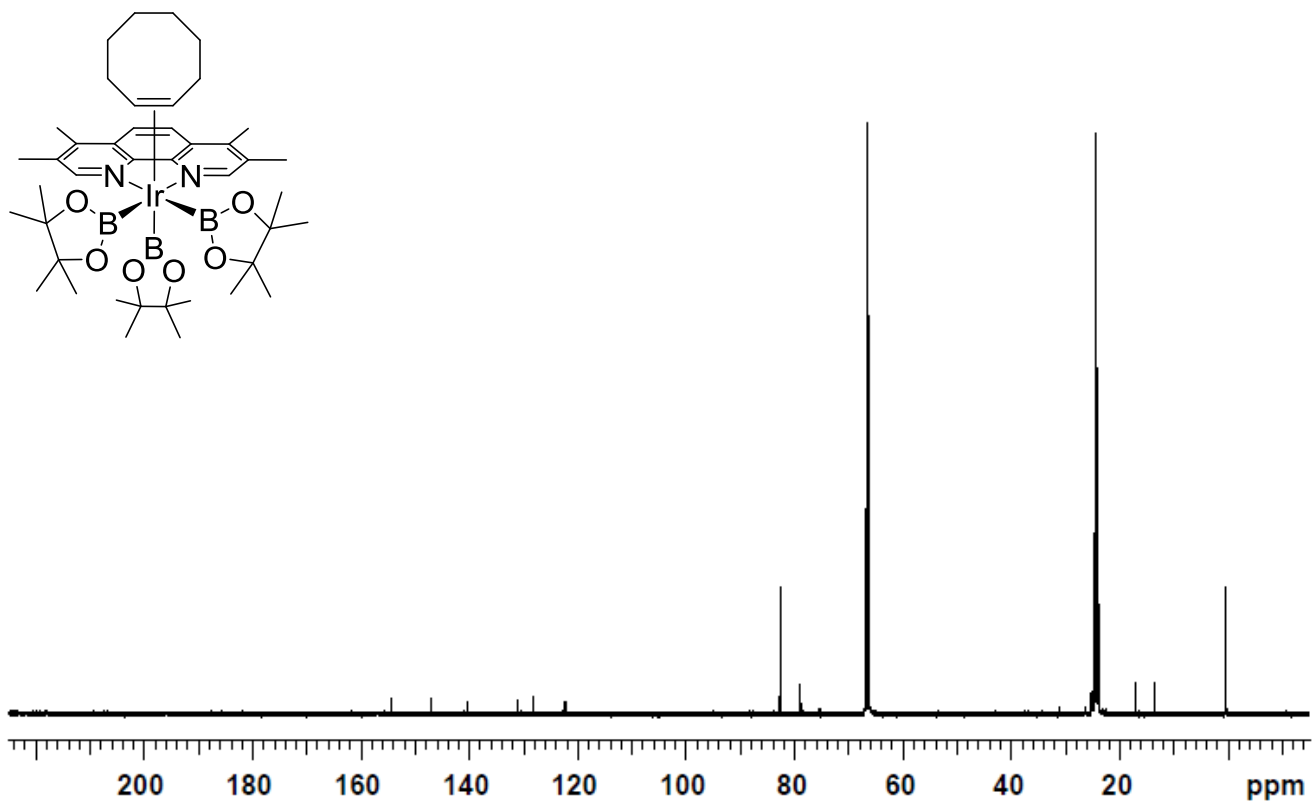


$^1\text{H}$  NMR (500 MHz,  $\text{THF}_d8$ ,  $-35^\circ\text{C}$ ) (tmphen)Ir(BPin) $_3$ (COE)

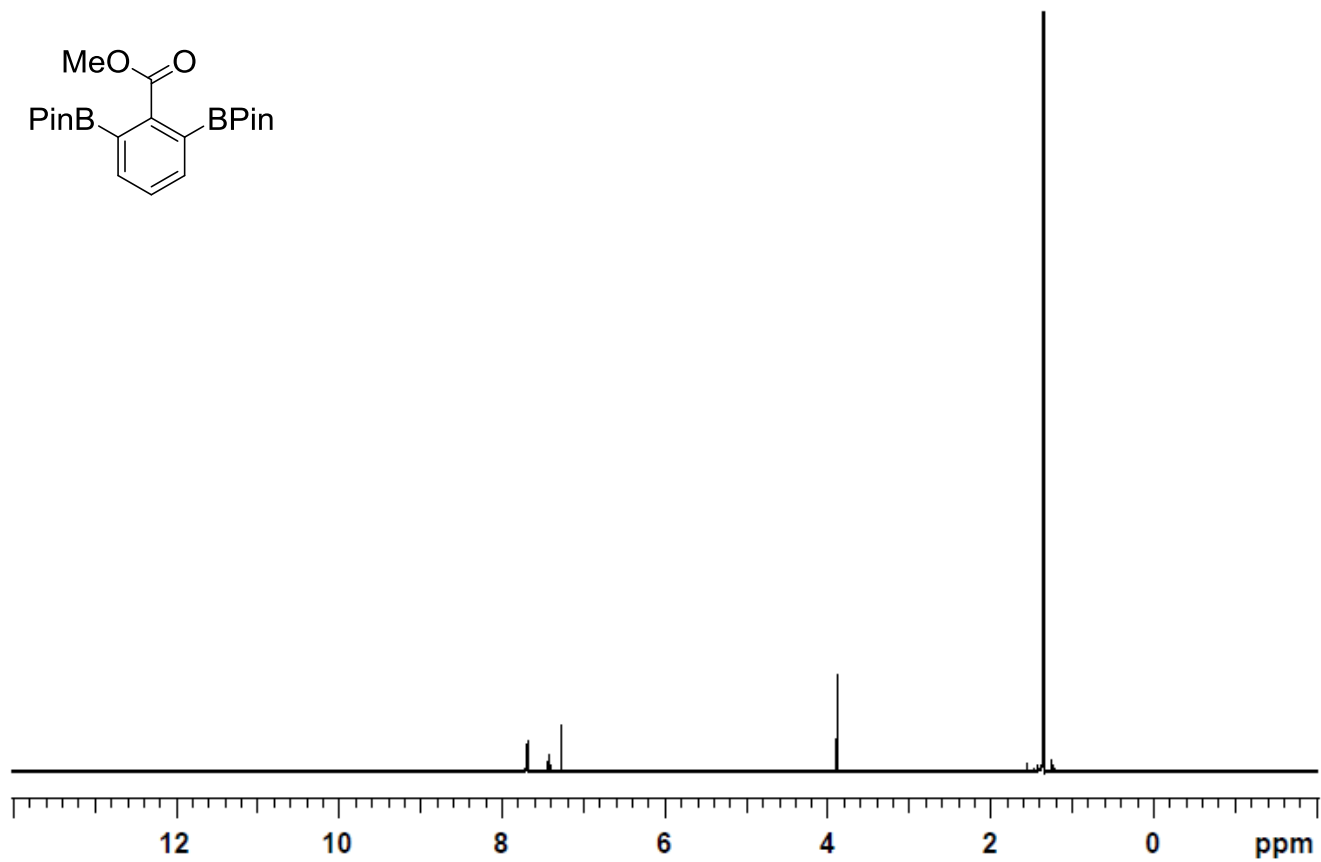
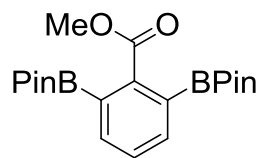




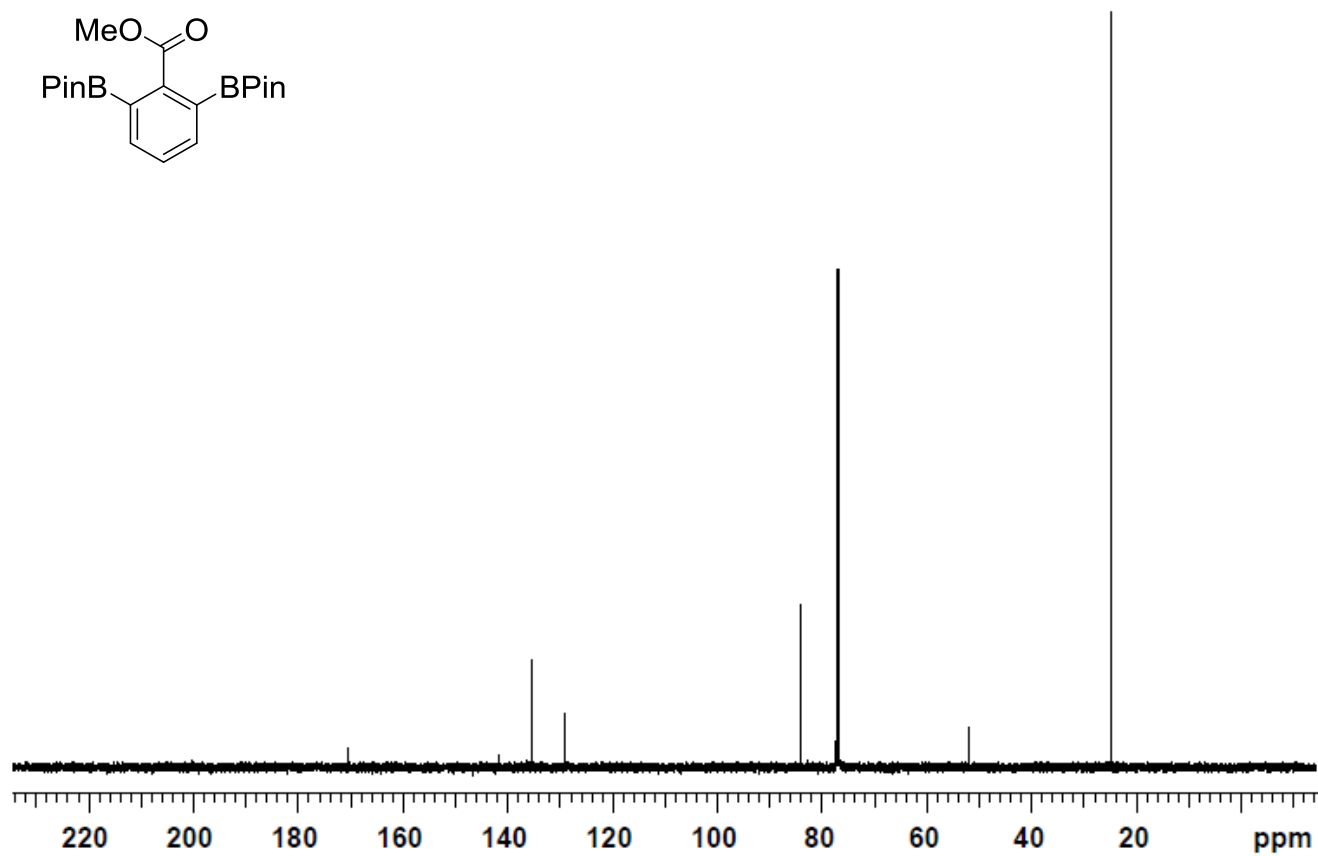
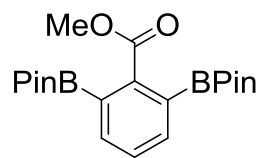
$^{13}\text{C}$  NMR (125 MHz,  $\text{THF}_d8$ ,  $-35^\circ\text{C}$ ) (tmphen)Ir(BPin) $_3$ (COE)



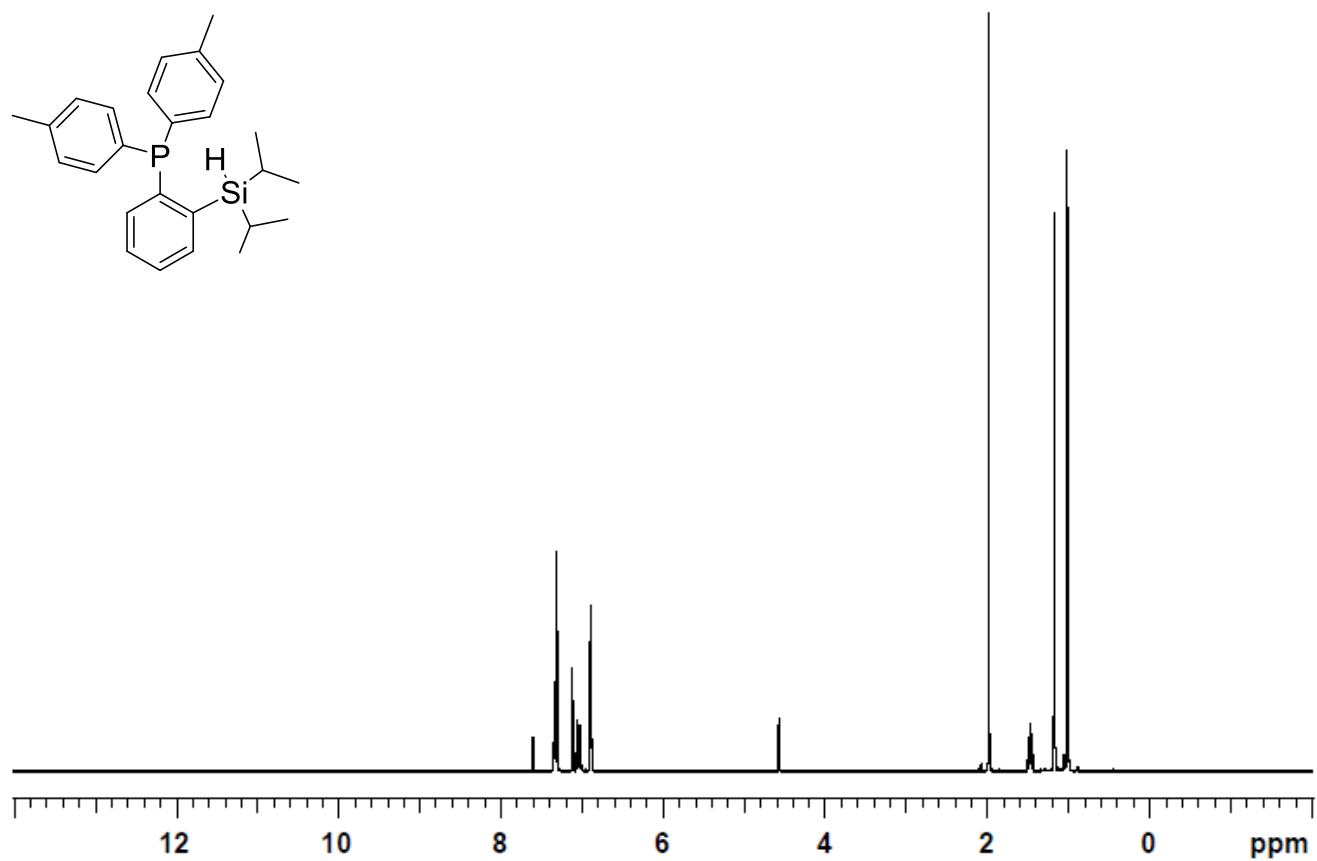
<sup>1</sup>H NMR (500 MHz, CDCl<sub>3</sub>) methyl 2,6-bis(4,4,5,5-tetramethyl-1,3,2-dioxaborolan-2-yl)benzoate (10c)



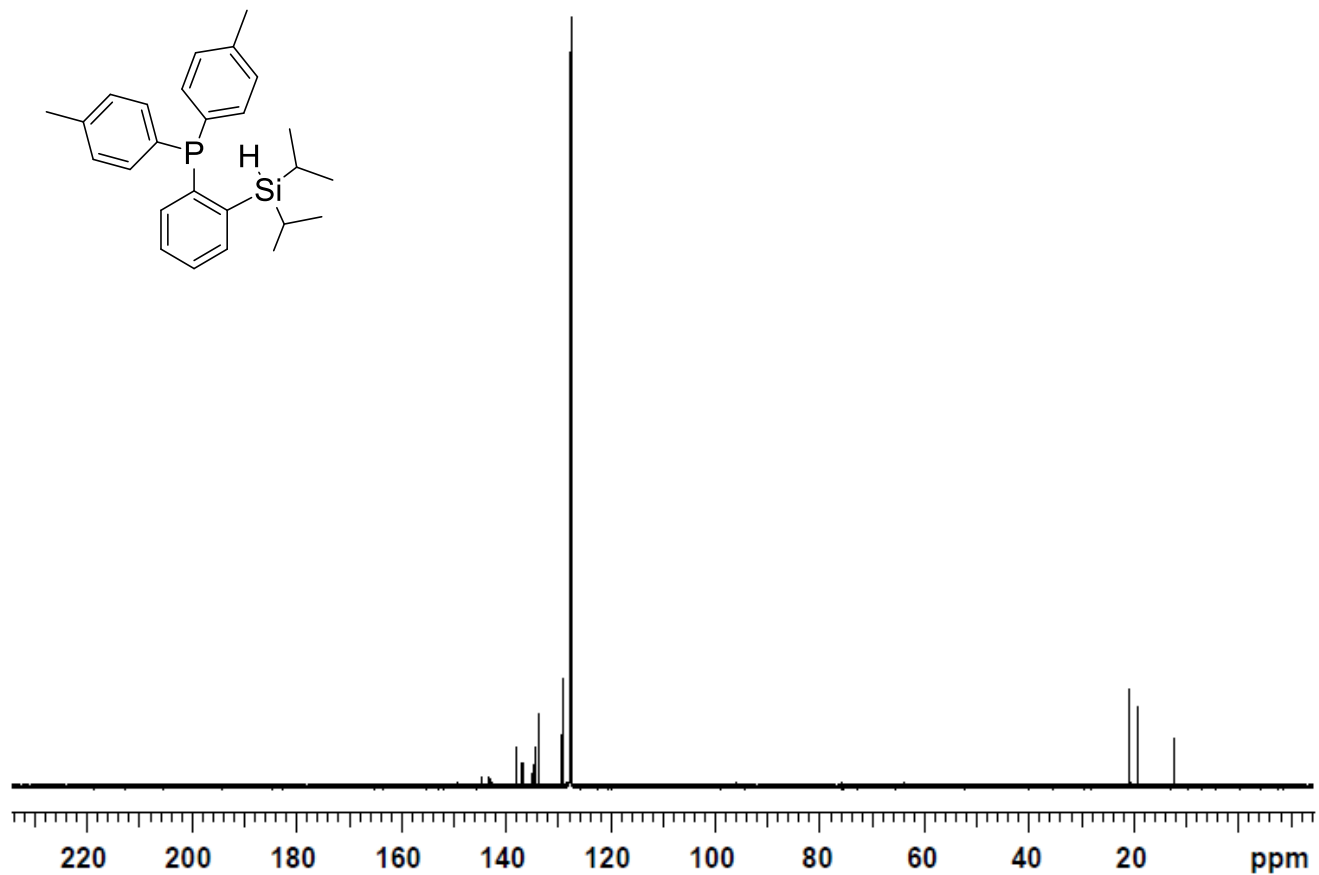
$^{13}\text{C}$  NMR (125 MHz,  $\text{CDCl}_3$ ) methyl 2,6-bis(4,4,5,5-tetramethyl-1,3,2-dioxaborolan-2-yl)benzoate (10c)



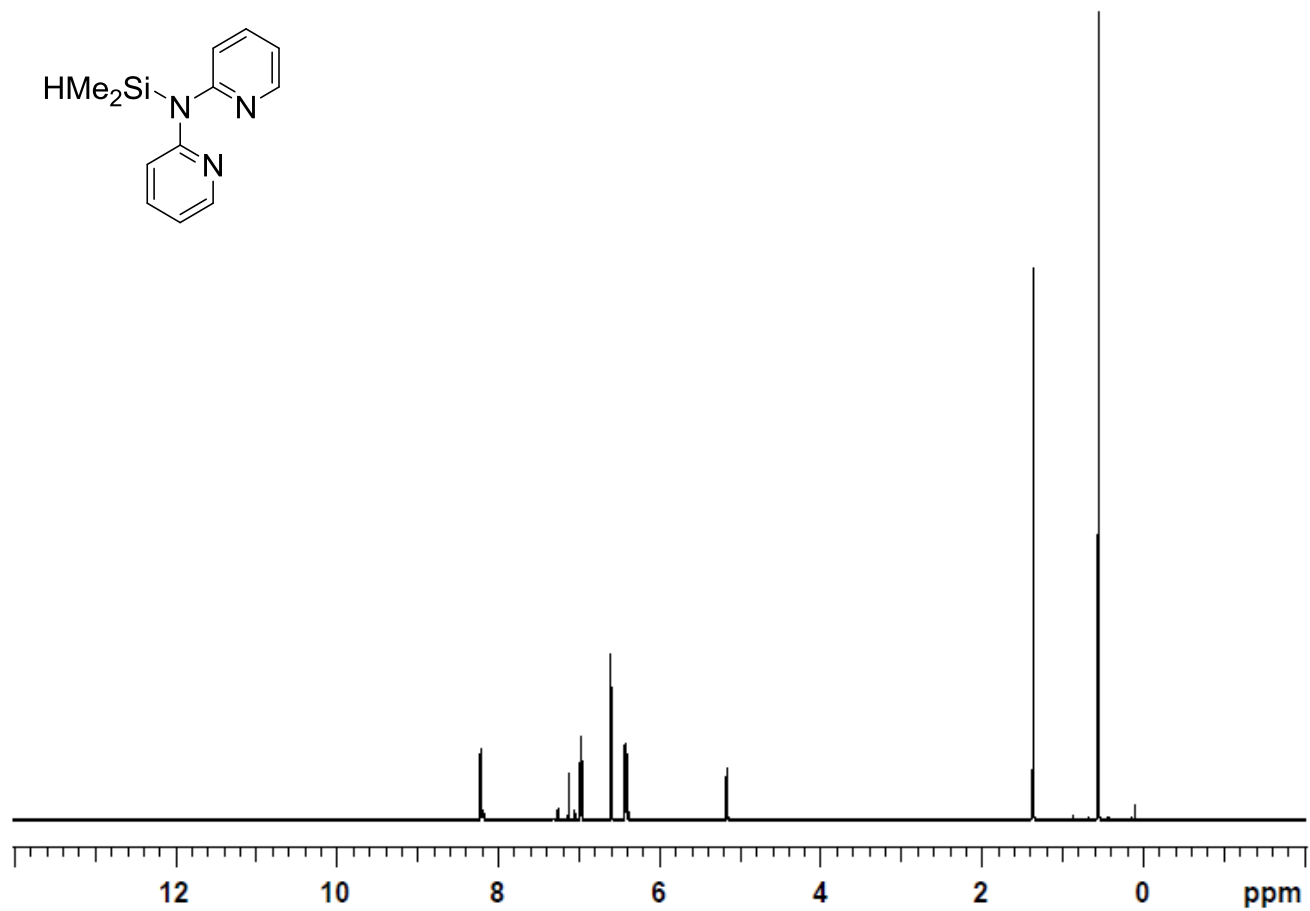
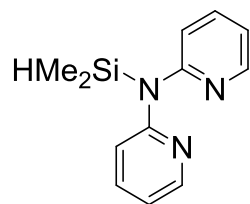
**$^1\text{H}$  NMR (500 MHz,  $\text{C}_6\text{D}_6$ ) (2-(diisopropylsilyl)phenyl)di-p-tolylphosphane (SiPbz)**



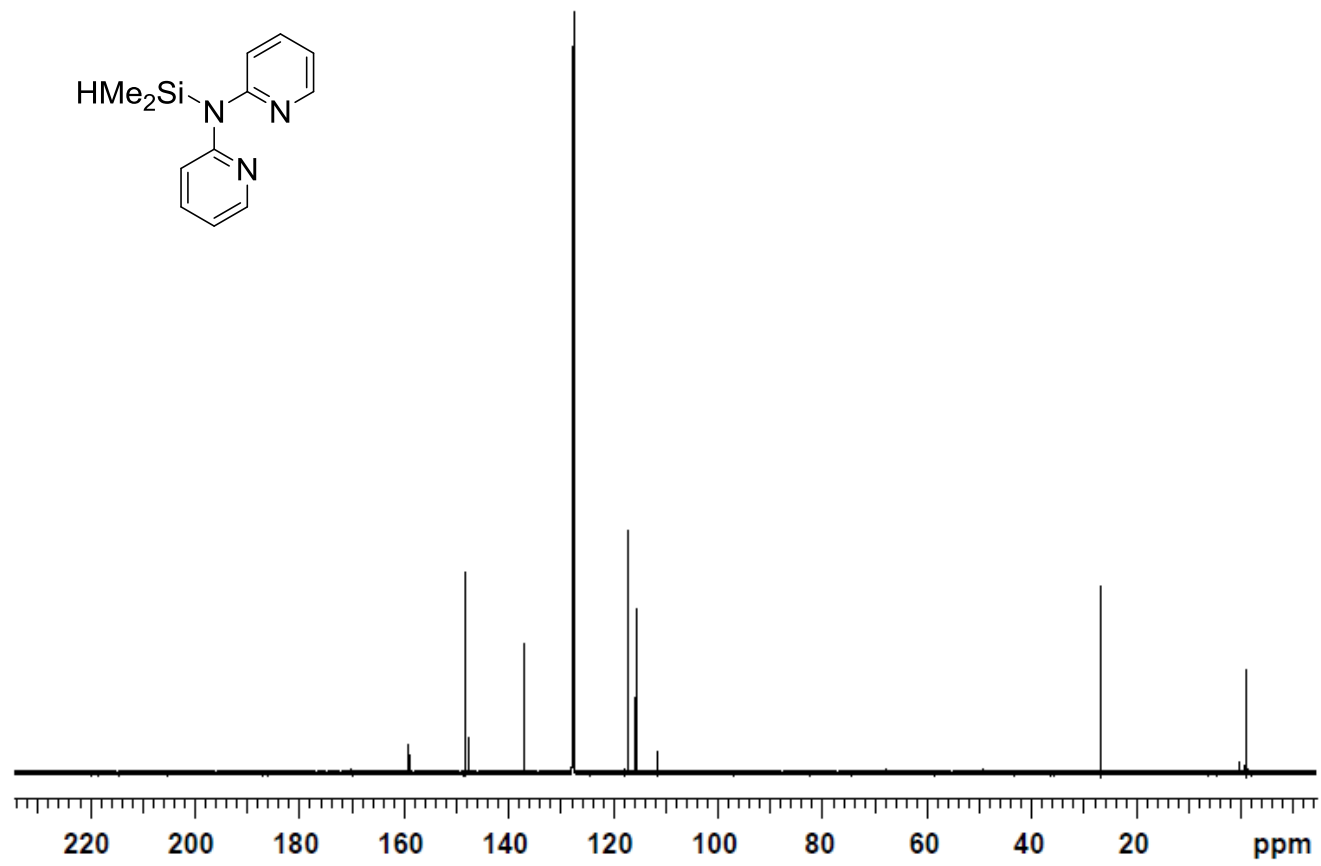
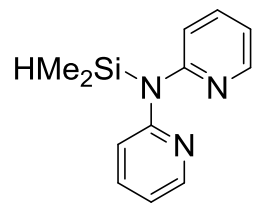
<sup>13</sup>C NMR (125 MHz, C<sub>6</sub>D<sub>6</sub>) (2-(diisopropylsilyl)phenyl)di-p-tolylphosphane (SiPbz)



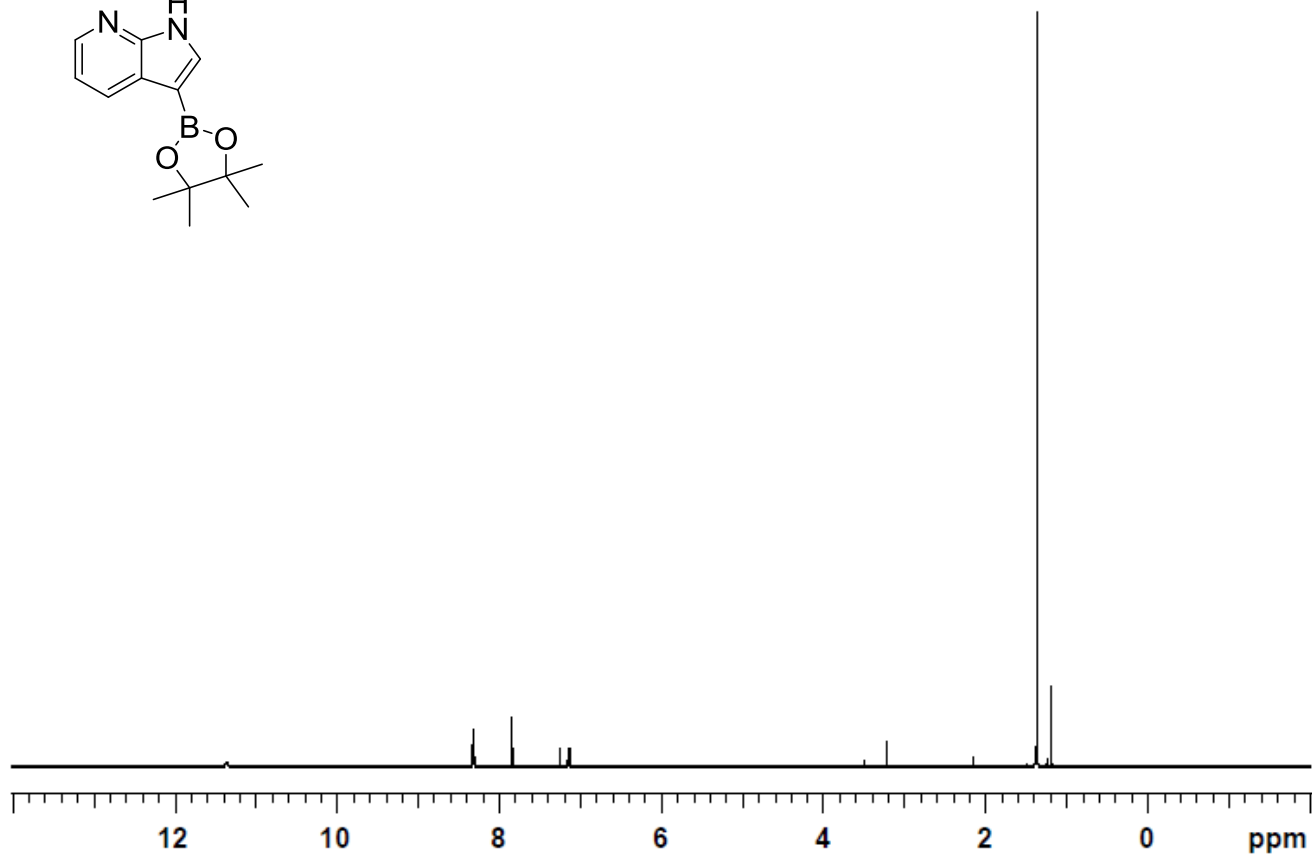
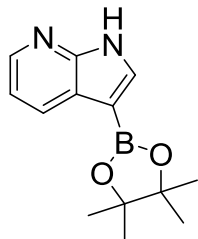
**<sup>1</sup>H NMR (500 MHz, C<sub>6</sub>D<sub>6</sub>) N-(dimethylsilyl)-N-(pyridin-2-yl)pyridin-2-amine (14b)**



<sup>13</sup>C NMR (125 MHz, C<sub>6</sub>D<sub>6</sub>) N-(dimethylsilyl)-N-(pyridin-2-yl)pyridin-2-amine (14b)

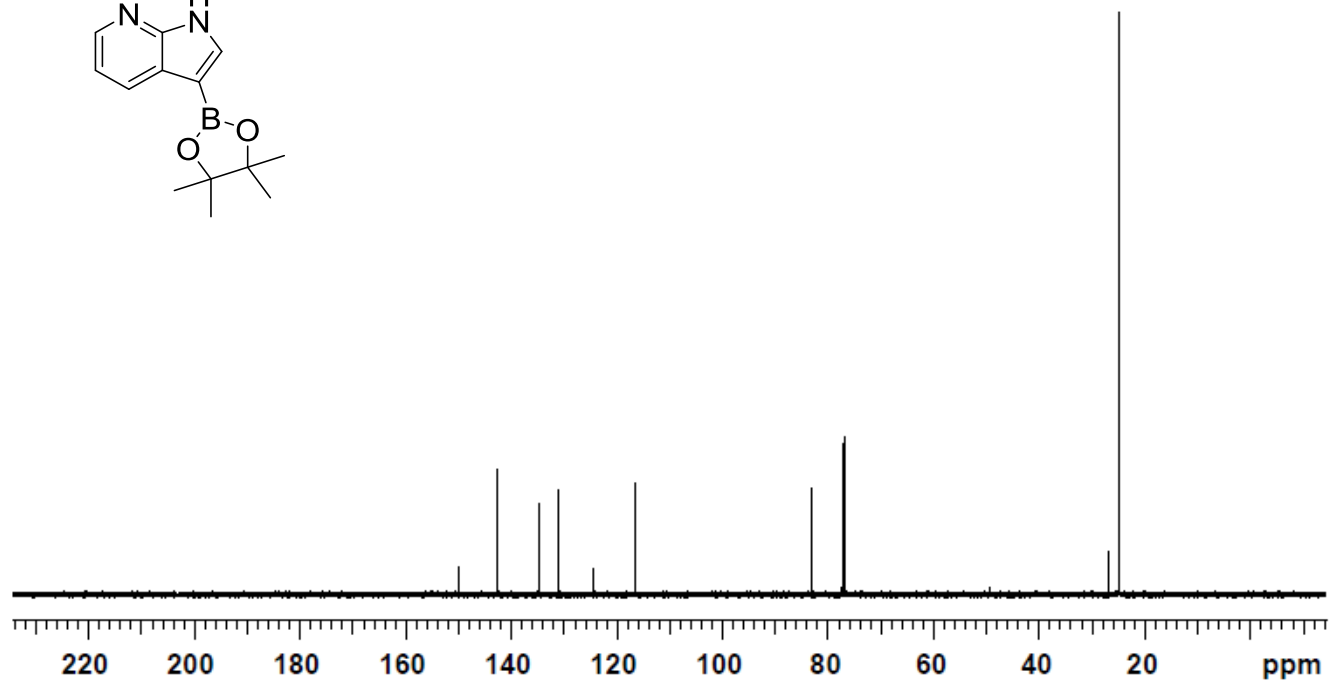
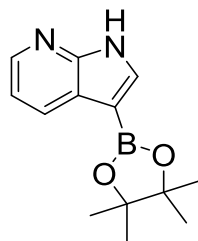


$^1\text{H}$  NMR (500 MHz,  $\text{CDCl}_3$ ) 3-(4,4,5,5-tetramethyl-1,3,2-dioxaborolan-2-yl)-7-azaindole (18a)

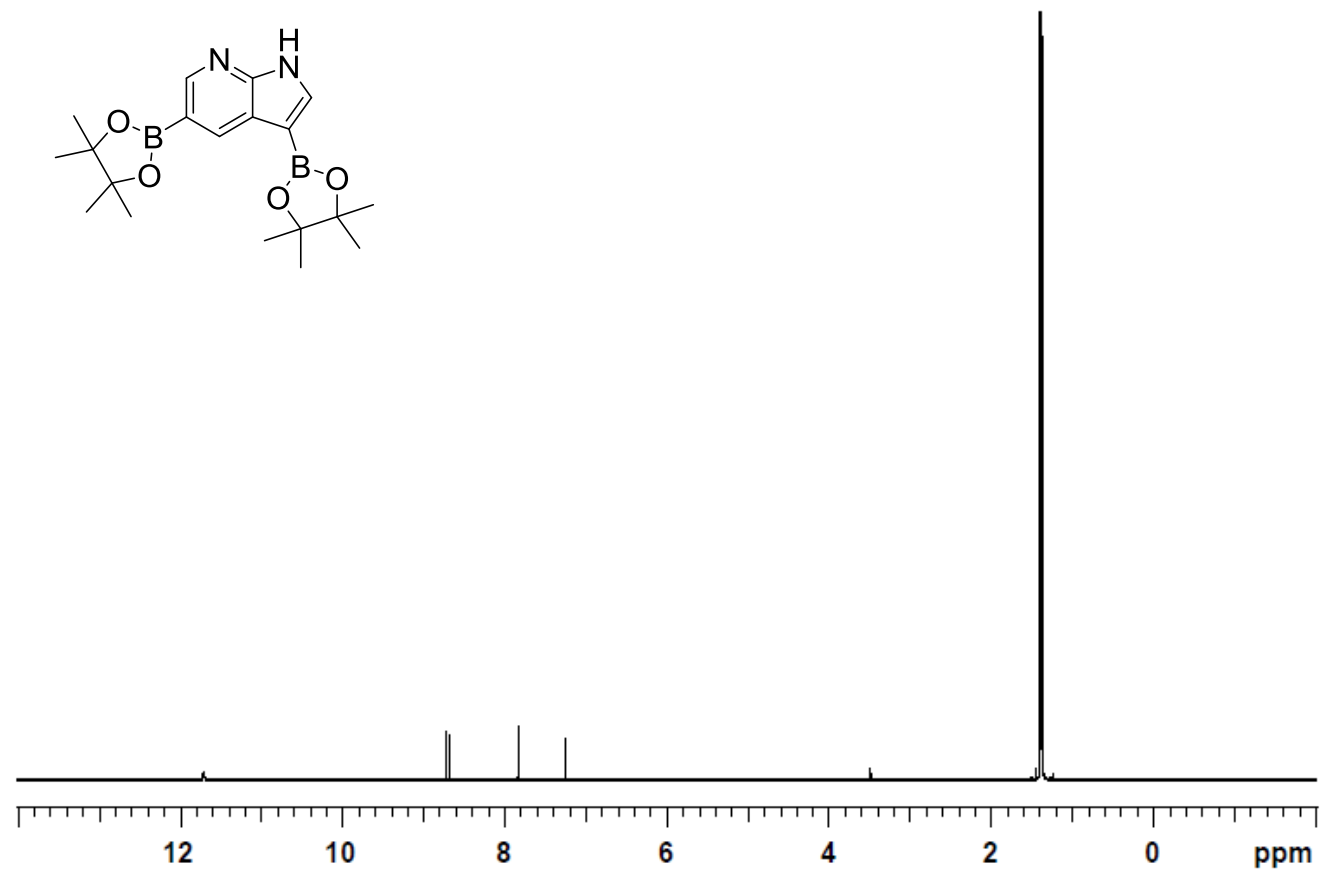




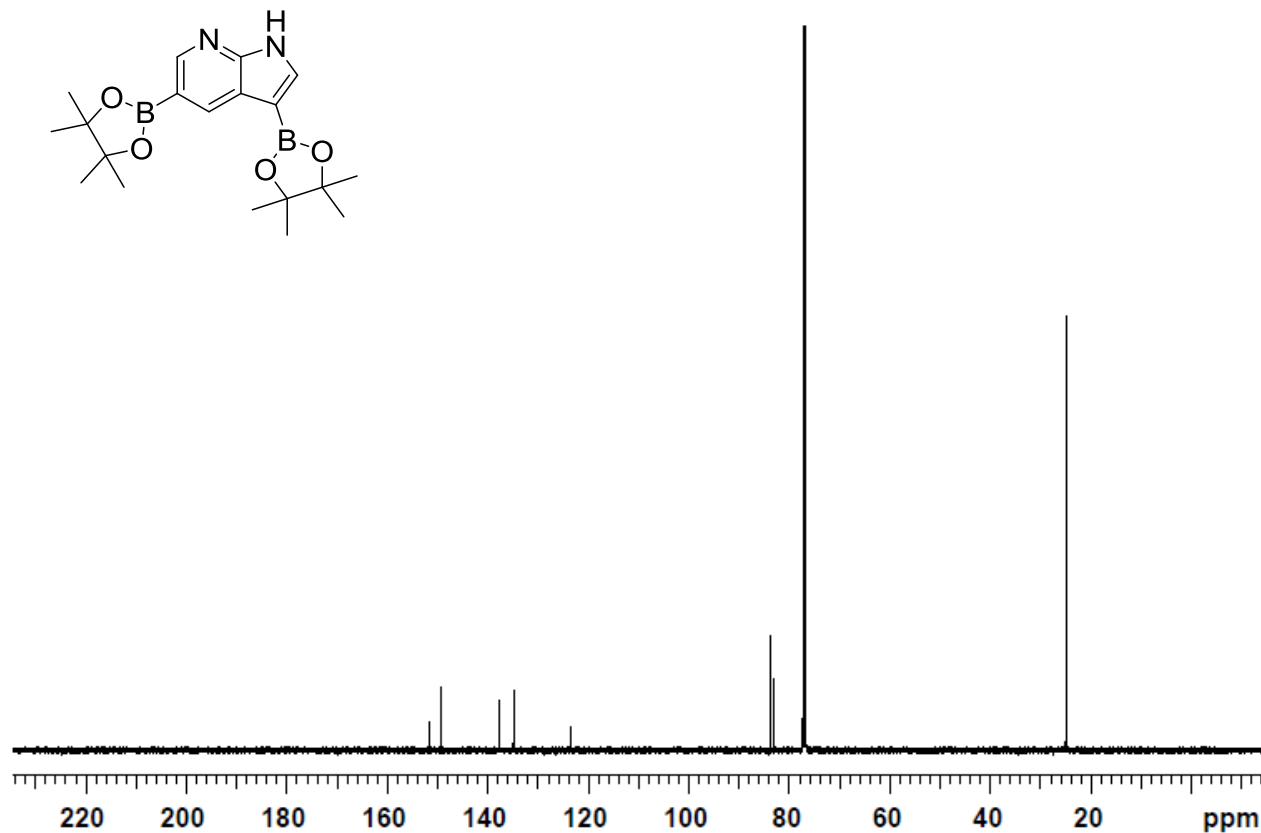
$^{13}\text{C}$  NMR (125 MHz,  $\text{CDCl}_3$ ) 3-(4,4,5,5-tetramethyl-1,3,2-dioxaborolan-2-yl)-7-azaindole (18a)



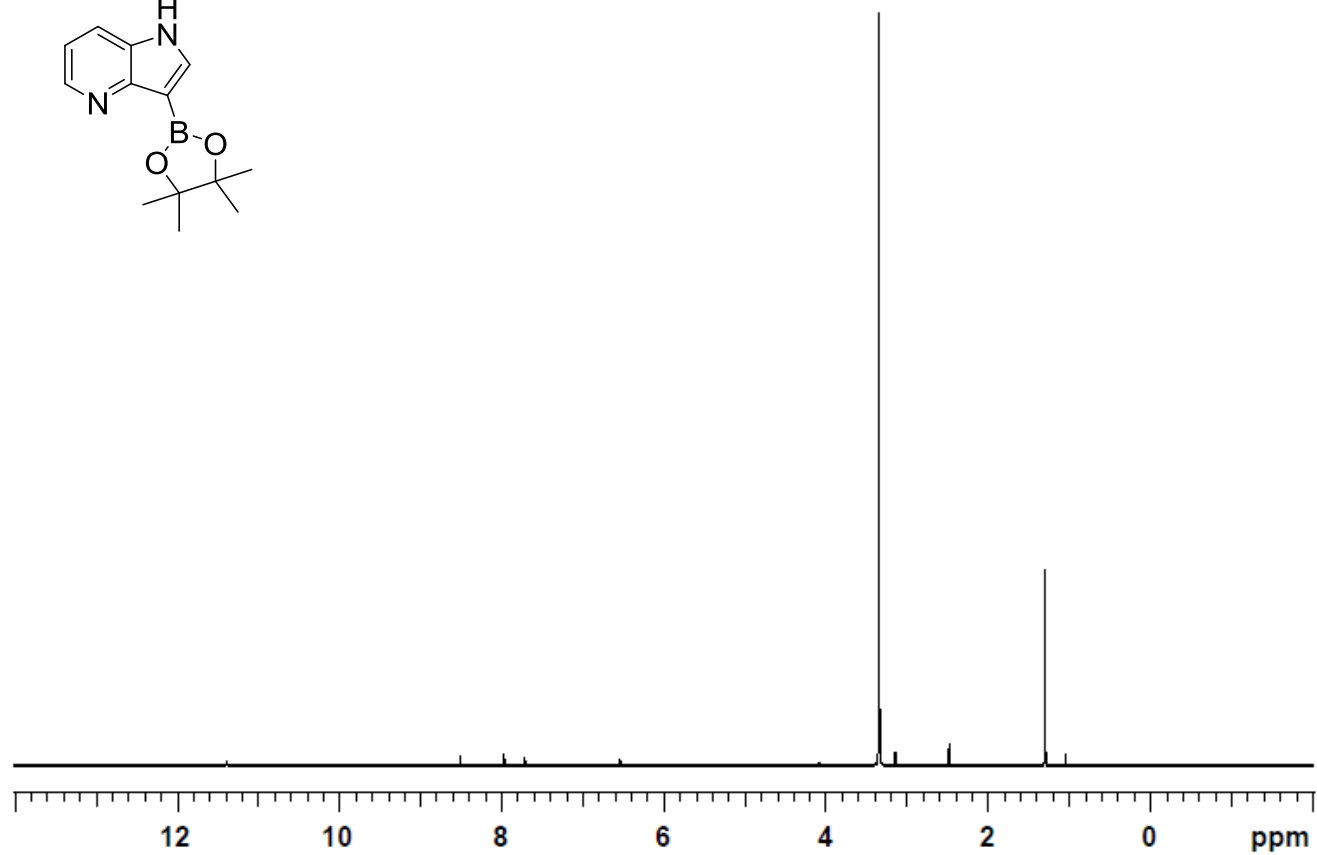
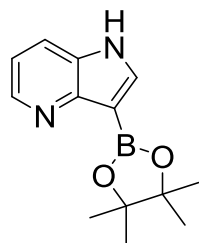
<sup>1</sup>H NMR (500 MHz, CDCl<sub>3</sub>) 3,5-bis(4,4,5,5-tetramethyl-1,3,2-dioxaborolan-2-yl)-7-azaindole (18b)



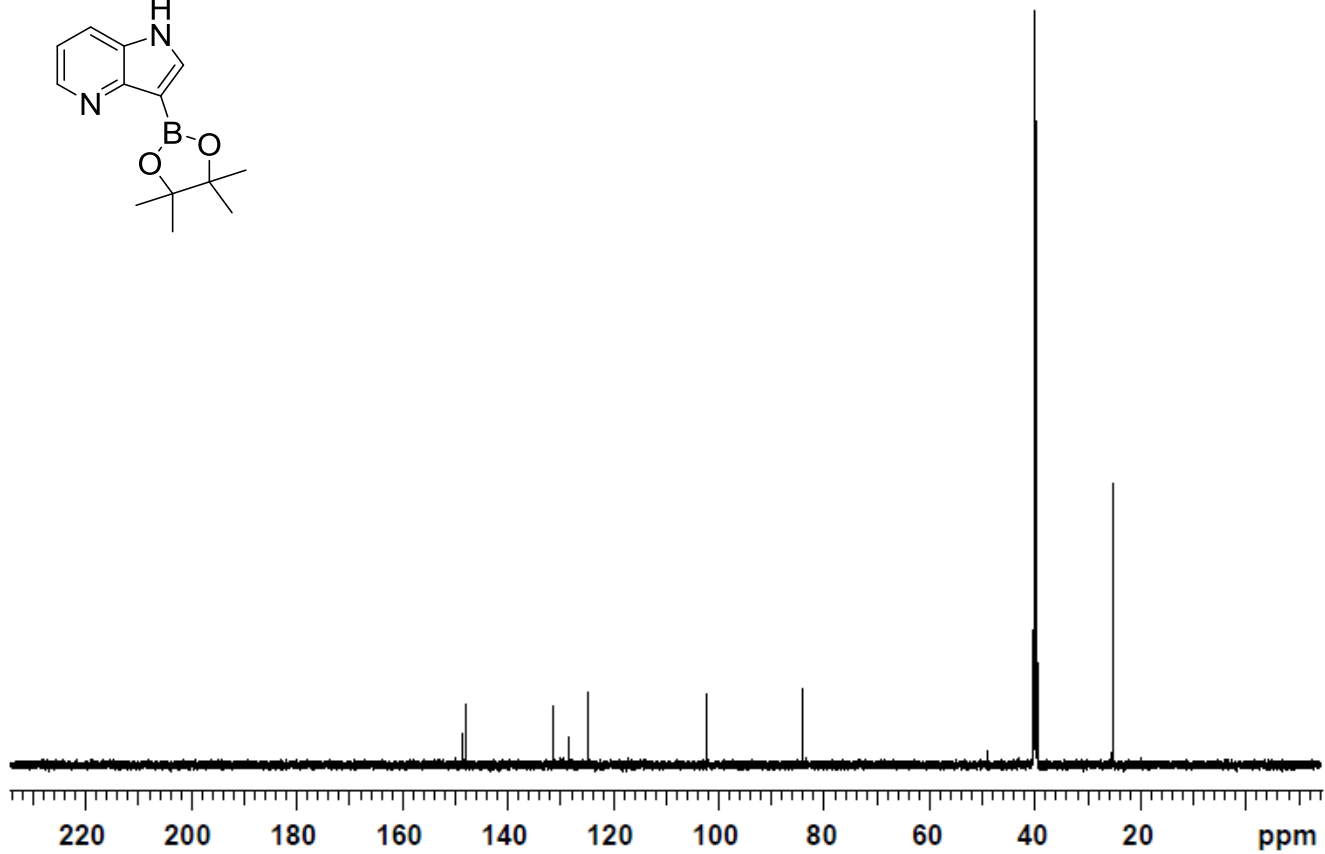
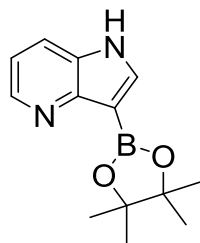
$^{13}\text{C}$  NMR (125 MHz,  $\text{CDCl}_3$ ) 3,5-bis(4,4,5,5-tetramethyl-1,3,2-dioxaborolan-2-yl)-7-azaindole (18b)



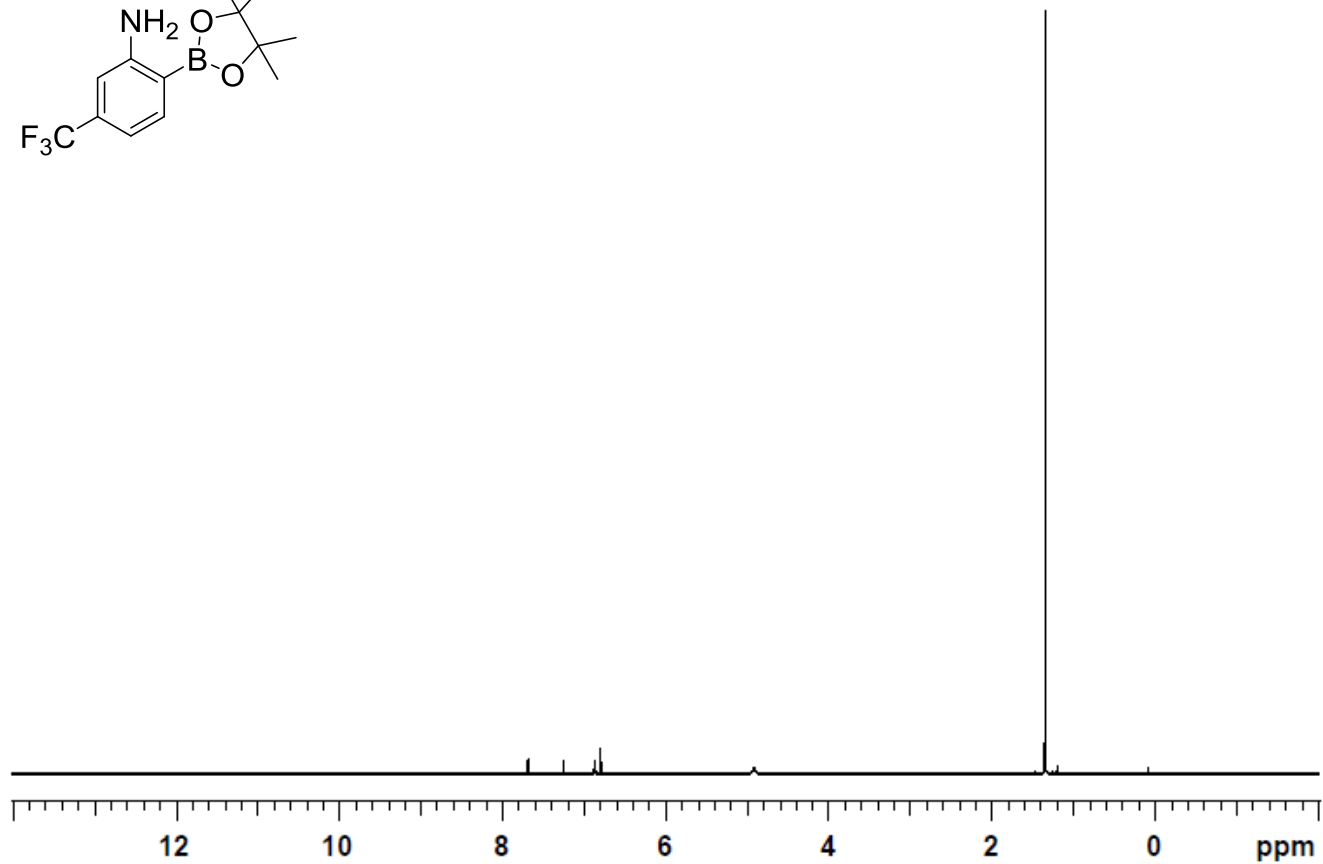
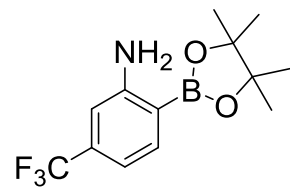
$^1\text{H}$  NMR (500 MHz,  $\text{DMSO}-d_6$ ) 3-(4,4,5,5-tetramethyl-1,3,2-dioxaborolan-2-yl)-4-azaindole (19)



$^{13}\text{C}$  NMR (125 MHz,  $\text{DMSO-d}_6$ ) 3-(4,4,5,5-tetramethyl-1,3,2-dioxaborolan-2-yl)-4-azaindole (19)

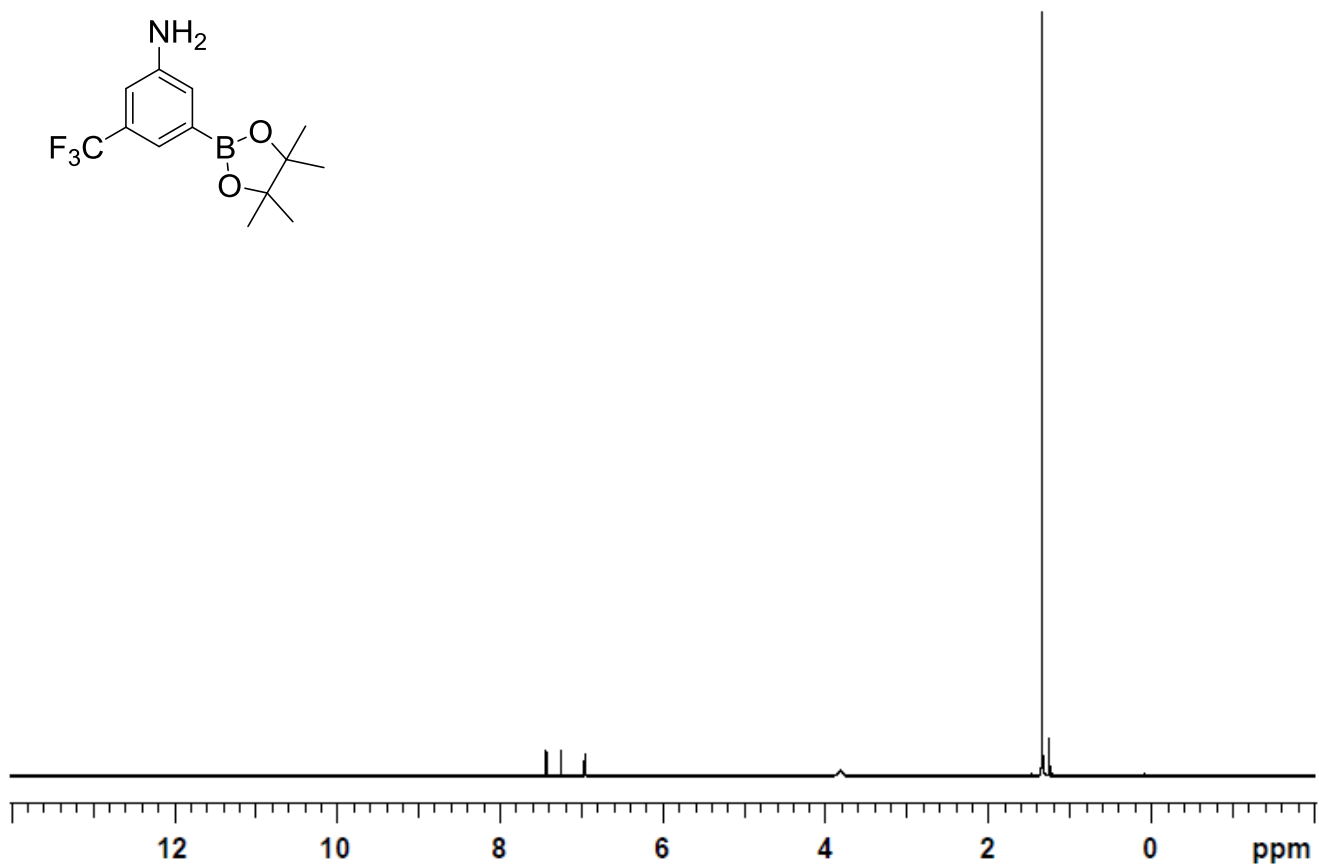


<sup>1</sup>H NMR (500 MHz, CDCl<sub>3</sub>) 2-(4,4,5,5-tetramethyl-1,3,2-dioxaborolan-2-yl)-5-(trifluoromethyl)-benzenamine (20f)



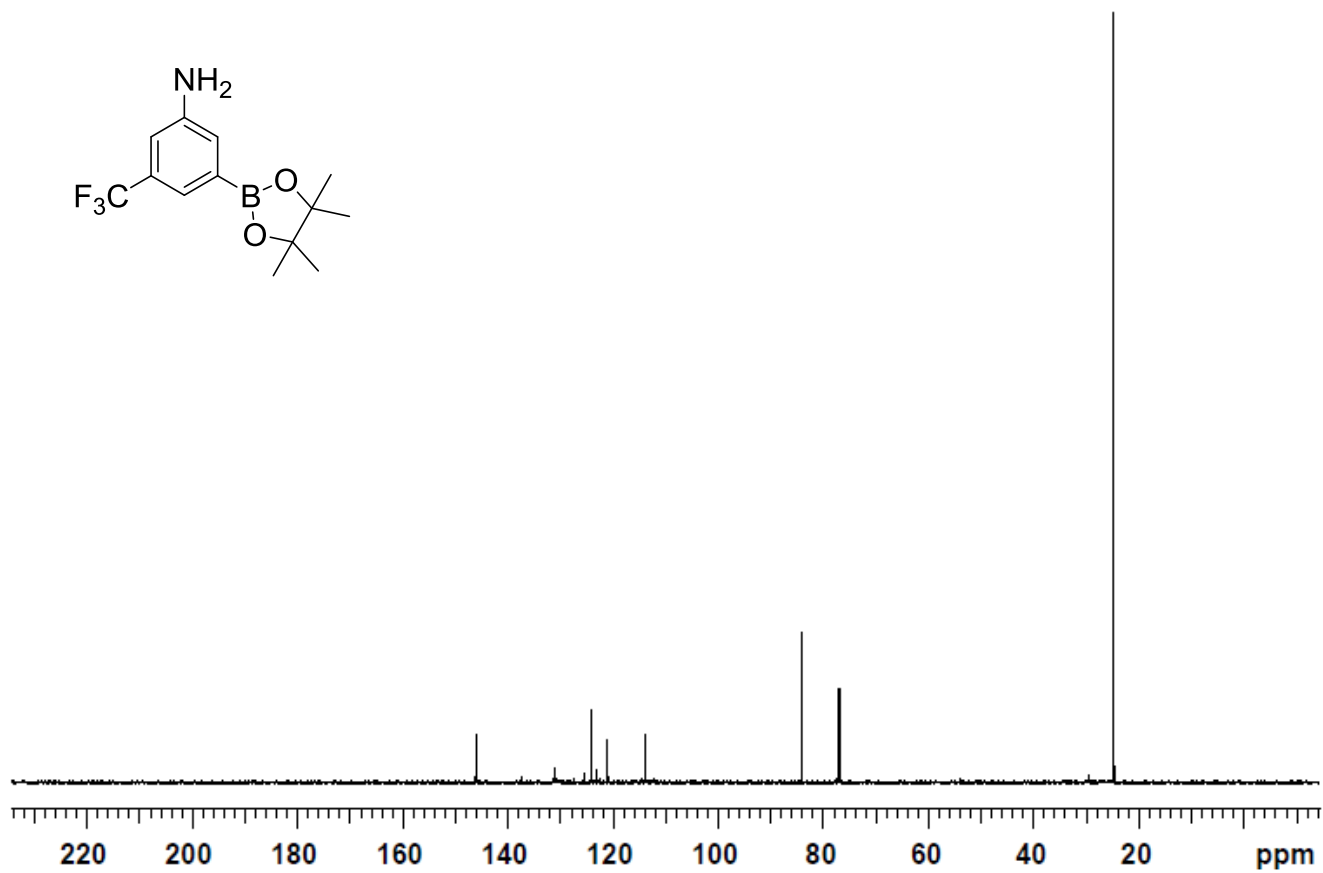
<sup>13</sup>C NMR (125 MHz, CDCl<sub>3</sub>) 2-(4,4,5,5-tetramethyl-1,3,2-dioxaborolan-2-yl)-5-(trifluoromethyl)-benzenamine (20f)



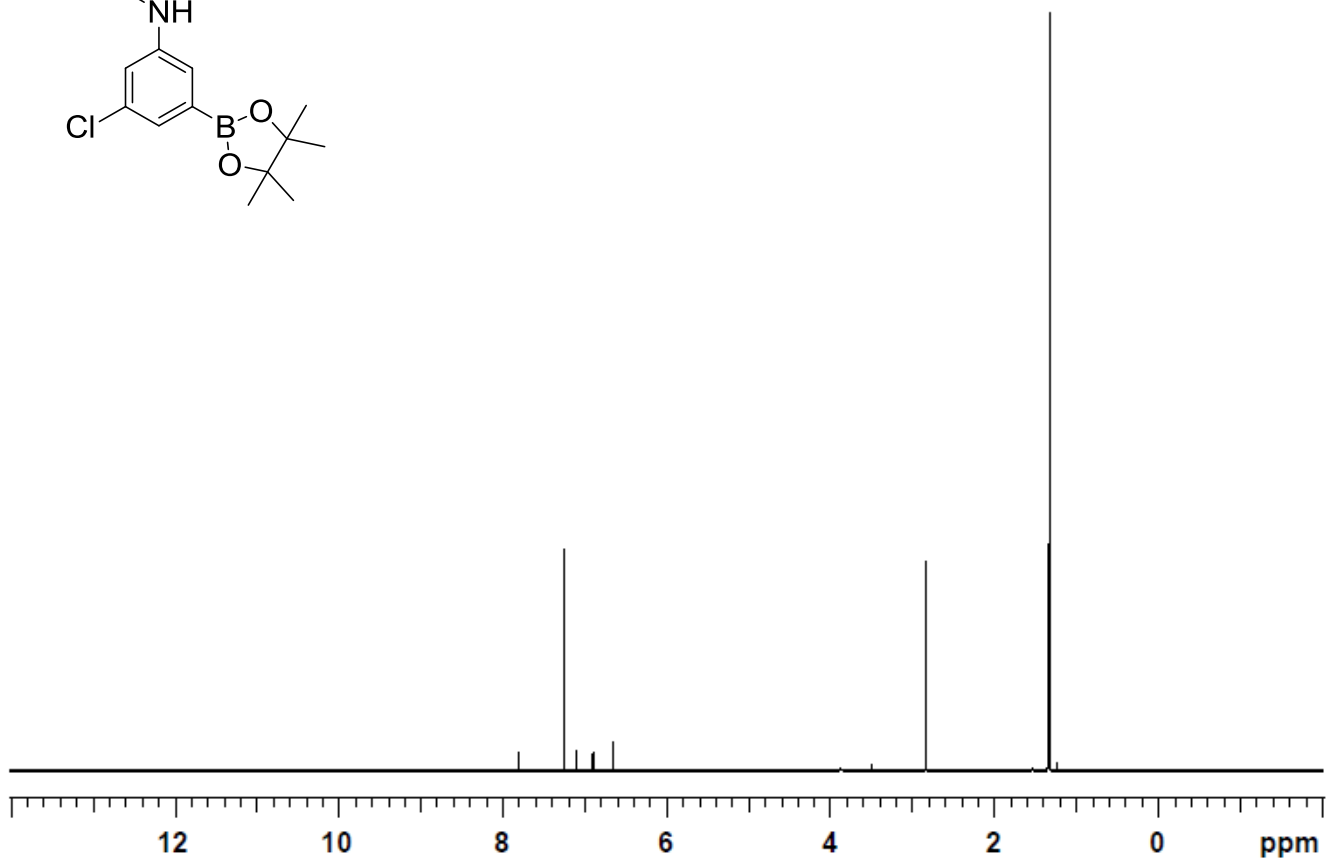
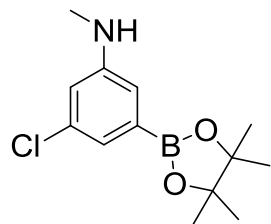


$^{13}\text{C}$  NMR (125 MHz,  $\text{CDCl}_3$ ) 3-(4,4,5,5-tetramethyl-1,3,2-dioxaborolan-2-yl)-5-(trifluoromethyl)-benzenamine (20e)

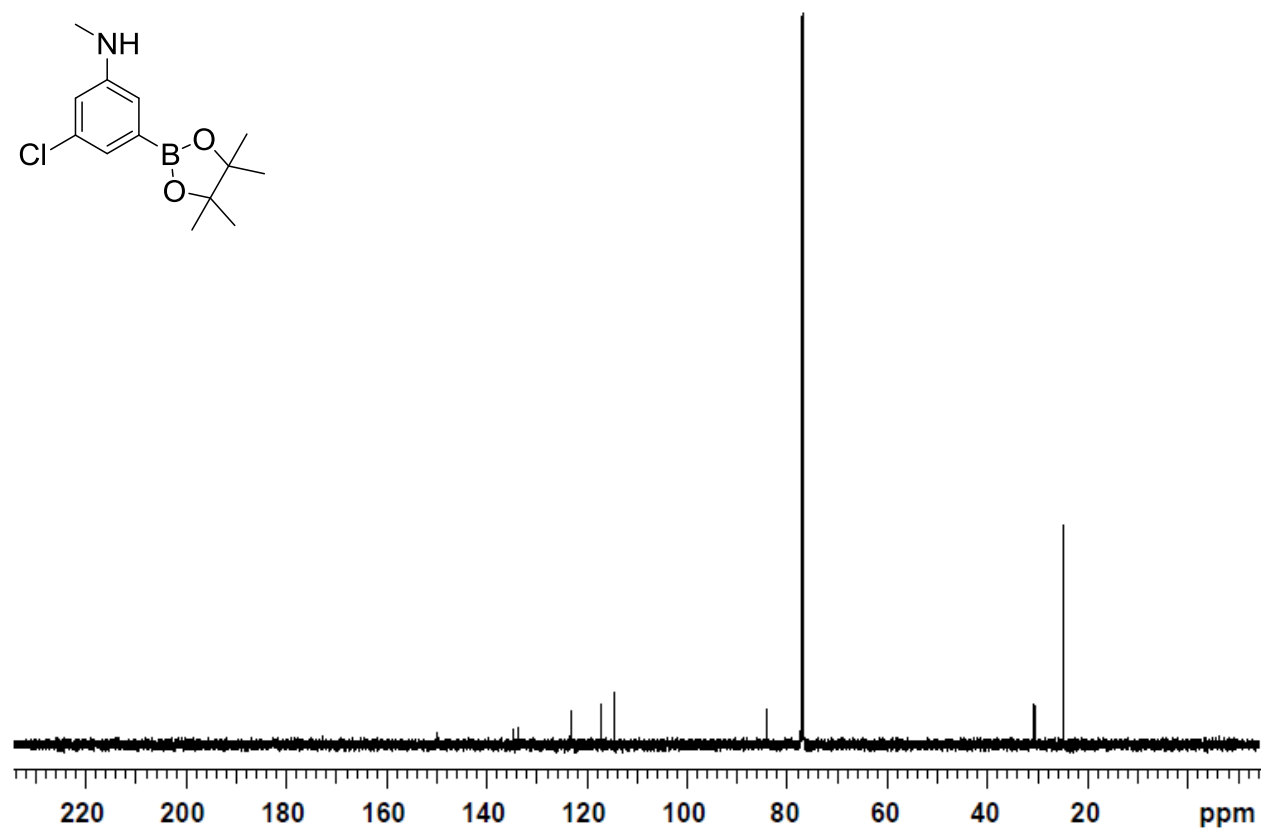
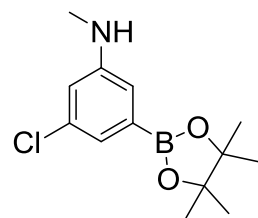




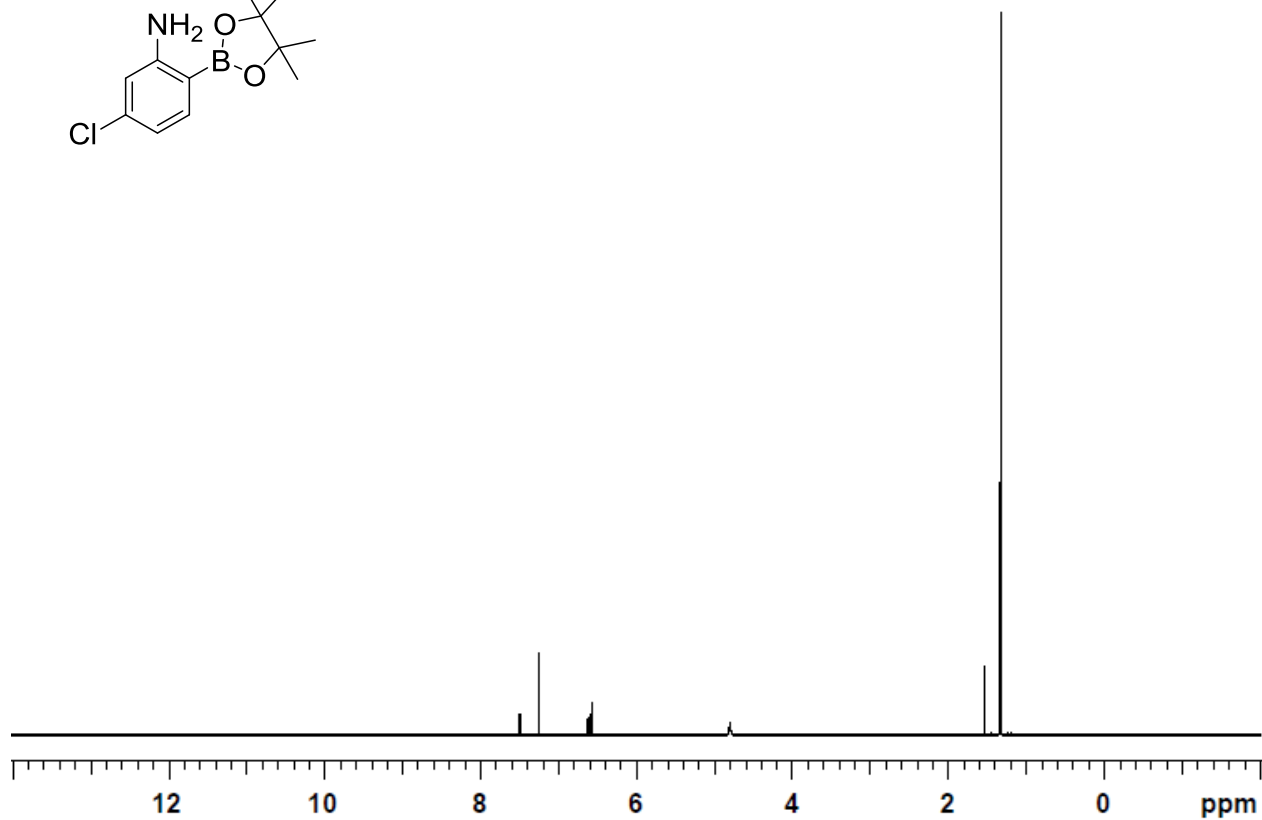
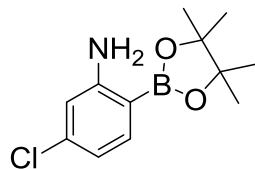
<sup>1</sup>H NMR (500 MHz, CDCl<sub>3</sub>) N-methyl-3-chloro-5-(4,4,5,5-tetramethyl-1,3,2-dioxaborolan-2-yl)-benzenamine (21b)



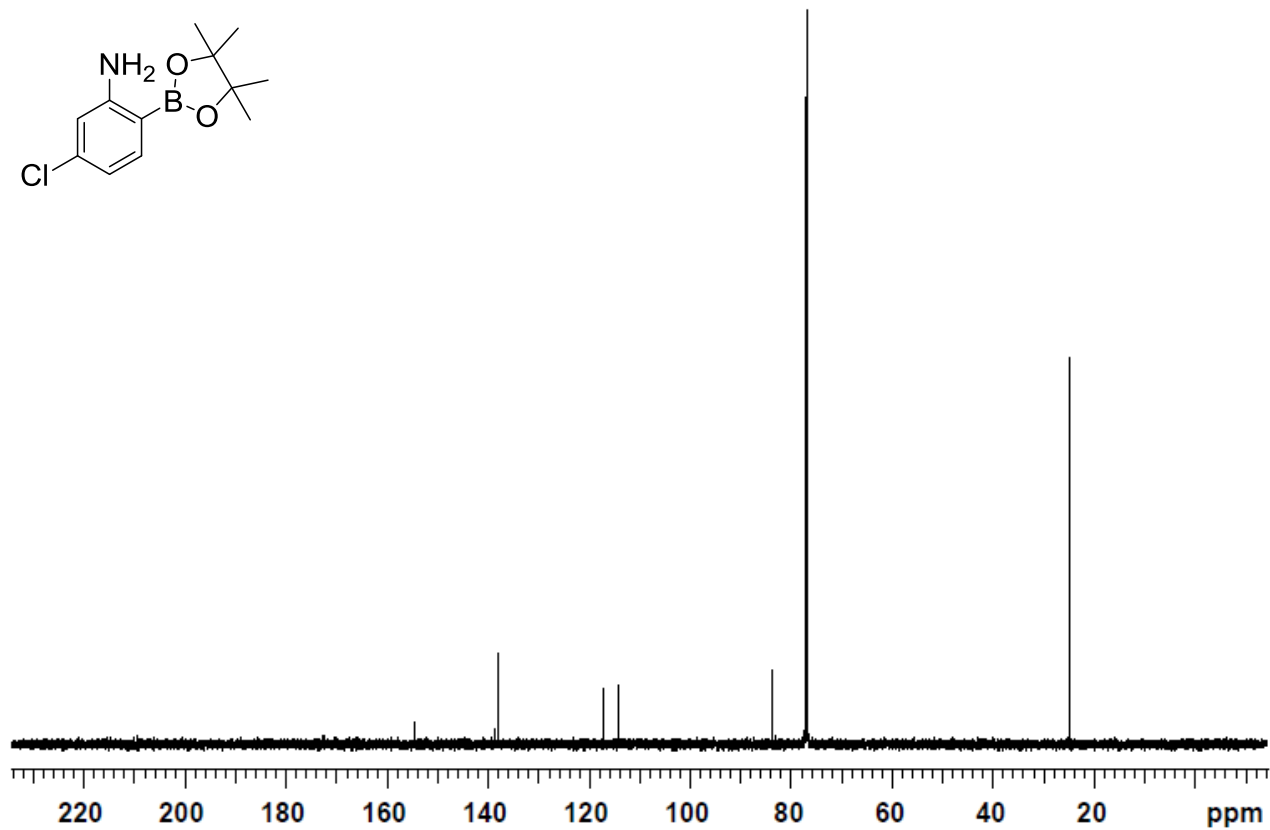
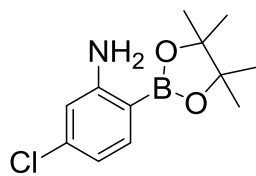
$^{13}\text{C}$  NMR (125 MHz,  $\text{CDCl}_3$ ) N-methyl-3-chloro-5-(4,4,5,5-tetramethyl-1,3,2-dioxaborolan-2-yl)-benzenamine (21b)



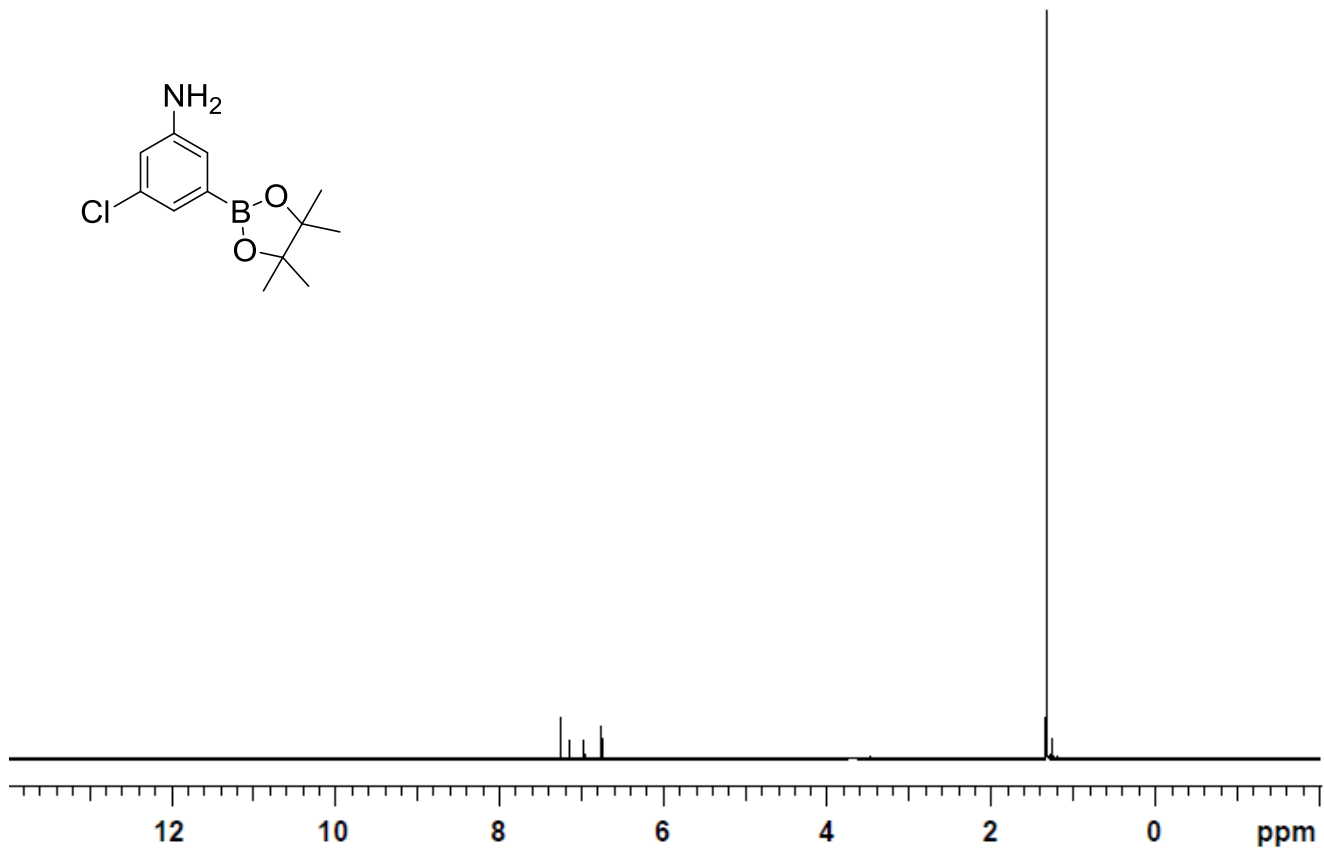
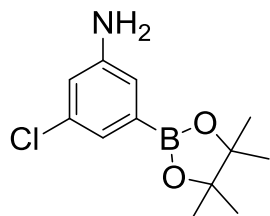
<sup>1</sup>H NMR (500 MHz, CDCl<sub>3</sub>) 5-chloro-2-(4,4,5,5-tetramethyl-1,3,2-dioxaborolan-2-yl)-benzenamine (22c)



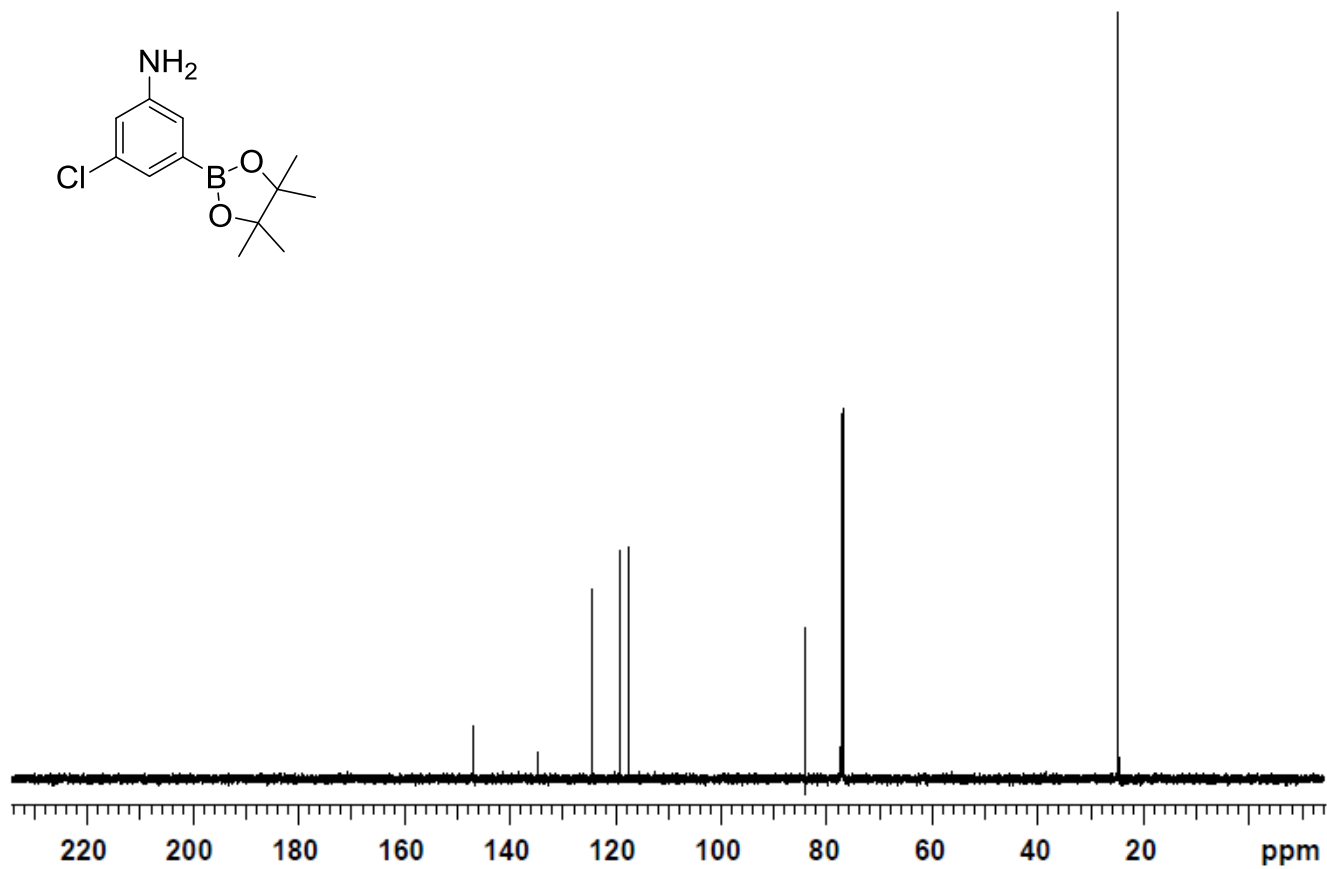
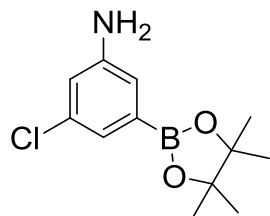
$^{13}\text{C}$  NMR (125 MHz,  $\text{CDCl}_3$ ) 5-chloro-2-(4,4,5,5-tetramethyl-1,3,2-dioxaborolan-2-yl)-benzenamine (22c)



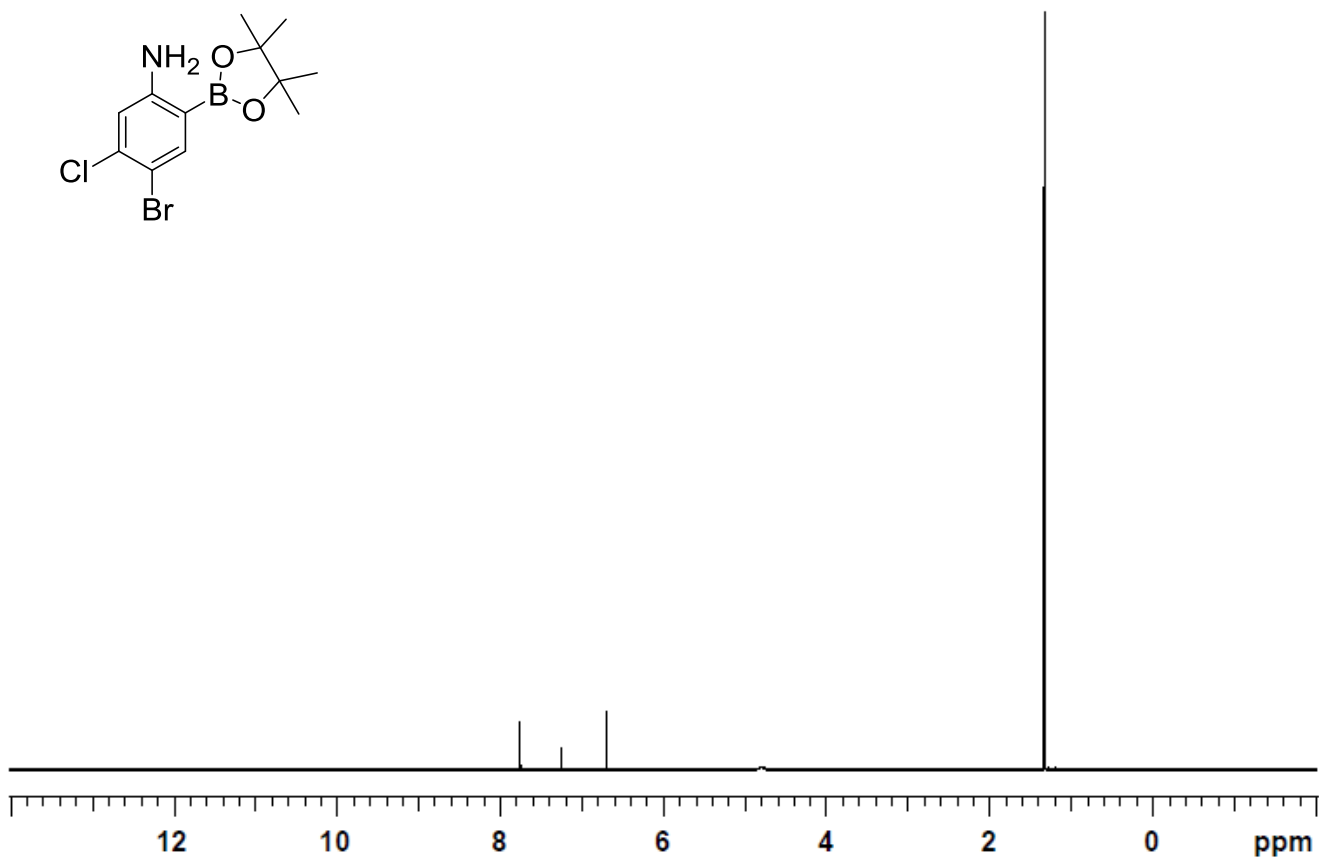
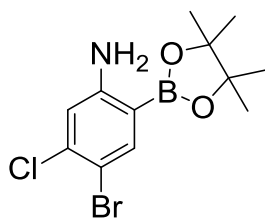
<sup>1</sup>H NMR (500 MHz, CDCl<sub>3</sub>) 3-chloro-5-(4,4,5,5-tetramethyl-1,3,2-dioxaborolan-2-yl)aniline (22b)



$^{13}\text{C}$  NMR (125 MHz,  $\text{CDCl}_3$ ) 3-chloro-5-(4,4,5,5-tetramethyl-1,3,2-dioxaborolan-2-yl)aniline (22b)

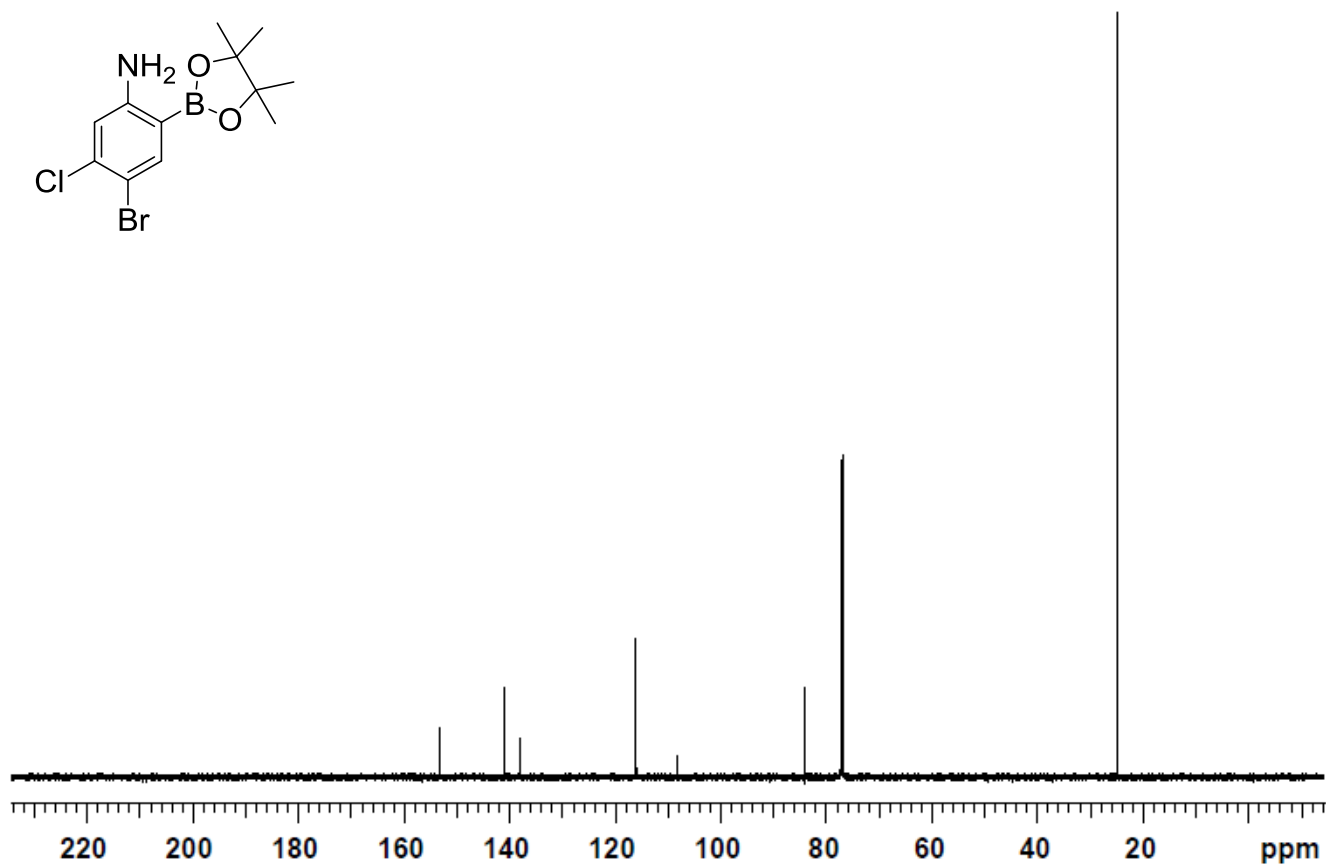
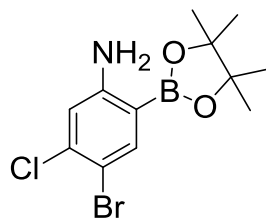


$^1\text{H}$  NMR (500 MHz,  $\text{CDCl}_3$ ) 4-bromo-5-chloro-2-(4,4,5,5-tetramethyl-1,3,2-dioxaborolan-2-yl)-benzamine (23)

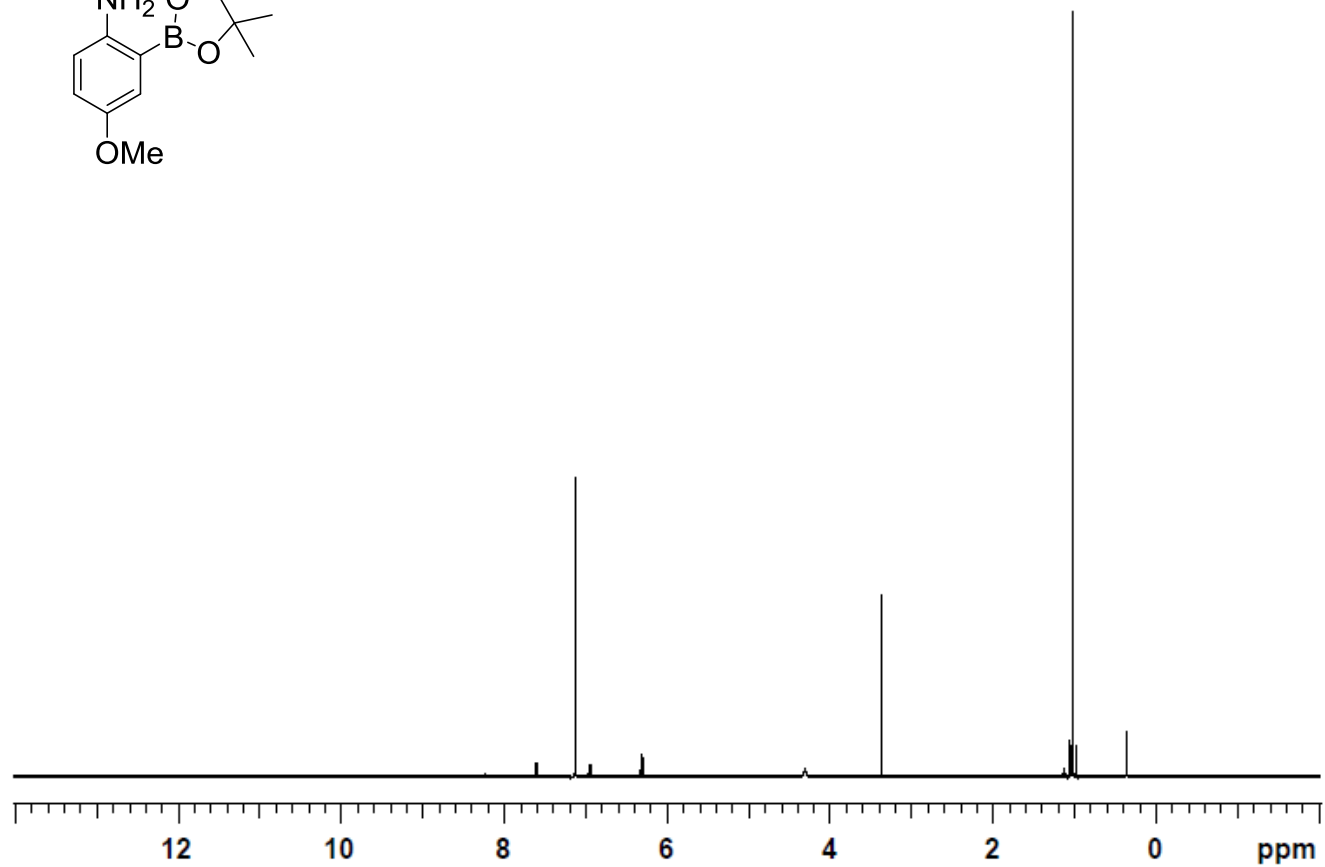
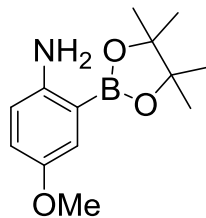




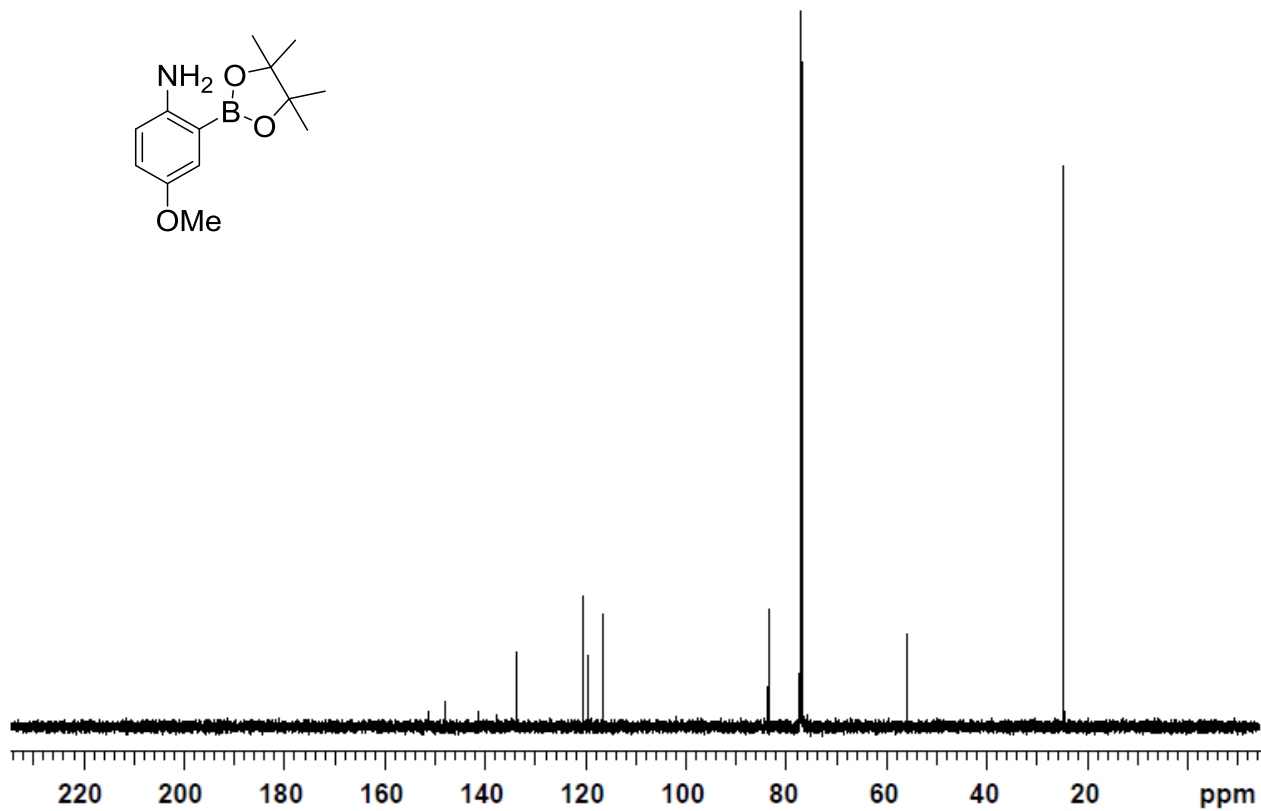
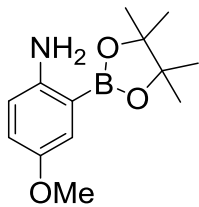
$^{13}\text{C}$  NMR (125 MHz,  $\text{CDCl}_3$ ) 4-bromo-5-chloro-2-(4,4,5,5-tetramethyl-1,3,2-dioxaborolan-2-yl)-benzamine (23)



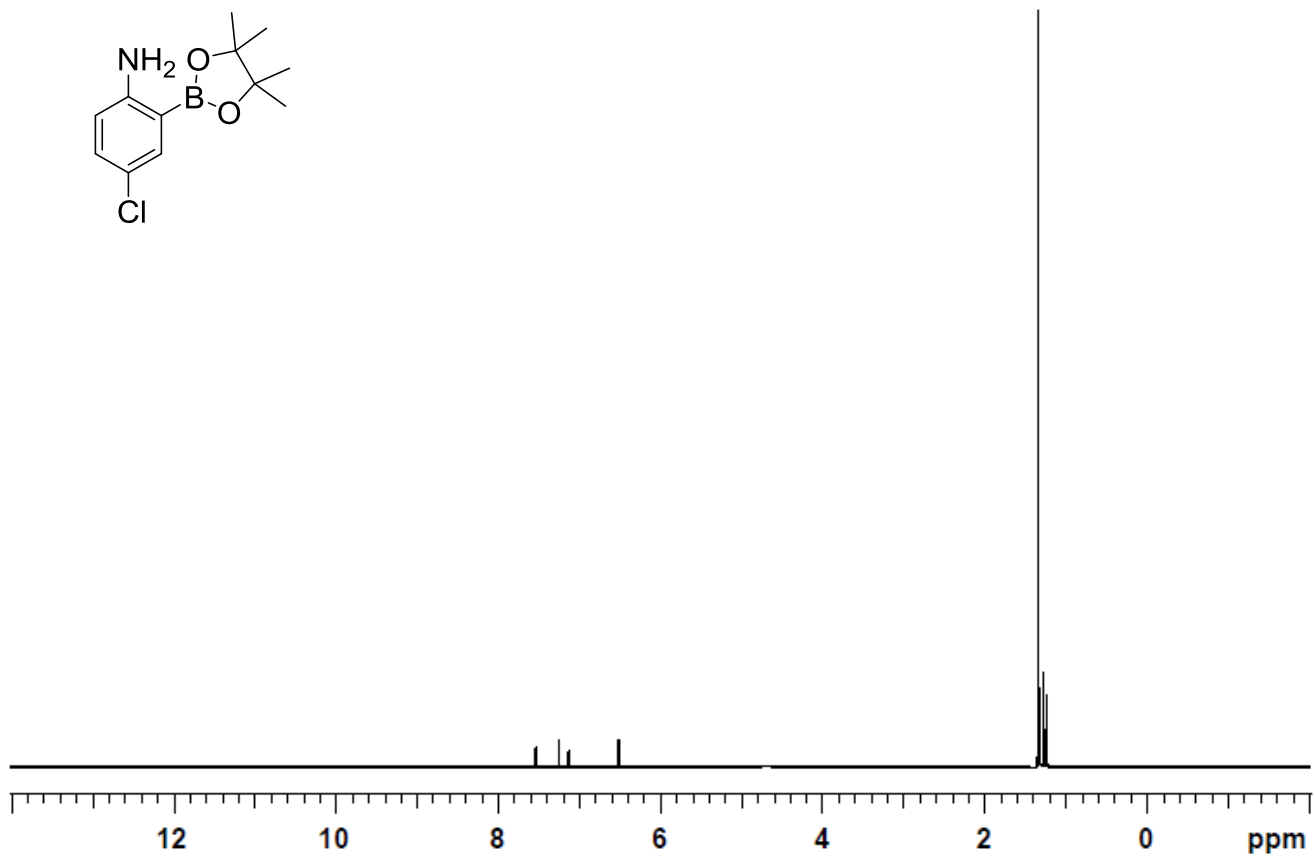
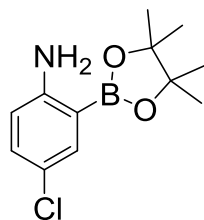
$^1\text{H}$  NMR (500 MHz,  $\text{C}_6\text{D}_6$ ) 4-methoxy-2-(4,4,5,5-tetramethyl-1,3,2-dioxaborolan-2-yl)-benzenamine (24)



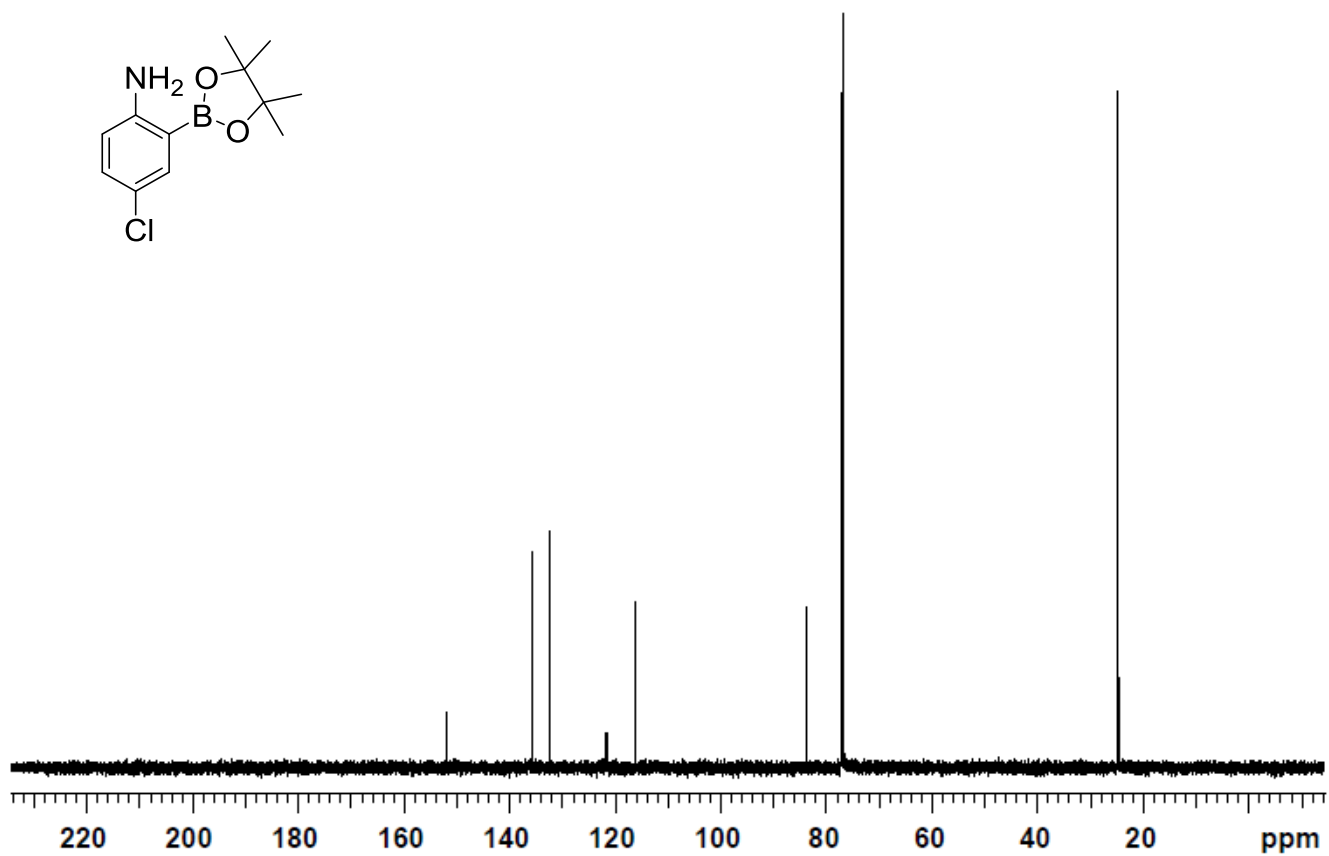
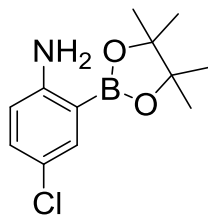
$^{13}\text{C}$  NMR (125 MHz,  $\text{CDCl}_3$ ) 4-methoxy-2-(4,4,5,5-tetramethyl-1,3,2-dioxaborolan-2-yl)-benzenamine (24)



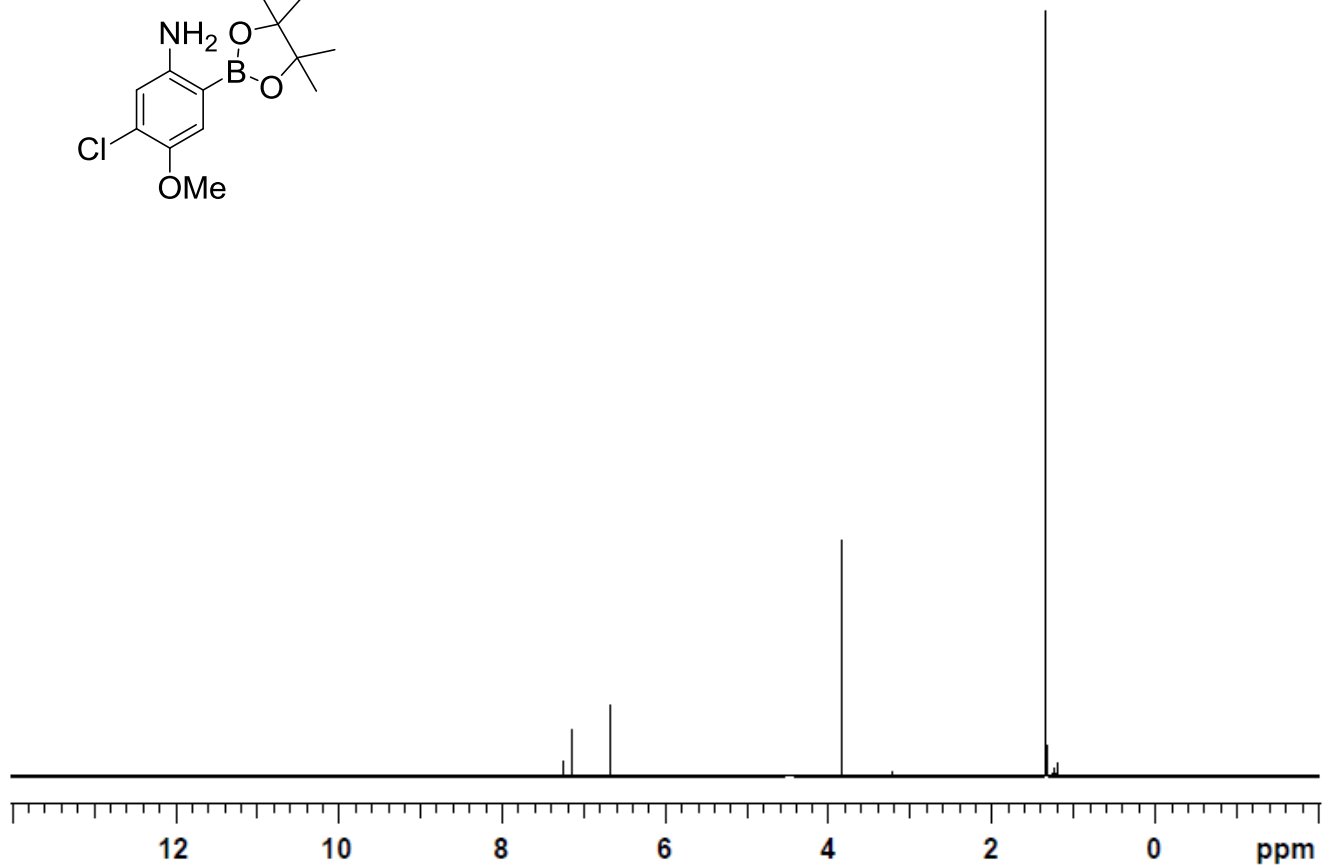
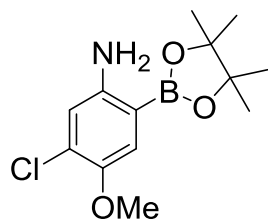
$^1\text{H}$  NMR (500 MHz,  $\text{CDCl}_3$ ) 4-chloro-2-(4,4,5,5-tetramethyl-1,3,2-dioxaborolan-2-yl)-benzenamine (25)



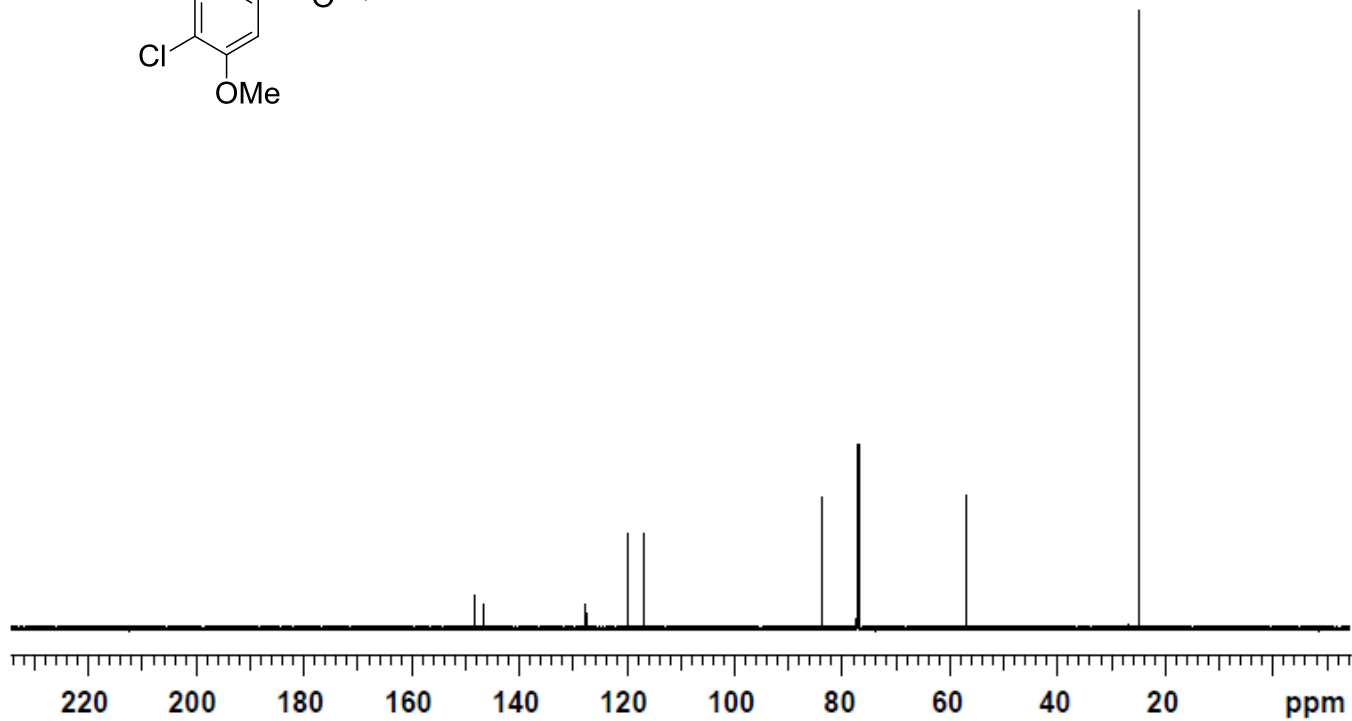
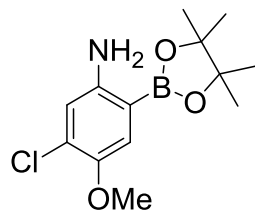
$^{13}\text{C}$  NMR (125 MHz,  $\text{CDCl}_3$ ) 4-chloro-2-(4,4,5,5-tetramethyl-1,3,2-dioxaborolan-2-yl)-benzenamine (25)



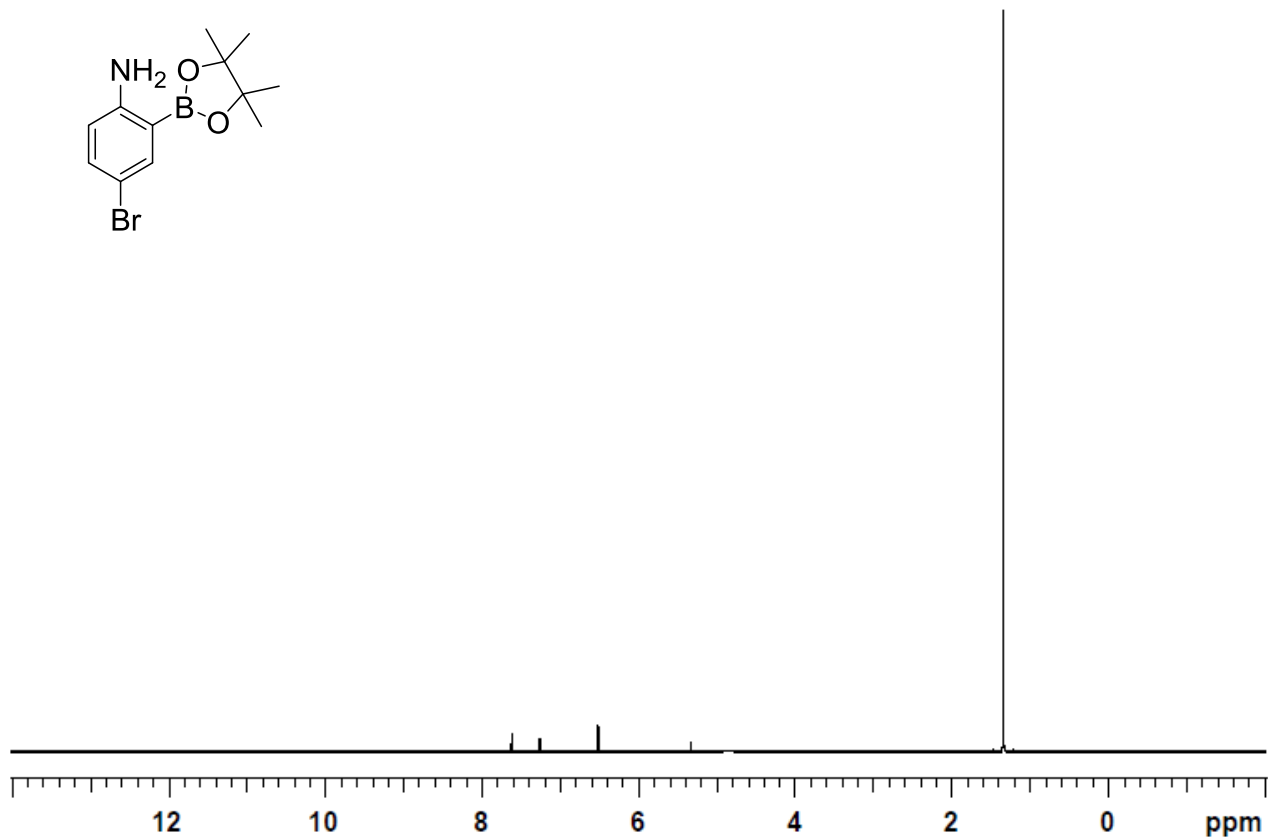
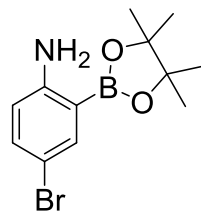
<sup>1</sup>H NMR (500 MHz, CDCl<sub>3</sub>) 5-chloro-4-methoxy-2-(4,4,5,5-tetramethyl-1,3,2-dioxaborolan-2-yl)-benzamine (27)



$^{13}\text{C}$  NMR (125 MHz,  $\text{CDCl}_3$ ) 5-chloro-4-methoxy-2-(4,4,5,5-tetramethyl-1,3,2-dioxaborolan-2-yl)-benzamine (27)

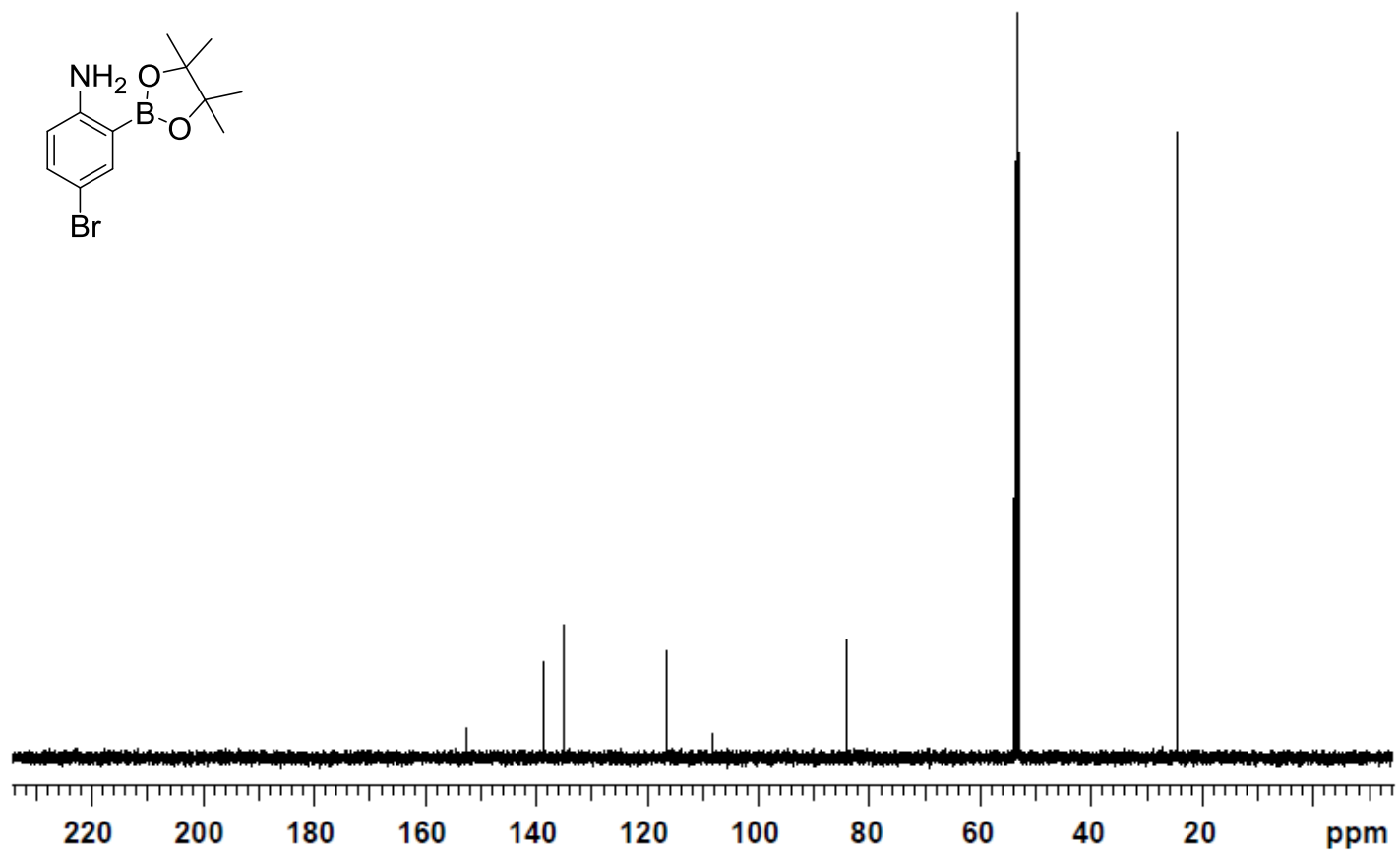
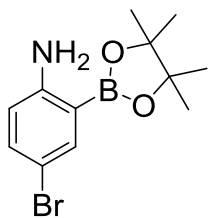


$^1\text{H}$  NMR (500 MHz,  $\text{CD}_2\text{Cl}_2$ ) 4-bromo-2-(4,4,5,5-tetramethyl-1,3,2-dioxaborolan-2-yl)-benzenamine (29)

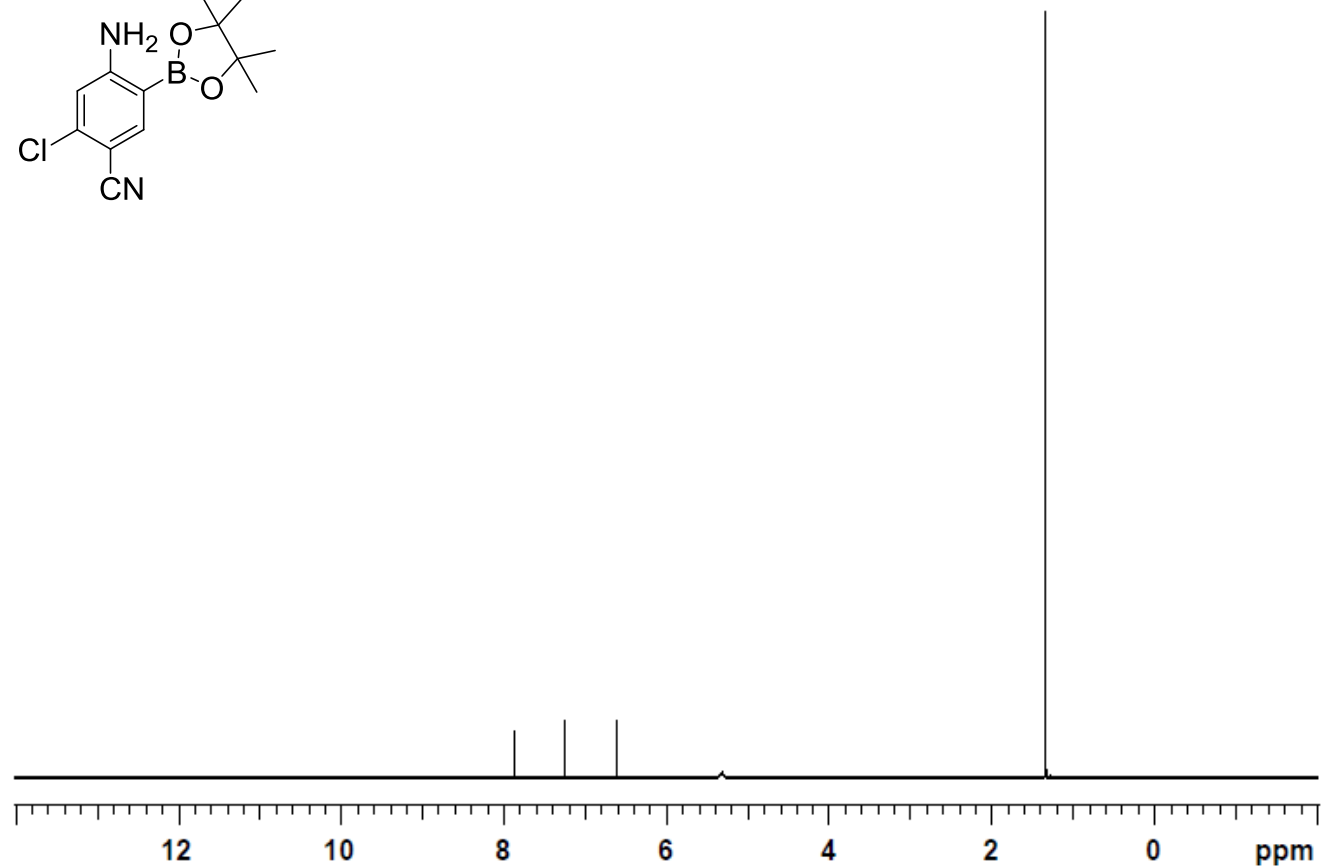
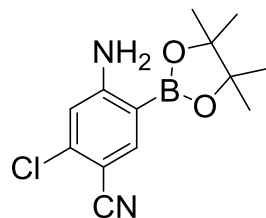




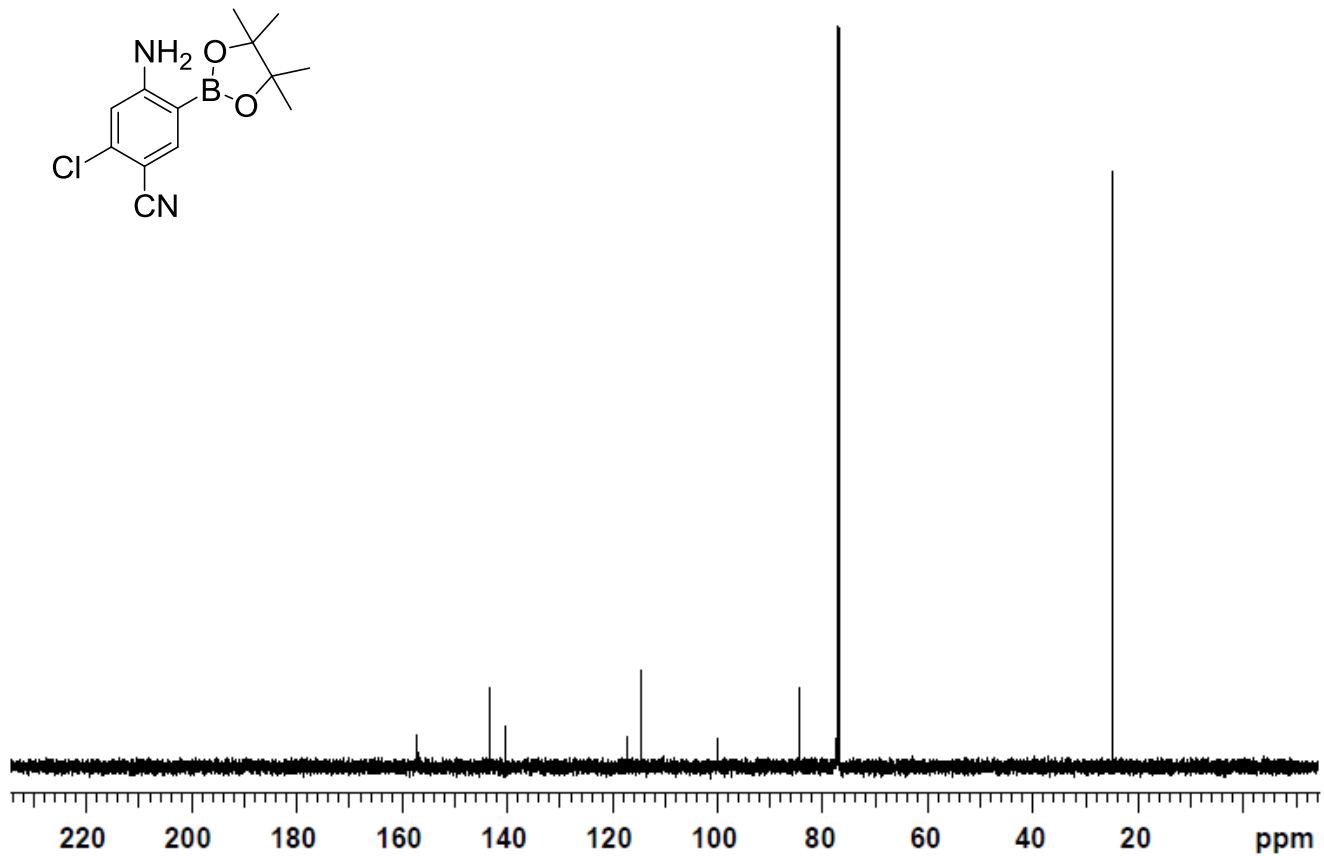
$^{13}\text{C}$  NMR (125 MHz,  $\text{CD}_2\text{Cl}_2$ ) 4-bromo-2-(4,4,5,5-tetramethyl-1,3,2-dioxaborolan-2-yl)-benzenamine (29)



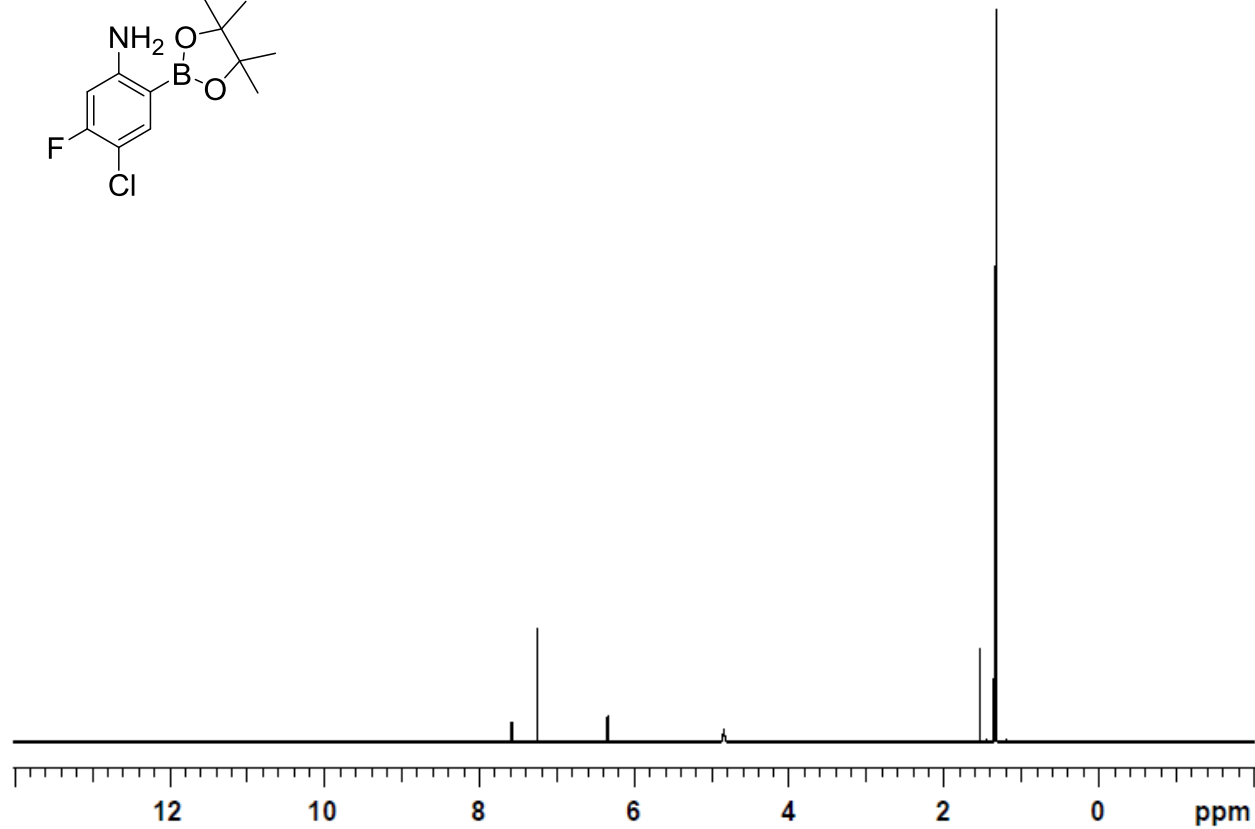
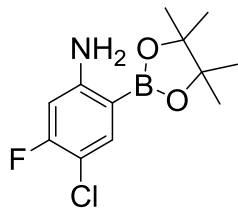
$^1\text{H}$  NMR (500 MHz,  $\text{CDCl}_3$ ) 4-amino-2-chloro-5-(4,4,5,5-tetramethyl-1,3,2-dioxaborolan-2-yl)-benzonitrile (30)



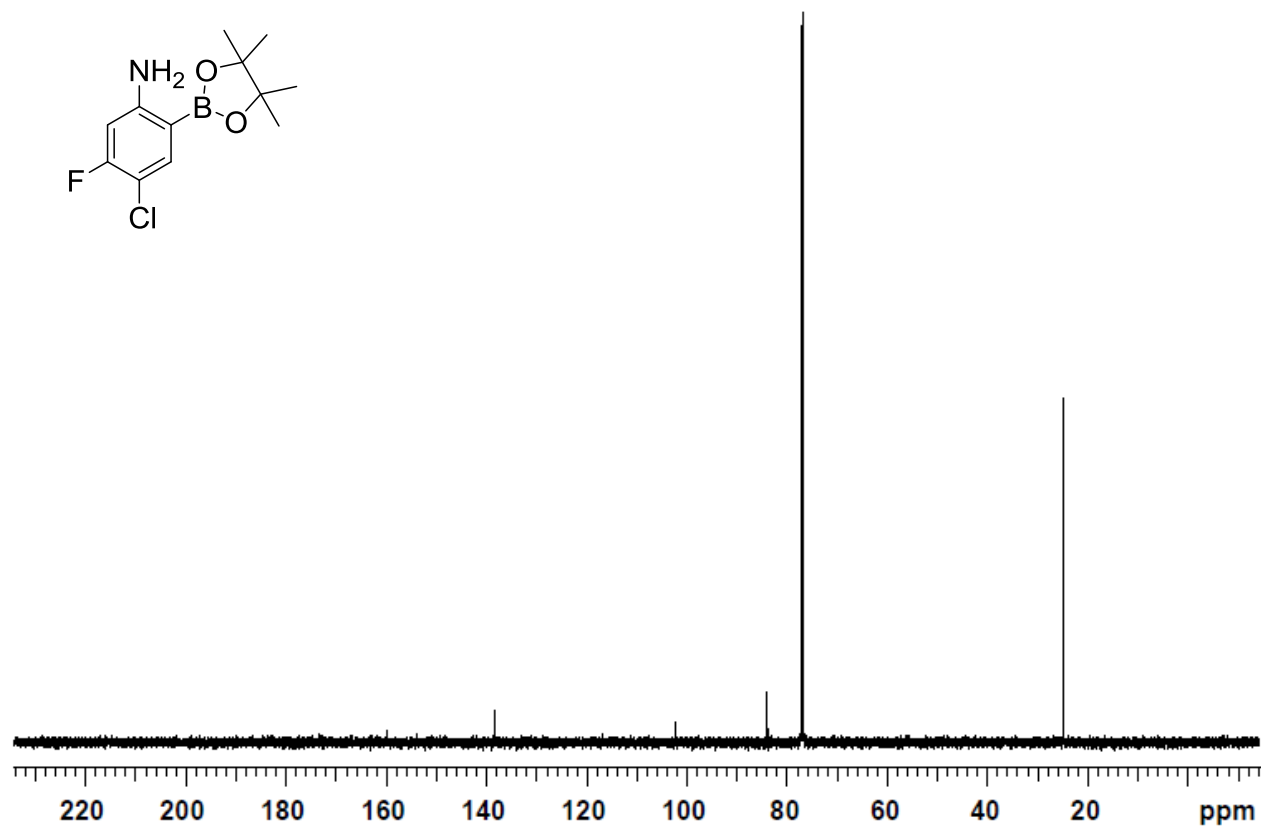
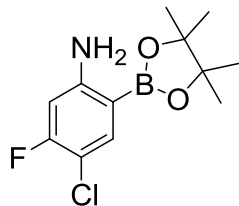
$^{13}\text{C}$  NMR (125 MHz,  $\text{CDCl}_3$ ) 4-amino-2-chloro-5-(4,4,5,5-tetramethyl-1,3,2-dioxaborolan-2-yl)-benzonitrile (30)



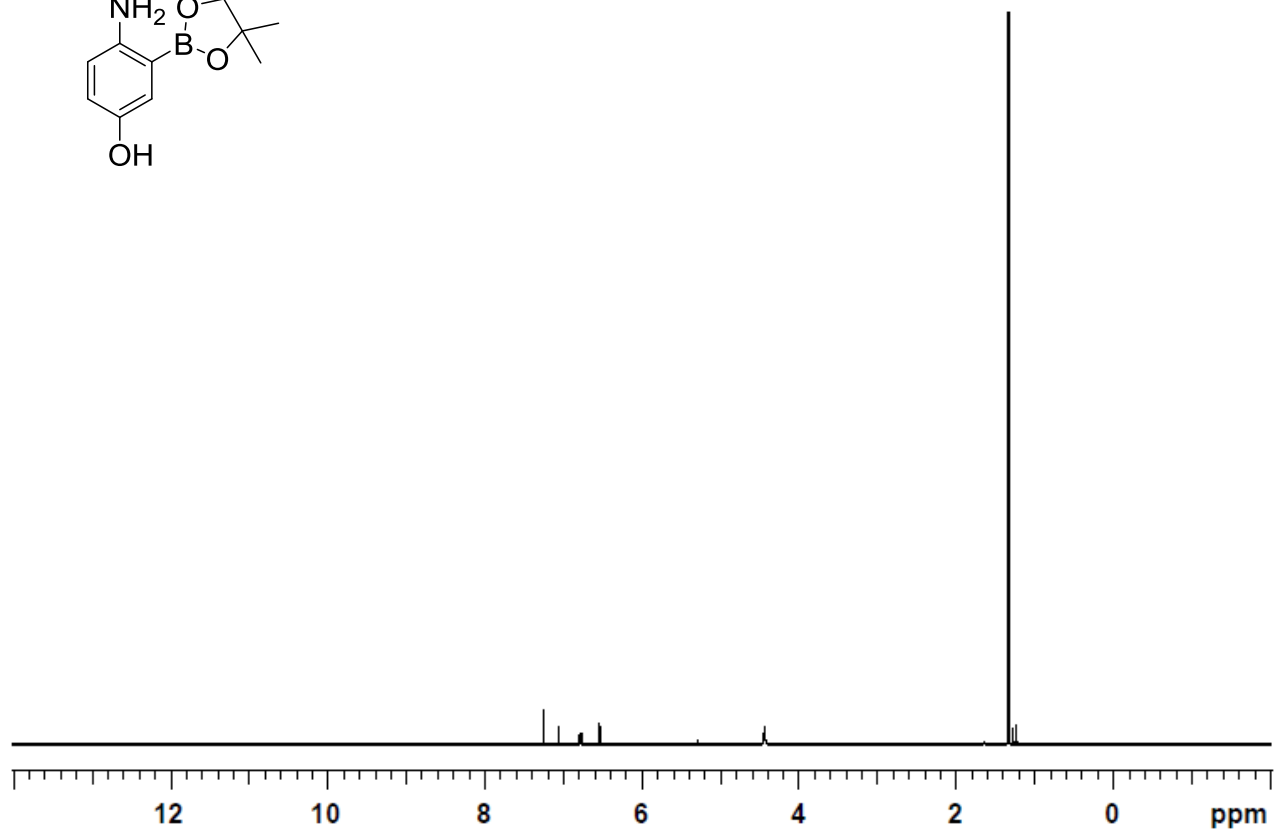
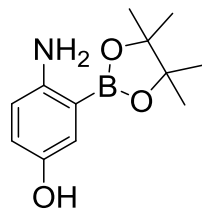
<sup>1</sup>H NMR (500 MHz, CDCl<sub>3</sub>) 4-chloro-5-fluoro-2-(4,4,5,5-tetramethyl-1,3,2-dioxaborolan-2-yl)-benzamine (31)



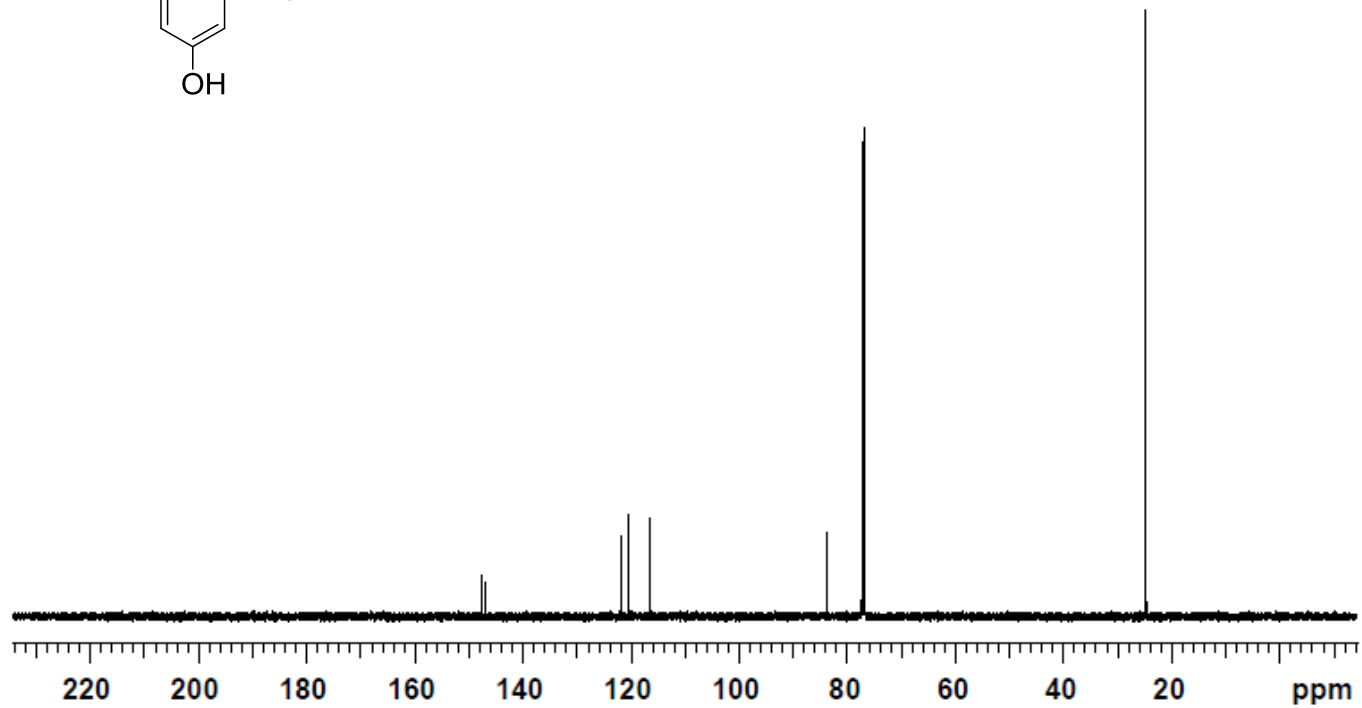
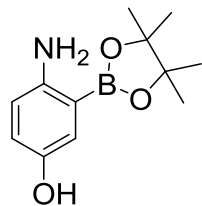
$^{13}\text{C}$  NMR (125 MHz,  $\text{CDCl}_3$ ) 4-chloro-5-fluoro-2-(4,4,5,5-tetramethyl-1,3,2-dioxaborolan-2-yl)-benzamine (31)



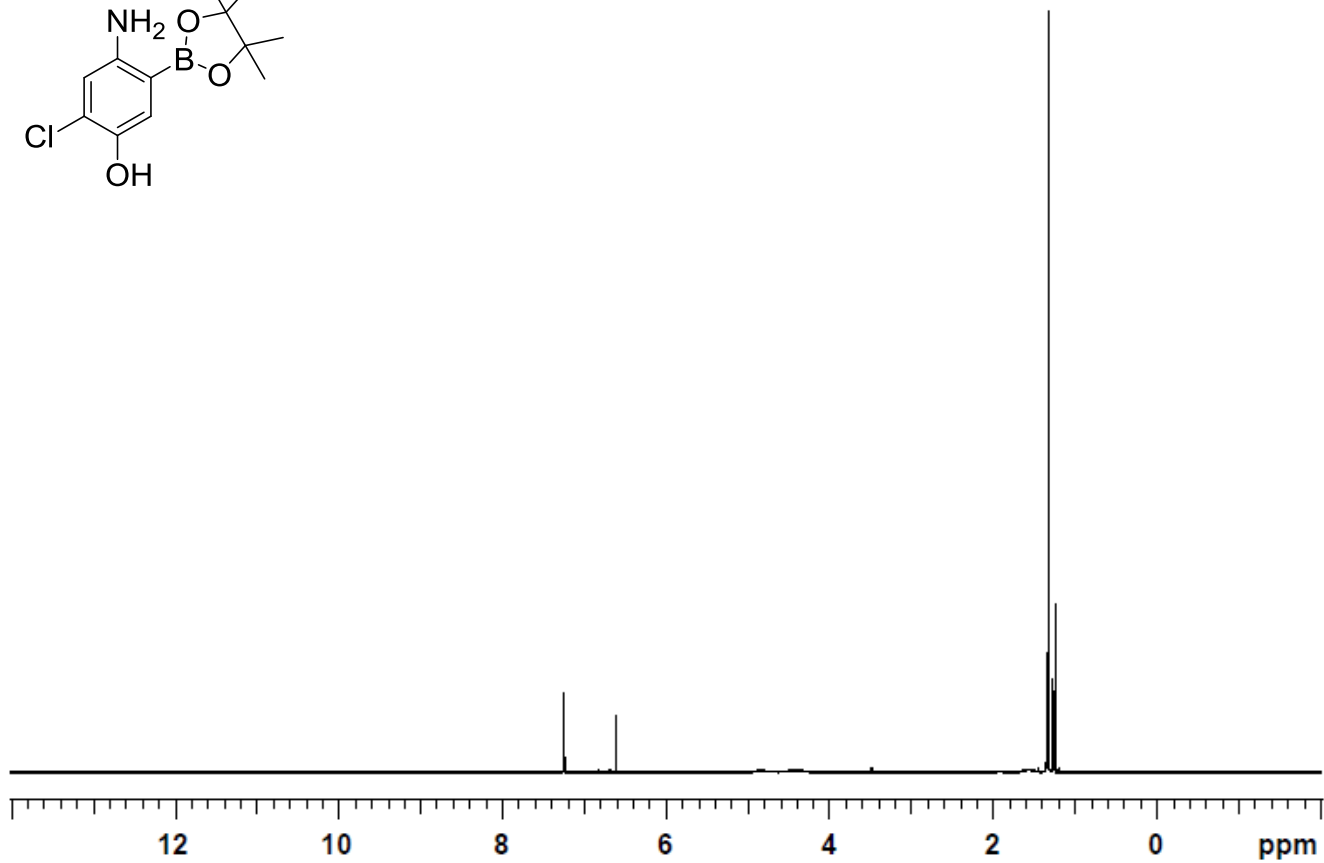
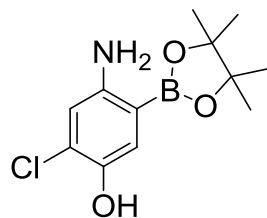
<sup>1</sup>H NMR (500 MHz, CDCl<sub>3</sub>) 4-amino-3-(4,4,5,5-tetramethyl-1,3,2-dioxaborolan-2-yl)-phenol (32)



$^{13}\text{C}$  NMR (125 MHz,  $\text{CDCl}_3$ ) 4-amino-3-(4,4,5,5-tetramethyl-1,3,2-dioxaborolan-2-yl)-phenol (32)

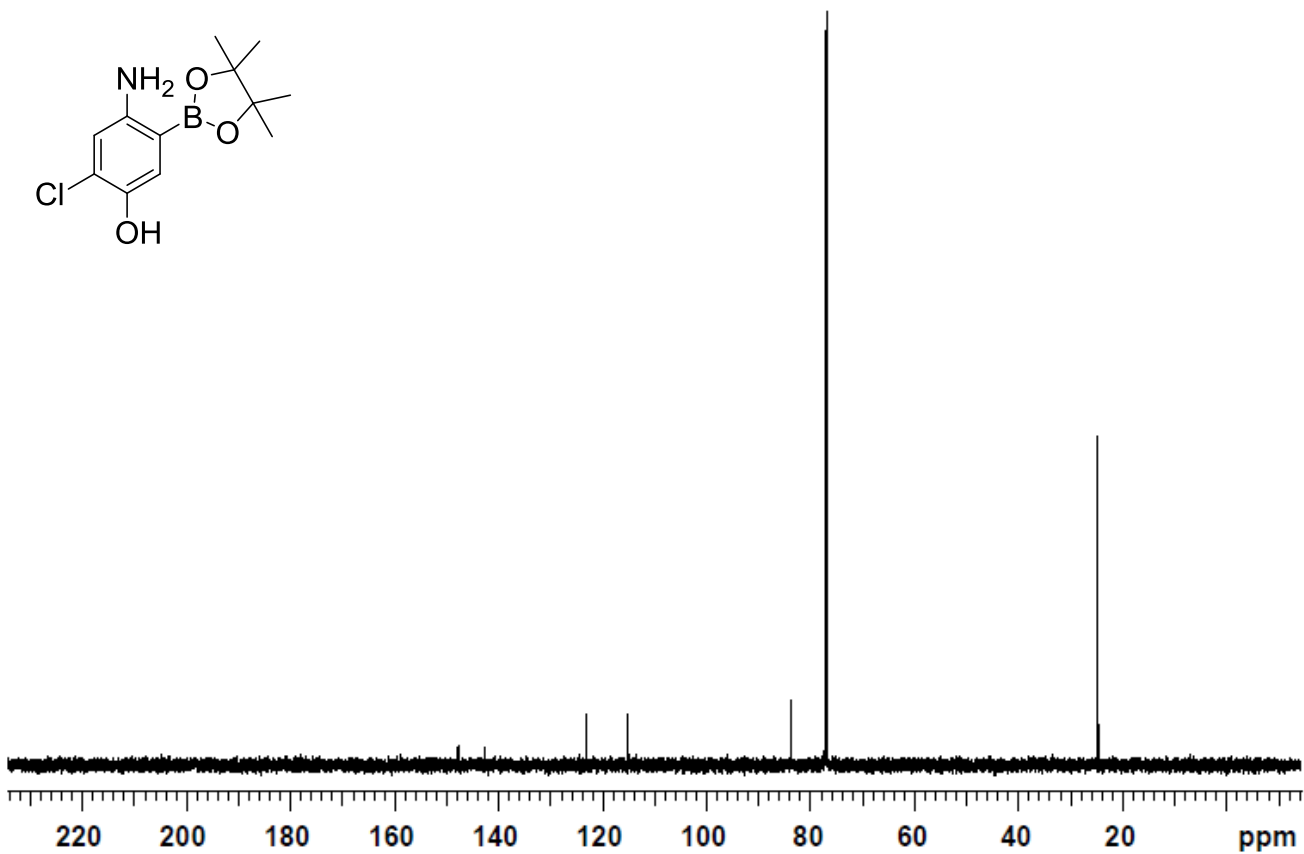


<sup>1</sup>H NMR (500 MHz, CDCl<sub>3</sub>) 4-amino-2-chloro-5-(4,4,5,5-tetramethyl-1,3,2-dioxaborolan-2-yl)-phenol (33)

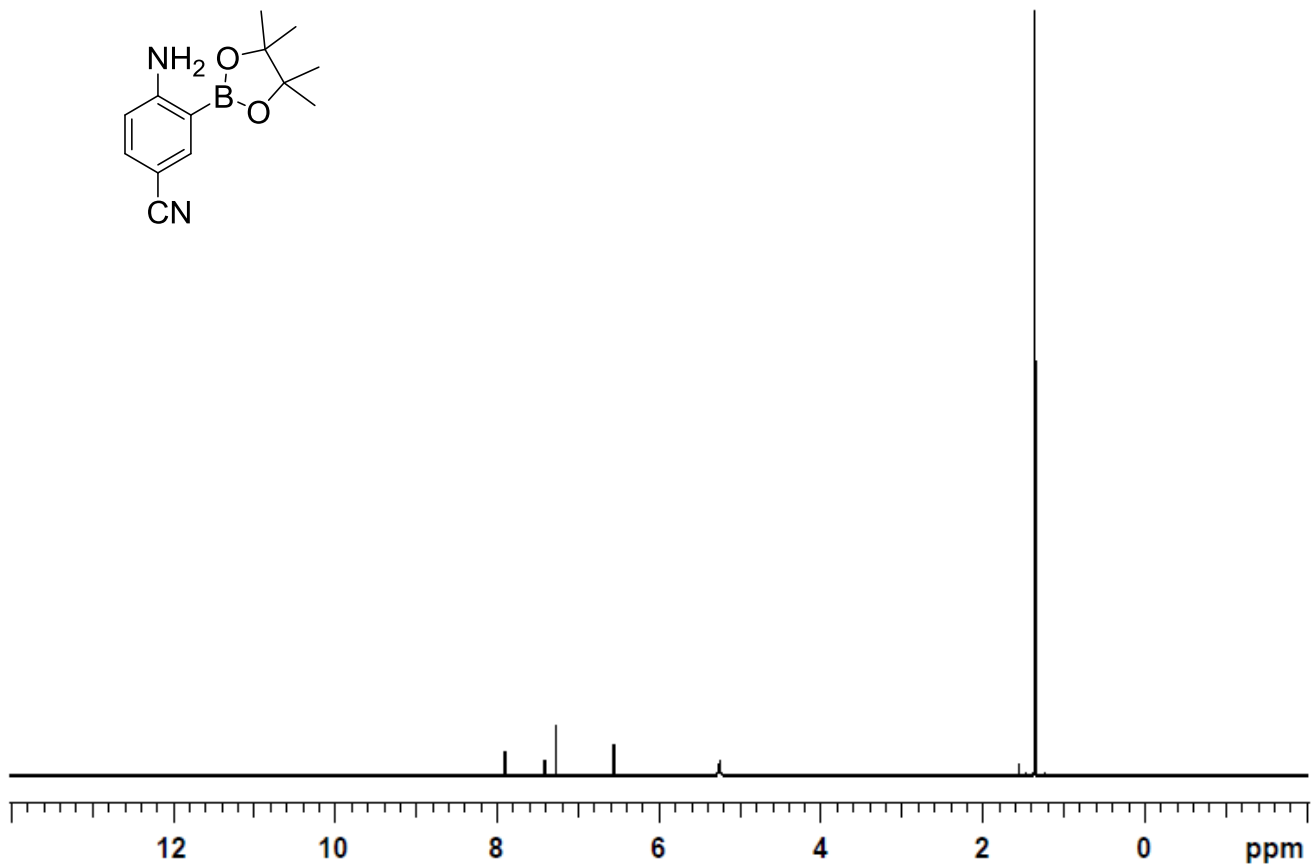
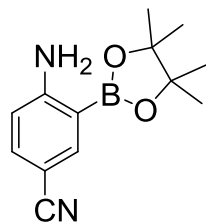




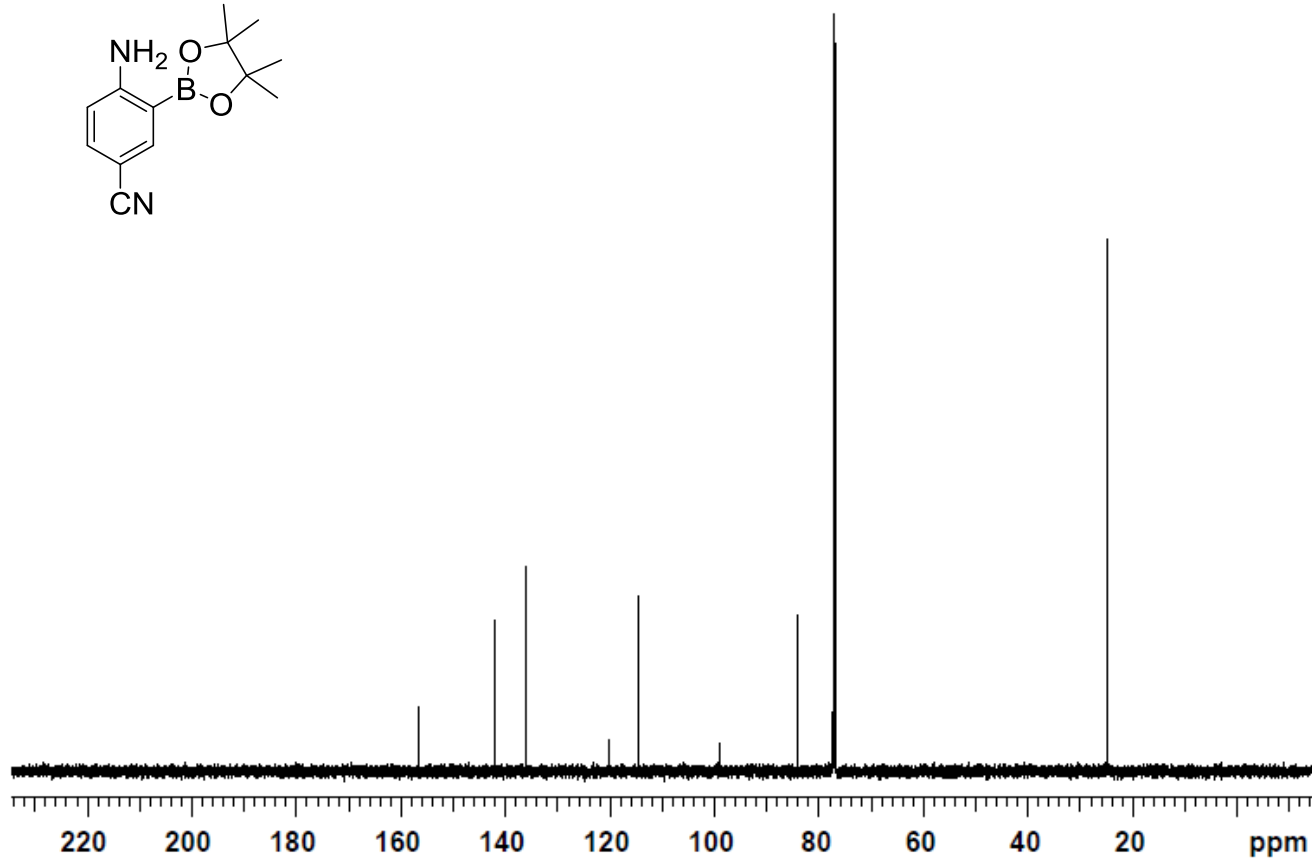
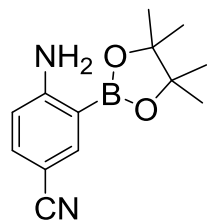
$^{13}\text{C}$  NMR (125 MHz,  $\text{CDCl}_3$ ) 4-amino-2-chloro-5-(4,4,5,5-tetramethyl-1,3,2-dioxaborolan-2-yl)-phenol (33)



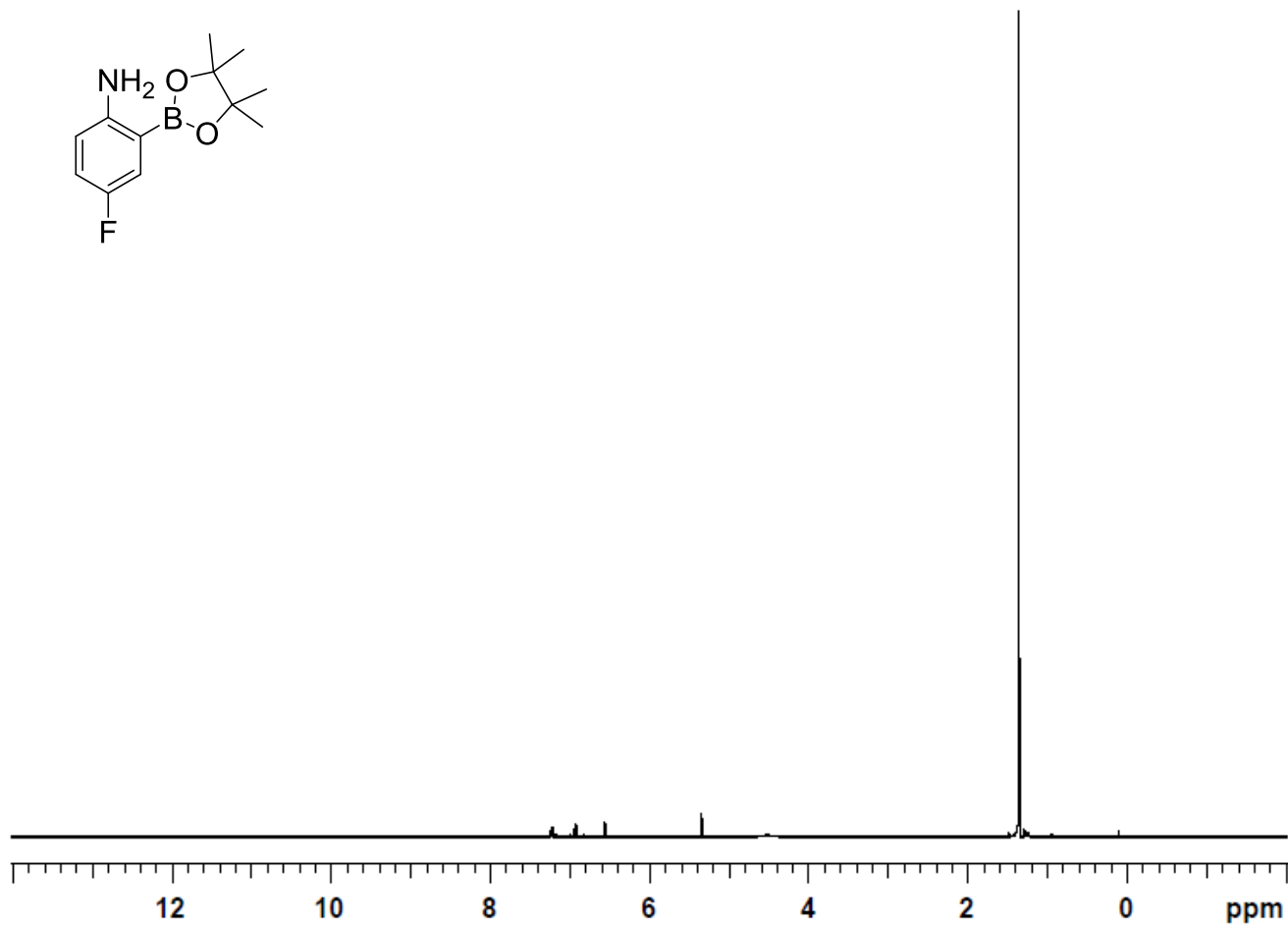
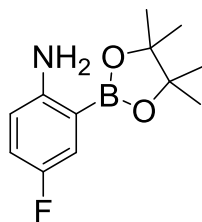
<sup>1</sup>H NMR (500 MHz, CDCl<sub>3</sub>) 4-amino-3-(4,4,5,5-tetramethyl-1,3,2-dioxaborolan-2-yl)benzonitrile (34)



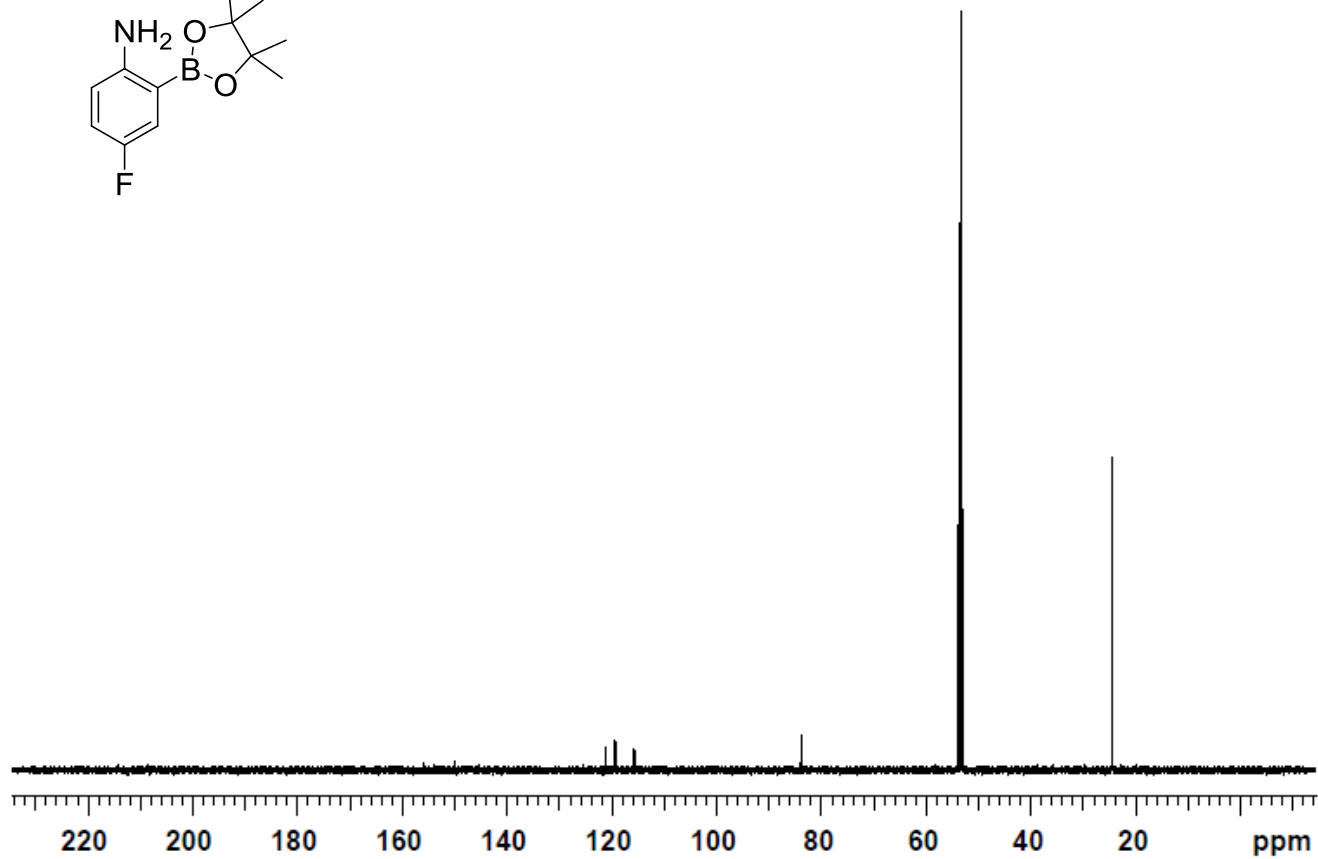
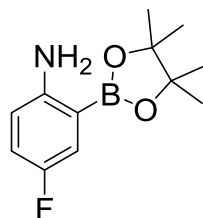
$^{13}\text{C}$  NMR (125 MHz,  $\text{CDCl}_3$ ) 4-amino-3-(4,4,5,5-tetramethyl-1,3,2-dioxaborolan-2-yl)benzonitrile (34)



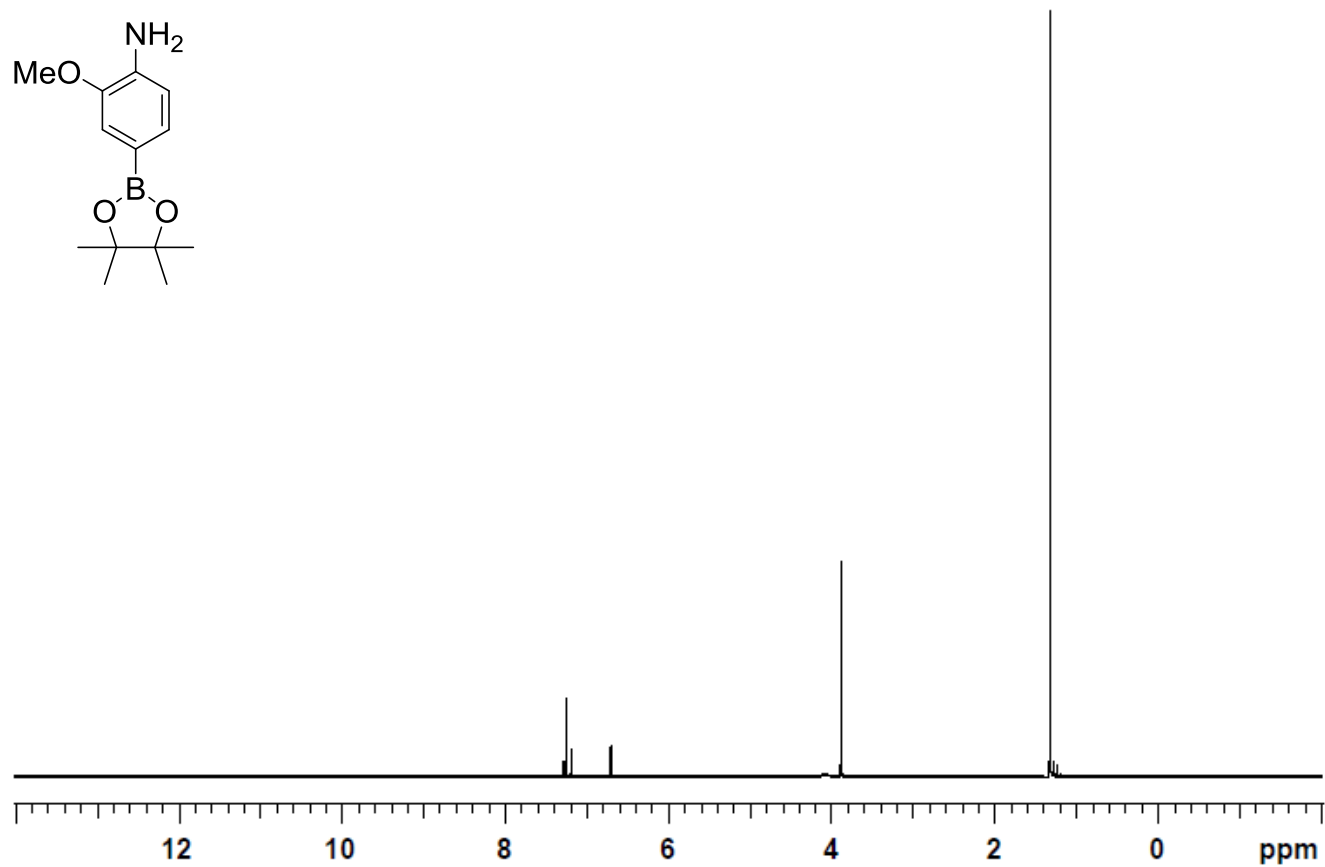
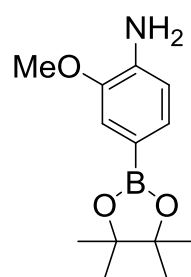
$^1\text{H}$  NMR (500 MHz,  $\text{CD}_2\text{Cl}_2$ ) 4-fluoro-2-(4,4,5,5-tetramethyl-1,3,2-dioxaborolan-2-yl)-benzamine (35)



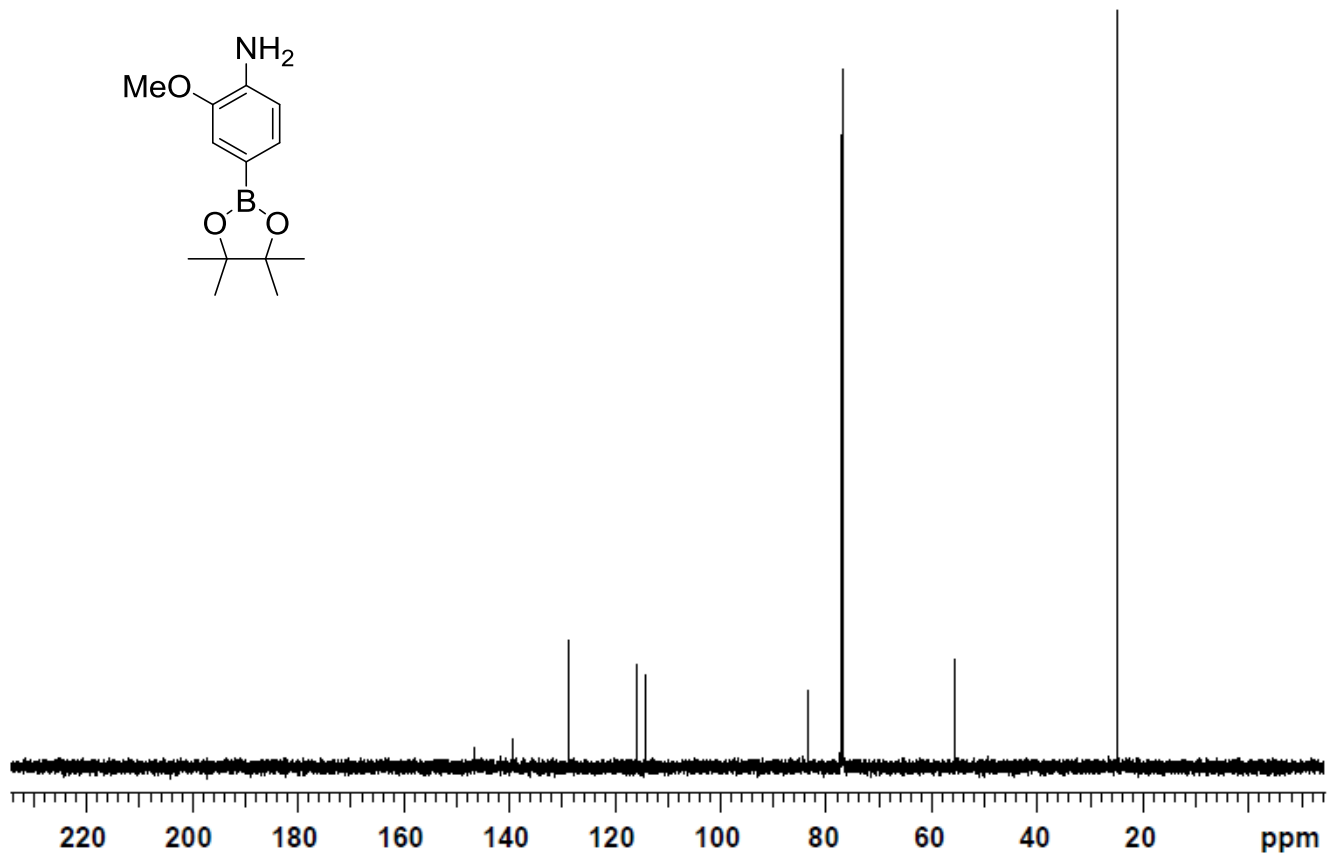
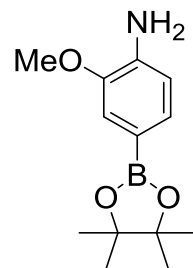
$^{13}\text{C}$  NMR (125 MHz,  $\text{CD}_2\text{Cl}_2$ ) 4-fluoro-2-(4,4,5,5-tetramethyl-1,3,2-dioxaborolan-2-yl)-benzamine (35)



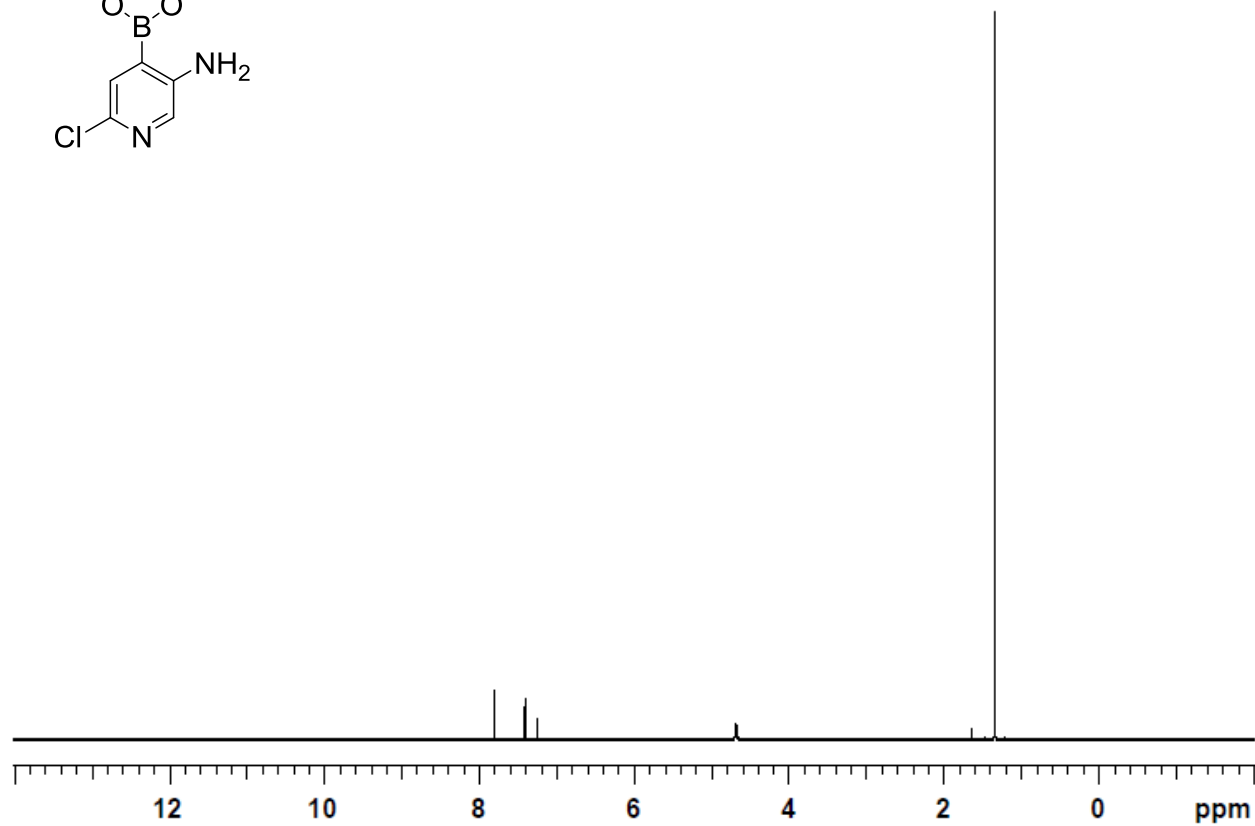
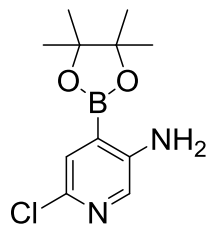
$^1\text{H}$  NMR (500 MHz,  $\text{CDCl}_3$ ) 2-methoxy-4-(4,4,5,5-tetramethyl-1,3,2-dioxaborolan-2-yl)-benzenamine (37)



$^{13}\text{C}$  NMR (125 MHz,  $\text{CDCl}_3$ ) 2-methoxy-4-(4,4,5,5-tetramethyl-1,3,2-dioxaborolan-2-yl)-benzenamine (37)

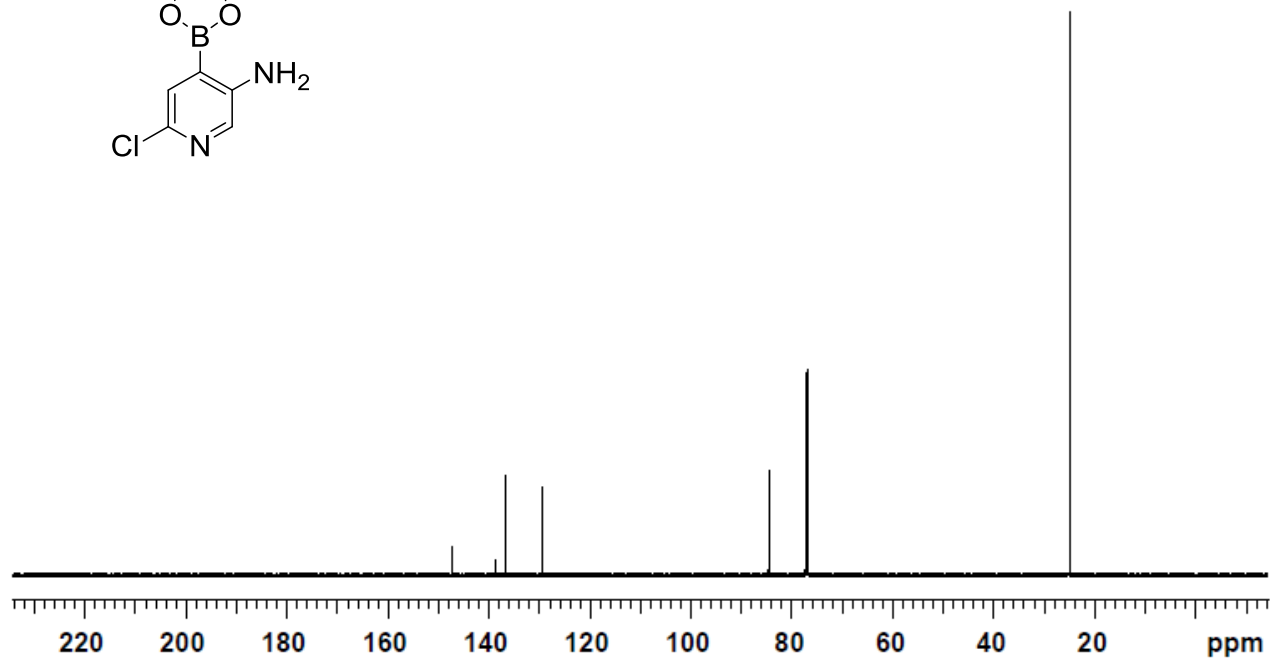
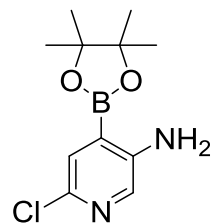


<sup>1</sup>H NMR (500 MHz, CDCl<sub>3</sub>) 5-amino-2-chloro-4-(4,4,5,5-tetramethyl-1,3,2-dioxaborolan-2-yl)-pyridine (38)

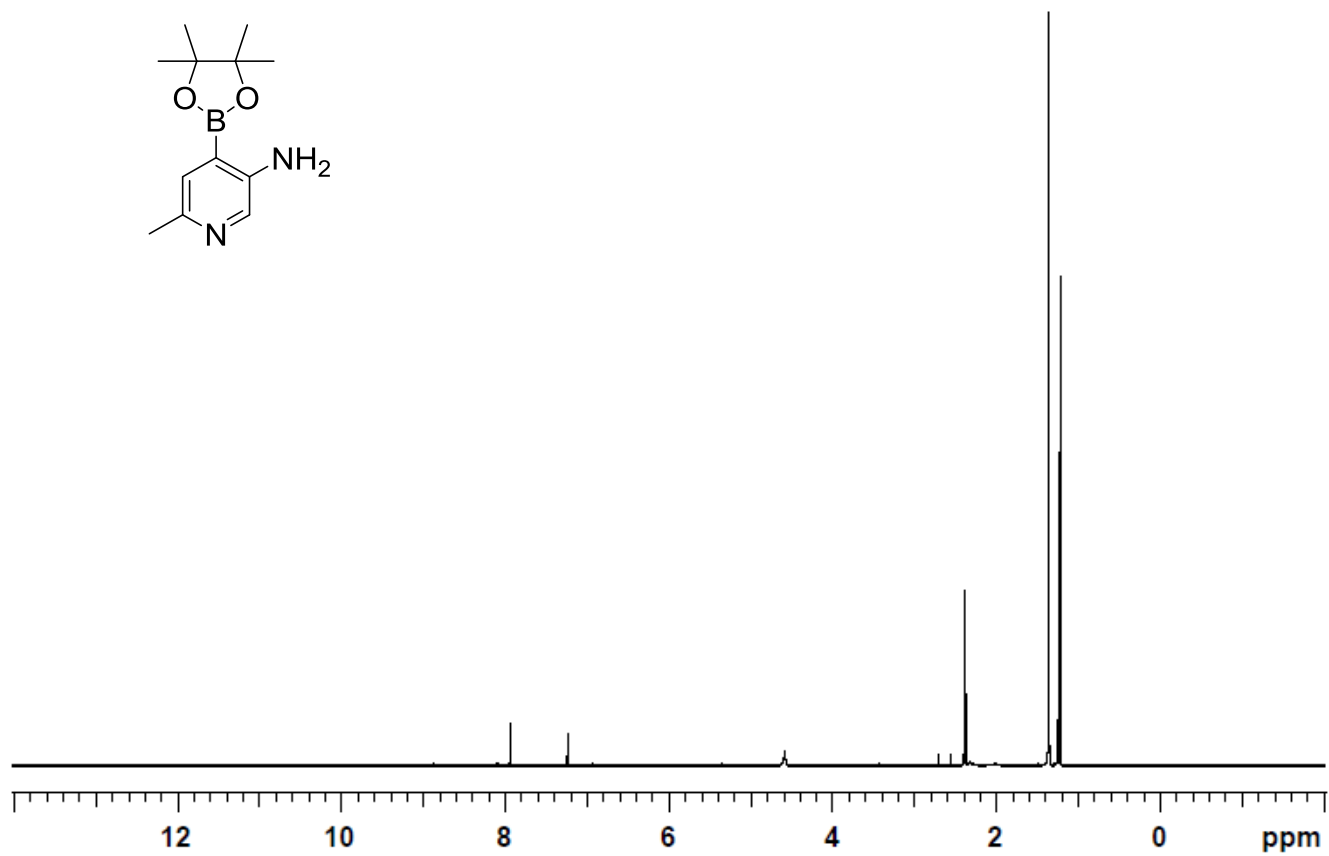
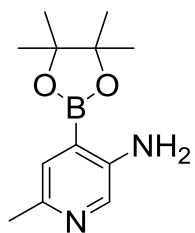




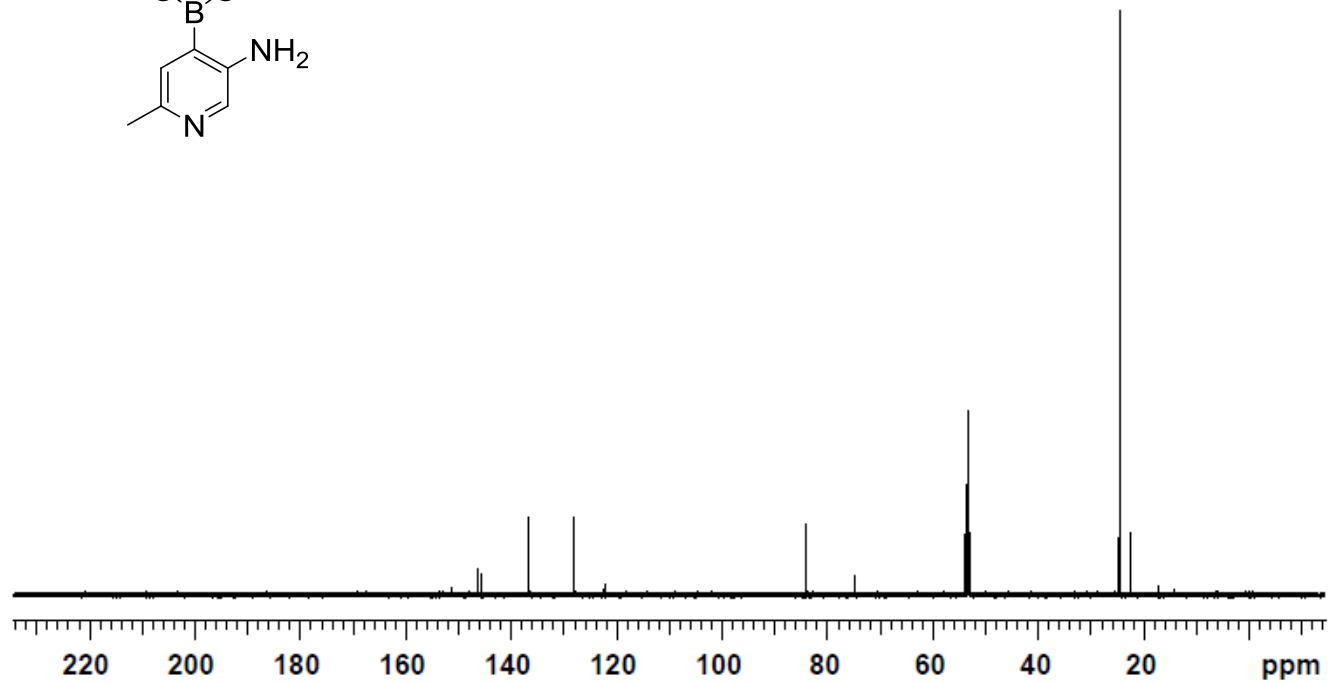
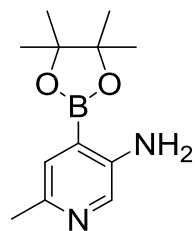
$^{13}\text{C}$  NMR (125 MHz,  $\text{CDCl}_3$ ) 5-amino-2-chloro-4-(4,4,5,5-tetramethyl-1,3,2-dioxaborolan-2-yl)-pyridine (38)



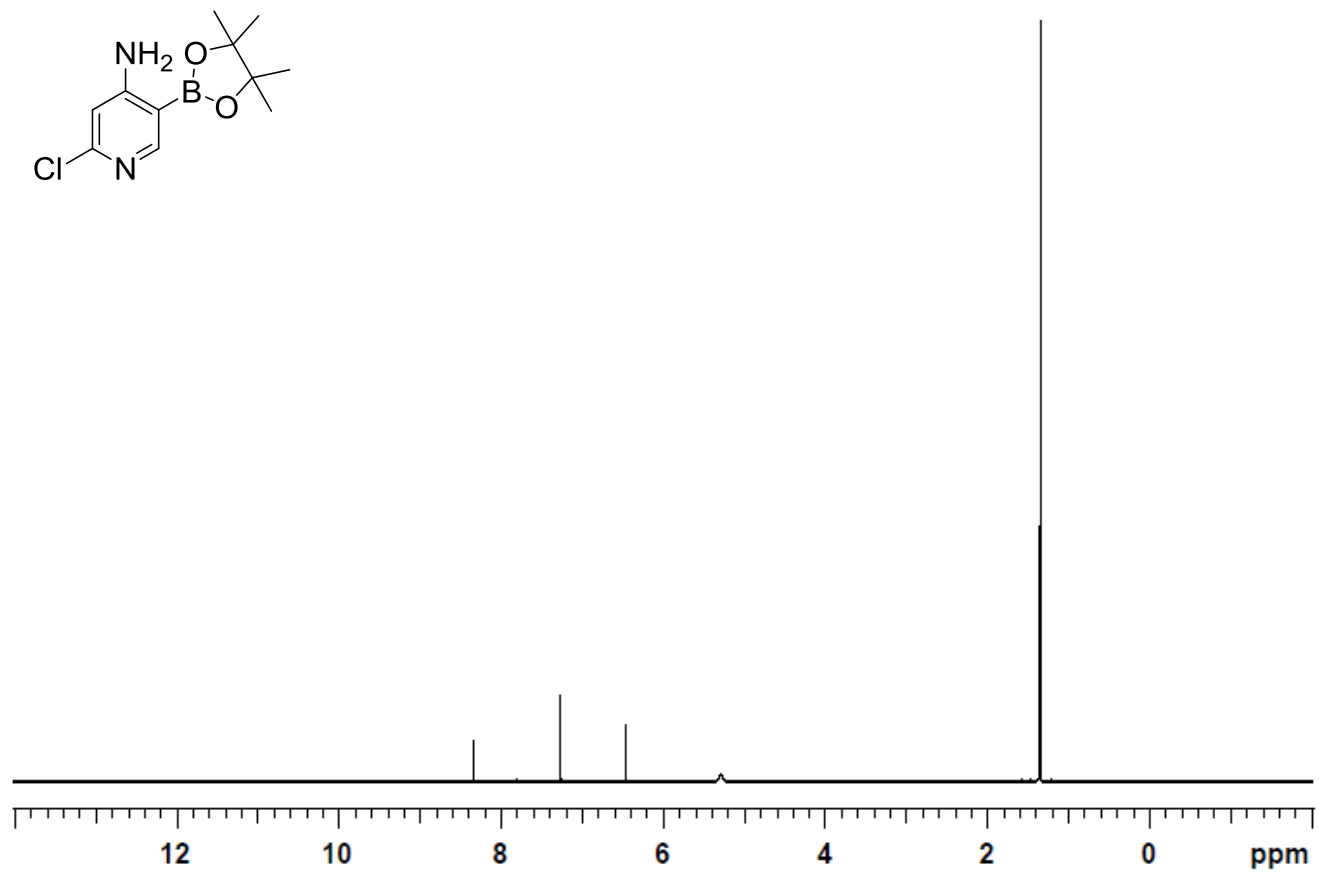
$^1\text{H}$  NMR (500 MHz,  $\text{CD}_2\text{Cl}_2$ ) 5-amino-4-(4,4,5,5-tetramethyl-1,3,2-dioxaborolan-2-yl)-2-methyl pyridine (39)



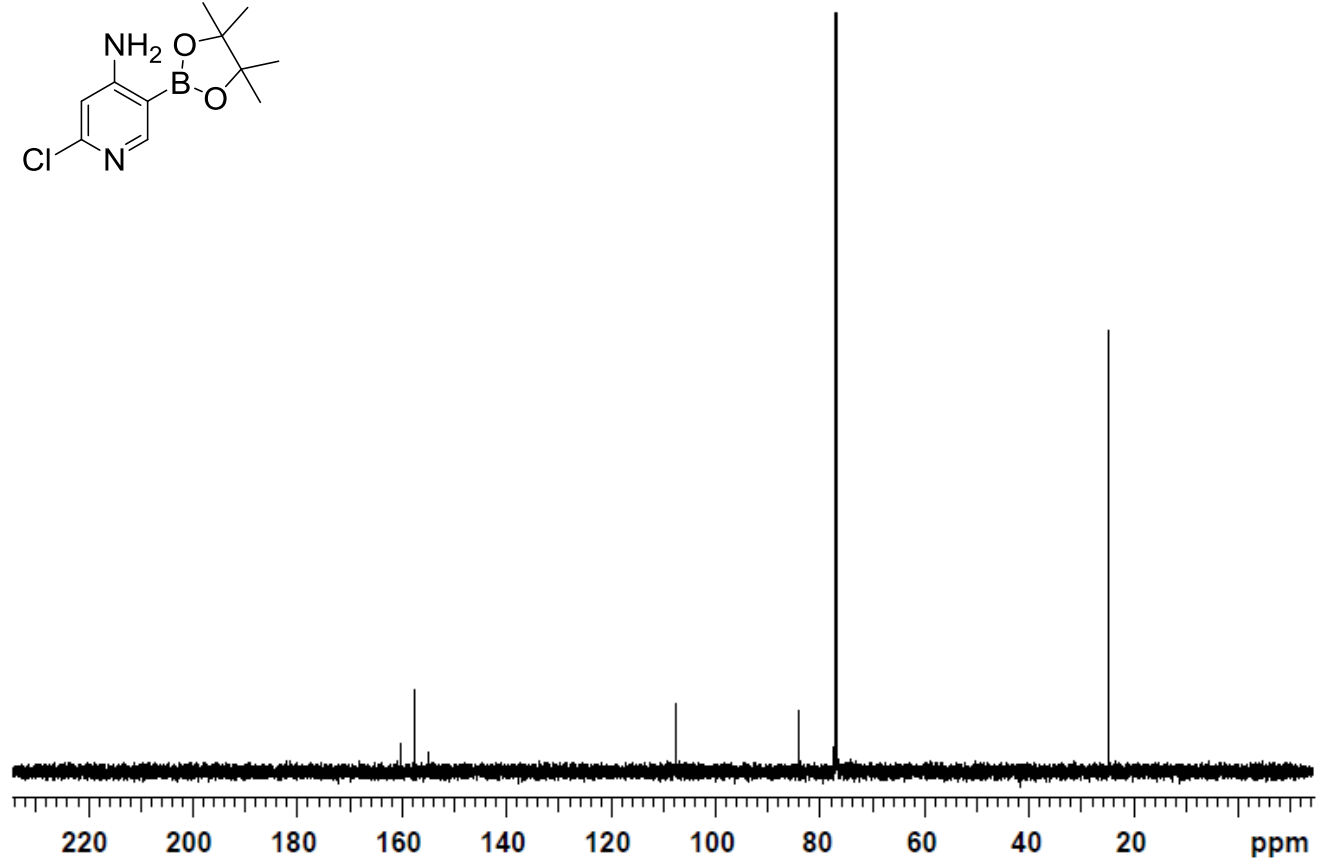
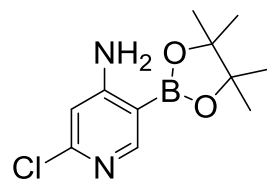
$^{13}\text{C}$  NMR (125 MHz,  $\text{CD}_2\text{Cl}_2$ ) 5-amino-4-(4,4,5,5-tetramethyl-1,3,2-dioxaborolan-2-yl)-2-methyl pyridine (39)



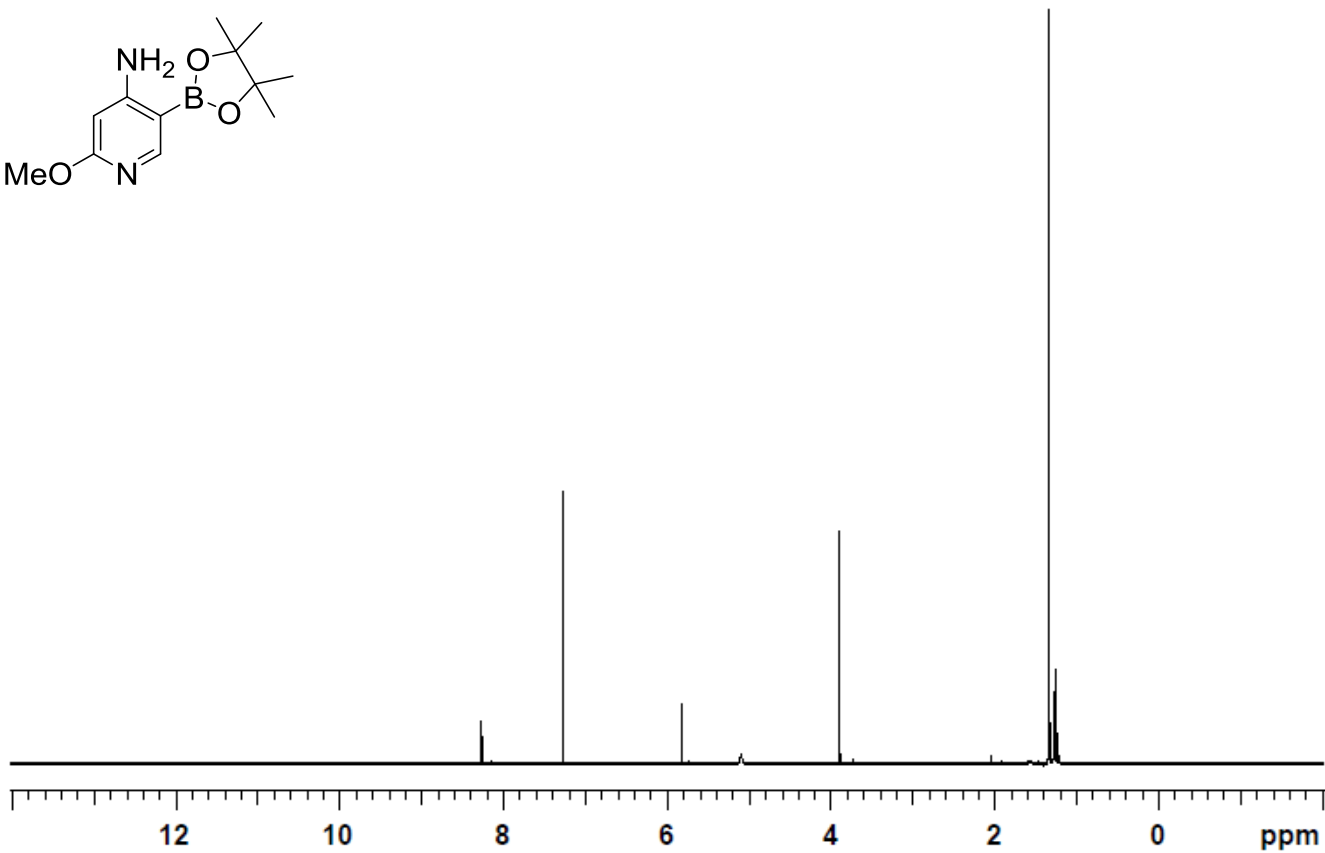
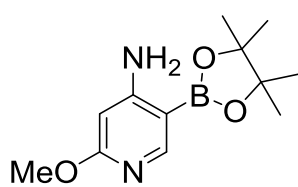
<sup>1</sup>H NMR (500 MHz, CDCl<sub>3</sub>) 2-chloro-5-(4,4,5,5-tetramethyl-1,3,2-dioxaborolan-2-yl)pyridin-4-amine (40)



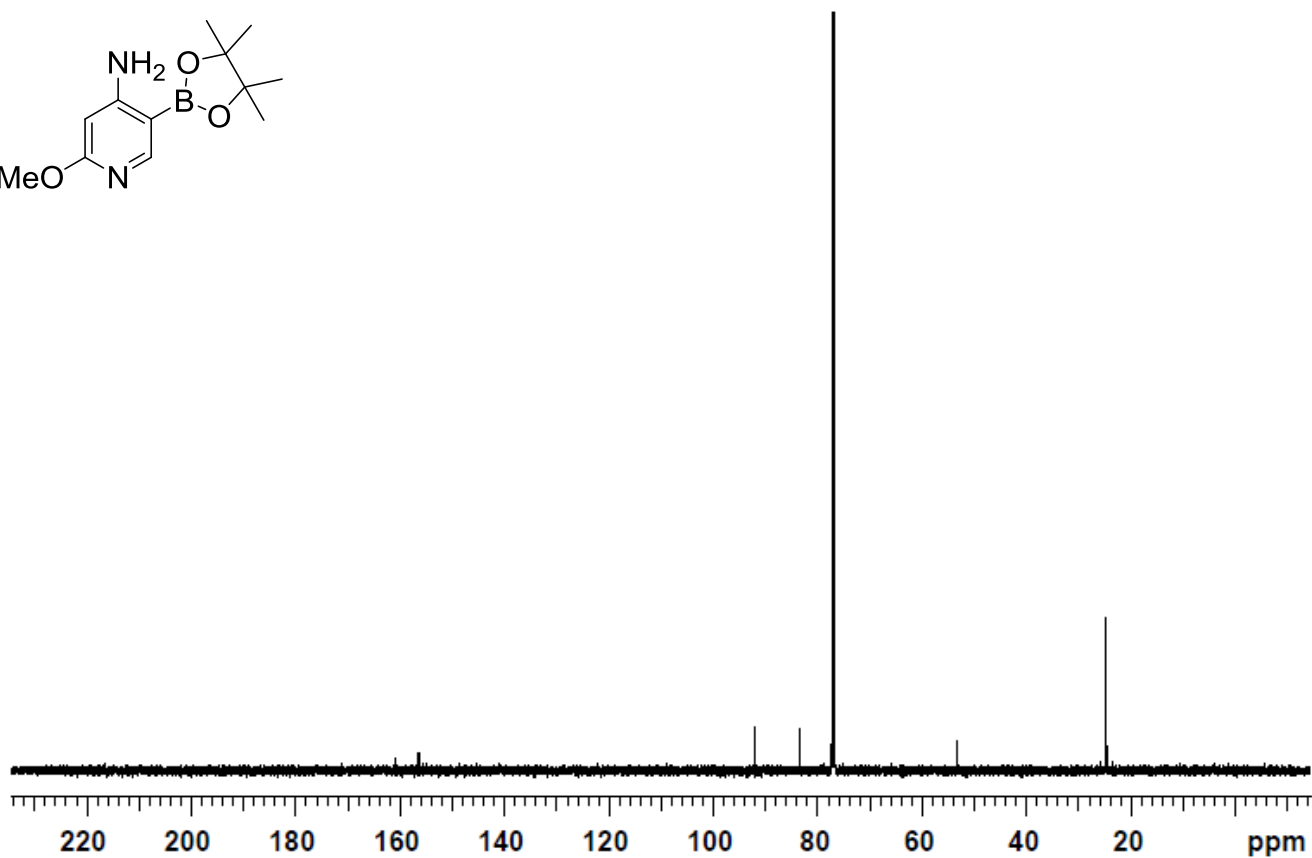
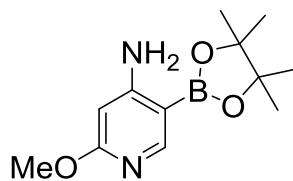
$^{13}\text{C}$  NMR (125 MHz,  $\text{CDCl}_3$ ) 2-chloro-5-(4,4,5,5-tetramethyl-1,3,2-dioxaborolan-2-yl)pyridin-4-amine (40)



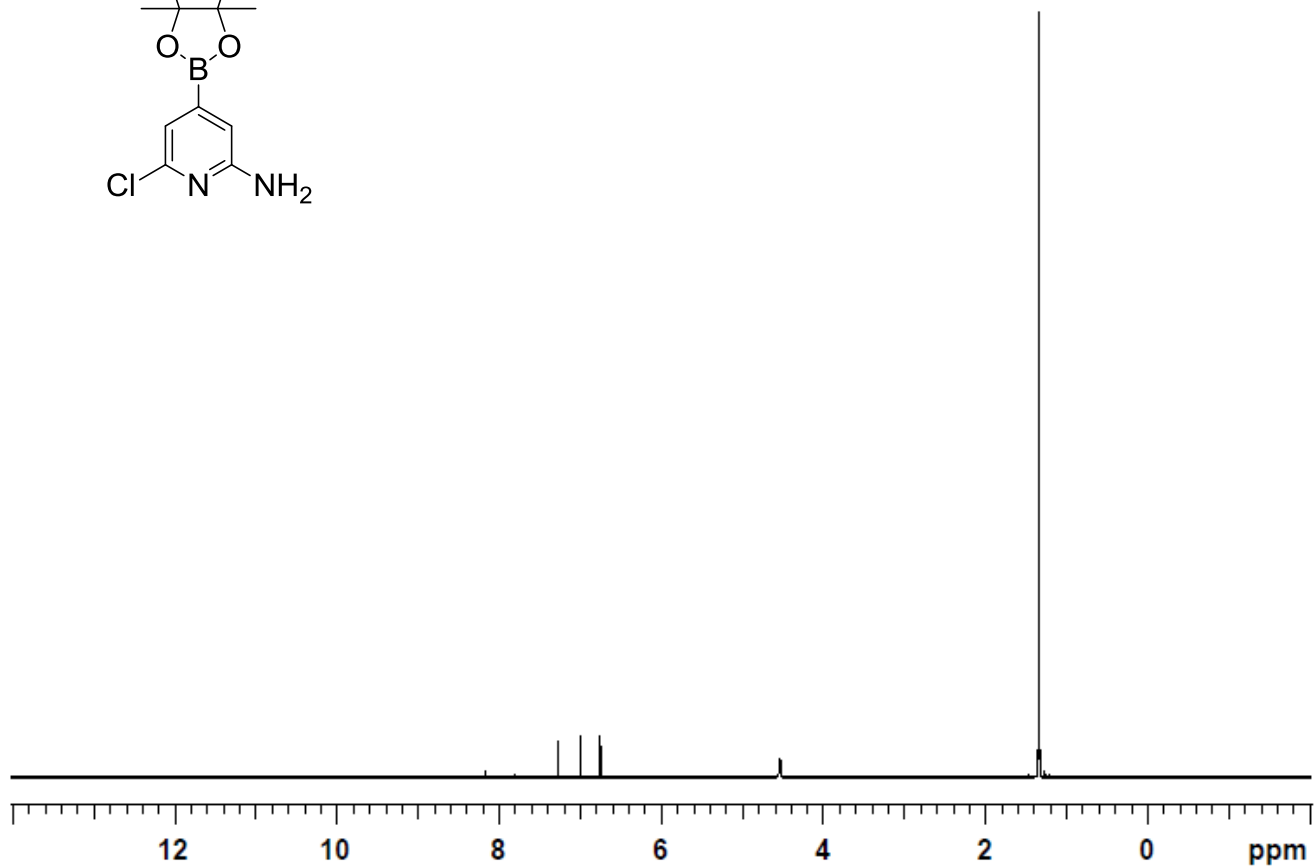
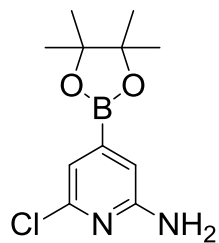
<sup>1</sup>H NMR (500 MHz, CDCl<sub>3</sub>) 2-methoxy-5-(4,4,5,5-tetramethyl-1,3,2-dioxaborolan-2-yl)pyridin-4-amine (41)



$^{13}\text{C}$  NMR (125 MHz,  $\text{CDCl}_3$ ) 2-methoxy-5-(4,4,5,5-tetramethyl-1,3,2-dioxaborolan-2-yl)pyridin-4-amine (41)

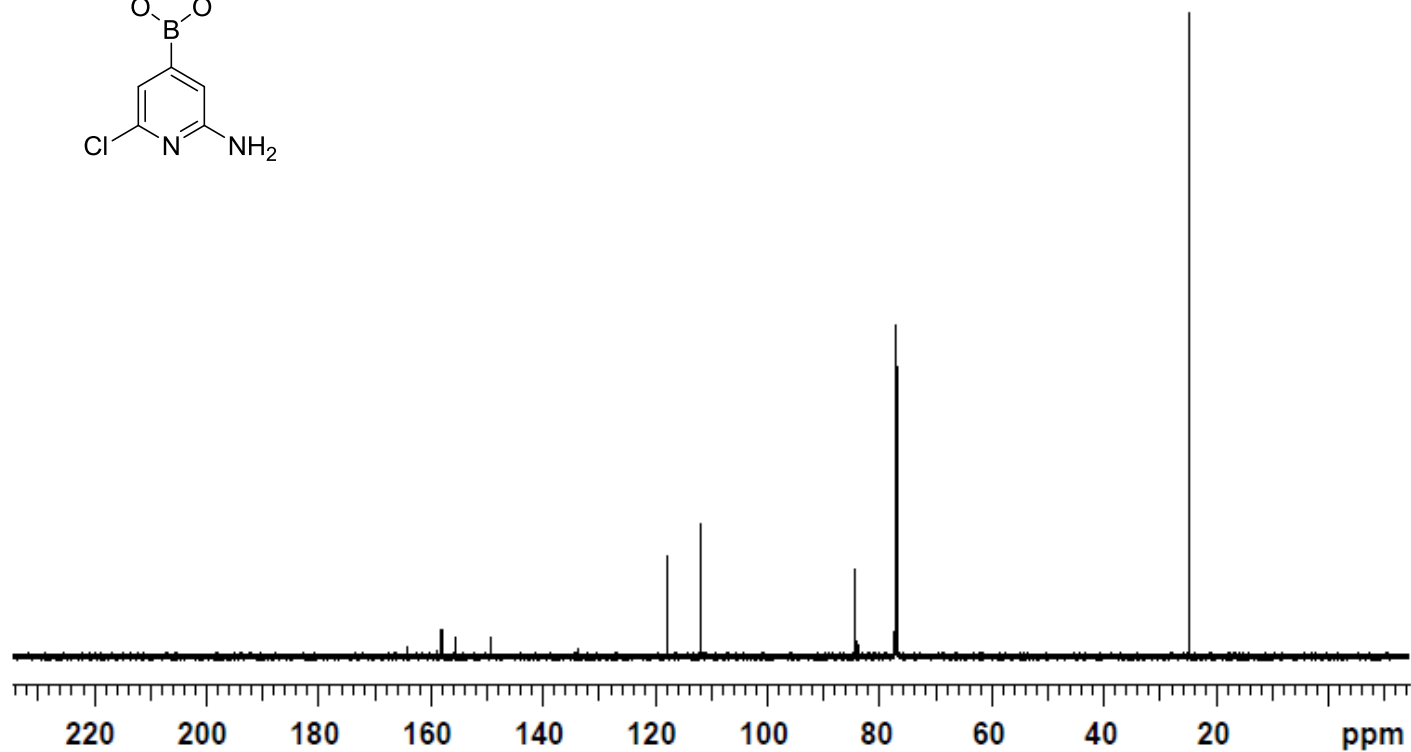
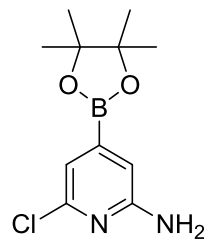


<sup>1</sup>H NMR (500 MHz, CDCl<sub>3</sub>) 6-chloro-4-(4,4,5,5-tetramethyl-1,3,2-dioxaborolan-2-yl)pyridin-2-amine (42)

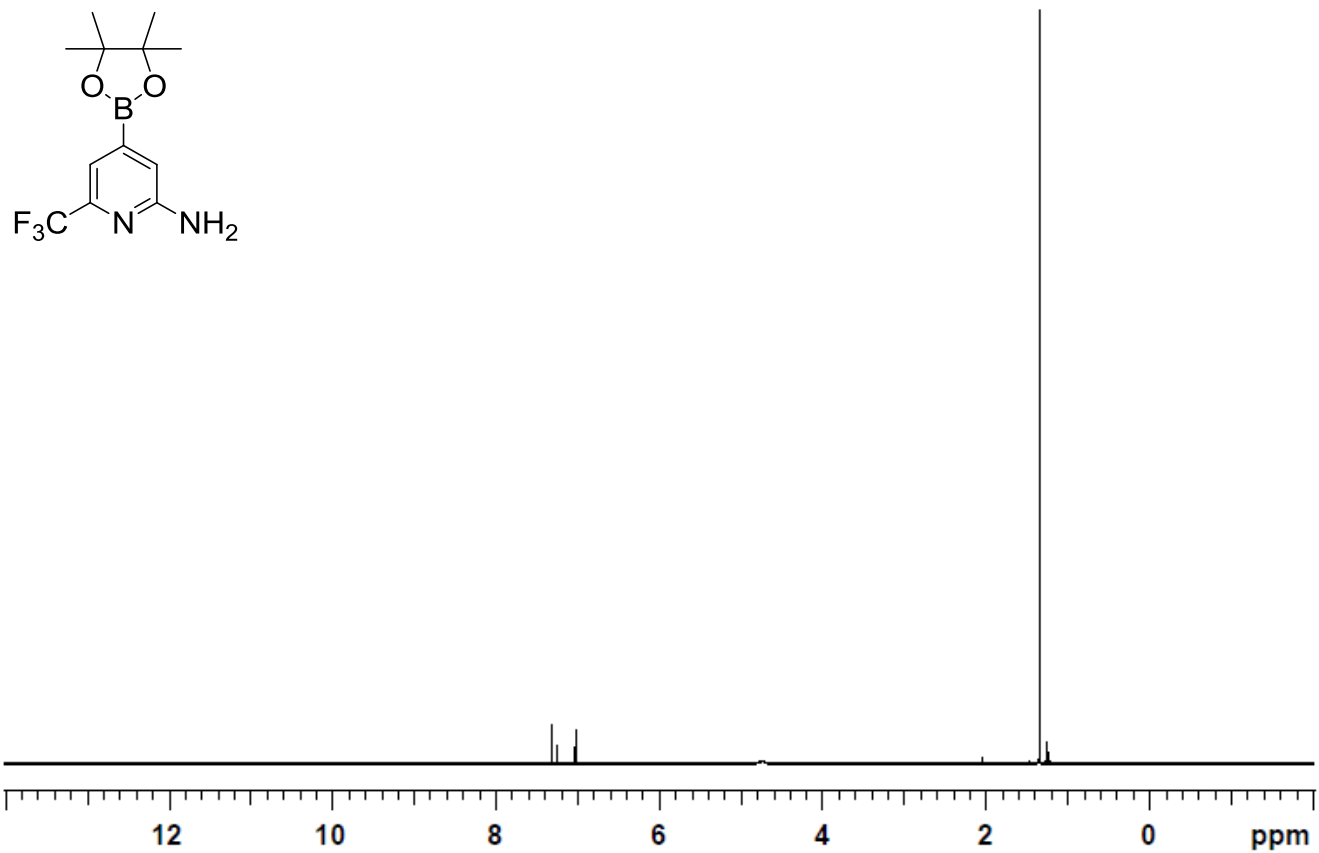




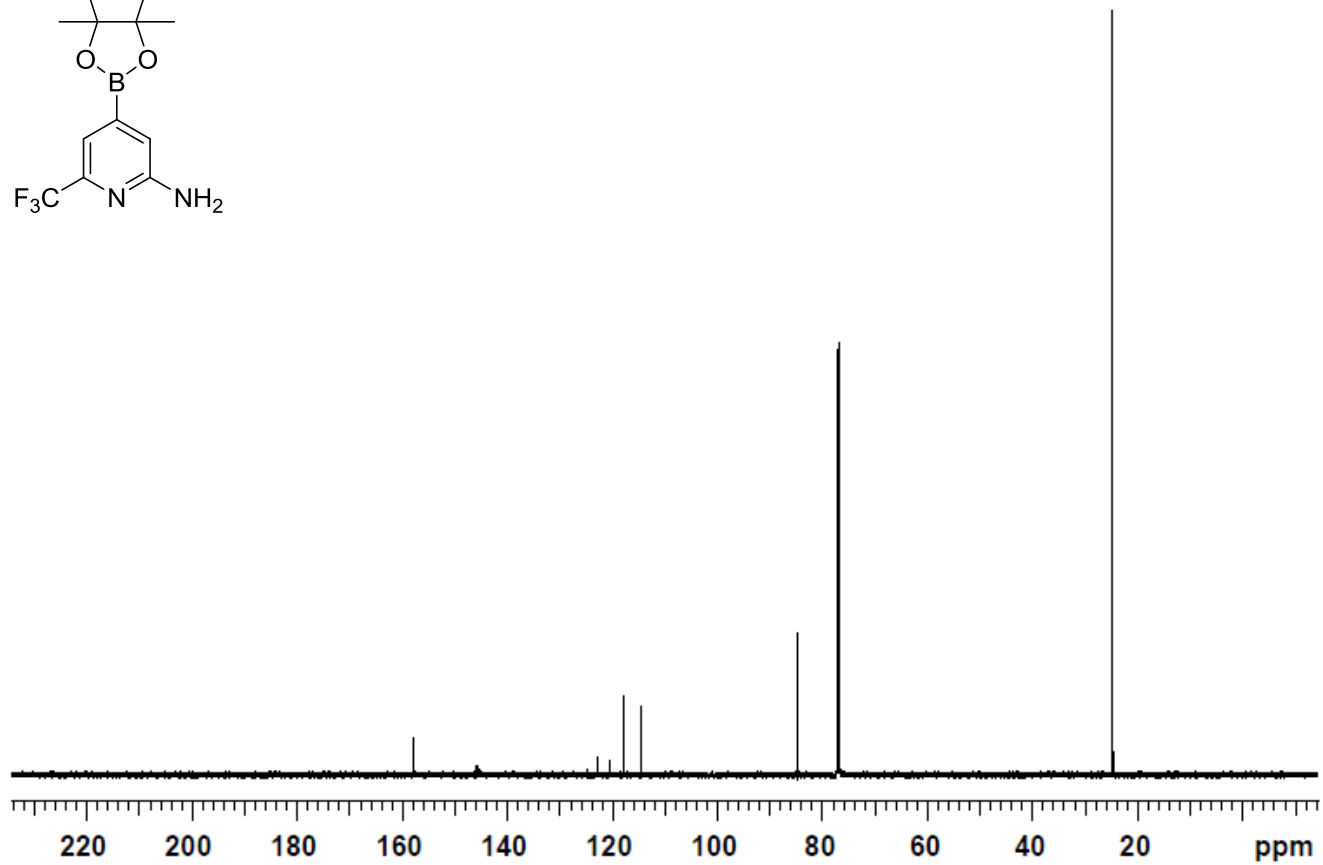
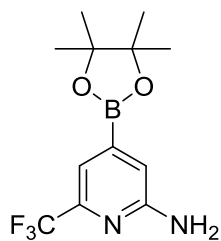
<sup>13</sup>C NMR (125 MHz, CDCl<sub>3</sub>) 6-chloro-4-(4,4,5,5-tetramethyl-1,3,2-dioxaborolan-2-yl)pyridin-2-amine (42)



<sup>1</sup>H NMR (500 MHz, CDCl<sub>3</sub>) 4-(4,4,5,5-tetramethyl-1,3,2-dioxaborolan-2-yl)-6-(trifluoromethyl)pyridin-2-amine (43)



$^{13}\text{C}$  NMR (125 MHz,  $\text{CDCl}_3$ ) 4-(4,4,5,5-tetramethyl-1,3,2-dioxaborolan-2-yl)-6-(trifluoromethyl)pyridin-2-amine (43)



## REFERENCES

## REFERENCES

- 1) Li, Z.; Liang, Z.; Wang, Y.; Pei, Y. *Res. Chem. Intermed.*, Ahead of Print.
- 2) Rosen, B. M.; Huang, C.; Percec, V. *Org. Lett.* **2008**, *10*, 2597-2600.
- 3) Jung, Y. C.; Mishra, R. K.; Yoon, C. H.; Jung, K. W. *Org. Lett.* **2003**, *5*, 2231-2234.
- 4) Lokare, K. S.; Staples, R. J.; Odom, A. L. *Organometallics* **2008**, *27*, 5130-5138.
- 5) Kallepalli, V. A.; Shi, F.; Paul, S.; Onyeozili, E. N.; Maleczka, R. E., Jr.; Smith, M. R., III *J. Org. Chem.* **2009**, *74*, 9199.
- 6) Takagi, J.; Sato, J.; Hartwig, J. F.; Ishiyama, T.; Miyaura, N. *Tetrahedron Lett.* **2002**, *43*, 5649.
- 7) Wheaton, S. L.; Humanayun, S. M.; Zhang, H.; Vogels, C. M.; Decken, A.; Westcott, S. A. *Cent. Eur. J. Chem.* **2010**, *8*, 725.